Geometry of the integrable multi-body systems and Exactly-solvable correlators in the fishnet theory

Dissertation

zur Erlangung des Doktorgrades
an der Fakultät für Mathematik,
Informatik und Naturwissenschaften

Fachbereich Physik
der Universität Hamburg

vorgelegt von
Enrico Olivucci

Hamburg

2020

Tag der Disputation: 24.06.2020
Folgende Gutachter empfehlen die Annahme der Dissertation:
Prof. Dr. G.E. Arutyunov
Prof. Dr. J. Teschner

Abstract

In this thesis, we present recent results obtained in the area of integrable models and focused on two main aspects of the discipline. The first part of the thesis concerns the geometric construction of specific multi-body integrable deformations of Calogero-Moser models via reduction methods - and the subsequent quantization. In particular, we provide a Poisson structure of the Ruijsenaars-Schneider model (i.e. the relativistic Calogero-Moser model) with hyperbolic potential and spin degrees of freedom, and we conjecture the trace formulae for the quantization of the spectral invariants of the Lax operator in the hyperbolic Ruijsenaars-Schneider model. In the second part of the thesis, we present a study of correlation functions in the fishnet theories arising as a double-scaling limit of γ-deformed $\mathcal{N} = 4$ SYM theory, via methods of exact solvability and integrability. In particular, we deal with the extension of the bi-scalar fishnet theory to any space-time dimensions, the computation of specific four-point functions at finite-coupling and the extraction from the operator product expansion of non-perturbative conformal data for the local operators.

Zusammenfassung

In dieser Arbeit präsentieren wir aktuelle Ergebnisse aus dem Bereich integrierbarer Modelle, die sich auf zwei Hauptaspekte der Disziplin konzentrieren. Der erste Teil der Arbeit befasst sich mit der geometrischen Konstruktion spezifischer integrierbarer Mehrkörperdeformationen von Calogero-Moser-Modellen mittels Reduktionsmethoden - und der anschließenden Quantisierung. Insbesondere liefern wir eine Poisson-Struktur des Ruijsenaars-Schneider-Modells (dh des relativistischen Calogero-Moser-Modells) mit hyperbolischem Potential und Spinfreiheitsgraden und vermuten die Spurenformeln für die Quantisierung der spektralen Invarianten des Lax-Operators in das hyperbolische Ruijsenaars-Schneider-Modell. Im zweiten Teil der Arbeit präsentieren wir eine Untersuchung der Korrelationsfunktionen in den Fischnetz-Theorien, die sich als doppelte Skalierungsgrenze der γ-deformierten $\mathcal{N} = 4$ SYM Theorie ergeben, über Methoden der exakten Lösbarkeit und Integrierbarkeit. Insbesondere befassen wir uns mit der Erweiterung der bi-skalaren Fischnetz-Theorie auf beliebige Raum-Zeit-Dimensionen, der Berechnung spezifischer Vierpunktfunktionen bei endlicher Kopplung und der Extraktion nicht störender konformer Daten aus dem Operatorprodukt für die lokale Betreiber.

This thesis is based on the following papers:

- G. Arutyunov, R. Klabbers and E. Olivucci, *“Quantum Trace Formulae for the Integrals of the Hyperbolic Ruijsenaars-Schneider model”*, JHEP **05**, 069 (2019), [arXiv:1902.06755].
- G. Arutyunov and E. Olivucci, *“Hyperbolic spin Ruijsenaars-Schneider model from Poisson reduction”*, [arXiv:1906.02619], (to appear in “Proceedings of the Steklov Institute of Mathematics”).
- V. Kazakov and E. Olivucci, *“Biscalar Integrable Conformal Field Theories in Any Dimension”*, Phys. Rev. Lett. **121**, no.13, 131601 (2018), [arXiv:1801.09844].
- S. Derkachov, V. Kazakov and E. Olivucci, *“Basso-Dixon Correlators in Two-Dimensional fishnet CFT”*, JHEP **04**, 032 (2019), [arXiv:1811.10623].
- S. Derkachov and E. Olivucci, *“Exactly solvable magnet of conformal spins in four dimensions”*, [arXiv:1912.07588].
- V. Kazakov, E. Olivucci and M. Preti, *“Generalized fishnets and exact four-point correlators in chiral CFT_4”*, JHEP **06**, 078 (2019), [arXiv:1901.00011].

Contents

Chapter 1
Introduction

> "Nissuna umana investigazione si può dimandare vera scienza, s'essa non passa per le matematiche dimostrazioni."
>
> "No human investigation can claim to be real science, if it doesn't go through mathematical proofs."
>
> *Leonardo Da Vinci*
> *Trattato della Pittura, ∼ 1540*

The theoretical description of any natural phenomena consist in a mathematical model that encodes its dynamics, that is the way according to which the state of things changes in time giving rise to the phenomenon. Any such model (dynamical system) is defined by a set of numeric variables which give a complete description of the configuration of the system at a certain time t (degrees of freedom) together with their dependence in time (evolution rule). Usually the evolution rule is not explicitly known for a given dynamical system, but we can still define the system by a set of differential equations in the time variable (equations of motion) whose solution is the evolution rule. This scheme, first elaborated for classical mechanics, can be extended to any field of theoretical physics, including quantum mechanics and quantum field theory. In fact, this thesis concerns various models of classical mechanics, quantum mechanics, and quantum field theory whose time-evolution is triggered by the Hamiltonian function of the degrees of freedom, or in other words by the energy of the system.

The crucial goal in the study of any dynamical system is to collect as much knowledge as possible on its evolution rule. In the most optimistic hypothesis it is possible to determine it exactly, solving the equations of motion. We refer to this condition as exact solvability of a model. A systematic way to investigate the features of exact solvability is given by the notion of integrability of the dynamical system, according to the theorems of Liouville [1] and its global version by Arnol'd [2] (see also [3, 4] for an extended treatment of this subject). The general idea of integrability is that if a Hamiltonian system with N degrees of freedom has N independent conserved quantities (integrals of motion) that generate N commuting symmetries of the Hamiltonian function (involution property), it is always possible to separate the variables by a canonical transformation so that the equations of motion can be solved by quadrature. In other words an integrable system, after a suitable canonical transformation, has conserved momenta, i.e. a Hamiltonian independent from the coordinates (free motion). Along with the notion of integrability in classical mechanics, it is possible to formulate its extensions to the quantum theory - where Poisson brackets between functions are quantized into commutators of linear operators - which have several realizations in terms of the Bethe ansatz, quantum separation of variables, Baxter equations [5–8].

The theory of integrable models has shown formidable applications to the solution of highly non-trivial problems in theoretical physics, covering topics ranging from spin lattices [9, 10], systems of coupled particles on a line [11, 12], to the spectrum of string theories and QFTs in the AdS/CFT correspondence [13, 14]. In this thesis we will touch upon many of these aspects, with the goal to to shed more light on the origin of integrability. The general approach that we will adopt for the systems of interacting particles and lattice spins under study, is an algebraic analysis of their Poisson structure aimed at revealing their integrability. Concretely, we will make use of the Lax pair methods [15] and their quantum counterpart (quantum inverse scattering method [10, 16]).

The special attention reserved in this thesis to field theories with conformal symmetry is due to the wide interest that they attracted in theoretical physics, ranging from critical phenomena to quantum gravity. For the sake of exact-solvability and integrability, conformal field theories [17] provide an amazing environment for developing toy models. Indeed, tight constraints imposed by conformal symmetry allow for significant simplification of correlation functions. For instance, the computation of two-point correlators is reduced to finding the spectrum of a quantum operator (Dilation), while three-point functions are fixed by symmetry up to a constant. Moreover, computations of Feynman diagrams of the perturbative series for conformal correlators are greatly helped by the simple power-law behavior of the propagators.

The thesis is divided into two parts, reflecting the two research areas approached during the doctoral period. Below we outline the content of the thesis and explain our main achievements.

The *first part* of this thesis deals with the study of integrable models of many particles which mutually interact in one spatial dimension. In particular, we study the relativistic Calogero-Moser models, also known as Ruijsenaars-Schneider models [18]. The first representative of the class of Calogero-Moser integrable dynamical systems was studied by F. Calogero in 1969 for $N = 3$ particles [11], and its Hamiltonian for generic N reads

$$\mathcal{H}_{CM}(q,p) = \sum_{i=1}^{N} p_i^2 + \sum_{i\neq j} \frac{\gamma}{(q_i - q_j)^2}\,. \tag{1.0.1}$$

Further on, several deformation of the Calogero-Moser model were introduced and shown to be integrable and solvable; among these we must mention the deformation of the rational potential $1/(q_i - q_j)^2$ to a trigonometric/hyperbolic or elliptic function [12]. Doing so, one gives rise to a hierarchy of integrable models where the elliptic one stands at the top and the other models can be obtained by sending to infinity the fundamental periods of the torus on which the elliptic model is defined. The models of Calogero-Moser hierarchy have been well studied together with their quantum versions, and have found applications to several problems in theoretical physics, ranging from the low-energy spectrum of super-symmetric gauge theories [19] to recent advancements in conformal field theory [20]. Analogues features hold for the Ruijsenaars-Schneider (RS) models [18, 21]; they form a hierarchy of integrable models, each of them being the relativistic counterpart of a corresponding model in the Caloger-Moser hierarchy. In this thesis we deal with the hyperbolic RS model in the perspective of reduction techniques, according to which we aim at obtaining a non-trivial integrable model starting from a highly symmetric dynamical system with more degrees of freedom and a simple evolution rule.

In the chapter “Symmetry and reduction” (1) we briefly present the reduction procedure by the Poisson action of a Poisson-Lie group [22] on the phase space of a dynamical system, introducing the definitions of momentum map and the Dirac's classification of constraints. Furthermore we provide details on a particular symplectic manifold, the Heisenberg double of a Poisson-Lie group, which is the natural starting point for the reduction of Ruijsenaars-Schneider hyperbolic models performed in the successive chapters of part I.

In the second chapter (2) we give an explicit realization of the reduction for the hyperbolic model of the RS hierarchy, starting from a trivial dynamics defined on the Heisenberg double of the Poisson-Lie group $\mathrm{GL}(N,\mathbb{C})$. We present an original result about the quantum model consisting in a remarkably simple conjecture, based on a guess over reduction procedure, for the quantum traces of powers of the Lax matrix $\mathrm{tr}(L^k)$, a complete family of integrals of motion. These quantities generate the center of the semi-dynamical reflection equation (see [23]) which defines the algebra of quantum Lax operators. Furthermore we provide details about the affine quantum model obtained by introduction of a spectral parameter.

The third and last chapter (3) of the first part deals with the higher-rank realization of the RS hyperbolic model. This dynamical system, better known after the name of “spin Ruijsenars-Schneider model” has been first formulated by I. Krichever and A. Zabrodin [24], by stating its equation of motion but without providing its Poisson structure. Here we present as an original result a Poisson structure for the spin model. This has been obtained by means of a Poisson reduction of a phase space consisting of the Heisenberg double of $\mathrm{GL}(N, \mathbb{C})$ enlarged with the degrees of freedom of higher-rank twisted harmonic oscillators. We provide the explicit solution to the equations of motion and explain its features of degenerate integrability [25].

The *second part* of the thesis deals with quantum conformal field theory (CFT) and with integrability methods applied to field theoretical computations. In the past two decades there has been an exceptionally fruitful interest in integrability techniques for the computations of correlation functions in the context of the AdS/CFT correspondence [26]. In particular the most advanced results have been obtained in the super-symmetric and conformal $\mathcal{N} = 4$ SYM theory [13, 27], which is the natural background of the second part of this thesis. All the scientific content we present – apart from statements and formulas with an explicit reference to the literature – are original contributions contained in the papers [28–31].

The first chapter (1) introduces a special strong deformation limit for the $\mathcal{N} = 4$ SYM theory (double-scaling limit), which leads to the loss of gauge symmetry and super-symmetry but – at the same time – preserves the conformality of the resulting theory, which in addition enjoys a much simpler field content (three complex scalars and three fermions). This limiting procedure, firstly proposed by V. Kazakov and O. Gurdogan in [32], provides an amazing toy model to explore the properties of CFTs in space-time dimensions higher than $d = 2$ and their relation to integrable spin chains with conformal symmetry $SO(1, d + 1)$. It is worth mentioning that all the features of such field theories are always discussed within the planar limit. In this context the integrability methods appear as a tool for computing exact correlators, by mapping the conformal Feynman integrals to the Hamiltonian of an integrable spin magnet. This chapter presents the general properties of the doubly-scaled theory, basing the discussion on the fact that its Feynman diagrams present a simple and regular topology.

The second chapter (2) presents the definition of the bi-scalar fishnet theory (or simply "fishnet theory"), a reduction of the double-scaling limit of $\mathcal{N} = 4$ SYM with only two scalar fields. We generalize the fishnet theory to any space-time dimension and by an "anisotropic" deformation consisting in different scaling dimensions for the two scalar fields. Tuning the space-time dimension d and the deformation parameter ω, one can regard fishnet theory as an interpolation between other known integrable models. For example, setting $d = 2$ and $\omega \to 0$ the spin chain of fishnet theory coincides with that of the BFKL (Balitski-Kuraev-Fadin-Lipatov) model [33] for the scattering of high-energy gluons in quantum chromodynamics.

In the third chapter (3) we perform for the first time an explicit computation of a specific class of four-point functions for the fishnet theory in two and four space-time dimensions. The corresponding Feynman integrals admit a determinant representation in terms of ladder integrals (computed in $4D$ by [34]) and we express the integrals as an expansion over the spectrum of quantum separated variables in the conformal spin magnet with open boundaries. A remarkable aspect of these results is the first-principle check of the bootstrap conjectures of [35].

Finally, the last chapter (4) of this thesis aims at extending the results of [36, 37] about the CFT data of local operators in fishnet theory, to the entire double-scaling limit of $\mathcal{N} = 4$ SYM theory, definitely richer in matter content due to the inclusion of fermionic fields with Yukawa interactions. In addition we show how the integrability of conformal Feynman diagrams in the spin-chain vacuum sector $\mathrm{tr}[\phi_1^L]$ is described by the same model of the simpler bi-scalar reduction. Finally, we point out the presence of logarithmic multiplets in the mixing of local operators, previously noticed for the bi-scalar theory [38, 39], which arise as a consequence of non-hermitian interactions. These results consist in drawing a first step back towards the original - undeformed - $\mathcal{N} = 4$ SYM theory.

In the end of this thesis we give an appendix containing technical computations that are required to justify some statements in the main text. An exhaustive bibliography can be consulted at the end of this thesis, collecting references from both the two parts.

Part I

Geometry of the integrable multi-body systems

Chapter 1
Symmetry and reduction

1.1 Introduction

In this chapter we present through some definitions and examples the basic idea that the Poisson-Lie symmetry of a dynamical system may be exploited to obtain an integrable model by a reduction of the degrees of freedom. This basic idea will be applied in the subsequent chapters to models of point-like interacting particles in one spatial dimension going under the general name of Calogero-Moser systems and their various deformations.

In order to introduce the basic notions, let us consider a dynamical systems with N degrees of freedom. The configurations of N particles at a certain time can be described by N real numbers $q^i = (q^1, \dots, q^N)$ which constitute a point of an N-dimensional (real) manifold M. The phase space of the system is the cotangent bundle T^*M over M, that is the vector bundle of 1-forms on M. The dimension of the cotangent bundle is then $2N$ and one can introduce a system of local coordinates (p_i, q^i), where p_i are coordinates on fibers. In other words, the 1-form on M defined by a point (p_i, q^i) of the cotangent bundle $\alpha(p_i, q^i) = p_i dq^i$ can be regarded as a 1-form (canonical) on T^*M. As a consequence it is always possible to associate to such a dynamical system a closed (exact) form $\omega = d\alpha$ which is indeed non-degenerate:

$$\omega = d\alpha = dp_i \wedge dq^i \,. \tag{1.1.1}$$

The coordinates on M describe the degrees of freedom and are called positions $\{q^i\}$, while the coordinates on the fiber are the momenta $\{p_i\}$. In general, the state of a dynamical system with N degrees of freedom is described by a point on a $2N$-dimensional symplectic manifold $\mathscr{P}$.

A Hamiltonian dynamical system is characterized by the existence of a function of the phase space $\mathcal{H} = \mathcal{H}(q, p)$ such that the given differential equations for the time evolution of an observable $f = f(q, p)$ can be expressed via the following Poisson bracket

$$\frac{d}{dt} f(q,p) = \{\mathcal{H}, f\}(q,p) = J_{ij}(q,p)\, \partial^i \mathcal{H}(q,p)\, \partial^j f(q,p) \,, \tag{1.1.2}$$

where the Poisson tensor J is a $2N \times 2N$ matrix given by the inverse of the symplectic form: $J = \omega^{-1}$.

A Hamiltonian symmetry is a canonical transformation which leaves the Hamiltonian $\mathcal{H}$ invariant

$$(q,p) \;\to\; (Q(q,p), P(q,p))\,, \quad \mathcal{H}(Q(q,p), P(q,p)) = \mathcal{H}(q,p)\,. \tag{1.1.3}$$

As such it is a diffeomorphism of the phase space that transforms solutions of the equations of motion into solutions[1]. A consequence of a Hamiltonian symmetry is the existence of conserved quantities - the generators of the infinitesimal symmetry transformations, that form (a representation of) the Lie algebra $\mathfrak{g}$ of the symmetry Lie group G. In this thesis we will deal with the Poisson-Lie symmetry – the generalization of the Hamiltonian symmetry to the Poisson action of a Poisson-Lie group G on the phase space $\mathscr{P}$ of a dynamical system.

Under suitable additional hypothesis on how the group G acts on the phase space $\mathscr{P}$, the existence of a symmetry allows to reduce the number of degrees of freedom of the system by means of the so-called Poisson reduction [40, 41], which leads to the definition of a new Hamiltonian system (reduced) whose dynamics is usually more-complicated than the non-reduced one. The reduction consists in eliminating a number of degrees of freedom by setting the conserved generators of the symmetry to some constant values, then to factor out some further redundant degrees of freedom by fixing the residual (gauge) symmetry of the level set of such integrals.

The present chapter will deal with the formulation and application of such techniques. The general task is to obtain from a simple dynamical system with many symmetries on a symplectic manifold $\mathscr{P}$, a reduced system on a symplectic submanifold $\mathscr{P}_{red}$ whose dynamics is much less trivial and which inherits enough involutive integrals of motion to satisfy Liouville's integrability.

1.2 Poisson-Lie groups

In order to explain the Poisson reduction techniques, we need the notion of Poisson-Lie group [22]. A Lie group G endowed with a Poisson structure, is called a Poisson-Lie group if the group multiplication $G \times G \to G$ is a Poisson mapping, where the space $G \times G$ is equipped with the product Poisson structure.
Let $\{\ ,\ \}$ be a Poisson bracket on G. The Poisson-Lie property requires that, for any two smooth functions f, h on the group, it holds:

$$\{f,h\}(g_1 g_2) = \{R_{g_2} f, R_{g_2} h\}(g_1) + \{L_{g_1} f, L_{g_1} h\}(g_2)\,, \tag{1.2.1}$$

where $L_h f(g) = f(h \cdot g) = R_g f(h)$. This definition is equivalent to ask that the Poisson tensor $J(g)$ satisfies the following equation:

$$J(g_1 g_2) = J(g_2) + \mathrm{Ad}_{g_2^{-1}} \otimes \mathrm{Ad}_{g_2^{-1}} J(g_1)\,, \tag{1.2.2}$$

[1] The symmetry of the system can be of more general type, for example discrete symmetries generated by finite groups. Here we refer to the continuous, smooth case which allows to define a symmetry according to Noether's theorem.

where $J(g) = J^{ij}(g)\, e_i \wedge e_j \in \mathfrak{g} \wedge \mathfrak{g}$, $\{e_i\}$ are basis elements of the Lie algebra $\mathfrak{g}$ and Ad is the adjoint action of the group[2]. In particular for $g_2 = e$ the former equation implies $J(e) = 0$, so the Poisson bracket on G degenerates at the group origin and a Poisson-Lie group can not be a symplectic manifold.

We will consider a class of Poisson-Lie groups whose Poisson tensor J has the form

$$J(g) = \mathrm{Ad}_{g^{-1}} \otimes \mathrm{Ad}_{g^{-1}} r - r\,, \tag{1.2.3}$$

where[3]

$$r \equiv r^{ij}\, e_i \wedge e_j \equiv \tfrac{1}{2} r^{ij} \big(e_i \otimes e_j - e_j \otimes e_i \big)\,, \tag{1.2.4}$$

is a constant element of $\mathfrak{g} \wedge \mathfrak{g}$. The corresponding Poisson bracket, known as Sklyanin bracket, takes a simple form between the generators of the coordinate ring of the group

$$\{g_1, g_2\}_G = [r, g_1 g_2]\,, \tag{1.2.5}$$

for $g_1 = g \otimes \mathbb{1}_G$ and $g_2 = \mathbb{1}_G \otimes g$. Such bracket appears often in the theory of integrable systems and we will encounter it several times in the next three chapters. In this context a condition on r, resulting from the imposition of the Jacobi identity, is:

$$[r_{12}, r_{13}] + [r_{13}, r_{23}] + [r_{12}, r_{23}] = -c^2 [e_i, e_j] \otimes e_i \otimes e_j\,, \tag{1.2.6}$$

where r_{ij} is the r-matrix (1.2.4) acting on the i-th and j-th spaces, and $c^2 \in \mathbb{R}$ is a constant. Equation (1.2.6) is known as modified classical Yang-Baxter equation (mCYBE). For $c = 0$ we say that the r-matrix solves the classical Yang-Baxter equation (CYBE), while the choices $\Im(c) = 0$ and $\Re(c) = 0$ are called respectively "split" and "non-split" solutions.

The Poisson-Lie property (1.2.1) implies that the space $\mathfrak{g}^*$ of linear functionals over the Lie algebra $\mathfrak{g}$ is itself a Lie algebra (dual Lie algebra) whose commutator is defined by a co-cycle on $\mathfrak{g}$ induced by the Poisson tensor $J(g)$. Namely, we can define the co-cycle $\delta \in \mathfrak{g} \wedge \mathfrak{g}$ as

$$\delta(X) = \frac{d}{ds} J(e^{-sX}) \mid\,, \quad X \in \mathfrak{g}\,. \tag{1.2.7}$$

Then, the commutator of the dual Lie algebra is given, for any two elements $\ell, \ell' \in \mathfrak{g}^*$, by

$$\langle [\ell, \ell']_{\mathfrak{g}^*}, X \rangle = \langle \ell \otimes \ell', \delta(X) \rangle\,, \tag{1.2.8}$$

[2]Let us think in terms of groups of matrices: the adjoint action of the group element h on a matrix M is the conjugation hMh^{-1}.

[3]To render J skew-symmetric, it is enough to require that the symmetric part of $r = r^{ij} e_i \otimes e_j$ is Ad-invariant. Since this symmetric part decouples from J, we can assume from the beginning that r is an element in $\mathfrak{g} \wedge \mathfrak{g}$.

where $X \in \mathfrak{g}$ and $\langle \cdot, \cdot \rangle$ is the pairing between $\mathfrak{g}$ and its dual space $\mathfrak{g}^*$. We assume from now on that the r-matrix (1.2.4) is a split solution of the (1.2.6), with $c^2 = 1$. Then, we can define a linear operator $\mathbf{r} : \mathfrak{g}^* \to \mathfrak{g}$ as

$$\ell \in \mathfrak{g}^* \ \mapsto \ \mathbf{r}(\ell) = r^{ij} \langle \ell, e_i \rangle e_j \,, \tag{1.2.9}$$

and the commutator in the dual Lie algebra, for a Poisson-Lie group with Sklyanin bracket (1.2.5), is realized as

$$\langle [\ell, \ell']_{\mathfrak{g}^*}, X \rangle = -\langle \ell, [\mathbf{r}(\ell'), X] \rangle \,. \tag{1.2.10}$$

As a further consequence of the Poisson-Lie property, one might define a connected Lie group as “exponentiation” of the dual algebra $\mathfrak{g}^*$, which we call dual Lie group G^*. The group multiplication on G^* can be defined in the embedding $G^* \to G \times G$. Indeed, one can first define an embedding of $\mathfrak{g}^*$ into two copies of $\mathfrak{g}$ as

$$\ell \in \mathfrak{g}^* \ \mapsto \ (\ell_+, \ell_-) = \frac{1}{2}(\mathbf{r}(\ell) + \ell, \mathbf{r}(\ell) - \ell) \in (\mathfrak{g}, \mathfrak{g}) \,, \tag{1.2.11}$$

then considering to “exponentiate” the map to the dual group, that is to associate to $u \in G^*$ a pair $(u_+, u_-) \in G \times G$ such that if $u = \mathbb{1} + s\ell + O(s^2)$ then $(u_+, u_-) = (\mathbb{1} + s\ell_+, \mathbb{1} + s\ell_-) + O(s^2)$. According to this decomposition the multiplication law of G^* is just the usual matrix multiplication by components

$$(u_+, u_-) \cdot (v_+, v_-) = (u_+ v_+, u_- v_-) \,, \tag{1.2.12}$$

The group G^* can be embedded into G by a map σ

$$\sigma(u_+, u_-) = u_+ u_-^{-1} = u \,. \tag{1.2.13}$$

Conversely, assuming σ is a global diffeomorphism $G^* \simeq G$, for a given $u \in G$ an element (u_+, u_-) is defined as a unique solution of the factorization problem $u = u_+ u_-^{-1}$. We remark that according to (1.2.12) the inverse of u is $\sigma(u_+^{-1}, u_-^{-1}) = u_+^{-1} u_-$, that is not the matrix inverse of u. In general, the multiplication of two elements in the embedding is then given by

$$v \star u = v_+ u_+ u_-^{-1} v_-^{-1} = v_+ u v_-^{-1} \,. \tag{1.2.14}$$

The dual group G^* equipped with the brackets

$$\begin{aligned} \{u_{+1}, u_{+2}\}_{G^*} &= -\tfrac{1}{2}[r, u_{+1} u_{+2}] \,, \qquad & \{u_{+1}, u_{-2}\}_{G^*} &= -[r_+, u_{+1} u_{-2}] \,, \\ \{u_{-1}, u_{-2}\}_{G^*} &= -\tfrac{1}{2}[r, u_{-1} u_{-2}] \,, \qquad & \{u_{-1}, u_{+2}\}_{G^*} &= -[r_-, u_{-1} u_{+2}] \,, \end{aligned} \tag{1.2.15}$$

where $r_\pm = r \pm C/2$ and $C = e_i \otimes e_i$ is the split-Casimir of the algebra $\mathfrak{g}$, is a Poisson-Lie group. Further, under the map (1.2.13) the Poisson structure (1.2.15) induces the following Poisson structure on G

$$\{u_1, u_2\}_{\hat{G}} = -\tfrac{1}{2} r u_1 u_2 - \tfrac{1}{2} u_1 u_2 r + u_1 r_- u_2 + u_2 r_+ u_1 \,. \tag{1.2.16}$$

This structure is Poisson-Lie with respect to the product (1.2.14), i.e.,

$$\{v_1 \star u_1, v_2 \star u_2\}_{G^* \times \hat{G}} = \{u_1, u_2\}_{\hat{G}}(v \star u)\,,$$

where in the right hand side the subscript $\hat{G}$ refers to the bracket (1.2.16), while $\{\ ,\ \}_{G^* \times \hat{G}}$ in the left hand side refers to the product Poisson structure. In this way we model the Poisson-Lie group G^* as the manifold G with the Poisson brackets (1.2.16) and the composition law (1.2.14). In the context of the Poisson-Lie theory (1.2.16) and (1.2.15) are known as the Semenov-Tian-Shansky brackets [40].

1.2.1 Momentum map

In this section we summarize the features of a dynamical system which enjoys symmetry under the action of a Poisson-Lie group G on the phase space $\mathscr{P}$. Our task is to explain the procedure of Poisson reduction [40] in the formalism of the momentum map introduced in [41]. We will require that the action $G \times \mathscr{P} \to \mathscr{P}$ is a Poisson map between the Poisson manifolds $G \times \mathscr{P}$ and $\mathscr{P}$:

$$\{f_x, h_x\}_G(g) + \{f_g, h_g\}_{\mathscr{P}}(x) = \{f, h\}_{\mathscr{P}}(g \cdot x)\,, \tag{1.2.17}$$

where $f_x(g) = f(g \cdot x)$, $f_g(x) = f(g \cdot x)$ and the subscripts distinguish the Poisson bracket on the group and on the phase space. This condition is the requirement of a "Poisson action". In the case of the trivial Poisson bracket on G, i.e. $\{g_1, g_2\}_G = 0$ this action is called "Hamiltonian" and it takes a simpler form

$$\{f_g, h_g\}_{\mathscr{P}}(x) = \{f, h\}_{\mathscr{P}}(g \cdot x)\,. \tag{1.2.18}$$

A Poisson action of a Poisson-Lie group G on a symplectic manifold $\mathscr{P}$ defines a map $\mathcal{M}$ with values in the dual Lie group G^*

$$\mathcal{M}:\ \mathscr{P} \to G^*\,, \tag{1.2.19}$$

which generates the infinitesimal group action on the algebra of functions of the phase space. Let us call ξ_X the vector field of the infinitesimal transformation associated to an element $X \in \mathfrak{g}$

$$\xi_X f(p) = \frac{d}{ds} f(e^{-sX} \cdot p)\mid_{s=0} \tag{1.2.20}$$

where $e^{-sX} \cdot p \in \mathscr{P}$ is the result of the action of $e^{-sX} \in G$ on the phase space point p. Then the momentum map $\mathcal{M}$ is a generator of the group action in the Poisson algebra:

$$\xi_X f = \langle X, \{\mathcal{M}, f\}_{\mathscr{P}} \star \mathcal{M}^{-1} \rangle\,. \tag{1.2.21}$$

Here we emphasize that $\{\mathcal{M}, f\}_{\mathscr{P}}$ and $\mathcal{M}^{-1}$ in the right hand side of the last formula are multiplied by using the composition law of G^*, in the embedding $G^* \hookrightarrow G$.

The momentum map $\mathcal{M}$ satisfies some properties. First, it is a Poisson map[4] between the Poisson manifolds $\mathscr{P}$ and G^*, that is

$$\{\mathcal{M}^* f, \mathcal{M}^* h\}_{\mathscr{P}}(p) = \{f, h\}_{G^*}(\mathcal{M}(p)), \tag{1.2.22}$$

for any two functions f, h on the dual Lie group G^*. For the components of the momentum map the last formula specifies to

$$\{\mathcal{M}_1, \mathcal{M}_2\}_{\mathscr{P}}(p) = \Phi_{ij}(\mathcal{M}(p)) e^i \mathcal{M}(p) \otimes e^j \mathcal{M}(p), \tag{1.2.23}$$

where $\mathcal{M}_1 = \mathcal{M} \otimes \mathbb{1}_{G^*}$, $\mathcal{M}_2 = \mathbb{1}_{G^*} \otimes \mathcal{M}$, and Φ_{ij} is a Poisson tensor on G^*. It follows that the infinitesimal action of the group G on $\mathscr{P}$ is intertwined with an infinitesimal action on G^* defined by

$$\xi_i \mathcal{M}(p) = \Phi_{ij}(p) e^j \mathcal{M}(p). \tag{1.2.24}$$

Secondly, the map $X \to \xi_X$ is a homomorphism of the Lie algebra $\mathfrak{g}$ into the algebra of vector fields on $\mathscr{P}$, that is

$$[\xi_X, \xi_Y] = \xi_{[X,Y]}. \tag{1.2.25}$$

This property can be satisfied in accord with (1.2.24) if we impose that the tensor Φ endows G^* with the structure of a Poisson-Lie group, so that

$$\Phi(\mathcal{M} \star \mathcal{M}') = \Phi(\mathcal{M}) + \mathrm{Ad}_{\mathcal{M}} \otimes \mathrm{Ad}_{\mathcal{M}} \Phi(\mathcal{M}'), \tag{1.2.26}$$

for each $\mathcal{M}, \mathcal{M}' \in G^*$, and it coincides with the Poisson-Lie structure defined by the bracket (1.2.16). In this case, the action of G on $\mathscr{P}$ is intertwined with the coadjoint action of G on the dual Lie group G^*

$$\mathcal{M}(g \cdot p) = \mathrm{Ad}^*_g \mathcal{M}(p). \tag{1.2.27}$$

It follows that a Poisson-Lie orbit of G on $\mathscr{P}$ is mapped by $\mathcal{M}$ into a coadjoint orbit on G^*.

Now, let's assume that the Poisson action of the Poisson-Lie group G on the phase space $\mathscr{P}$ is a symmetry of the dynamical system. This means that the Hamiltonian $\mathcal{H}$ is invariant under the symmetry

$$\xi_X \mathcal{H} = \langle X, \{\mathcal{M}, \mathcal{H}\}_{\mathscr{P}} \star \mathcal{M}^{-1} \rangle = 0, \quad \forall X \in \mathfrak{g}, \tag{1.2.28}$$

It follows that the components of the matrix $\mathcal{M} = \mathcal{M}(p)$ are conserved quantities along the time evolution of the system, i.e. integrals of the motion. In other words the existence of a Poisson symmetry means that the evolution of the system in the phase space, occurs on the level set of the generators of the symmetry

$$\mathcal{S} = \{p \in \mathscr{P} \,|\, \mathcal{M}(p) = \mathcal{M}(p_0)\}, \tag{1.2.29}$$

[4]Here we are making some assumptions on the group which are verified in the examples of the next chapters. In general, this condition should be relaxed by asking a more general Poisson structure on G^* that includes an extension by central terms [42].

where we called p_0 the initial condition. Thus the dynamical system is subject to dim $\mathfrak{g}$ constraints

$$\mathcal{M}_{ij} = \mathcal{M}_{ij}(p_0)\,, \tag{1.2.30}$$

which can be classified into two classes [43]:

- Constraints of the first class correspond to those components of the momentum map $\mathcal{M}_\alpha$ which Poisson commute with all the others on the constrained surface. So, on the surface $\mathcal{S}$ one has that $\{\mathcal{M}_\alpha, \mathcal{M}_{\alpha'}\}_{\mathscr{P}} = 0$, $\forall\alpha'$.
- Constraints of the second class are all the others. For every point $p \in \mathscr{P}$ which lies in a neighborhood of the constrained surface $\mathcal{S}$

$$\det(\Psi)(p) \neq 0\,,\ \ \Psi_{\beta\beta'}(p) = \{\mathcal{M}_\beta, \mathcal{M}_{\beta'}\}_{\mathscr{P}}(p)\,, \tag{1.2.31}$$

  and so the matrix Ψ can be inverted in each point of $\mathcal{S}$.

The geometrical meaning of the two classes of constraints coincides with the splitting of the group action into two components. The momentum map elements associated to first class constraints generate the component of the group action tangent to the constrained surface, while the elements of the second class generate the components of the action in a (skew-)orthogonal direction.

The restriction of the phase space to $\mathcal{S}$ does not conclude the reduction procedure as the first class components generate the isotropy subgroup $G_{iso} \subset G$ of the constrained surface. Its action is well defined on $\mathcal{S}$ and defines the "gauge" transformations. Since the observable quantities are invariant under the action of G_{iso}, such gauge freedom is redundant and generates unphysical degrees of freedom, so it must be fixed to complete the reduction. The fully reduced phase space $\mathscr{P}_{red} = \mathcal{S}/G_{iso}$ has now real dimension

$$\dim\ \mathscr{P}_{red} = \dim\ \mathscr{P} - \dim\ \mathfrak{g} - \dim\ \mathfrak{g}_{iso}\,, \tag{1.2.32}$$

and can be endowed with a symplectic structure according to [41][5]. This statement completes the procedure of Poisson reduction, and in the following chapters we will give some explicit examples.

Once the symplectic form is defined, one needs to write explicitly the Poisson structure on $\mathscr{P}_{red}$. In the simplified situation in which all the constraints are of the first class, the restriction of the original Poisson brackets on $\mathscr{P}$ to the reduced phase space $\mathscr{P}_{red}$ is enough. Otherwise, the presence of second class constraints requires the definition of the Dirac bracket. The latter is defined for any two functions f and h on a neighborhood of $\mathcal{S}$ as

$$\{f, h\}_{\rm D} = \{f, h\} - \{f, \mathcal{M}_{\bar\alpha}\}\Psi^{-1}_{\bar\alpha\bar\beta}\{\mathcal{M}_{\bar\beta}, h\}\,. \tag{1.2.33}$$

With respect to the Dirac bracket, any function on the phase space Poisson commutes with all the second class constraints, i.e.

$$\{f, \mathcal{M}_\beta\}_{\rm D} = \{f, \mathcal{M}_\beta\} - \{f, \mathcal{M}_\gamma\}\Psi^{-1}_{\gamma\delta}\{\mathcal{M}_\delta, \mathcal{M}_\beta\} = \{f, \mathcal{M}_\beta\} - \{f, \mathcal{M}_\beta\} = 0\,,$$

[5] Under some additional hypothesis on the group action discussed in the paper [41].

thus, in particular, all the constraints are of the first class.

In order to compute the Poisson bracket of two functions $\hat{f}, \hat{h}$ on $\mathscr{P}_{red}$ (physical observables) one needs to take any G_{iso}-invariant extensions f, h without loss of generality, compute their Dirac bracket in a neighborhood of the reduced phase space and then restrict the result to $\mathscr{P}_{red}$

$$\{\hat{f}, \hat{h}\}_{\mathscr{P}_{red}}(x) = \{f, h\}_{\mathrm{D}}(x), \qquad x \in \mathscr{P}_{red}. \tag{1.2.34}$$

Symplectic reduction In the simplified situation in which the Poisson structure on G is trivial, that is the dual group G^* is abelian, we can write $\mathcal{M} = \exp(\mu)$ where $\mu \in \mathfrak{g}^*$ is called "momentum map" of the Hamiltonian action. In this case the definition (1.2.21) reduces to

$$\xi_X f = \langle X, \{\mu, f\}_{\mathscr{P}} \rangle, \tag{1.2.35}$$

so that for each Lie algebra element there is an associated function

$$f_X(p) = \langle X, \mu(p) \rangle, \tag{1.2.36}$$

such that $\xi_X h = \{f_X, h\}$. It is possible to require that the Hamiltonian functions f_X satisfy the property

$$f_{[X,Y]} = \{f_X, f_Y\}_{\mathscr{P}}. \tag{1.2.37}$$

The last requirement together with the Poisson property for the map μ fixes completely the Poisson bracket between components of the moment map to be

$$\{\mu_1, \mu_2\}_{\mathscr{P}} = \langle \mu, [e_i, e_j] \rangle\, e^i \wedge e^j, \tag{1.2.38}$$

Obviously, (1.2.38) coincides with the Kirillov-Kostant bracket for the coordinates μ_i on $\mathfrak{g}^*$ amalgamated into

$$\mu = \mu_i e^i. \tag{1.2.39}$$

A straightforward consequence of (1.2.37) is the equivariance of the momentum map, namely

$$\xi_X f_Y(p) = \langle \mu(p), [X, Y] \rangle = \langle -\mathrm{ad}^*_X \mu(p), Y \rangle, \tag{1.2.40}$$

and so $\xi_X \mu(p) = -\mathrm{ad}^*_X \mu(p)$, which can be integrated as

$$\mu(g \cdot p) = \mathrm{Ad}^*_g \mu(p). \tag{1.2.41}$$

In simple words, the momentum map intertwines the Hamiltonian action of G on the symplectic manifold $\mathscr{P}$ with the action of G on the dual Lie algebra $\mathfrak{g}^*$ (coadjoint action). The geometric picture for this statement is that an orbit on $\mathscr{P}$ is mapped by μ into an orbit in $\mathfrak{g}^*$ (co-adjoint orbit).

According to Marsden and Weinstein [44], if an Hamiltonian action is proper and free, the restriction of the symplectic form ω of $\mathscr{P}$ to $\mathscr{P}_{red}$ defines a symplectic structure on the reduced manifold, which is then the phase space of the reduced dynamical system. The symplectic reduction follows the same line of the Poisson reduction previously presented. In the Hamiltonian case the constraints are given by the components of the momentum map $\mu(p) \in \mathfrak{g}^*$, and are classified into first-class and second-class following Dirac. The definition of the Dirac bracket on the constrained surface is given by (1.2.33), where $\mathcal{M}$ should be substituted by μ.

1.2.2 Heisenberg double

It is known that the relativistic Calogero-Moser model (also known as Ruijsennars-Schneider model) of N interacting particles in one dimension is an integrable system and that it can be obtained via a Hamiltonian reduction of a dynamical system having as phase space the cotangent bundle of the Lie group $G = \mathrm{GL}(N, \mathbb{C})$ (see [3]). Starting from this result, that will be discussed to some detail in the next sections, we introduce a deformation of the cotangent bundle of a Lie group to a symplectic manifold going under the name of Heisenberg double of a Poisson-Lie group G. The reason for studying such deformation is that the Heisenberg double of $G = \mathrm{GL}(N, \mathbb{C})$ is the initial phase space for the Poisson reduction that leads to the N-particles RS model with hyperbolic potential.
Given a Lie group G such that its Lie algebra $\mathfrak{g}$ is factorizable[6], the Heisenberg double $D_+(G)$ is a symplectic manifold given by the direct product $G \times G$ equipped with the (non-degenerate) Poisson structure among the coordinates $(x, y) \in G \times G$:

$$\begin{aligned} \{x_1, x_2\} &= -\left(\tfrac{1}{2} r x_1 x_2 + x_1 x_2 \tfrac{1}{2} r\right), \\ \{y_1, y_2\} &= -\left(\tfrac{1}{2} r y_1 y_2 + y_1 y_2 \tfrac{1}{2} r\right), \\ \{x_1, y_2\} &= -\left(r_+ x_1 y_2 + x_1 y_2 r_+\right), \\ \{y_1, x_2\} &= -\left(r_- y_1 x_2 + y_1 x_2 r_-\right), \end{aligned} \tag{1.2.42}$$

where the subscript indexes label the corresponding matrix spaces $x_1 = x \otimes \mathbb{1}$, $x_2 = \mathbb{1} \otimes x$. The interpretation of $D_+(G)$ as a deformation of the cotangent bundle $T^*G \simeq G \times \mathfrak{g}$ requires the introduction of the following factorization, valid for almost every element[7] of $D_+(G)$:

$$(x, y) = (\mathcal{L}_+, \mathcal{L}_-)(g^{-1}, g^{-1}) = (\mathcal{L}_+ g^{-1}, \mathcal{L}_- g^{-1}) . \tag{1.2.43}$$

Here $(\mathcal{L}_+, \mathcal{L}_-)$ is the representative of an element from G^* corresponding in the embedding $G^* \hookrightarrow G \times G$, which at the infinitesimal level is given by the decomposition of the dual Lie algebra element ℓ into two Lie algebra elements (ℓ_+, ℓ_-) explained in (1.2.9). Similarly, (g, g) is an image of $g \in G$ under the diagonal embedding $G \hookrightarrow G \times G$. The matrix elements of $\mathcal{L}_\pm$ and g give a new system of generators of the coordinate ring of the double. They are rational functions of x and y with singularities at those points where factorization (1.2.43) fails. In terms of this new

[6] This means that there exist a solution $\hat{r}$ of the CYBE, such that $\hat{r}_{12} + \hat{r}_{21}$ defines a non-degenerate ad-invariant scalar product on $\mathfrak{g}^*$. Concretely we will have $\hat{r} = r_+$ and $\hat{r}_{12} + \hat{r}_{21} = C_{12}$.

[7] For our treatment D is assumed to be connected and simply connected. We multiply $(\mathcal{L}_+, \mathcal{L}_-)$ by the inverse $(g, g)^{-1}$ so that to have the standard definition of the right action of G on a manifold which in the present case is D.

coordinates system, the Poisson structure of the Heisenberg double is given by the usual brackets of G^*

$$\begin{aligned} \{\mathcal{L}_{+1}, \mathcal{L}_{+2}\} &= -\tfrac{1}{2}[r, \mathcal{L}_{+1}\mathcal{L}_{+2}]\,, \qquad \{\mathcal{L}_{+1}, \mathcal{L}_{-2}\} = -[r_+, \mathcal{L}_{+1}\mathcal{L}_{-2}]\,, \\ \{\mathcal{L}_{-1}, \mathcal{L}_{-2}\} &= -\tfrac{1}{2}[r, \mathcal{L}_{-1}\mathcal{L}_{-2}]\,, \qquad \{\mathcal{L}_{-1}, \mathcal{L}_{+2}\} = -[r_-, \mathcal{L}_{-1}\mathcal{L}_{+2}]\,, \end{aligned} \tag{1.2.44}$$

together with the usual Sklyanin brackets for the Poisson-Lie group G

$$\{g_1, g_2\} = [r, g_1 g_2]\,,$$

and the mixed brackets between elements of G and G^*, which make the structure non-degenerate:

$$\{\mathcal{L}_{+1}, g_2\} = \mathcal{L}_{+1} g_2 r_+\,, \qquad \{\mathcal{L}_{-1}, g_2\} = \mathcal{L}_{-1} g_2 r_-\,. \tag{1.2.45}$$

The subgroup $G^* \subset D_+(G)$, as well as G, is a Poisson-Lie subgroup, its Poisson structure given by (1.2.44). The Poisson-Lie group G acts on G^* by dressing transformations [40]. Modeling G^* over G, these transformations take the form of the adjoint action[8]

$$\mathcal{L} \to h\mathcal{L}h^{-1}\,, \qquad h \in G\,, \tag{1.2.46}$$

and they are Poisson maps of the Semenov-Tian-Shansky bracket provided the Poisson-Lie structure on G is given by (1.2.5). The non-abelian moment map of this action is $\mathcal{L}$. It is well known that the symplectic leaves of (1.2.44) coincide with the orbits of (1.2.46).

Adjoint action In order to complete the picture for reduction, we consider that the Poisson-Lie group G acts on its Heisenberg double with a Poisson action. In order to write it we introduce a new coordinate system on the double which will be widely used in the next chapters

$$A = \mathcal{L} = \mathcal{L}_+\mathcal{L}_-^{-1}\,, \;\; B = \mathcal{L}_+ g \mathcal{L}_-^{-1}\,. \tag{1.2.47}$$

In this paragraph we will deal with the following action of the group G on its Heisenberg double

$$(A, B) \longrightarrow (hAh^{-1}, hBh^{-1})\,. \tag{1.2.48}$$

This action is Poisson, and its non-abelian momentum map is given by $(\mathcal{M}_+, \mathcal{M}_-)$: $D_+(G) \to G^*$

$$\mathcal{M}_+ = \mathcal{L}_+\mathcal{L}'_+\,, \quad \mathcal{M}_- = \mathcal{L}_-\mathcal{L}'_-\,,$$

where we used also the primed factorization

$$(x, y) = (g', g')(\mathcal{L}_+^{-1}, \mathcal{L}_-^{\prime -1}) = (\mathcal{L}_+, \mathcal{L}_-)(g^{-1}, g^{-1})\,. \tag{1.2.49}$$

[8]This is in fact the coadjoint action of G on G^*.

The Poisson brackets between the components of the matrices $\mathcal{M}_+$ and $\mathcal{M}_-$ are inherited form those of the double, and read

$$\begin{aligned}\{\mathcal{M}_{+1},\mathcal{M}_{+2}\} &= -\tfrac{1}{2}[r,\mathcal{M}_{+1}\mathcal{M}_{+2}]\,, \quad \{\mathcal{M}_{+1},\mathcal{M}_{-2}\} = -[r_+,\mathcal{M}_{+1}\mathcal{M}_{-2}]\,,\\ \{\mathcal{M}_{-1},\mathcal{M}_{-2}\} &= -\tfrac{1}{2}[r,\mathcal{M}_{-1}\mathcal{M}_{-2}]\,, \quad \{\mathcal{M}_{-1},\mathcal{M}_{+2}\} = -[r_-,\mathcal{M}_{-1}\mathcal{M}_{+2}]\,.\end{aligned} \tag{1.2.50}$$

which are the Semenov-Tian-Shanky brackets. Indeed, in the embedding formalism $\mathcal{M} \in G$

$$\mathcal{M} = \mathcal{M}_+(\mathcal{M}_-)^{-1} = \mathcal{L}_+ x^{-1} y \mathcal{L}_-^{-1}\,, \tag{1.2.51}$$

such brackets take the Semenov-Tian-Shansky form

$$\{\mathcal{M}_1,\mathcal{M}_2\} = -r_+\mathcal{M}_1\mathcal{M}_2 - \mathcal{M}_1\mathcal{M}_2 r_- + \mathcal{M}_1 r_- \mathcal{M}_2 + \mathcal{M}_2 r_+ \mathcal{M}_1\,. \tag{1.2.52}$$

Taking $X \in \mathfrak{g}$, one can compute the infinitesimal actions

$$\xi_X \mathcal{L} = \langle X, \{\mathcal{M},\mathcal{L}\} \star \mathcal{M}^{-1}\rangle = -[X,\mathcal{L}]\,, \tag{1.2.53}$$

and

$$\xi_X g = \langle X, \{\mathcal{M},g\} \star \mathcal{M}^{-1}\rangle = -[\mathrm{Ad}^*_{\mathcal{L}^{-1}} X, g]\,, \tag{1.2.54}$$

which are indeed the infinitesimal forms of (1.2.48).

Relation to the cotangent bundle Having advanced into the structure of the Heisenberg double, we can now explain in which sense this phase space can be viewed as a deformation of the cotangent bundle T^*G.
The formula $\mathcal{L} = \mathcal{L}_+\mathcal{L}_-^{-1}$ gives an embedding $G^* \hookrightarrow G$ and, alternatively, having $\mathcal{L} \in G$ the components $\mathcal{L}_\pm$ are found by solving the factorization problem in G for which we assume a unique solution. The Poisson structure of D_+ in terms of generators $(\mathcal{L}, g)$ is then

$$\begin{aligned}\frac{1}{\varkappa}\{\mathcal{L}_1,\mathcal{L}_2\} &= -r_+\mathcal{L}_1\mathcal{L}_2 - \mathcal{L}_1\mathcal{L}_2 r_- + \mathcal{L}_1 r_- \mathcal{L}_2 + \mathcal{L}_2 r_+ \mathcal{L}_1\,,\\ \frac{1}{\varkappa}\{\mathcal{L}_1,g_2\} &= g_2\,\mathcal{L}_{+1} C_{12} \mathcal{L}_{-1}^{-1}\,,\\ \frac{1}{\varkappa}\{g_1,g_2\} &= -[r,g_1 g_2]\,.\end{aligned} \tag{1.2.55}$$

Since a re-scaling of the Poisson bracket is always possible, we introduced here the parameter $\varkappa \in \mathbb{C}$, which enters the Poisson brackets as a non-trivial deformation parameter, if we assume that the coordinate functions also exhibit some non-trivial scaling with $\varkappa$. Most importantly, a connection to the Poisson structure of the cotangent bundle arises in the limit $\varkappa \to 0$ provided we assume the following behavior of $\mathcal{L}_\pm$ in this limit

$$\mathcal{L}_\pm = \mathbb{1} + \varkappa \ell_\pm + \ldots\,, \quad \ell_\pm = r_\pm \ell\,,$$

while g remains unchanged. In this scaling limit

$$\mathcal{L} = \mathbb{1} + \varkappa\ell + \ldots\,, \qquad \mathcal{M} = \mathbb{1} - \varkappa\, g(\ell g^{-1} - \ell) + \ldots = \mathbb{1} - \varkappa\mu + \ldots \tag{1.2.56}$$

and the Poisson structure (1.2.55) turns into

$$\begin{aligned} \{g_1, g_2\} &= 0 \\ \{\ell_1, g_2\} &= C_{12} g_2 \\ \{\ell_1, \ell_2\} &= \frac{1}{2}[C_{12}, \ell_1 - \ell_2]\,, \end{aligned}$$

which define the symplectic structure of T^*G. Thus, formulae (1.2.55) are deformed counterparts of the Poisson structure of the cotangent bundle (in the left parametrization).

The idea of constructing integrable many-body systems via symplectic (Hamiltonian) reduction goes back to the Kazhdan-Konstant-Steinberg paper [45], where the Calogero-Moser models with rational and trigonometric potentials have been obtained from $T^*\mathfrak{g}$ and T^*G, respectively. In the next two chapters we show the Poisson reduction techniques applied to the Heisenberg double of a Lie group of matrices $G = \mathrm{GL}(N, \mathbb{C})$ in order to obtain the Ruijsenaars-Schneider (RS) model with hyperbolic potential. Once this system is obtained one can take the degenerate limit to the RS rational model or to the Calogero-Moser hyperbolic model by tuning in a suitable way the deformation parameters. In particular we will present results about the quantization of the system and its higher-rank realization (or "spin model").

It is important to remark here that in the following we will deal with holomorphic integrable systems, defined on a complex algebraic manifold $\mathscr{P}$ (the phase space) with an associated non-degenerate closed holomorphic $(2,0)$-form ω (the symplectic form) and an abelian sub-variety of $\mathscr{P}$, Lagrangian with respect to ω. In this context the complex canonical variables p_i and q^i are treated as holomorphic (complex) coordinates on $\mathscr{P}$. Such a setup can simplify crucially the reduction techniques, then once the reduction is performed and an algebraic integrable system is constructed, one can impose suitable reality conditions, compatible with natural physical requirements, such as positivity of the Hamiltonian, etc.

Chapter 2
Quantum Hyperbolic Ruijsenaars-Schneider model

2.1 Introduction

The Ruijsenaars-Schneider (RS) models [18, 21] continue to provide an outstanding theoretical laboratory for the study of various aspects of Liouville integrability, both at the classical and quantum level, see, for instance, [46–50]. Also, new interesting applications of these models were recently found in conformal field theories [20].

In this chapter we study some aspects related to the quantum integrability of the RS model with the hyperbolic potential. The definition of quantum integrability relies on the existence of a quantization map which maps a complete involutive family of classical integrals of motion into a set of commuting operators on a Hilbert space. In general, there are different ways to choose a functional basis for this involutive family which is mirrored by the ring structure of the corresponding commuting operators. In particular, a classical integrable structure, most conveniently encoded into a Lax pair (L, M), produces a set of canonical integrals which are simply the eigenvalues of the Lax matrix. Their commutativity relies on the existence of the classical r-matrix [15]. Provided this matrix exists one can build up different classical involutive families represented, for instance, by elementary symmetric functions of the eigenvalues of L or, alternatively, by traces $\mathrm{Tr}L^k$ for $k \in \mathbb{Z}$. Concerning the particular class of the RS hyperbolic models, the quantization of a family of elementary symmetric functions associated to a properly chosen L is well known and given by the Macdonald operators [21, 51]. In this chapter we conjecture the quantum analogues of $\mathrm{Tr}L^k$ built up in terms of the same L-operator that is used to generate Macdonald operators through the determinant type formulae [52, 53]. In fact there appear two commuting families $I_k^{\pm}$ that are given by the quantum trace formulae

$$I_k^{\pm} = \mathrm{Tr}_{12}\left(C_{12}^{\tau_2} L_1 \bar{R}_{21}^{\tau_2} R_{\pm 12}^{\tau_2} L_1 \ldots L_1 \bar{R}_{21}^{\tau_2} R_{\pm 12}^{\tau_2} L_1\right) ,$$

as quantization of the classical integrals $\mathrm{Tr}L^k$. In particular, R and $\bar{R}$ are two quantum dynamical R-matrices that depend rationally on the variables $\mathcal{Q}_i = e^{q_i}$, where q_i, $i = 1, \ldots, N$ are coordinates, and satisfy a system of equations of Yang-Baxter type. Also, R is a parametric solution of the standard quantum Yang-Baxter equation.[1] Departing from $I_k^{\pm}$ and introducing $q = e^{-\hbar}$, we then find that these integrals are related to the Macdonald operators $\mathcal{S}_k$ through the q-deformed analogues of the determinant formulae that in the classical case relate the coefficients of characteristic polynomial of L with invariants constructed out of $\text{Tr}L^k$. The commutativity of $I_k^{\pm}$ and their relation to Macdonald operators has been checked by explicit computation for sufficiently large values of N.

We arrive to this expression for $I_k^{\pm}$ through the following chain of arguments. It is known that the Calogero-Moser models and their RS generalizations can be obtained at the classical level through the Hamiltonian or Poisson reduction applied to a system exhibiting free motion on one of the suitably chosen initial finite- or infinite-dimensional phase spaces [45–47, 54–56]. For instance, the RS model with the rational potential is obtained by the Hamiltonian reduction of the cotangent bundle $T^*G = G \times \mathfrak{g}$, where G ia Lie group and $\mathfrak{g}$ is its Lie algebra. In [57] the corresponding reduction was developed for the Lie group $G = \text{GL}(N, \mathbb{C})$ by employing a special parametrization for the Lie algebra-valued element $\ell = TQT^{-1} \in \mathfrak{g}$, where Q is a diagonal matrix and T is an element of the Frobenius group $F \subset G$. An analogous parametrization is used for the group element $g = UP^{-1}T^{-1} \in G$, where U is Frobenius and P is diagonal. If one writes $Q_i = q_i$ and $P_i = \exp p_i$, then (p_i, q_i) is a system of canonical variables with the Poisson bracket $\{p_i, q_j\} = \delta_{ij}$. In the new variables the Poisson structure of the cotangent bundle is then described in terms of the triangular dynamical matrix r satisfying the classical Yang-Baxter equation (CYBE) and of another matrix $\bar{r}$. The cotangent bundle is easily quantized, in particular, the algebra of quantum T-generators is $T_1T_2 = T_2T_1R_{12}$ and its consistency is guaranteed by the fact that the matrix R, being a quantization of r, is triangular, $R_{12}R_{21} = \mathbb{1}$, and obeys the quantum Yang-Baxter equation. The quantum L-operator is then introduced as $L = T^{-1}gT$ and it is an invariant under the action of F. In [57] the same formula for I_k as given above[2] was derived by eliminating from the commuting operators $\text{Tr}g^k = \text{Tr}TL^kT^{-1}$ the element T.

To build up the hyperbolic RS model, one can start from the Heisenberg double associated to a Lie group G. As a manifold, the Heisenberg double is $G \times G$ and it has a well-defined Poisson structure being a deformation of the one on T^*G [40]. However, an attempt to repeat the same steps of the reduction procedure meets an obstacle: since the action of G on the Heisenberg double is Poisson, rather than Hamiltonian, the Poisson bracket of two Frobenius invariants, $\{L_1, L_2\}$, is not closed, i.e. it is not expressed via L's alone. Moreover, for the same reason, the Poisson bracket $\{p_i, p_j\}$ does not vanish on the Heisenberg double. On the other hand, a part of the non-abelian moment map generates second class constraints and to find the Poisson structure on the reduced manifold one has to resort to the Dirac bracket

[1] For the definition of other quantities, see the main text.
[2] In the rational case there is only one family, $R_{\pm 12} \to R_{12}$.

construction.[3] In this chapter we work out the Dirac brackets for Frobenius invariants and show in detail how the cancellation of the non-invariant terms happens on the constraint surface. This leads to the canonical set of brackets for the degrees of freedom (p_i, q_i) on the reduced manifold, the physical phase space of the RS model. However, continuing along the same path as in the rational case [57] does not seem to yield $\{T, L\}$ and $\{T, T\}$ brackets. The variable T is not invariant with respect to the stability subgroup of the moment map and computation of such brackets requires fixing a gauge, which makes the whole approach rather obscure. Moreover, the very simple and elegant bracket $\{L_1, L_2\}$ emerging on the reduced phase space looks the same as in the rational case, with one exception: now the r-matrix r_{12} entering this bracket is not skew-symmetric, i.e. $r_{12} \neq r_{21}$. We then find a quantization of r_{12}: a simple quantum R-matrix R_+ satisfying $R_{+12}R_{-21} = \mathbb{1}$, where R_{-12} is another solution of the quantum Yang-Baxter equation. In the absence of the triangular property for R_{+12}, assuming, for instance, the same algebra for T's as in the rational case - that is $T_1T_2 = T_2T_1R_{+12}$ - would be inconsistent. Thus, at this point we simply conjecture that the integrals of the hyperbolic model have absolutely the same form as in the rational case, with the exception that the rational R-matrices are replaced by their hyperbolic analogues, which we explicitly find. That this conjecture yields integrals of motion can then be verified by tedious but direct computation and indeed holds true. Working out explicit expressions for these integrals for small numbers N of particles we find the determinant formulae relating these integrals to the standard basis of Macdonald operators. The rest of the chapter is devoted to the model whose formulation includes the spectral parameter. Neither for the rational nor for the hyperbolic case the spectral parameter is actually needed to demonstrate their Liouville integrability, but its introduction leads to interesting algebraic structures and clarifies the origin of the shifted Yang-Baxter equation [58] and its scale-violating solutions.

The chapter is organized as follows. In the next section we show how to obtain the hyperbolic RS model by the Poisson reduction of the Heisenberg double. This includes the derivation of the Poisson algebra of the Lax matrix via the Dirac bracket construction. We also introduce the spectral parameter and build up the theory based on spectral parameter-dependent (baxterized) r-matrices. We also describe a freedom in the definition of r-matrices that does not change the Poisson algebra of L's. In section 2.3 we consider the corresponding quantum theory. Finding the hyperbolic quantum R-matrices $R_\pm$ and $\bar{R}$, we conjecture our main formula for the quantum integrals $I_k^\pm$ and explain how it is related to the basis of the Macdonald operators. The rest of the section is devoted to the quantum baxterized R-matrices and the quantum L-operator algebra. We show that in spite of the fact that the constant R-matrices satisfy the usual system of quantum Yang-Baxter equations, their baxterized counterparts instead obey its modification that involves rescalings

[3] In [58] this problem was avoided by looking at those entries of L only that commute with the second class constraints.

of the spectral parameter with the quantum deformation parameter $q = e^{-\hbar}$. Some technical details are relegated to two appendices. All considerations are done in the context of holomorphic integrable systems.

2.2 The classical model from reduction

2.2.1 Moment map and Lax matrix

We start with recalling the construction of the classical Heisenberg double associated to the group $G = \mathrm{GL}(N, \mathbb{C})$. Let the entries of matrices $A, B \in G$ generate the coordinate ring of the algebra of functions on the Heisenberg double. The Heisenberg double is a Poisson manifold with the following Poisson brackets

$$\begin{aligned} \{A_1, A_2\} &= \varkappa\,(-r_-\, A_1 A_2 - A_1 A_2\, r_+ + A_1\, r_- A_2 + A_2\, r_+ A_1)\ , \\ \{A_1, B_2\} &= \varkappa\,(-r_-\, A_1 B_2 - A_1 B_2\, r_- + A_1\, r_- B_2 + B_2\, r_+ A_1)\ , \\ \{B_1, A_2\} &= \varkappa\,(-r_+\, B_1 A_2 - B_1 A_2\, r_+ + B_1\, r_- A_2 + A_2\, r_+ B_1)\ , \\ \{B_1, B_2\} &= \varkappa\,(-r_-\, B_1 B_2 - B_1 B_2\, r_+ + B_1\, r_- B_2 + B_2\, r_+ B_1)\ , \end{aligned} \tag{2.2.1}$$

where the parameter $\varkappa$ in this chapter will be set to be one. Here and elsewhere in the chapter we use the standard notation where the indexes 1 and 2 denote the different matrix spaces. The matrix quantities $r_\pm$ are the following r-matrices

$$\begin{aligned} r_+ &= +\frac{1}{2}\sum_{i=1}^{N} E_{ii}\otimes E_{ii} + \sum_{i<j}^{N} E_{ij}\otimes E_{ji}\,, \\ r_- &= -\frac{1}{2}\sum_{i=1}^{N} E_{ii}\otimes E_{ii} - \sum_{i>j}^{N} E_{ij}\otimes E_{ji}\,, \end{aligned} \tag{2.2.2}$$

In the following we also need the split Casimir

$$C = \sum_{i,j=1}^{N} E_{ij}\otimes E_{ji}\,, \tag{2.2.3}$$

whose action on the tensor product $\mathbb{C}^N \otimes \mathbb{C}^N$ is a permutation. In these formulae E_{ij} stand for the standard matrix units. The r-matrices (2.2.2) satisfy the classical Yang-Baxter equation (CYBE) and have the following properties: $r_+ - r_- = C$ and $r_{\pm 21} = -r_{\mp 12}$. Moreover the matrix $r = \frac{1}{2}(r_+ + r_-)$, is a skew-symmetric split solution to the modified classical Yang-Baxter equation.

The variables (A, B) can be interpreted as a pair of monodromies of a flat connection on a punctured torus around its two fundamental cycles [59]. The monodromies are not gauge invariants as they undergo an adjoint action of the group of residual gauge transformations which coincides with G

$$A \to hAh^{-1}\,, \qquad B \to hBh^{-1}\,. \tag{2.2.4}$$

If G is a Poisson-Lie group with the Sklyanin bracket

$$\{h_1, h_2\} = -\varkappa[r_\pm, h_1 h_2]\,, \tag{2.2.5}$$

then the transformations (2.2.4) are the Poisson maps for the structure (2.2.1). The non-abelian moment map $\mathcal{M}$ of this action is given by

$$\mathcal{M} = BA^{-1}B^{-1}A \tag{2.2.6}$$

and it generates the following infinitesimal transformations of (A, B)

$$\begin{aligned} \{\mathcal{M}_1, A_2\} &= -(r_+\mathcal{M}_1 - \mathcal{M}_1 r_-)A_2 + A_2(r_+\mathcal{M}_1 - \mathcal{M}_1 r_-)\,, \\ \{\mathcal{M}_1, B_2\} &= -(r_+\mathcal{M}_1 - \mathcal{M}_1 r_-)B_2 + B_2(r_+\mathcal{M}_1 - \mathcal{M}_1 r_-)\,. \end{aligned} \tag{2.2.7}$$

The Poisson algebra between the entries of $\mathcal{M}$ is given by the Semenov-Tian-Shansky bracket

$$\frac{1}{\varkappa}\{\mathcal{M}_1, \mathcal{M}_2\} = -r_+\mathcal{M}_1\mathcal{M}_2 - \mathcal{M}_1\mathcal{M}_2 r_- + \mathcal{M}_1 r_- \mathcal{M}_2 + \mathcal{M}_2 r_+ \mathcal{M}_1\,. \tag{2.2.8}$$

In the rest of this chapter we will set $\varkappa$ to one.

The Poisson algebra (2.2.1) has two obvious involutive subalgebras – one is generated by $\mathrm{Tr}A^k$ and the other by $\mathrm{Tr}B^k$, where $k \in \mathbb{Z}$. There is yet another involutive family which will play an essential role the next chapter, namely,

$$H_k = \mathrm{Tr}(BA^{-1})^k = \mathrm{Tr}(A^{-1}B)^k\,, \quad k \in \mathbb{Z}\,. \tag{2.2.9}$$

The fact that $\{H_k, H_m\} = 0$ for any $k, m \in \mathbb{Z}$ can be verified by direct computation. A deeper observation is that the map

$$A \to A\,, \quad B \to BA^{-1}\,, \tag{2.2.10}$$

is a canonical transformation, i.e. under this map the Poisson structure (2.2.1) remains invariant. Note that all the involutive families mentioned above are generated by invariants of the adjoint action (2.2.4).

To perform the reduction, we fix the moment map to the following value

$$\mathcal{M} = \exp(\gamma n)\,, \tag{2.2.11}$$

where n is the Lie algebra element

$$n = \mathbf{e} \otimes \mathbf{e}^\tau - \mathbb{1}\,, \tag{2.2.12}$$

where $\mathbf{e}$ is an N-dimensional vector with all its entries equal to unity, $\mathbf{e}^\tau = (1, \ldots, 1)$, and γ is a formal parameter which will be eventually interpreted as the coupling constant. Fixing this value of the moment map is motivated a posteriori by the fact that the dynamical model arising on the reduced space will have a close connection to the RS model we are after.

We are thus led to find all A, B that solve the following matrix equation

$$BA^{-1}B^{-1}A = e^{-\gamma}\mathbb{1} - e^{-\gamma}\frac{1-e^{N\gamma}}{N}\mathbf{e}\otimes\mathbf{e}^{\tau}\,, \tag{2.2.13}$$

where on the right-hand side we worked out the explicit form of the exponential $\exp(\gamma n)$. In the following we adopt the concise notation

$$\theta = e^{-\gamma}\,, \qquad \beta = -e^{-\gamma}\frac{1-e^{N\gamma}}{N} = -\frac{\theta}{N}(1-\theta^{-N})\,. \tag{2.2.14}$$

To solve (2.2.13), we introduce a convenient representation for A and B:

$$A = T\mathcal{Q}T^{-1}\,, \tag{2.2.15}$$

$$B = UP^{-1}T^{-1}\,. \tag{2.2.16}$$

Here $\mathcal{Q}$ and P are two diagonal matrices and $T, U \in G$ are two Frobenius matrices, i.e. they satisfy the Frobenius condition

$$T\mathbf{e} = \mathbf{e}\,, \qquad U\mathbf{e} = \mathbf{e} \tag{2.2.17}$$

and, therefore, belong to the Frobenius subgroup F of G.

Introducing $W = T^{-1}U \in F$, equation (2.2.13) takes the form

$$\mathcal{Q}^{-1}W^{-1}\mathcal{Q}W = \theta\mathbb{1} + \beta\mathbf{e}\otimes\mathbf{e}^{\tau}U\,, \tag{2.2.18}$$

where we used the fact that $U \in F$. Furthermore, we write

$$\mathcal{Q}^{-1}W^{-1}\mathcal{Q} - \theta W^{-1} = \beta\mathbf{e}\otimes\mathbf{e}^{\tau}UW^{-1} = \beta\mathbf{e}\otimes\mathbf{e}^{\tau}T\,.$$

This equation can be elementary solved for W^{-1} and we get

$$W^{-1} = \sum_{i,j=1}^{N}\frac{\beta}{\mathcal{Q}_i^{-1} - \theta\mathcal{Q}_j^{-1}}\frac{c_j}{\mathcal{Q}_j}E_{ij}\,, \tag{2.2.19}$$

where we introduced $c_j = (\mathbf{e}^{\tau}T)_j$. The condition $W^{-1} \in F$ gives a set of equations to determine the coefficients c_j:

$$\sum_{j=1}^{N} V_{ij}\frac{c_j}{\mathcal{Q}_j} = 1\,, \qquad \forall i\,.$$

Here V is a Cauchy matrix with entries

$$V_{ij} = \frac{\beta}{\mathcal{Q}_i^{-1} - \theta\mathcal{Q}_j^{-1}}\,.$$

We apply the inverse of V

$$V_{ij}^{-1} = \frac{1}{\beta(\mathcal{Q}_i^{-1} - \theta^{-1}\mathcal{Q}_j^{-1})}\frac{\prod_{a=1}^{N}(\theta\mathcal{Q}_i^{-1} - \mathcal{Q}_a^{-1})}{\prod_{a\neq i}^{N}(\mathcal{Q}_i^{-1} - \mathcal{Q}_a^{-1})}\frac{\prod_{a=1}^{N}(\theta^{-1}\mathcal{Q}_j^{-1} - \mathcal{Q}_a^{-1})}{\prod_{a\neq j}^{N}(\mathcal{Q}_j^{-1} - \mathcal{Q}_a^{-1})}\,,$$

to obtain the following formula for the coefficients c_j

$$c_j = \mathcal{Q}_j \sum_{j=1}^{N} V_{ij}^{-1} = N\frac{1-\theta}{1-\theta^N} \prod_{a\neq j}^{N} \frac{\mathcal{Q}_j - \theta\mathcal{Q}_a}{\mathcal{Q}_j - \mathcal{Q}_a} . \tag{2.2.20}$$

Finally, inverting W^{-1} we find W itself

$$W_{ij}(\mathcal{Q}) = \frac{\mathcal{Q}_i}{c_i}(V^{-1})_{ij} = \frac{\prod\limits_{a\neq i}^{N}(\mathcal{Q}_j^{-1} - \theta\mathcal{Q}_a^{-1})}{\prod\limits_{a\neq j}^{N}(\mathcal{Q}_j^{-1} - \mathcal{Q}_a^{-1})} . \tag{2.2.21}$$

It is obvious, that eq.(2.2.13) becomes equivalent to the following two constraints

$$U = TW(\mathcal{Q}) , \qquad \mathbf{e}^\tau T = c^\tau , \tag{2.2.22}$$

where $T, U \in F$, and the quantities $W(\mathcal{Q})$, $c(\mathcal{Q})$ are given by (2.2.21) and (2.2.20), respectively. Any solution of $\mathbf{e}^\tau T = c^\tau$ can be constructed as $T = hT_0$, where T_0 is a particular solution of this equation and h is a Frobenius group element which satisfies the additional constraint $\mathbf{e}^\tau h = \mathbf{e}^\tau$. In fact, the subgroup of $\digamma \subset F \subset G$ determined by the conditions

$$\digamma = \{h \in G : \ h\mathbf{e} = \mathbf{e}, \quad \mathbf{e}^\tau h = \mathbf{e}^\tau\} , \tag{2.2.23}$$

constitutes the stability group[4] of the moment map determined by the element n. Note that $\dim_{\mathbb{C}} F = N^2 - N$ and $\dim_{\mathbb{C}} \digamma = (N-1)^2$.

Now we can define a family of G-invariant dynamical systems[5] taking the combination $L = W(\mathcal{Q})P^{-1}$ as their Lax matrix. Explicitly,

$$L = \sum_{i,j=1}^{n} \frac{(1-\theta)\mathcal{Q}_i}{\mathcal{Q}_i - \theta\mathcal{Q}_j} \prod_{a\neq j}^{N} \frac{\theta\mathcal{Q}_j - \mathcal{Q}_a}{\mathcal{Q}_j - \mathcal{Q}_a} P_j^{-1} E_{ij} . \tag{2.2.24}$$

After specifying the proper reality conditions, this L becomes nothing else but the Lax matrix of the RS family with the hyperbolic potential. Note that on the constrained surface the A, B-variables take the following form

$$A(P, \mathcal{Q}, h) = hT_0 Q T_0^{-1} h^{-1} , \qquad B(P, \mathcal{Q}, h) = hT_0 L T_0^{-1} h^{-1} , \quad h \in \digamma .$$

The reduced phase space can be singled out by fixing the gauge to, for instance, $h = 1$. Its dimension over $\mathbb{C}$ is $2N^2 - (N^2-1) - \dim_{\mathbb{C}} \digamma = 2N$.

[4] We do not include in $\digamma$ the one dimensional dilatation subgroup $\mathbb{C}^* \simeq \{h \in G : \ h = c\mathbb{1}, \ c \neq 0\}$, because its action on the phase space is not faithful.

[5] The systems whose Hamiltonians are invariant under the action of G.

2.2.2 Poisson structure on the reduced phase space

Now we turn to the analysis of the Poisson structure of the reduced phase space. We find from (2.2.1) the following formula

$$\{\mathcal{Q}_j, B\} = B \sum_{kl} T_{lj} \mathcal{Q}_j T^{-1}_{jk} E_{lk} \,. \tag{2.2.25}$$

Next, we need to determine the bracket between $\mathcal{Q}_j$ and P_i. We have

$$\{\mathcal{Q}_j, P_i\} = \frac{\delta P_i}{\delta A_{mn}}\{\mathcal{Q}_j, A_{mn}\} + \frac{\delta P_i}{\delta B_{mn}}\{\mathcal{Q}_j, B_{mn}\} \,.$$

Here the first bracket on the right-hand side vanishes because all $\mathcal{Q}_j$ commute with A.[6] To compute the second bracket, we consider the variation of $B = UP^{-1}T^{-1}$

$$U^{-1}\delta B\, TP = U^{-1}\delta U - P^{-1}\delta P \,.$$

Note that this formula does not include the variation δT. This is because T is solely determined by A, so so is its variation. The condition $\delta U \mathbf{e} = 0$ allows one to find

$$\frac{\delta P_i}{\delta B_{mn}} = -\sum_r P_i U^{-1}_{im} (TP)_{nr} \,.$$

We thus have

$$\{\mathcal{Q}_j, P_i\} = -\sum_r P_i U^{-1}_{im} (TP)_{nr} (BT)_{mj} \mathcal{Q}_j T^{-1}_{jn} = -\mathcal{Q}_i P_i \delta_{ij} \,, \tag{2.2.26}$$

and similarly one can check the bracket $\{\mathcal{Q}_i, \mathcal{Q}_j\} = 0$. These formulae suggests to employ the exponential parametrisation for both P and $\mathcal{Q}$, that is, to set

$$P_i = \exp p_i \,, \qquad \mathcal{Q}_i = \exp q_i \,,$$

where (p_i, q_i) satisfy the canonical relations $\{p_i, q_j\} = \delta_{ij}$.

An $\mathcal{F}$-invariant extension of the Lax matrix away from the reduced phase space is naturally given by the following Frobenius invariant

$$L = T^{-1} B T \,, \tag{2.2.27}$$

where T is an element of the Frobenius group entering the factorization (2.2.15). The Poisson bracket of $\mathcal{Q}_j$ with components of L is computed in a straightforward manner

$$\{\mathcal{Q}_j, L_{mn}\} = \{\mathcal{Q}_j, (T^{-1}BT)_{mn}\} = \sum_p (T^{-1}B)_{mp} \sum_{kl} T_{lj} \mathcal{Q}_j T^{-1}_{jk} (E_{lk})_{ps} T_{sn} = L_{mn} \mathcal{Q}_n \delta_{jn} \,,$$

[6] The spectral invariants of A are central in the Poisson subalgebra of A, the latter is described by the Semenov-Tian-Shansky bracket [40] given by the first line in (2.2.1).

which is perfectly compatible with the form (2.2.24) of the Lax matrix on the reduced space. In matrix form the previous formula reads as

$$\{\mathcal{Q}_1, L_2\} = \mathcal{Q}_1 L_2 \overline{C}_{12}\,, \qquad \bar{C}_{12} = \sum_{j=1}^{N} E_{jj} \otimes E_{jj}\,. \tag{2.2.28}$$

As to the brackets between the entries of L, this time they cannot be represented in terms of L alone but also involve T. Ultimately, such a structure is a consequence of the fact that the action of the Poisson-Lie group G on the phase space is Poisson rather than Hamiltonian, so that there is an obstruction for the Poisson bracket of two Frobenius invariants to also be such an invariant. In addition, computing the Dirac brackets of L one cannot neglect a non-trivial contribution from the second class constraints and, therefore, the analysis of the Poisson structure for L requires, as an intermediate step, to understand the nature of the constraints (2.2.13) imposed in the process of reduction. The same argument holds for the Poisson brackets between any of the Frobenius invariants $W = T^{-1}U$ and P, showing as a particular case that P_i's have a non-vanishing Poisson algebra on the Heisenberg double[7]. We save the details of the corresponding analysis for appendix A.2 and present here the final result for the Poisson bracket between the entries of the Lax matrix on the reduced phase space

$$\{L_1, L_2\} = r_{12} L_1 L_2 - L_1 L_2 \underline{r}_{12} + L_1 \bar{r}_{21} L_2 - L_2 \bar{r}_{12} L_1\,. \tag{2.2.29}$$

Clearly, the bracket (2.2.29) has the same form as the corresponding bracket for the rational RS model [57] albeit with new dynamical r-matrices for which we got the following explicit expressions [8]

$$\begin{aligned} r &= \sum_{i\neq j}^{N} \left(\frac{\mathcal{Q}_j}{\mathcal{Q}_{ij}} E_{ii} - \frac{\mathcal{Q}_i}{\mathcal{Q}_{ij}} E_{ij} \right) \otimes (E_{jj} - E_{ji})\,, \\ \bar{r} &= \sum_{i\neq j}^{N} \frac{\mathcal{Q}_i}{\mathcal{Q}_{ij}} (E_{ii} - E_{ij}) \otimes E_{jj}\,, \\ \underline{r} &= \sum_{i\neq j}^{N} \frac{\mathcal{Q}_i}{\mathcal{Q}_{ij}} (E_{ij} \otimes E_{ji} - E_{ii} \otimes E_{jj})\,, \end{aligned} \tag{2.2.30}$$

where we introduced the notation $\mathcal{Q}_{ij} = \mathcal{Q}_i - \mathcal{Q}_j$. This structure can be obtained as well after the computation of the Dirac brackets of W and P on the reduced phase space

$$\{W_1, W_2\} = [r_{12}, W_1 W_2] \tag{2.2.31}$$

[7] At the level of quantization, this fact prevents one from obtaining the quantum RS model starting from the algebra of the quantum Heisenberg double. Indeed, doing so one should later restore the canonical commutation relations of (P, Q) sub-algebra by imposing an analogue of the Dirac constraints at the quantum level.

[8] The quadratic and linear forms of the r-matrix structure for the RS model have been investigated in [60–64].

$$\{W_1, P_2\} = [\bar{r}_{12}, W_1] P_2 \tag{2.2.32}$$
$$\{P_1, P_2\} = 0\,, \tag{2.2.33}$$

using the decomposition $L = WP^{-1}$. Remarkably the imposition of Dirac constraints makes the Poisson subalgebra $\{P_i\}$ abelian, allowing the interpretation of components $p_i = \log P_i$ as particle momenta. Concerning the properties of the matrices (2.2.30) and the Lax matrix, we note the following: first, $\underline{r}$ is expressed via r and $\bar{r}$ as

$$\underline{r}_{12} = r_{12} + \bar{r}_{21} - \bar{r}_{12}\,. \tag{2.2.34}$$

Second, the matrix r is degenerate, $\det r = 0$, and it obeys the characteristic equation $r^2 = -r$. Moreover, in contrast to the rational case [57], r is not symmetric, rather it has the property

$$r_{12} + r_{21} = C_{12} - \mathbb{1} \otimes \mathbb{1}\,. \tag{2.2.35}$$

Third, it is a matter of straightforward calculation to verify that the Lax matrix (2.2.24) obeys the Poisson algebra relations (2.2.29), provided the bracket between the components of $\mathcal{Q}$ and P is given by (2.2.26),(2.2.33). Finally, as a consequence of the Jacobi identities, the matrices (2.2.30) satisfy a system of equations of Yang-Baxter type. In particular, for r one has just the standard CYBE

$$[r_{12}, r_{13}] + [r_{12}, r_{23}] + [r_{13}, r_{23}] = 0\,. \tag{2.2.36}$$

In addition, there are two more equations involving r and $\bar{r}$

$$\begin{aligned} &[\bar{r}_{12}, \bar{r}_{13}] + \{\bar{r}_{12}, p_3\} - \{\bar{r}_{13}, p_2\} = 0\,, \\ &[r_{12}, \bar{r}_{13}] + [r_{12}, \bar{r}_{23}] + [\bar{r}_{13}, \bar{r}_{23}] + \{r_{12}, p_3\} = 0\,. \end{aligned} \tag{2.2.37}$$

The matrix $\underline{r}$ satisfies the classical analogue of the Gervais-Neveu-Felder equation [65, 66]

$$[\underline{r}_{12}, \underline{r}_{13}] + [\underline{r}_{12}, \underline{r}_{23}] + [\underline{r}_{13}, \underline{r}_{23}] + \{\underline{r}_{12}, p_3\} - \{\underline{r}_{13}, p_2\} + \{\underline{r}_{23}, p_1\} = 0\,. \tag{2.2.38}$$

It is elementary to verify that the quantities

$$I_k = \mathrm{Tr} L^k \tag{2.2.39}$$

are in involution with respect to (2.2.30). This property of I_k is, of course, inherited from the same property for $\mathrm{Tr} B^k$ on the original phase space (2.2.1). We refer to (2.2.39) as the *classical trace formula.*

2.2.3 Introduction of a spectral parameter

Here we introduce a Lax matrix depending on a spectral parameter and discuss the associated algebraic structures and an alternative way to exhibit commuting integrals.

To start with, we point out one important identity satisfied by the Lax matrix (2.2.24). According to the moment map equation (2.2.18), we have

$$\theta \mathcal{Q}^{-1} W \mathcal{Q} = W \Big[\mathbb{1} + \frac{\beta}{\theta} \mathbf{e} \otimes \mathbf{e}^{\tau} U \Big]^{-1}, \tag{2.2.40}$$

The inverse on the right-hand side of the last expression can be computed with the help of the well-known Sherman-Morrison formula and we get

$$\theta \mathcal{Q}^{-1} W \mathcal{Q} = W \Big[\mathbb{1} - \frac{1-\theta^N}{N} \mathbf{e} \otimes \mathbf{e}^{\tau} U \Big] = W - \frac{1-\theta^N}{N} \mathbf{e} \otimes c^{\tau} W, \tag{2.2.41}$$

where we used the fact that W is a Frobenius matrix, so that $W\mathbf{e} = \mathbf{e}$. Here the vector c has components (2.2.20) and satisfies the relation $\mathbf{e}^{\tau} T = c^{\tau}$. Multiplying both sides of (2.2.22) with P^{-1} we obtain the following identity

$$\theta \mathcal{Q}^{-1} L \mathcal{Q} = L - \frac{1-\theta^N}{N} \mathbf{e} \otimes c^{\tau} L, \tag{2.2.42}$$

for the Lax matrix (2.2.24).

Evidently, we can consider

$$L' = \theta \mathcal{Q}^{-1} L \mathcal{Q} \tag{2.2.43}$$

as another Lax matrix since the evolution equation of the latter is of the Lax form

$$\dot{L}' = [M', L'], \qquad M' = \mathcal{Q}^{-1} M \mathcal{Q} - \mathcal{Q}^{-1} \dot{\mathcal{Q}}, \tag{2.2.44}$$

where M is defined by the Hamiltonian flow of L. Note that one can add to M' any function of L' without changing the evolution equation for L', which defines a class of equivalent M''s. Now, it turns out that due to the special dependence of L on the momentum, M and M' fall in the same equivalence class. To demonstrate this point, it is enough to consider the simplest Hamiltonian $H = \mathrm{Tr}\, L$ for which the matrix M is given by

$$M = \sum_{i \neq j}^{N} \frac{\mathcal{Q}_j}{\mathcal{Q}_{ij}} L_{ij} (E_{ii} - E_{ij}), \tag{2.2.45}$$

It follows from (2.2.28) that for the flow generated by this Hamiltonian

$$\mathcal{Q}^{-1} \dot{\mathcal{Q}} = \mathcal{Q}^{-1} \{H, \mathcal{Q}\} = -\sum_{i=1}^{N} L_{ii} E_{ii}.$$

Therefore,

$$M' = \mathcal{Q}^{-1} M \mathcal{Q} - \mathcal{Q}^{-1} \dot{\mathcal{Q}} = \sum_{i \neq j}^{N} \frac{\mathcal{Q}_j}{\mathcal{Q}_{ij}} L_{ij} \Big(E_{ii} - \frac{\mathcal{Q}_j}{\mathcal{Q}_i} E_{ij} \Big) + \sum_{i=1}^{N} L_{ii} E_{ii}.$$

Taking into account that $\mathcal{Q}_j/(\mathcal{Q}_{ij}\mathcal{Q}_i) = 1/\mathcal{Q}_{ij} - 1/\mathcal{Q}_i$, we then find

$$M' = \sum_{i\neq j}^{N} \frac{\mathcal{Q}_j}{\mathcal{Q}_{ij}} L_{ij}(E_{ii} - E_{ij}) + \sum_{i\neq j}^{N} \mathcal{Q}_i^{-1} L_{ij} \mathcal{Q}_j E_{ij} + \sum_{i=1}^{N} L_{ii} E_{ii} = M + L' .$$

Hence, M' is in the same equivalence class as M and, therefore, we can take the dynamical matrix M to be the same for both L and L'.

The above observation motivates us to introduce a Lax matrix depending on a spectral parameter just as a linear combination of L and L'. Namely, we can define

$$L(\lambda) = L - \frac{1}{\lambda} L' , \tag{2.2.46}$$

where $\lambda \in \mathbb{C}$ is the spectral parameter. The matrix $L(\lambda)$ has a pole at zero and the original matrix L is obtained from $L(\lambda)$ in the limit $\lambda \to \infty$, in particular,

$$H = \lim_{\lambda\to\infty} \mathrm{Tr} L(\lambda) = \mathrm{Tr} L . \tag{2.2.47}$$

The evolution equation for $L(\lambda)$ must, therefore, be of the form

$$\dot{L}(\lambda) = \{H, L(\lambda)\} = [M, L(\lambda)] , \tag{2.2.48}$$

where M is the expression (2.2.45).

The next task is to compute the Poisson brackets between the components of (2.2.46). We aim at finding a structure similar to (2.2.29), namely,

$$\begin{aligned} \{L_1(\lambda), L_2(\mu)\} = r_{12}(\lambda,\mu) L_1(\lambda) L_2(\mu) - L_1(\lambda) L_2(\mu) \underline{r}_{12}(\lambda,\mu) \\ + L_1(\lambda) \bar{r}_{21}(\mu) L_2(\mu) - L_2(\mu) \bar{r}_{12}(\lambda) L_1(\lambda) , \end{aligned} \tag{2.2.49}$$

where $r(\lambda,\mu)$, $\underline{r}(\lambda,\mu)$ and $\bar{r}(\lambda)$ are some spectral-parameter-dependent r-matrices. We show how to derive these r-matrices in appendix A.2. Our considerations are essentially based on the identity (2.2.42). To state the corresponding result, we need the matrix

$$\sigma_{12} = \sum_{i\neq j}^{N} (E_{ii} - E_{ij}) \otimes E_{jj} . \tag{2.2.50}$$

The minimal solution[9] for the spectral-dependent r-matrices realising the Poisson algebra (2.2.49) is then found to be

$$\begin{aligned} r_{12}(\lambda,\mu) &= \frac{\lambda r_{12} + \mu r_{21}}{\lambda - \mu} + \frac{\sigma_{12}}{\lambda - 1} - \frac{\sigma_{21}}{\mu - 1} , \\ \bar{r}_{12}(\lambda) &= \bar{r}_{12} + \frac{\sigma_{12}}{\lambda - 1} , \\ \underline{r}_{12}(\lambda,\mu) &= r_{12}(\lambda,\mu) + \bar{r}_{21}(\mu) - \bar{r}_{12}(\lambda) = \frac{\lambda \underline{r}_{12} + \mu \underline{r}_{21}}{\lambda - \mu} . \end{aligned} \tag{2.2.51}$$

[9] The explanation of its minimal character will be given later.

The matrices r and $\underline{r}$ are skew-symmetric in the sense that

$$r_{12}(\lambda,\mu) = -r_{21}(\mu,\lambda)\,, \qquad \underline{r}_{12}(\lambda,\mu) = -\underline{r}_{21}(\mu,\lambda)\,. \tag{2.2.52}$$

Further, one can establish implications of the Jacobi identity satisfied by (2.2.49) for these r-matrices. Introducing the dilatation operator acting on the spectral parameter

$$D_\lambda = \lambda\frac{\partial}{\partial\lambda}\,,$$

we find that the r-matrix $r(\lambda,\mu)$ does not satisfy the standard CYBE but rather the following modification thereof

$$\begin{aligned}&[r_{12}(\lambda,\mu), r_{13}(\lambda,\tau)] + [r_{12}(\lambda,\mu), r_{23}(\mu,\tau)] + [r_{13}(\lambda,\tau), r_{23}(\mu,\tau)] = \\ &\quad = -(D_\lambda + D_\mu)r_{12}(\lambda,\mu) + (D_\lambda + D_\tau)r_{13}(\lambda,\tau) - (D_\tau + D_\mu)r_{23}(\mu,\tau)\,.\end{aligned} \tag{2.2.53}$$

Following [54], we refer to (2.2.53) as the shifted classical Yang-Baxter equation. This equation can be rewritten in the form of the standard Yang-Baxter equation

$$[\hat{r}_{12}(\lambda,\mu), \hat{r}_{13}(\lambda,\tau)] + [\hat{r}_{12}(\lambda,\mu), \hat{r}_{23}(\mu,\tau)] + [\hat{r}_{13}(\lambda,\tau), \hat{r}_{23}(\mu,\tau)] = 0\,.$$

for the matrix differential operator

$$\hat{r}(\lambda,\mu) = r(\lambda,\mu) - D_\lambda + D_\mu\,. \tag{2.2.54}$$

There are also two more equations involving the matrix $\bar{r}$

$$\begin{aligned}&[r_{12}(\lambda,\mu), \bar{r}_{13}(\lambda) + \bar{r}_{23}(\mu)] + [\bar{r}_{13}(\lambda), \bar{r}_{23}(\mu)] + P_3^{-1}\{r_{12}(\lambda,\mu), P_3\} = \\ &\quad = -(D_\lambda + D_\mu)r_{12}(\lambda,\mu) + (D_\lambda\bar{r}_{13}(\lambda) - D_\mu\bar{r}_{23}(\mu))\end{aligned} \tag{2.2.55}$$

and

$$\begin{aligned}&[\bar{r}_{12}(\lambda), \bar{r}_{13}(\lambda)] + P_3^{-1}\{\bar{r}_{12}(\lambda), P_3\} - P_2^{-1}\{\bar{r}_{13}(\lambda), P_2\} = \\ &\quad = -D_\lambda(\bar{r}_{12}(\lambda) - \bar{r}_{13}(\lambda)).\end{aligned} \tag{2.2.56}$$

One can check that relations (2.2.53), (2.2.55) and (2.2.56) guarantee the fulfilment of the Jacobi identity for the brackets (2.2.28) and (2.2.29). Note that $\underline{r}$ is scale-invariant: $(D_\lambda + D_\mu)\underline{r}(\lambda,\mu) = 0$, implying that it depends on the ratio λ/μ. This property does not hold, however, for r and $\bar{r}$.

The solution we found for the spectral-dependent dynamical r-matrices is minimal in the sense that there is a freedom to modify these r-matrices without changing the Poisson bracket (2.2.49). First of all, there is a trivial freedom of shifting r and $\underline{r}$ as

$$r_{12} \to r_{12} + f(\lambda/\mu)\mathbb{1}\otimes\mathbb{1}\,, \quad \underline{r}_{12} \to \underline{r}_{12} + f(\lambda/\mu)\mathbb{1}\otimes\mathbb{1}\,, \tag{2.2.57}$$

where f is an arbitrary function of the ratio of the spectral parameters. This redefinition affects neither the bracket (2.2.29) nor equations (2.2.53), (2.2.55), (2.2.56).

Second, one can redefine $\bar{r}$ and r as

$$\begin{aligned} r(\lambda,\mu) &\to r(\lambda,\mu) - s(\lambda)\otimes \mathbb{1} + \mathbb{1}\otimes s(\mu) \\ \bar{r}(\lambda) &\to \bar{r}(\lambda) - s(\lambda)\otimes \mathbb{1}\,, \end{aligned} \tag{2.2.58}$$

where $s(\lambda)$ is an arbitrary matrix function of the spectral parameter. Owing to the structure of the bracket (2.2.49) this redefinition of the r-matrices produces no effect on the latter, as $\underline{r}$ remains unchanged, while the matrix s decouples from the right-hand side of the LL bracket (see (2.2.49)). For generic $s(\lambda)$, redefinition (2.2.58) affects[10], however, equations (2.2.53), (2.2.55), (2.2.56). In particular, there exists a choice of $s(\lambda)$ which turns the shifted Yang-Baxter equations for $\bar{r}$ and r into the conventional ones, where the derivative terms on the right hand side of (2.2.53), (2.2.55) and (2.2.56) are absent. One can take, for instance,

$$s(\lambda) = \frac{1}{N}\sum_{i\neq j}^{N}\frac{\mathcal{Q}_i}{\mathcal{Q}_{ij}}(E_{ii}-E_{ij}) + \frac{1}{\lambda-1}\frac{1}{N}\sum_{i\neq j}^{N}(E_{ii}-E_{ij})\,. \tag{2.2.59}$$

With the last choice the matrix $\bar{r}(\lambda)$ becomes

$$\bar{r}(\lambda) = \frac{1}{\lambda-1}\sum_{i\neq j}\frac{\lambda\mathcal{Q}_i-\mathcal{Q}_j}{\mathcal{Q}_{ij}}(E_{ii}-E_{ij})\otimes\Big(E_{jj}-\frac{1}{N}\mathbb{1}\Big)\,,$$

while for $r(\lambda,\mu)$ one finds

$$r_{12}(\lambda,\mu) = \frac{\lambda r_{12}^m + \mu r_{21}^m}{\lambda-\mu} + \frac{\rho_{12}}{\lambda-1} - \frac{\rho_{21}}{\mu-1}\,, \tag{2.2.60}$$

where

$$\rho_{12} = \sum_{i\neq j}(E_{ii}-E_{ij})\otimes\Big(E_{jj}-\frac{1}{N}\mathbb{1}\Big)$$

and the modified r-matrix is

$$\begin{aligned} r_{12}^m = &\sum_{i\neq j}^{N}\Big(\frac{\mathcal{Q}_j}{\mathcal{Q}_{ij}}E_{ii} - \frac{\mathcal{Q}_i}{\mathcal{Q}_{ij}}E_{ij}\Big)\otimes(E_{jj}-E_{ji}) \\ &- \frac{1}{N}\sum_{i\neq j}\frac{\mathcal{Q}_i}{\mathcal{Q}_{ij}}(E_{ii}-E_{ij})\otimes\mathbb{1} + \frac{1}{N}\sum_{i\neq j}\frac{\mathcal{Q}_i}{\mathcal{Q}_{ij}}\mathbb{1}\otimes(E_{ii}-E_{ij})\,. \end{aligned} \tag{2.2.61}$$

The modified r-matrix still solves the CYBE and obeys the same relation (2.2.35).

There is no symmetry operating on r-matrices that would allow one to remove the scale-non-invariant terms from these matrices. Clearly, the r-matrices satisfying the shifted version of the Yang-Baxter equations have a simpler structure than their cousins subjected to the standard Yang-Baxter equations. This fact plays an important role when it comes to quantization of the corresponding model and the

[10] An example of such a redefinition that does not affect the shifted Yang-Baxter equation corresponds to the choice $s(\lambda) = f(\lambda)\mathbb{1}$, where f is an arbitrary function of λ.

associated algebraic structures. We also point out that the r-matrices we found here through considerations in appendix A.2 also follow from the elliptic r-matrices of [54] upon their hyperbolic degeneration, albeit modulo the shift symmetries (2.2.57) and (2.2.58).

From (2.2.49) one then finds

$$\{\mathrm{Tr}_1 L_1(\lambda), L_2(\mu)\} = [\mathrm{Tr}_1 L_1(\lambda)(r_{12}(\lambda,\mu) + \bar{r}_{21}(\mu)), L_2(\mu)]\,,$$

which, upon taking the limit $\lambda \to \infty$, yields the Lax equation (2.2.48) with M given by (2.2.45). The conserved quantities are, therefore, $I_k(\lambda) = \mathrm{Tr}L(\lambda)^k$, $k \in \mathbb{Z}$. The determinant $\det(L(\lambda) - \zeta\mathbb{1})$, which generates $I_k(\lambda)$ in the power series expansion over the parameter ζ, defines the classical spectral curve

$$\det(L(\lambda) - \zeta\mathbb{1}) = 0\,, \qquad \zeta, \lambda \in \mathbb{C}\,. \tag{2.2.62}$$

2.3 Quantum model

2.3.1 Quantum Heisenberg double

At the classical level we obtained the hyperbolic RS model by means of the Poisson reduction of the Heisenberg double. It is therefore natural to start with the quantum analogue of the Heisenberg double. The Poisson algebra (2.2.1) can be straightforwardly quantized in the standard spirit of deformation theory. We thus introduce an associative unital algebra generated by the entries of matrices A, B modulo the relations [67]

$$\begin{aligned}
\mathcal{R}_-^{-1} A_2 \mathcal{R}_+ A_1 &= A_1 \mathcal{R}_-^{-1} A_2 \mathcal{R}_+\,,\\
\mathcal{R}_-^{-1} B_2 \mathcal{R}_+ A_1 &= A_1 \mathcal{R}_-^{-1} B_2 \mathcal{R}_-\,,\\
\mathcal{R}_+^{-1} A_2 \mathcal{R}_+ B_1 &= B_1 \mathcal{R}_-^{-1} A_2 \mathcal{R}_+\,,\\
\mathcal{R}_-^{-1} B_2 \mathcal{R}_+ B_1 &= B_1 \mathcal{R}_-^{-1} B_2 \mathcal{R}_+\,,
\end{aligned} \tag{2.3.1}$$

and they can be regarded as the quantization of the Poisson relations (2.2.1). The quantum $\mathcal{R}$-matrices here are defined as follows: first, we consider the following well-known solution of the quantum Yang-Baxter equation

$$\mathcal{R} = \sum_{i\neq j}^{n} E_{ii} \otimes E_{jj} + e^{\hbar/2} \sum_{i=1}^{n} E_{ii} \otimes E_{ii} + (e^{\hbar/2} - e^{-\hbar/2}) \sum_{i>j}^{n} E_{ij} \otimes E_{ji}\,. \tag{2.3.2}$$

Using this $\mathcal{R}$ one can construct two more solutions $\mathcal{R}_\pm$ of the quantum Yang-Baxter equation, namely,

$$\mathcal{R}_{+12} = \mathcal{R}_{21}\,, \qquad \mathcal{R}_{-12} = \mathcal{R}_{12}^{-1}\,. \tag{2.3.3}$$

These solutions are, therefore, related as

$$\mathcal{R}_{+21}\mathcal{R}_{-12} = \mathbb{1}\,, \tag{2.3.4}$$

and they also satisfy

$$\mathcal{R}_+ - \mathcal{R}_- = (e^{\hbar/2} - e^{-\hbar/2})\, C\,, \tag{2.3.5}$$

where C is the split Casimir. In the limit $\hbar \to 0$ the matrices $R_\pm$ expand as

$$\mathcal{R}_\pm = 1 + \hbar r_\pm + \mathcal{O}(\hbar)\,, \tag{2.3.6}$$

where $r_\pm$ are the classical r-matrices (2.2.2). Further, we point out that $\hat{\mathcal{R}}_\pm = C\mathcal{R}_\pm$ satisfy the Hecke condition

$$\widehat{\mathcal{R}}^2_\pm \mp (e^{\hbar/2} - e^{-\hbar/2})\hat{\mathcal{R}}_\pm - \mathbb{1} = \big(\hat{\mathcal{R}}_\pm - e^{\pm\hbar/2}\mathbb{1}\big)\big(\hat{\mathcal{R}}_\pm + e^{\mp\hbar/2}\mathbb{1}\big) = 0\,. \tag{2.3.7}$$

The first, or alternatively, the last line in (2.3.1) is a set of defining relations for the corresponding subalgebra that describes a quantization of the Semenov-Tian-Shansky bracket, the latter has a set of Casimir functions generated by $C_k = \mathrm{Tr}A^k$. In the quantum case an analogue $\mathrm{Tr}A^k$ can be defined by means of the quantum trace formula

$$C_k = \mathrm{Tr}_q A^k \;=\; \mathrm{Tr}(DA^k)\,, \quad q \,=\, e^{-\hbar}\,,$$

where D is a diagonal matrix $D = \mathrm{diag}(q, q^2, \ldots, q^n)$. The elements C_k are central in the subalgebra generated by A. Indeed, by successively using the permutation relations for A, one gets

$$A_2 \mathcal{R}_+ A_1^k \mathcal{R}_+^{-1} = \mathcal{R}_- A_1^k \mathcal{R}_-^{-1} A_2\,.$$

We then multiply both sides of this relation by D_1 and take the trace in the first matrix space

$$A_2 \mathrm{Tr}_1\,(D_1 \mathcal{R}_+ A_1^k \mathcal{R}_+^{-1}) = \mathrm{Tr}_1\,(D_1 \mathcal{R}_- A_1^k \mathcal{R}_-^{-1}) A_2\,.$$

It remains to notice that $\mathrm{Tr}_1\,(D_1 \mathcal{R}_+ A_1^k \mathcal{R}_+^{-1}) = \mathrm{Tr}_1\,(D_1 \mathcal{R}_- A_1^k \mathcal{R}_-^{-1}) = \mathrm{Tr}_q A^k \cdot \mathbb{1}$, so that

$$A\, \mathrm{Tr}_q A^k = \mathrm{Tr}_q A^k\, A\,, \tag{2.3.8}$$

i.e. $\mathrm{Tr}_q A^k$ is central in the subalgebra generated by A. Analogously, the $I_k = \mathrm{Tr}_q B^k$ are central in the algebra generated by B and, in particular, the I_k form a commutative family.

In principle, we can start with (2.3.1) and try to develop a proper parametrization of the (A, B) generators suitable for reduction. It is an interesting path that should lead to understanding how to implement the Dirac constraints at the quantum level. We will find, however, a short cut to the algebra of the quantum L-operator.

2.3.2 Quantum R-matrices and the L-operator

An alternative route to the quantum R-matrices and to the corresponding L-operator algebra is based on the observation that in the classical theory, the Poisson brackets between the entries of the Lax matrix have the same structure (2.2.29) for both rational and hyperbolic cases. As a consequence, the equations satisfied by the classical rational and hyperbolic r-matrices are also the same. This should also be applied to the equations obeyed by the corresponding quantum R-matrices. We thus assume that the matrices R and $\bar{R}$ for the hyperbolic RS model satisfy the system of equations

$$R_{12}R_{13}R_{23} = R_{23}R_{13}R_{12} \tag{2.3.9}$$

and

$$R_{12}\bar{R}_{13}\bar{R}_{23} = \bar{R}_{23}\bar{R}_{13}P_3R_{12}P_3^{-1}, \tag{2.3.10}$$

$$\bar{R}_{12}P_2\bar{R}_{13}P_2^{-1} = \bar{R}_{13}P_3\bar{R}_{12}P_3^{-1}\,. \tag{2.3.11}$$

and have the standard semi-classical limit where they match the classical r-matrices (2.2.30). Here and in the following (Q_i, P_i) satisfy the quantum algebra

$$Q_iQ_j = Q_jQ_i \qquad P_iP_j = P_jP_i \qquad [P_i, Q_j] = (e^{\hbar} - 1)Q_jP_j\delta_{ij}\,, \tag{2.3.12}$$

being the standard quantization of the Poisson algebra on the reduced phase space (2.2.26),(2.2.33). In fact, it is not difficult to guess a proper solution for these R-matrices based on the analogy with the rational case. For R we can take

$$R = \exp \hbar r\,, \tag{2.3.13}$$

where r is given on the first line of (2.2.30). In the following we adopt the notation $R_+ = R$. Since the classical r-matrix satisfies the property $r^2 = -r$, the exponential in (2.3.13) can be easily evaluated and we find

$$R_+ = \mathbb{1} + (1-q)\sum_{i\neq j}^{N}\left(\frac{\mathcal{Q}_j}{\mathcal{Q}_{ij}}E_{ii} - \frac{\mathcal{Q}_i}{\mathcal{Q}_{ij}}E_{ij}\right)\otimes(E_{jj} - E_{ji})\,. \tag{2.3.14}$$

A direct check shows that (2.3.14) is a solution of (2.3.9).

In comparison to the rational model, a new feature is that there exists yet another solution R_- of the Yang-Baxter equation, namely,

$$R_- = \mathbb{1} - (1-q^{-1})\sum_{i\neq j}^{N}(E_{ii} - E_{ij})\otimes\left(\frac{\mathcal{Q}_i}{\mathcal{Q}_{ij}}E_{jj} - \frac{\mathcal{Q}_j}{\mathcal{Q}_{ij}}E_{ji}\right)\,. \tag{2.3.15}$$

These solutions are related as

$$R_{+21}R_{-12} = \mathbb{1}\,, \tag{2.3.16}$$

i.e. precisely in the same way as their non-dynamical counterparts, cf. (2.3.4). Furthermore, the matrices $R_\pm$ satisfy equation

$$R_+ - qR_- = (1-q)C\,. \tag{2.3.17}$$

They are also of Hecke type and the matrices $\hat{R}_\pm = CR_\pm$ have the following property

$$\big(\hat{R}_\pm - \mathbb{1}\big)\big(\hat{R}_\pm + q^{\pm 1}\mathbb{1}\big) = 0\,. \tag{2.3.18}$$

Concerning the generalization of equation (2.3.10) to the hyperbolic case, we can imagine two different versions - one involving R_+ and another R_-, that is,

$$R_{\pm 12}\bar{R}_{13}\bar{R}_{23} = \bar{R}_{23}\bar{R}_{13}P_3R_{\pm 12}P_3^{-1}, \tag{2.3.19}$$

It appears that there exists a unique matrix $\bar{R}$ which satisfies both these equations. It is given by

$$\bar{R} = \mathbb{1} - \sum_{i\neq j}^{N} \frac{q\mathcal{Q}_i - \mathcal{Q}_i}{q\mathcal{Q}_i - \mathcal{Q}_j}(E_{ii} - E_{ij}) \otimes E_{jj}\,. \tag{2.3.20}$$

and its inverse is

$$\bar{R}^{-1} = \mathbb{1} - (1-q)\sum_{i\neq j}^{N} \frac{\mathcal{Q}_i}{\mathcal{Q}_{ij}}(E_{ii} - E_{ij}) \otimes E_{jj}\,. \tag{2.3.21}$$

The matrix (2.3.20) also obeys (2.3.11),

$$\bar{R}_{12}P_2\bar{R}_{13}P_2^{-1} = \bar{R}_{13}P_3\bar{R}_{12}P_3^{-1}\,. \tag{2.3.22}$$

Introducing

$$\underline{R}_{12} = \bar{R}_{12}^{-1}R_{12}\bar{R}_{21}\,, \tag{2.3.23}$$

we find

$$\begin{aligned} \underline{R}_+ &= \mathbb{1} + (1-q)\sum_{i\neq j}^{N} \frac{\mathcal{Q}_i}{\mathcal{Q}_{ij}}(E_{ij}\otimes E_{ji} - E_{ii}\otimes E_{jj})\,, \\ \underline{R}_- &= \mathbb{1} - (1-q^{-1})\sum_{i\neq j}^{N} \frac{\mathcal{Q}_j}{\mathcal{Q}_{ij}}(E_{ij}\otimes E_{ji} - E_{ii}\otimes E_{jj})\,. \end{aligned} \tag{2.3.24}$$

These matrices satisfy the Gervais-Neveu-Felder equation

$$\underline{R}_{\pm 12}P_2^{-1}\underline{R}_{\pm 13}P_2\underline{R}_{\pm 23} = P_1^{-1}\underline{R}_{\pm 23}P_1\underline{R}_{\pm 13}P_3^{-1}\underline{R}_{\pm 12}P_3\,. \tag{2.3.25}$$

and are related to each other as

$$\underline{R}_{+21}\underline{R}_{-12} = \mathbb{1}\,. \tag{2.3.26}$$

They also have another important property, usually referred to as the zero weight condition [66],

$$[P_1P_2, \underline{R}_\pm] = 0\,. \tag{2.3.27}$$

Finally, the quantum L-operator is literally the same as its classical counterpart (2.2.24), of course with the natural replacement of p_i by the corresponding derivative

$$L = \sum_{i,j=1}^{N} \frac{\mathcal{Q}_i - \theta\mathcal{Q}_i}{\mathcal{Q}_i - \theta\mathcal{Q}_j}\, b_j \top_j E_{ij}\,, \qquad b_j \;=\; \prod_{a\neq j}^{N} \frac{\theta\mathcal{Q}_j - \mathcal{Q}_a}{\mathcal{Q}_j - \mathcal{Q}_a}\,, \tag{2.3.28}$$

where $\theta = e^{-\gamma}$ and $\top_j$ is the operator $\top_j = e^{-\hbar\frac{\partial}{\partial q_j}}$.[11] The operator $\top_i$ acts on smooth functions $f(\mathcal{Q}_1,\ldots,\mathcal{Q}_N)$ as

$$(\top_j f)(\mathcal{Q}_1,\ldots,\mathcal{Q}_N) = f(\mathcal{Q}_1,\ldots,q\mathcal{Q}_j\,,\ldots\mathcal{Q}_N)\,.$$

It is a straightforward exercise to check that this L-operator satisfies the algebraic relations

$$\begin{aligned} R_{+12}L_2\bar{R}_{12}^{-1}L_1 &= L_1\bar{R}_{21}^{-1}L_2\underline{R}_{+12}\,,\\ R_{-12}L_2\bar{R}_{12}^{-1}L_1 &= L_1\bar{R}_{21}^{-1}L_2\underline{R}_{-12}\,. \end{aligned} \tag{2.3.29}$$

with the R-matrices given by (2.3.14), (2.3.15), (2.3.20) and (2.3.24). The consistency of these relations follow from (2.3.16) and (2.3.26). One can alternatively derive equations (2.3.29) by direct quantization of (2.2.31)-(2.2.32), where the classical matrix is chosen to be r_{12} or, equivalently, $-r_{21}$

$$W_1W_2R_{\pm12} \;=\; R_{\pm12}W_2W_1\,, \tag{2.3.30}$$
$$W_1\bar{R}_{12}P_2 \;=\; \bar{R}_{12}P_2W_1\,, \tag{2.3.31}$$

whose consistency follows from the same R-matrices relations. The algebraic relation (2.3.30) is also known as the quantum Frobenius group condition [57].

Concerning commuting integrals, the Heisenberg double has a natural commutative family $I_k = \mathrm{Tr}_q B^k$. It is not clear, however, how these integrals can be expressed via L, because we are lacking an analogue of the quantum factorization formula $B = TLT^{-1}$, where T and L would be subjected to well-defined algebraic relations. Instead, what we could do is to conjecture the same formula as was obtained for quantum integrals in the rational case [57], where now the R-matrices are those of the hyperbolic model. Interestingly, the existence of two R-matrices, $R_\pm$, should give rise to two families of commuting integrals $I_k^\pm$. Borrowing the corresponding expression from the rational case [57], we conjecture the following quantum trace formulae

$$I_k^\pm = \mathrm{Tr}_{12}\left(C_{12}^{\tau_2}L_1\bar{R}_{21}^{\tau_2}R_{\pm12}^{\tau_2}L_1\ldots L_1\bar{R}_{21}^{\tau_2}R_{\pm12}^{\tau_2}L_1\right)\,, \tag{2.3.32}$$

as quantization of the classical integrals (2.2.39). In (2.3.32) the number k on the right-hand side gives a number of L_1's and τ_2 stands for the transposition in the second matrix space. In particular,

$$C_{12}^{\tau_2} = \sum_{i,j=1}^{N} E_{ij}\otimes E_{ij}$$

[11] In fact, $\top_j = P_j^{-1}$, we use $\top_j$ to signify that we talk about a particular representation for L.

is a one-dimensional projector and from (2.3.14), (2.3.15) and (2.3.20) we get

$$\bar{R}^{\tau_2}_{21}R^{\tau_2}_{+12} = \mathbb{1} + (1-q)\sum_{i,j}\frac{\mathcal{Q}_i}{\mathcal{Q}_i - q\mathcal{Q}_j}\,E_{ij}\otimes(E_{ij}-E_{jj})\,, \tag{2.3.33}$$

$$\bar{R}^{\tau_2}_{21}R^{\tau_2}_{-12} = \mathbb{1} + (1-q)\sum_{i,j}\left[\frac{\mathcal{Q}_j}{\mathcal{Q}_i - q\mathcal{Q}_j}\,E_{ij}\otimes(E_{ij}-E_{jj}) + \frac{1}{q}(E_{ii}-E_{ij})\otimes E_{jj}\right]. \tag{2.3.34}$$

Commutativity of $I^{\pm}_k$ is then verified by tedious but direct computation which we do not reproduce here, rather our goal is to present a formula which relates $I^{\pm}_k$ with the commuting family given by Macdonald operators.

We denote by $\{\mathcal{S}_k\}$ a commutative family of Macdonald operators, where

$$\mathcal{S}_k = \theta^{\frac{1}{2}k(k-1)}\sum_{\substack{J\subset\{1,\ldots,n\}\\ |J|=k}}\prod_{\substack{i\in J\\ j\notin J}}\frac{\theta\mathcal{Q}_i - \mathcal{Q}_j}{\mathcal{Q}_i - \mathcal{Q}_j}\prod_{i\in J}\top_i\,. \tag{2.3.35}$$

The Macdonald operators have the following generating function

$$:\det(L-\zeta\mathbb{1}):= \sum_{k=0}^{N}(-\zeta)^{N-k}\mathcal{S}_k\,,\qquad \mathcal{S}_0 = 1\,, \tag{2.3.36}$$

where ζ is a formal parameter, L is the Lax operator (2.3.28). Under the sign $::$ of normal ordering the operators p_j and q_j are considered as commuting and upon algebraic evaluation of the determinant all $\top_j$ are brought to the right. In the classical theory the normal ordering is omitted and the corresponding generating function yields classical integrals of motion that are nothing else but the spectral invariants of the Lax matrix.

We found an explicit formula that relates the families $\{I^{\pm}_k\}$ and $\mathcal{S}_k$. To present it, we need the notion of a q-number $[k]_q$ associated to an integer k

$$[k]_q = \sum_{n=0}^{k-1}q^n = \frac{1-q^k}{1-q}\,, \tag{2.3.37}$$

so that $[k]_1 = k$, which corresponds to the limit $\hbar\to 0$. Then $\mathcal{S}_k$ is expressed via I^{+}_m or I^{-}_m as

$$\mathcal{S}_k = \frac{1}{[k!]_{q^{\pm1}}}\begin{vmatrix} I^{\pm}_1 & [k-1]_{q^{\pm1}} & 0 & \cdots & 0\\ I^{\pm}_2 & I^{\pm}_1 & [k-2]_{q^{\pm1}} & \cdots & 0\\ \vdots & \vdots & . & \cdots & \vdots\\ I^{\pm}_{k-1} & I^{\pm}_{k-2} & . & \cdots & [1]_{q^{\pm1}}\\ I^{\pm}_k & I^{\pm}_{k-1} & . & \cdots & I^{\pm}_1 \end{vmatrix}. \tag{2.3.38}$$

These formulae can be inverted to express each integral $I_k^{\pm}$ as the determinant of a $k \times k$ matrix depending on $\mathcal{S}_j$, namely,

$$I_k^{\pm} = \begin{vmatrix} \mathcal{S}_1 & 1 & 0 & \cdots & 0 \\ [2]_{q^{\pm 1}}\mathcal{S}_2 & \mathcal{S}_1 & 1 & 0 & \cdots \\ \vdots & \vdots & \cdots & \cdots & 1 \\ [k]_{q^{\pm 1}}\mathcal{S}_k & \mathcal{S}_{k-1} & \mathcal{S}_{k-2} & \cdots & \mathcal{S}_1 \end{vmatrix} . \tag{2.3.39}$$

2.3.3 Spectral parameter and quantum L-operator

The quantum L-operator depending on the spectral parameter is naturally introduced as a normal ordered version of its classical counterpart

$$L(\lambda) = \frac{(1-\theta)}{\lambda} \sum_{i,j=1}^{N} \frac{\lambda \mathcal{Q}_i - \theta e^{-\hbar/2} \mathcal{Q}_j}{\mathcal{Q}_i - \theta \mathcal{Q}_j} b_j \top_j E_{ij} = L - \frac{\theta\, e^{\hbar/2}}{\lambda} \mathcal{Q}^{-1} L \mathcal{Q} \, , \tag{2.3.40}$$

where b_j are the same as in (2.3.28). This L-operator satisfies the following quadratic relation

$$R_{12}(\lambda,\mu) L_2(\mu) \bar{R}_{12}^{-1}(\lambda) L_1(\lambda) = L_1(\lambda) \bar{R}_{21}^{-1}(\mu) L_2(\mu) \underline{R}_{12}(\lambda,\mu) \, , \tag{2.3.41}$$

where

$$\underline{R}_{12}(\lambda,\mu) = \bar{R}_{12}^{-1}(\lambda) R_{12}(\lambda,\mu) \bar{R}_{21}(\mu) \, . \tag{2.3.42}$$

In (2.3.41) the quantum R-matrices are

$$\begin{aligned} R(\lambda,\mu) &= \frac{\lambda e^{\hbar/2} R_+ - \mu e^{-\hbar/2} R_-}{\lambda - \mu} - \frac{e^{\hbar/2} - e^{-\hbar/2}}{e^{\hbar/2}\lambda - 1} X_{12} + \frac{e^{\hbar/2} - e^{-\hbar/2}}{e^{-\hbar/2}\mu - 1} X_{21} \, . \\ \bar{R}(\lambda) &= \bar{R} - \frac{e^{\hbar} - 1}{e^{\hbar/2}\lambda - 1} X_{12} \, . \end{aligned} \tag{2.3.43}$$

Here R_+ and R_- are the solutions (2.3.14) and (2.3.15) of the quantum Yang-Baxter equation, $\bar{R}$ is (2.3.20) and we have introduced the matrix $X \equiv X_{12}$,

$$X = \sum_{i,j=1}^{N} E_{ij} \otimes E_{jj} \, . \tag{2.3.44}$$

This matrix satisfies a number of simple relations with $\bar{R}$ and $R_{\pm}$, which are

$$\bar{R} X = X \bar{R} \tag{2.3.45}$$

and

$$\begin{aligned} R_- X_{12} &= X_{12} R_- \, , \qquad & R_- X_{21} - X_{21} R_- &= (1-q^{-1})(X_{12} - X_{21}) \, , \\ R_+ X_{21} &= X_{21} R_+ \, , \qquad & R_+ X_{12} - X_{12} R_+ &= -(1-q)(X_{12} - X_{21}) \, . \end{aligned} \tag{2.3.46}$$

We also present the formula for the inverse of $\bar{R}(\lambda)$

$$\bar{R}(\lambda)^{-1} = \bar{R}^{-1} + \frac{e^{\hbar} - 1}{e^{\hbar/2}\lambda - e^{\hbar}} X_{12} \, . \tag{2.3.47}$$

With the help of this formula and (2.3.43) one can show that (2.3.42) boils down to

$$\underline{R}_{12}(\lambda,\mu) = \frac{\lambda e^{\hbar/2}\underline{R}_{+} - \mu e^{-\hbar/2}\underline{R}_{-}}{\lambda-\mu}\,, \tag{2.3.48}$$

where $\underline{R}_{\pm}$ are the same as given by (2.3.24). We note also the relation

$$R_{12}(\lambda,\mu)R_{21}(\mu,\lambda) = \underline{R}_{12}(\lambda,\mu)\underline{R}_{21}(\mu,\lambda) = \frac{(e^{\hbar/2}\lambda - e^{-\hbar/2}\mu)(e^{-\hbar/2}\lambda - e^{\hbar/2}\mu)}{(\lambda-\mu)^2}\mathbb{1}\,.$$

Finally, in addition to (2.3.42) there is one more relation between $R(\lambda,\mu)$ and $\underline{R}(\lambda,\mu)$, namely,

$$\underline{R}_{12}(\lambda,\mu) = P_1^{-1}\bar{R}_{21}(\mu)P_1R_{12}(\lambda,\mu)P_2^{-1}\bar{R}_{12}^{-1}(\lambda)P_2\,. \tag{2.3.49}$$

An interesting observation is that the combination

$$R^{\mathrm{YB}}(\lambda,\mu) = \frac{\lambda e^{\hbar/2}R_{+} - \mu e^{-\hbar/2}R_{-}}{\lambda-\mu}$$

solves the usual quantum Yang-Baxter equation with the spectral parameter. However, the full R-matrix in (2.3.43) differs from R^{YB} by the terms that violate scale invariance. As a result, this matrix obeys the shifted version of the quantum Yang-Baxter equation, namely,

$$R_{12}(\lambda,\mu)R_{13}(q\lambda,q\tau)R_{23}(\mu,\tau) = R_{23}(q\mu,q\tau)R_{13}(\lambda,\tau)R_{12}(q\lambda,q\mu)\,. \tag{2.3.50}$$

In addition, there are two more equations – the one involving both R and $\bar{R}$, and the other involving $\bar{R}$ only,

$$R_{12}(\lambda,\mu)\bar{R}_{13}(q\lambda)\bar{R}_{23}(\mu) = \bar{R}_{23}(q\mu)\bar{R}_{13}(\lambda)P_3R_{12}(q\lambda,q\mu)P_3^{-1}\,, \tag{2.3.51}$$

$$\bar{R}_{12}(\lambda)P_2\bar{R}_{13}(q\lambda)P_2^{-1} = \bar{R}_{13}(\lambda)P_3\bar{R}_{12}(q\lambda)P_3^{-1}\,. \tag{2.3.52}$$

It is immediately recognisable that equations (2.3.50), (2.3.51) and (2.3.52) are a quantum analogue (quantization) of the classical equations (2.2.53), (2.2.55) and (2.2.56), respectively. In the semi-classical expansion

$$R(\lambda,\mu) = \mathbb{1} + \hbar r(\lambda,\mu) + o(\hbar)\,, \quad \bar{R}(\lambda) = \mathbb{1} + \hbar r(\lambda) + o(\hbar) \tag{2.3.53}$$

the matrices (2.3.43) yield

$$\begin{aligned} r_{12}(\lambda,\mu) &= \frac{\lambda r_{12} + \mu r_{21}}{\lambda-\mu} + \frac{\sigma_{12}}{\lambda-1} - \frac{\sigma_{21}}{\mu-1} \\ &\qquad + \Big(\frac{1}{2}\frac{\lambda+\mu}{\lambda-\mu} - \frac{1}{\lambda-1} + \frac{1}{\mu-1}\Big)\mathbb{1}\otimes\mathbb{1}\,, \\ \bar{r}_{12}(\lambda) &= \bar{r}_{12} + \frac{\sigma_{12}}{\lambda-1} - \frac{\mathbb{1}\otimes\mathbb{1}}{\lambda-1}\,, \end{aligned}$$

which is different from the canonical classical r-matrices (2.2.51) by allowed symmetry shifts. Thus, (2.3.43) should be regarded as a quantization of the classical r-matrices satisfying the shifted Yang-Baxter equation. In this respect it is interesting to point out that the corresponding quantization of the r-matrices solving the usual CYBE remains unknown.

Finally, the algebra (2.3.41) should be completed by the following additional relations encoding the commutation properties of L with $\mathcal{Q}$

$$L_1\mathcal{Q}_2 = \mathcal{Q}_2 L_1 \theta_{12}\,, \quad \mathcal{Q}_1^{-1} L_2 = L_2 \mathcal{Q}_1^{-1}\theta_{12}\,, \tag{2.3.54}$$

where $\theta_{12} = \mathbb{1} - (1-q)\bar{C}_{12}$.

Now we derive a couple of important consequences of the algebraic relation (2.3.41). Namely, we establish the quantum Lax representation, similar to the rational case, and also prove the commutativity of the operators $\mathrm{Tr}L(\lambda)$ for different values of the spectral parameter.

Following considerations of the dynamics in the classical theory, we take $H = \lim\limits_{\lambda\to\infty} \mathrm{Tr}L(\lambda)$ as the Hamiltonian. From (2.3.41) we get

$$\mathrm{Tr}_1\Big[R_{21}(\mu,\lambda)L_1(\lambda)\bar{R}_{21}^{-1}(\mu)\Big]\, L_2(\mu) = L_2(\mu)\,\mathrm{Tr}_1\Big[\bar{R}_{12}^{-1}(\lambda)L_1(\lambda)\underline{R}_{21}(\mu,\lambda)\Big]\,, \tag{2.3.55}$$

where (2.3.48) was used. A straightforward computation reveals that the traces on the left and the right-hand side of the last expression are equal and that, for instance,

$$e^{\hbar/2}\mathrm{Tr}_1\Big[\bar{R}_{12}^{-1}(\lambda)L_1(\lambda)\underline{R}_{21}(\mu,\lambda)\Big] = \mathrm{Tr}L(\lambda)\,\mathbb{1} - M(\lambda,\mu)\,, \tag{2.3.56}$$

where

$$\begin{aligned} M(\lambda,\mu) &= (e^{\hbar}-1)\frac{\lambda}{\lambda-\mu}\frac{\mu-e^{-\hbar/2}}{\lambda-e^{\hbar/2}}\,L(\lambda) \\ &\quad + \frac{e^{\hbar}-1}{\lambda-e^{\hbar/2}}\sum_{i\neq j}^{N}\frac{\lambda e^{-\hbar}\mathcal{Q}_j - e^{-\hbar/2}\mathcal{Q}_i}{\mathcal{Q}_i - e^{-\hbar}\mathcal{Q}_j}L_{ij}(\lambda)(E_{ii}-E_{ij})\,. \end{aligned} \tag{2.3.57}$$

Thus, equation (2.3.55) turns into

$$\mathrm{Tr}L(\lambda)L(\mu) - L(\mu)\mathrm{Tr}L(\lambda) = [M(\lambda,\mu), L(\mu)]\,. \tag{2.3.58}$$

From (2.3.57) we, therefore, derive the quantum-mechanical operator M

$$\begin{aligned} M = \lim_{\lambda\to\infty} M(\lambda,\mu) &= (e^{\hbar}-1)\sum_{i\neq j}^{N}\frac{e^{-\hbar}\mathcal{Q}_j}{\mathcal{Q}_i - e^{-\hbar}\mathcal{Q}_j}L_{ij}(E_{ii}-E_{ij}) \\ &= (e^{\hbar}-1)\sum_{i\neq j}^{N} L_{ij}\frac{\mathcal{Q}_j}{\mathcal{Q}_{ij}}(E_{ii}-E_{ij})\,, \end{aligned} \tag{2.3.59}$$

where in the last expression we commuted the entries of L_{ij} to the left so that it formally coincides with its classical counterpart (2.2.45). In the limit $\lambda\to\infty$, (2.3.58) becomes the quantum Lax equation. Note that in the derivation of this equation we did not use any concrete form of L; we only use that it factorises as $L = WP^{-1}$, where W is a function of coordinates only.

Taking the trace of (2.3.58), one gets

$$\mathrm{Tr}L(\lambda)\mathrm{Tr}L(\mu) - \mathrm{Tr}L(\mu)\mathrm{Tr}L(\lambda) = \mathrm{Tr}[M(\lambda,\mu), L(\mu)]\,. \tag{2.3.60}$$

A priori the trace of the commutator on the right-hand side might not be equal to zero, because it involves matrices with operator-valued entries. An involved calculation that uses representation (2.3.40) shows that it nevertheless vanishes[12], identically for λ and μ. Fortunately, there is a simple and transparent way to show the commutativity of traces of the Lax operator, which directly relies on the algebraic relations (2.3.55), thus bypassing the construction of the quantum Lax pair. Indeed, let us multiply both sides of (2.3.41) with $P_2^{-1}\bar{R}_{12}(\lambda)P_2R_{12}^{-1}(\lambda,\mu)$ and take the trace with respect to both spaces. We get

$$\mathrm{Tr}_{12}\Big[P_2^{-1}\bar{R}_{12}(\lambda)P_2L_2(\mu)\bar{R}_{12}^{-1}(\lambda)L_1(\lambda)\Big] = \\ \mathrm{Tr}_{12}\Big[P_2^{-1}\bar{R}_{12}(\lambda)P_2R_{12}^{-1}(\lambda,\mu)L_1(\lambda)\bar{R}_{21}^{-1}(\mu)L_2(\mu)\underline{R}_{12}(\lambda,\mu)\Big]\,.$$

From (2.3.49) we have

$$P_2^{-1}\bar{R}_{12}(\lambda)P_2R_{12}^{-1}(\lambda,\mu) = \underline{R}_{12}^{-1}(\lambda,\mu)P_1^{-1}\bar{R}_{21}(\mu)P_1\,,$$

so that the right-hand side of the above equation can be transformed as

$$\mathrm{Tr}_{12}\Big[P_2^{-1}\bar{R}_{12}(\lambda)P_2L_2(\mu)\bar{R}_{12}^{-1}(\lambda)L_1(\lambda)\Big] = \\ \mathrm{Tr}_{12}\Big[\underline{R}_{12}^{-1}(\lambda,\mu)P_1^{-1}\bar{R}_{21}(\mu)P_1L_1(\lambda)\bar{R}_{21}^{-1}(\mu)L_2(\mu)\underline{R}_{12}(\lambda,\mu)\Big]\,. \tag{2.3.61}$$

Further progress is based on the fact that the matrices $\bar{R}_{12}(\lambda)$ and $\bar{R}_{12}^{-1}(\lambda)$ are diagonal in the second space. We represent it in factorised form

$$\bar{R}_{12}(\lambda) = \sum_{j=1}^{N} G_j(\lambda)\otimes E_{jj}\,, \tag{2.3.62}$$

see (2.3.43), (2.3.20) and (2.3.44). Therefore,

$$P_2^{-1}\bar{R}_{12}(\lambda)P_2 = \sum_{j=1}^{N} P_j^{-1}G_j(\lambda)P_j\otimes E_{jj}\,. \tag{2.3.63}$$

Although this expression involves the shift operator, it commutes with any function of coordinates q_j, because when pushed through (2.3.63), this function will undergo the shifts of q_j in opposite directions which compensate each other. Similarly,

$$\bar{R}_{12}^{-1}(\lambda) = \sum_{j=1}^{N} G_j(\lambda)^{-1}\otimes E_{jj} = \sum_{j=1}^{N}(\mathbb{1}\otimes E_{jj})(G_j(\lambda)^{-1}\otimes\mathbb{1})\,.$$

[12] For this result to hold, the presence in (2.3.57) of the first term proportional to $L(\lambda)$ is of crucial importance.

Consider first the left-hand side of (2.3.61)

$$\mathrm{Tr}_{12}\Big[\sum_{j=1}^{N}\sum_{k=1}^{N}(P_j^{-1}G_j(\lambda)P_j\otimes E_{jj}L(\mu)E_{kk})(G_k(\lambda)^{-1}\otimes\mathbb{1})L_1(\lambda)\Big]\,.$$

Using the cyclic property of the trace in the second space, this expression is equivalent to

$$\mathrm{Tr}_{12}\Big[\sum_{j=1}^{N}\sum_{k=1}^{N}(P_j^{-1}G_j(\lambda)P_j\otimes L(\mu)E_{jj}E_{kk})(G_k(\lambda)^{-1}\otimes\mathbb{1})L_1(\lambda)\Big]\,.$$

Taking into account that $L = WP^{-1}$ and the commutativity of $P_j^{-1}G_j(\lambda)P_j$ with any function of coordinates, we arrive at

$$\mathrm{Tr}_{12}\Big[\sum_{j=1}^{N}(\mathbb{1}\otimes W(\mu))(P_j^{-1}G_j(\lambda)P_j\otimes P_j^{-1}E_{jj})\bar{R}_{12}^{-1}(\lambda)L_1(\lambda)\Big] = \mathrm{Tr}L(\mu)\mathrm{Tr}L(\lambda)\,.$$

Now we look at the right-hand side of (2.3.61): using the cyclic property of the trace, the matrix $\underline{R}_{12}(\lambda,\mu)$ can be moved to the left where it cancels with its inverse. This manipulation is allowed because $L_1(\lambda)$ and $L_2(\mu)$ produce together a factor $P_1^{-1}P_2^{-1}$ with which $\underline{R}_{12}(\lambda,\mu)$ commutes due to the zero weight condition (2.3.27). Also, the individual entries of $\underline{R}_{12}(\lambda,\mu)$ are freely moved through $P_1^{-1}\bar{R}_{21}(\mu)P_1$, because of the diagonal structure of the latter matrix in the first matrix space, analogous to the similar property of (2.3.63). Then, to eliminate $\bar{R}_{21}(\mu)$, one employs the same procedure as was used for the left-hand side of (2.3.61) and the final result is $\mathrm{Tr}L(\lambda)\mathrm{Tr}L(\mu)$. This proves the commutativity of traces of the Lax matrix for different values of the spectral parameter.

We finally remark that writing the analogue of (2.3.36) with spectral parameter dependent Lax operator [52, 53]

$$:\det(L(\lambda)-\zeta\mathbb{1}):=\sum_{k=0}^{N}(-\zeta)^{N-k}\mathcal{S}_k(\lambda)\,, \tag{2.3.64}$$

the quantities $\mathcal{S}_k(\lambda)$ are commuting integrals and they are related to Macdonald operators (2.3.35) by a simple coupling- and spectral parameter-dependent re-scaling

$$\mathcal{S}_k(\lambda) \;=\; \lambda^{-k}(\lambda-\theta^k\, e^{-\hbar/2})(\lambda-e^{-\hbar/2})^{k-1}\,\mathcal{S}_k\,. \tag{2.3.65}$$

2.4 Conclusions

We have discussed the hyperbolic RS model in the context of Poisson reduction of the Heisenberg double [57]: we derive its Poisson structure and show that only on the reduced phase space does the Poisson algebra of the Lax matrix close and take a form very similar to the Lax matrix of the rational RS model [57]. We find a quantization of the L-operator algebra governed by new R matrices $R_{\pm}$, along with a quantization of the classical integrals in the form of quantum trace formulae I_k (see (2.3.32)). We show how these quantum integrals are related to the well-known Macdonald operators through determinant formulae. Along the way we present a second Lax matrix that we can use to introduce a spectral parameter in the model. At the classical level this yields r-matrices that satisfy the shifted Yang-Baxter equation due to scale-violating terms. We show that this L-operator algebra admits a quantization as well, with new R matrices satisfying the shifted quantum Yang-Baxter equation.

A particularly interesting observation is that one cannot obtain the quantum L-operator algebra from the quantum Heisenberg double in the same way as was done for the quantum cotangent bundle. It would be interesting to pursue the question whether and how one can impose the Dirac constraints after quantization in order to reconstruct the quantum L-operator algebra. A first step in that direction could be finding an analytic proof that the Dirac bracket for L on the reduced phase space is closed for general N. Another interesting question is to find the relation between our quantum trace formulae and the commuting traces obtained by the fusion procedure [23, 68] for the equations (2.3.29). In addition, it would be interesting to extend our results to the RS models with spin, in particular, to those discussed in [48], as well as to find an analogue of the formulae (2.3.32) for the model with elliptic potential or for other series of Lie algebras. Constructing the quantum spin versions of these models could further aid the understanding of the RS type models that appear in the study of conformal blocks as in [20].

Chapter 3
Hyperbolic Ruijsenaars-Schneider model with spins

3.1 Introduction

The Ruijsenaars-Schneider (RS) integrable models [18, 21] continue to deliver rich mathematical structures that are worth further exploring. One particular aspect concerns the introduction of spin degrees of freedom. Recall that a spin generalization of the RS model with the most general elliptic potential was proposed in [24] as a dynamical system describing the evolution of poles of elliptic solutions of the non-abelian 2d Toda chain. This is a system of N particles on a line with internal degrees of freedom represented by two ℓ-dimensional vectors attached to each of the particles. The proposed spin RS model is given in terms of equations of motion for the particle coordinates q_i, $i = 1, \ldots, N$ and the spin variables[1] $\mathbf{a}_{i\alpha}$ and $\mathbf{c}_{\alpha i}$, where $\alpha = 1, \ldots, \ell$. The knowledge of the equations of motion contains but unfortunately does not immediately yield the Hamiltonian structure behind this dynamical system.

In [69] it was established the underlying Hamiltonian structure for the case of rational degeneration of the elliptic spin RS model. This was done by relaying on the observation that goes back to [45] and further developed in [70]-[47] that the Calogero-Moser-Sutherland and Ruijsenaars-Schneider models can be obtained by means of the Hamiltonian or Poisson reduction procedure applied to a suitably chosen initial phase space. In the case of the rational spin RS model the suitable initial phase space $\mathscr{P}$ appears to be the direct product $\mathscr{P} = T^*G \times \Sigma$, where T^*G is the cotangent bundle to a Lie group G with the Lie algebra $\mathfrak{g}$ and Σ is the symplectic manifold of $N\ell$ pairs of canonical variables (oscillators). This phase space is a Poisson manifold which carries the Hamiltonian action of G. Choosing $G = \mathrm{GL}(N, \mathbb{C})$ the Hamiltonian reduction of $\mathscr{P}$ by the action of G yields the desired Poisson structure of the spin RS model [69]. The Poisson brackets of the invariant spin variables appear rather involved. Although it was possible to guess a natural generalization of the Poisson structure for "collective" spin variables $f_{ij} = \sum_\alpha \mathbf{a}_{i\alpha}\mathbf{c}_{\alpha j}$ to the hyperbolic

[1] We follow the notation of [69].

spin RS model, the progress of finding the Poisson structure of individual spins in the hyperbolic case was delayed for years. Quite recently this structure has been found [48] confirming the conjecture in [69] on the brackets of collective spin variables. The approach of [48], see also [71, 72], is based on the quasi-Hamiltonian reduction procedure, where one starts from an initial manifold $\mathscr{P}$ supplied with a quasi-Poisson structure and which carries a free action of a Lie group G. Although $\mathscr{P}$ is not Poisson, the quotient $\mathscr{P}/G$ inherits the well-defined Poisson structure from the quasi-Poisson structure on $\mathscr{P}$. Picking as $\mathscr{P}$ a representation space of a framed Jordan quiver, it was shown in [48] that the reduction of this by G yields the Poisson structure of invariant spins that perfectly fits the hyperbolic (trigonometric complex) spin RS model. The Liouville integrability and superintegrability (degenerate integrability) of the spin RS model also follow from this approach.

Having established these nice results, one still may wonder if there would exist a conventional way of getting the spin hyperbolic RS model by the usual Poisson reduction but applied to a more complicated initial phase space being the next in the deformation hierarchy after $T^*G \times \Sigma$ responsible for the rational model. Indeed, the spinless hyperbolic RS model follows from the Poisson reduction applied to the Heisenberg double $D_+(G)$ of G, as has been recently discussed in [73]. The Poisson structure of the Heisenberg double [40] is a deformation of the one of T^*G. From the point of view of the deformation theory, it is then natural to replace the moment map on Σ, taking values into the dual Lie algebra $\mathfrak{g}^*$, with a non-abelian moment map defined on a suitable deformation of Σ and which takes values in the dual Poisson-Lie group G^*. The main question is how to realize the quadratic Poisson structure of G^* in terms of $N\ell$-pairs of oscillators that should replace those used to represent the linear Kirillov-Kostant bracket in the rational case. In this chapter we solve this problem and reconstruct the spin hyperbolic RS model in the standard framework of the Poisson reduction.

The main tool in our approach is a Poisson pencil of a constant and quadratic Poisson structures on an oscillator manifold $\Sigma_{N,\ell}$ spanned by $2N\ell$ dynamical variables $a_{i\alpha}, b_{\alpha i}$. When the coefficient $\varkappa$ in front of the quadratic structure vanishes, one obtains the standard canonical relations of the $N\ell$ conjugate pairs. In fact there are two different quadratic structures, to distinguish between them we label the corresponding Poisson manifolds as $\Sigma^{\pm}_{N,\ell}$. These Poisson manifolds carry Poisson actions of two different Poisson-Lie groups – the particle group $\mathrm{GL}(N,\mathbb{C})$ and the spin group $\mathrm{GL}(\ell,\mathbb{C})$, acting by linear transformations on the oscillator indexes i and α, respectively. Starting from the initial phase space $\mathscr{P} = D_+(G) \times \Sigma^{\pm}_{N,\ell}$ and reducing this manifold by the action of the particle group, we obtain the spin RS model with the Poisson structure inherited from that on $\mathscr{P}$. The equations of motion for the spins are the same regardless of which manifold $\Sigma^{\pm}_{N,\ell}$ we use, and they coincide with those that follow from the Poisson structure of spins found in [48] through the quasi-Hamiltonian reduction. The construction of conserved quantities, both Poisson commutative and non-commutative, is straightforward and follows the same pattern as in the rational case. The spin group continues to act on the reduced phase space as a Poisson-Lie symmetry and its presence explains the superintegrability of the model. In fact, there are higher symmetries whose generators are polynomial in the spin variables and which arise from conjunction of the spin symmetries with abelian symmetries generated by higher commuting charges. We show that the Poisson structure of the currents encoding these symmetries is a quadratic deformation of the linear bracket of the rational model. This quadratic part appears as an affine version of the Poisson-Lie structure on G^*.

Concluding the brief discussion of our approach, we point out that it would be interesting to extend it to account for the most general elliptic spin model. Also, since we are building on the classical r-matrix formalism, the recognition of various r-matrix structures might help to pave the way for quantizing the spin model which currently remains another open problem.

The chapter is organized as follows. In section 3.2 we introduce the oscillator manifold. In section 3.3 we discuss the Poisson action of a Poisson-Lie group on the product of two manifolds. In section (3.4) we solve the moment map equation obtaining the Lax matrix of the spin RS model on the reduced phase space. The Poisson brackets of G-invariant variables are studied in section 3.5 and section 3.6 is devoted to the discussion of symmetries of the model responsible for its superintegrable status. We conclude this section by showing what superintegrability implies for solvability of the equations of motion. Some technical details are collected in appendix. All the considerations in the chapter are done in the context of holomorphic integrability.

3.2 Oscillator manifold

We introduce a manifold $\Sigma_{N,\ell}$ as the product of two linear spaces of all rectangular $N\times\ell$-matrices

$$\Sigma_{N,\ell} \,=\, \mathrm{Mat}_{N,\ell}(\mathbb{C})\times \mathrm{Mat}_{\ell,N}(\mathbb{C})\,, \tag{3.2.1}$$

where N is the number of particles of the model and ℓ is the length of spin vectors. Let (a,b) be two arbitrary $N\times\ell$- and $\ell\times N$-matrices. Their entries

$$a_{i\alpha}\equiv(a)_{i\alpha}\,,\;\; b_{\alpha j}\equiv(b)_{\alpha j}\qquad i=1,\ldots,N\,,\quad \alpha=1,\ldots,\ell\,. \tag{3.2.2}$$

provide a global coordinate system on $\Sigma_{N,\ell}$. We call $a_{i\alpha}$ and $b_{\alpha j}$ oscillators and refer to $\Sigma_{N,\ell}$ as to an oscillator manifold.

Now we endow $\Sigma_{N,\ell}$ with two different $\pm$-structures of a Poisson manifold $\Sigma^{\pm}_{N,\ell}$ by defining the following Poisson brackets $\{\,,\,\}_{\pm}$ between oscillators

$$\begin{aligned}
\{a_1,a_2\}_{\pm} &= \varkappa\,(\,r\,a_1a_2\mp a_1a_2\,\rho)\,,\\
\{b_1,b_2\}_{\pm} &= \varkappa\,(\,b_1b_2\,r\,\mp\,\rho\,b_1b_2)\,,\\
\{a_1,b_2\}_{\pm} &= \varkappa\,(-b_2\,r_+\,a_1\,\pm\,a_1\,\rho_{\mp}\,b_2\,)\,-C^{\rm rec}_{12}\,,\\
\{b_1,a_2\}_{\pm} &= \varkappa\,(-b_1\,r_-\,a_2\,\pm\,a_2\,\rho_{\pm}\,b_1\,)\,+C^{\rm rec}_{21}\,.
\end{aligned} \tag{3.2.3}$$

Here we have introduced a "rectangular split Casimir"

$$C_{12}^{\mathrm{rec}} = \sum_{i=1}^{N}\sum_{\alpha=1}^{\ell} E_{i\alpha}\otimes E_{\alpha i}\,, \tag{3.2.4}$$

where $(E_{i\alpha})_{j\beta} = \delta_{ij}\delta_{\alpha\beta}$. The matrices $\rho_\pm$ are the following analogues of $r_\pm$ in the spin space

$$\rho_\pm = \pm\frac{1}{2}\sum_{\alpha=1}^{\ell} E_{\alpha\alpha}\otimes E_{\alpha\alpha} \pm \sum_{\alpha\lessgtr\beta}^{\ell} E_{\alpha\beta}\otimes E_{\beta\alpha} \tag{3.2.5}$$

and $\rho = \frac{1}{2}(\rho_+ + \rho_-)$. One also has

$$\rho_+ - \rho_- = C_{12}^{\mathrm{s}} = \sum_{\alpha,\beta=1}^{\ell} E_{\alpha\beta}\otimes E_{\beta\alpha}\,. \tag{3.2.6}$$

For $\varkappa = 0$ the brackets (3.2.3) turn into the standard oscillator algebra formed by $N\ell$ pairs of canonically conjugate variables

$$\{a_{i\alpha}, b_{\beta j}\} = -\delta_{ij}\delta_{\alpha\beta}\,. \tag{3.2.7}$$

The brackets (3.2.3) satisfy the Jacobi identity for any $\varkappa$, i.e. the constant and quadratic structures in (3.2.3) form a Poisson pencil being a one-parametric deformation of the canonical relations (3.2.7). It remains to note that if we define

$$\omega = \mathbb{1} + \varkappa ab\,, \tag{3.2.8}$$

where ab is an $N\times N$-matrix being a natural product of two rectangular matrices, then due to (3.2.3), ω will satisfy the Poisson algebra

$$\frac{1}{\varkappa}\{\omega_1,\omega_2\} = r_+\omega_1\omega_2 + \omega_1\omega_2 r_- - \omega_1 r_-\omega_2 - \omega_2 r_+\omega_1\,, \tag{3.2.9}$$

which is different from (1.2.52) by an overall sign only. In particular, the contribution of the spin matrices $\rho, \rho_\pm$ completely decouples. Thus, formulae (3.2.8) give a realization of the Semenov-Tian-Shansky bracket in terms of the oscillator algebra (3.2.3). We also point out the Poisson relations between ω and oscillators

$$\frac{1}{\varkappa}\{\omega_1, a_2\} = (r_+\omega_1 - \omega_1 r_-)a_2\,, \qquad \frac{1}{\varkappa}\{\omega_1, b_2\} = -b_2(r_+\omega_1 - \omega_1 r_-)\,. \tag{3.2.10}$$

In deriving (3.2.9) and (3.2.10) one has to use the relations

$$a_1 C_{21}^{\mathrm{rec}} = C_{12}a_2\,, \qquad C_{12}^{\mathrm{rec}} b_1 = b_2 C_{12}\,, \qquad C_{12}^{\mathrm{s}} b_1 b_2 = b_1 b_2 C_{12}\,.$$

Importantly, one can now verify that if we allow G to act infinitesimally on oscillators as

$$\delta_X a_{i\alpha} = (\mathrm{Ad}^*_\omega X\, a)_{i\alpha} \qquad \delta_X b_{\alpha i} = -(b\,\mathrm{Ad}^*_\omega X\,)_{\alpha i}\,, \qquad X\in\mathfrak{g}\,, \tag{3.2.11}$$

then this action $G \times \Sigma^{\pm}_{N,\ell} \to \Sigma^{\pm}_{N,\ell}$ is a mapping of Poisson manifolds provided G is equipped with the Sklyanin bracket (2.2.5). Here $\mathrm{Ad}^*_g X$ for $g \equiv (g_+, g_-) \in G^*$ is the coadjoint (dressing) action of G^* on the Lie algebra $\mathfrak{g}$. If we factorize $\omega = \omega_+\omega_-^{-1}$ according to (1.2.13), then $(\omega_+^{-1}, \omega_-^{-1}) \in G^*$ is the moment map for the Poisson action (3.2.11). Under (1.2.13) it defines the following element of G

$$\mathcal{N} = \omega_+^{-1}\omega_- \in G\,. \tag{3.2.12}$$

The fact that $\mathcal{N}$ generates the action (3.2.11) can be deduced from the Poisson brackets (3.2.10) together with the fact that $\omega \star \{\mathcal{N}, \,.\,\} = -\{\omega, \,.\,\} \star \mathcal{N}$. The Poisson algebra of $\mathcal{N}$ coincides with (1.2.52).

Further, the oscillator manifolds carries an action of the spin Poisson-Lie group $S = \mathrm{GL}(\ell, \mathbb{C})$

$$a_{i\alpha} \longrightarrow (ag)_{i\alpha}\,, \qquad b_{\alpha i} \longrightarrow (g^{-1}b)_{\alpha i}\,, \quad g \in S\,. \tag{3.2.13}$$

This action is Poisson provided the Poisson-Lie structure on S is taken for $\Sigma^{\pm}_{N,\ell}$ to be

$$\{g_1, g_2\} = \pm\varkappa[\rho, g_1 g_2]\,. \tag{3.2.14}$$

3.3 Poisson-Lie group action on a product manifold

Let $\mathscr{P}_1$ and $\mathscr{P}_2$ be two Poisson manifolds with brackets $\{\cdot\,,\cdot\}_{\mathscr{P}_1}$ and $\{\cdot\,,\cdot\}_{\mathscr{P}_2}$ that carry the Poisson action of a Poisson-Lie group G. Let $\mathcal{M}_i : \mathscr{P}_i \to G^*$ be the corresponding non-abelian moment maps which are assumed to be Poisson. Then, one can define the Poisson action of G on the product manifold $\mathscr{P} = \mathscr{P}_1 \times \mathscr{P}_2$ by taking the product[2] of the moment maps [74][3]

$$\mathcal{M} = \mathcal{M}_1 \star \mathcal{M}_2\,,$$

and allowing it to act on functions on $\mathscr{P}$ by means of the formula

$$\xi_X f = \langle X, \{\mathcal{M}, f\}_{\mathscr{P}} \star \mathcal{M}^{-1}\rangle\,, \quad f \in \mathrm{Fun}(\mathscr{P})\,, \tag{3.3.1}$$

where ξ_X is a vector field corresponding to $X \in \mathfrak{g}$ and $\langle\cdot\,,\cdot\rangle$ is the canonical pairing between $\mathfrak{g}$ and $\mathfrak{g}^*$. We have

$$\xi_X f = \langle X, \{\mathcal{M}_1, f\}_{\mathscr{P}_1}\mathcal{M}_1^{-1} + \mathcal{M}_1\{\mathcal{M}_2, f\}_{\mathscr{P}_2}\mathcal{M}_2^{-1}\mathcal{M}_1^{-1}\rangle\,. \tag{3.3.2}$$

Let $\xi^{(1)}_X$ and $\xi^{(2)}_X$ be the fundamental vector fields induced by the group action on $\mathscr{P}_1$ and $\mathscr{P}_2$, respectively. Formula (3.3.2) is equivalent to the statement that at a point $x = (x_1, x_2) \in \mathscr{P}$, where $x_1 \in \mathscr{P}_1$ and $x_2 \in \mathscr{P}_2$, the vector field ξ_X is defined as

$$\xi_X(x) = \xi^{(1)}_X(x_1) + \xi^{(2)}_{\mathrm{Ad}^*_{\mathcal{M}_1^{-1}(x_1)}X}(x_2)\,, \tag{3.3.3}$$

[2]The product is naturally taken in G^*.

[3]We are grateful to László Fehér for drawing our attention to this chapter.

where Ad^*_h, $h \in G^*$ is the coadjoint action of G^* on G which is also an example of dressing transformations [40]. One can show that the map $X \to \xi_X$, where ξ_X is defined by (3.3.3), is the Lie algebra homomorphism, so that ξ_X is the fundamental vector field of the group action on G [3, 74]. Since G^* is a Poisson-Lie group, $\mathcal{M}$ will have the same Poisson brackets between its entries as $\mathcal{M}_1$ or $\mathcal{M}_2$.

To construct the Hamiltonian structure of the spin RS model, we take the product of symplectic manifolds $\mathscr{P}_1 = D_+(G)$ and $\mathscr{P}_2 = \Sigma^{\pm}_{N,\ell}$,

$$\mathscr{P} = D_+(G) \times \Sigma^{\pm}_{N,\ell}\,. \tag{3.3.4}$$

Here the Poisson structure on the Heisenberg double $D_+(G)$ is given by (2.2.1) and that on the oscillator manifold is (3.2.3). We define the Poisson action of G on $\mathscr{P}$ through its moment map

$$\mathcal{M} \star \mathcal{N} = \mathcal{M}_+ \mathcal{N} \mathcal{M}_-^{-1}\,, \tag{3.3.5}$$

where $\mathcal{N}$ is the moment map (3.2.12) of the action (3.2.11) and $\mathcal{M}$ is (2.2.6). Since $\mathcal{M}$ and $\mathcal{N}$ are elements of G^* modeled by G, we multiply them with the star product. To obtain the RS model on the reduced phase space, we fix the moment map to the following value

$$\mathcal{M} \star \mathcal{N} = \theta\, \mathbb{1}\,, \tag{3.3.6}$$

where $\mathbb{1}$ is the group identity in G and θ is the coupling constant. Since the right hand side of (3.3.6) is proportional to the identity, the stability group of the moment map coincides with the whole group G and, therefore, all the entries of $\mathcal{M} \star \mathcal{N}$ are constraints of the first class. Equation (3.3.6) can be written as the following equation in G

$$\mathcal{M} = \theta\, \omega_+ \omega_-^{-1} = \theta\, \omega\,. \tag{3.3.7}$$

Some comments are in order. The choice of the initial manifold (3.3.4), as well as the use of relevant reduction techniques to obtain the spin RS models on the reduced phase space was already suggested earlier, see e.g. [25, 69]. Also, a similar construction was developed in [47], where G was taken to be the compact Lie group $\mathrm{U}(N)$. In this case the underlying Lie bialgebra $(\mathfrak{g}, \mathfrak{g}^*)$ is not factorizable and the corresponding double $\mathscr{D}$ can be identified with the complexification of $\mathfrak{g} = \mathfrak{su}(N)$. The dynamical system one finds on the reduced phase space coincides with the trigonometric spin RS model. The point, however, is that working with the collective spin variable ω alone leaves invisible the evolution of individual spin components of a spin vector associated to each particle. The aim of our present construction is to further resolve $\omega \in G^*$ in terms of internal spin degrees of freedom and obtain the dynamical equations for individual spins, as in [24].

3.4 Reduction

We can now develop the reduction procedure starting from the initial phase space (3.3.4)

$$\mathscr{P} = D_+(G) \times \Sigma^{\pm}_{N,\ell} \,. \tag{3.4.1}$$

The moment map equation (3.3.7) takes the form

$$BA^{-1}B^{-1}A = \theta(\mathbb{1} + \varkappa ab) \,. \tag{3.4.2}$$

The reduced phase space $\mathscr{P}$ is obtained by factoring solutions of (3.4.2) by the action of the group G

$$\mathscr{P} = \{\text{Solutions of } (3.4.2)\}/G \,.$$

Note that for our reduction procedure the parameter $\varkappa$ controlling the Poisson brackets (2.2.1) of the Heisenberg double and the brackets (3.2.3) of the oscillator manifold is chosen to be the one and the same.

We point out that under the Poisson action on the product manifold (3.4.1) the transformation of oscillators get simplified over the hypersurface defined by (3.4.2). Indeed recalling (3.3.3) and (3.2.11), we get

$$\delta_X a_{i\alpha} \;=\; (\mathrm{Ad}^*_{\omega\star\mathcal{M}^{-1}}X\,a)_{i\alpha} \qquad \delta_X b_{\alpha i} \;=\; -(b\,\mathrm{Ad}^*_{\omega\star\mathcal{M}^{-1}}X\,)_{\alpha i}\,, \qquad X\in\mathfrak{g}\,, \tag{3.4.3}$$

and since $\omega\star\mathcal{M}^{-1} = \omega_+\mathcal{M}_+^{-1}\mathcal{M}_-\omega_-^{-1} \equiv \theta^{-1}\mathbb{1}$ the action of $\mathrm{Ad}^*_{\omega\star\mathcal{M}^{-1}}$ is ineffective and the oscillators transform as

$$a_{i\alpha} \;\longrightarrow\; (h\,a)_{i\alpha} \qquad b_{\alpha i} \;\longrightarrow\; (b\,h^{-1})_{\alpha i}\,, \qquad h = e^X \in G\,. \tag{3.4.4}$$

The most efficient way to factor out solutions by the action of G is to reformulate and solve the moment map equation (3.4.2) in terms of gauge-invariant variables. To this end, following [73] we introduce a new coordinate system on the diagonalizable locus of the Heisenberg double

$$A = T\mathcal{Q}T^{-1}\,, \qquad B = UP^{-1}T^{-1}\,, \tag{3.4.5}$$

where $\mathcal{Q}$ and P are diagonal matrices with entries

$$\mathcal{Q}_{ij} \;=\; \delta_{ij}\mathcal{Q}_j \qquad P_{ij} \;=\; \delta_{ij}P_j\,. \tag{3.4.6}$$

The matrices T, U are Frobenius, i.e. they are subjected to the following constraints

$$\sum_{j=1}^N T_{ij} \;=\; \sum_{j=1}^N U_{ij} = 1\,, \qquad \forall\, i = 1,\ldots,N\,. \tag{3.4.7}$$

Imposition of these constraints renders decomposition (3.4.5) unique.

Under the transformations (3.2.11) the new variables transform as follows

$$\mathcal{Q} \;\to\; \mathcal{Q}\,, \qquad P \;\to\; P\,d_T^{-1}\,d_U\,, \qquad T \;\to\; h\,T\,d_T\,, \qquad U \;\to\; h\,U\,d_U\,, \tag{3.4.8}$$

where $(d_X)_{ij} = \delta_{ij} \sum_{k=1}^{N} (hX)_{ik}$ for any $X \in \mathrm{GL}(N, \mathbb{C})$. In particular, $\mathcal{Q}$ is invariant under the G-action.

Substituting (3.4.5) into (3.4.2), we will get

$$U\mathcal{Q}^{-1}U^{-1}T\mathcal{Q}T^{-1} = \theta(\mathbb{1} + \varkappa ab)\,,$$

where, in particular, the momentum variable P has completely decoupled. There are different ways to solve the above equation, we follow the one which relies on the simplest invariant spin variables. We have

$$T^{-1}U\mathcal{Q}^{-1} = \theta(\mathcal{Q}^{-1}T^{-1}U + \varkappa T^{-1}\, ab\, T\mathcal{Q}^{-1}T^{-1}U)\,,$$

Following the spinless pattern in [57, 73], we introduce the Frobenius matrix $W = T^{-1}U$ and reintroduce the momentum P by multiplying from the right both sides of the equations above by P^{-1},

$$WP^{-1}\mathcal{Q}^{-1} - \theta\mathcal{Q}^{-1}WP^{-1} = \theta\varkappa T^{-1}\, ab\, A^{-1}BT\,, \tag{3.4.9}$$

Note that under (3.2.11) the variable WP^{-1} is not invariant, rather it transforms as

$$WP^{-1} \;\rightarrow\; d_T^{-1}(WP^{-1})d_T\,.$$

On the other hand, a matrix $T^{-1}a$ transforms as

$$T^{-1}a \;\rightarrow\; d_T^{-1}T^{-1}h^{-1}ha = d_T^{-1}T^{-1}a\,,$$

where we have taken into account the transformation law (3.2.11) for the spin variables. This suggests to introduce a diagonal matrix t with entries

$$t_{ij} = \delta_{ij}\sum_{\alpha=1}^{\ell}(T^{-1}a)_{i\alpha}\,. \tag{3.4.10}$$

Multiplying (3.4.9) from the left and from the right by t^{-1} and t, respectively, projects the moment map equation of the space of G-invariants

$$t^{-1}WP^{-1}t\mathcal{Q}^{-1} - \theta\mathcal{Q}^{-1}\,t^{-1}WP^{-1}t = \theta\varkappa\, t^{-1}T^{-1}abA^{-1}BTt\,.$$

Introducing the G-invariant combinations

$$L = t^{-1}WP^{-1}t\,\mathcal{Q}^{-1}\,, \qquad \mathbf{a} = t^{-1}T^{-1}a\,, \qquad \mathbf{c} = bA^{-1}BTt\,, \tag{3.4.11}$$

we rewrite the moment map equation in its final invariant form

$$L - \theta\mathcal{Q}^{-1}L\mathcal{Q} = \theta\varkappa\,\mathbf{ac}\,. \tag{3.4.12}$$

The last equation is elementary solved for L

$$L = \theta\varkappa\sum_{i,j=1}^{N}\frac{\mathcal{Q}_i}{\mathcal{Q}_i - \theta\mathcal{Q}_j}(\mathbf{ac})_{ij}\,E_{ij}\,. \tag{3.4.13}$$

The quantity (3.4.13) is the Lax matrix of the hyperbolic spin RS model, as can be seen by by introducing the following parametrization

$$\theta = e^{-2\gamma}\,, \qquad \mathcal{Q}_i = e^{2q_i}\,, \qquad q_{ij} = q_i - q_j\,, \tag{3.4.14}$$

so that L takes the familiar form

$$L = \varkappa e^{-2\gamma} \sum_{i,j}^{N} \frac{e^{q_{ij}+\gamma}}{2\sinh(q_{ij}+\gamma)} f_{ij}\, E_{ij}\,, \qquad f_{ij} \equiv (\mathbf{ac})_{ij}\,.$$

Computing the trace of L^k,

$$\mathrm{Tr}L^k = \mathrm{Tr}(WP^{-1}\mathcal{Q}^{-1})^k = \mathrm{Tr}(UP^{-1}T^{-1}T\mathcal{Q}^{-1}T^{-1})^k = \mathrm{Tr}(BA^{-1})^k\,, \tag{3.4.15}$$

we recognize that $\mathrm{Tr}L^k$ originate from the G-invariant involutive family (2.2.9). Thus, $\mathrm{Tr}L^k$ are in involution. We take $H = H_1$ as the Hamiltonian.

3.5 Poisson brackets of G-invariants

As we have found, the reduced phase space $\mathscr{P}$ has a natural parametrization in terms of the following G-invariant variables

$$\mathbf{a}_{i\alpha}\,,\ \mathbf{c}_{\alpha i}\,,\ \mathcal{Q}_i\,, \qquad i = 1,\ldots,N,\ \ \alpha = 1,\ldots,\ell\,. \tag{3.5.1}$$

Note that by construction the spin variables $\mathbf{a}_{i\alpha}$ are constrained to satisfy

$$\sum_{\alpha=1}^{\ell} \mathbf{a}_{i\alpha} = 1\,, \tag{3.5.2}$$

which can be regarded as the Frobenius condition in the spin space. The Lax matrix (3.4.13) depends on the collective spin variables f_{ij} only, which allows to perform the $\mathrm{GL}(\ell,\mathbb{C})$-rotations

$$\mathbf{a}_{i\alpha} \;\to\; \frac{1}{u_i}\mathbf{a}_{i\beta}\,(g^{-1})^{\beta}_{\alpha}\,, \quad \mathbf{c}_{\alpha i} \;\to\; u_i g_{\alpha\beta}\,\mathbf{c}^{\beta}_i\,, \quad u_i = \sum_{\alpha,\beta=1}^{\ell} \mathbf{a}_{i\beta}\,(g^{-1})^{\beta}_{\alpha}\,, \qquad g \in \mathrm{GL}(\ell,\mathbb{C})\,,$$

without changing f_{ij} and preserving the Frobenius condition (3.5.2).

Now we are in a position to determine the Poisson brackets between the variables (3.5.1) constituting the phase space. For that we need the Poisson brackets between $T, U, \mathcal{Q}$ and P variables of the double which have been computed in [73] (see previous chapter). The brackets between invariant spins and $\mathcal{Q}$ are then

$$\{\mathcal{Q}_i, \mathbf{a}_{j\alpha}\} = 0\,, \qquad \{\mathcal{Q}_i, \mathbf{c}_{\alpha j}\} = \delta_{ij}\,\mathbf{c}_{\alpha j}\,\mathcal{Q}_j\,. \tag{3.5.3}$$

For the brackets of spins between themselves we find

$$\{\mathbf{a}_1, \mathbf{a}_2\}_{\pm} = \varkappa\big[(r^{\bullet} \mp Y)\mathbf{a}_1\mathbf{a}_2 \mp \mathbf{a}_1\mathbf{a}_2\rho \mp \mathbf{a}_1 X_{21}\,\mathbf{a}_2 \pm \mathbf{a}_2\,X_{12}\,\mathbf{a}_1\big]\,, \tag{3.5.4}$$

$$\{\mathbf{a}_1,\mathbf{c}_2\}_\pm = \varkappa\big[\mathbf{c}_2(r^*_{12}\pm Y)\mathbf{a}_1 \pm \mathbf{a}_1\rho_\mp\mathbf{c}_2 \pm \mathbf{a}_1\mathbf{c}_2X_{21} \mp X^\mp_{12}\mathbf{a}_1\mathbf{c}_2\big] + K_{21}\,\mathbf{a}_1 Z_2 - C^{\rm rec}_{12}Z_2\,,$$
$$\{\mathbf{c}_1,\mathbf{a}_2\}_\pm = \varkappa\big[\mathbf{c}_1(-r^*_{21}\pm Y)\mathbf{a}_2 \pm \mathbf{a}_2\rho_\pm\mathbf{c}_1 \mp \mathbf{a}_2\mathbf{c}_1X_{12} \pm X^\mp_{21}\mathbf{a}_2\mathbf{c}_1\big] - K_{12}\,\mathbf{a}_2 Z_1 + C^{\rm rec}_{21}Z_1\,,$$
$$\{\mathbf{c}_1,\mathbf{c}_2\}_\pm = \varkappa\big[\mathbf{c}_1\mathbf{c}_2\,(r^\circ\mp Y) \mp \rho\mathbf{c}_1\mathbf{c}_2 \pm \mathbf{c}_1\,X^\mp_{12}\mathbf{c}_2 \mp \mathbf{c}_2\,X^\mp_{21}\mathbf{c}_1\big] + \mathbf{c}_2K_{12}Z_1 - \mathbf{c}_1K_{21}Z_2\,,$$

where we introduced the matrices $Z = \mathcal{Q}^{-1}L\mathcal{Q}$ and

$$\begin{aligned} X_{12} &= \sum_{i\beta\sigma\delta}(\mathbf{a}_1\rho)_{i\beta\sigma\delta}\,E_{ii}\otimes E_{\sigma\delta}\,, \qquad & X^\pm_{12} &= \sum_{i\beta\sigma\delta}(\mathbf{a}_1\rho^\pm)_{i\beta\sigma\delta}\,E_{ii}\otimes E_{\sigma\delta}\,,\\ K_{12} &= \sum_{i\sigma} E_{\sigma i}\otimes E_{ii}\,, & Y_{12} &= \sum_{i\beta k\delta}(\mathbf{a}_1\mathbf{a}_2\rho)_{i\beta k\delta}\,E_{ii}\otimes E_{kk}\,. \end{aligned} \tag{3.5.5}$$

While the matrices $r^\bullet, r^*, r^\circ$ depend on coordinates $\mathcal{Q}_i$ and they are defined as follows:

$$r^\bullet = \frac{1}{2}\sum_{i,j=1}^N \frac{\mathcal{Q}_i+\mathcal{Q}_j}{\mathcal{Q}_i-\mathcal{Q}_j}\,(E_{ii}-E_{ij})\otimes(E_{jj}-E_{ji})\,,$$
$$r^* = \frac{1}{2}\sum_{i,j=1}^N \frac{\mathcal{Q}_i+\mathcal{Q}_j}{\mathcal{Q}_i-\mathcal{Q}_j}\,(E_{ij}-E_{ii})\otimes E_{jj}\,,\quad r^\circ = \frac{1}{2}\sum_{i,j=1}^N \frac{\mathcal{Q}_i+\mathcal{Q}_j}{\mathcal{Q}_i-\mathcal{Q}_j}\,(E_{ii}\otimes E_{jj} - E_{ij}\otimes E_{ji})\,.$$

Writing the brackets (3.5.4) for the choice "−" in components one finds that for $N = 1,2$ and any spin ℓ, either $\ell = 1,2$ and any number of particles N, it coincides with the result obtained in [48] by means of a quasi-Hamiltonian reduction.[4] There are further immediate consequences of our findings. First, the rational limit of (3.5.4), which consists in re-scaling $q_i \to \varkappa q_i$, $\gamma \to \varkappa\gamma$ with further sending $\varkappa$ to zero, reproduces the Poisson structure of invariant spins established in [69]. Second, the Poisson algebra of collective spin variables f_{ij} that follows from (3.5.4) is in general different from the result conjectured in [69], and their difference written in the matrix form is

$$\mp f_1f_2\,Y \mp Y f_1 f_2 \pm f_1\,Y f_2 \pm f_2\,Y f_1\,. \tag{3.5.6}$$

As a result, the Lax matrix (3.4.13) does not satisfies the same Poisson algebra as in the spinless case, due to the contributions of Y_{12}. The Poisson bracket between Lax matrices reads

$$\begin{aligned} \frac{1}{\varkappa}\{L_1,L_2\}_\pm =& (r_{12}\mp Y)L_1L_2 - L_1L_2(\underline{r}_{12}\pm Y) +\\ &+ L_1(\bar r_{21}\pm Y)L_2 - L_2(\bar r_{12}\mp Y)L_1\,, \end{aligned} \tag{3.5.7}$$

where the dynamical r-matrices are [73]

$$\begin{aligned} r &= \sum_{i\neq j}^N\Big(\frac{\mathcal{Q}_j}{\mathcal{Q}_{ij}}E_{ii} - \frac{\mathcal{Q}_i}{\mathcal{Q}_{ij}}E_{ij}\Big)\otimes(E_{jj}-E_{ji})\,,\\ \bar r &= \sum_{i\neq j}^N \frac{\mathcal{Q}_i}{\mathcal{Q}_{ij}}(E_{ii}-E_{ij})\otimes E_{jj}\,, \qquad \underline{r} = \sum_{i\neq j}^N \frac{\mathcal{Q}_i}{\mathcal{Q}_{ij}}(E_{ij}\otimes E_{ji} - E_{ii}\otimes E_{jj})\,, \end{aligned} \tag{3.5.8}$$

[4] We thank to Maxime Fairon for pointing out the difference between the Poisson brackets (3.5.4) and those of [48] for a generic choice of N and ℓ. We provide an explicit comparison in appendix A.3.

where similarly to the rational case we introduced the notation $\mathcal{Q}_{ij} = \mathcal{Q}_i - \mathcal{Q}_j$.

The bracket (3.5.7) has the general form of the r-matrix structure compatible with involutivity of the spectral invariants of L, but the $\mathcal{Q}$-dependent r-matrices of the spinless case receive now an extra contribution from the spin variables. As to the Poisson structure of [48], the corresponding LL-algebra is given by (3.5.7) where Y should be taken to zero.

3.6 Superintegrability

Here we explain how superintegrability of the spin RS model follows from our approach. Consider the following two families of functions on the Heisenberg double

$$J_n^+ = \mathrm{Tr}\big[\mathrm{S}(BA^{-1})^n\big]\,, \qquad J_n^- = \mathrm{Tr}\big[\mathrm{S}(A^{-1}B)^n\big]\,, \qquad n\in\mathbb{Z}\,,$$

where S is an arbitrary $N\times N$-matrix which has a vanishing Poisson bracket with both A and B. Using (2.2.1), it is elementary to find $\{H_m, J_n^{\pm}\} = 0$, where $H_m = \mathrm{Tr}(BA^{-1})^m$ constitute a commutative family containing the Hamiltonian H_1. Thus, $J_n^{\pm}$ are integrals of motion. We take as S a matrix $\mathrm{S}^{\alpha\beta}$ with entries $(\mathrm{S}^{\alpha\beta})_{ij} = a_{i\alpha}b_{\beta j}$. Thus, on the initial phase space $\mathscr{P}$ we have two families of integrals

$$J_n^{+\alpha\beta} = \mathrm{Tr}\big[\mathrm{S}^{\alpha\beta}(BA^{-1})^n\big]\,, \quad J_n^{-\alpha\beta} = \mathrm{Tr}\big[\mathrm{S}^{\alpha\beta}(A^{-1}B)^n\big]\,, \quad \forall\ \alpha,\beta = 1,\ldots,\ell \tag{3.6.1}$$

These integrals are actually functions on the reduced phase space $\mathcal{P}$ as they can be expressed in terms of gauge-invariant variables. Indeed, we have $BA^{-1} = Tt\,L\,t^{-1}T^{-1}$ and $A^{-1}B = Tt(\mathcal{Q}^{-1}L\mathcal{Q})t^{-1}T^{-1}$, so that

$$BA^{-1} = A^{-1}B(B^{-1}ABA^{-1}) = A^{-1}BTt(\mathcal{Q}^{-1}L^{-1}\mathcal{Q}L)t^{-1}T^{-1}$$

and, therefore,

$$J_n^{+\alpha\beta} = \mathrm{Tr}\big[\mathbf{S}^{\alpha\beta}\mathcal{Q}^{-1}L^{-1}\mathcal{Q}L^n\big]\,, \qquad J_n^{-\alpha\beta} = \mathrm{Tr}\big[\mathbf{S}^{\alpha\beta}\mathcal{Q}^{-1}L^{n-1}\mathcal{Q}\big]\,,$$

where the matrix $\mathbf{S}^{\alpha\beta}$ comprises invariant spins $(\mathbf{S}^{\alpha\beta})_{ij} = \mathbf{a}_{i\alpha}\mathbf{c}_{\beta j}$. Clearly, $J_0^{+\alpha\beta} = J_0^{-\alpha\beta} = \mathrm{Tr}\,\mathrm{S}^{\alpha\beta}$. In the rational limit J_n^+ and J_n^- collapse to the same conserved quantities $J_n^{\alpha\beta}$ introduced in [69].

Because $J_n^{\pm\alpha\beta}$ are gauge invariants, their Poisson algebra computed on $\mathscr{P}$ straightforwardly descends on the reduced phase space. To compute the Poisson brackets of the integrals, we start with

$$\begin{aligned}\frac{1}{\varkappa}\{\mathrm{S}_1^{\alpha\beta},\mathrm{S}_2^{\gamma\delta}\}_{\pm} = \frac{1}{\varkappa}C_{12}\big(\delta^{\beta\gamma}\mathrm{S}_2^{\alpha\delta} - \delta^{\alpha\delta}\mathrm{S}_1^{\gamma\beta}\big) + r\mathrm{S}_1^{\alpha\beta}\mathrm{S}_2^{\gamma\delta} + \mathrm{S}_1^{\alpha\beta}\mathrm{S}_2^{\gamma\delta}\,r - \mathrm{S}_2^{\gamma\delta}\,r_+\mathrm{S}_1^{\alpha\beta} - \mathrm{S}_1^{\alpha\beta}r_-\mathrm{S}_2^{\gamma\delta}\\ \pm\Big[\rho_{\alpha\mu,\gamma\nu}\,\mathrm{S}_1^{\mu\beta}\mathrm{S}_2^{\nu\delta} + \mathrm{S}_1^{\alpha\mu}\mathrm{S}_2^{\gamma\nu}\rho_{\mu\beta,\nu\delta} - \mathrm{S}_2^{\gamma\nu}\rho_{\pm\alpha\mu,\nu\delta}\mathrm{S}_1^{\mu\beta} - \mathrm{S}_1^{\alpha\mu}\rho_{\mp\mu\beta,\gamma\nu}\mathrm{S}_2^{\nu\delta}\Big]\,,\end{aligned} \tag{3.6.2}$$

where the indexes $1,2$ are associated to the $N\times N$ matrix spaces. In deriving the last formula we used the properties of the spin ρ-matrices $\rho^T = -\rho$ and $\rho_{\pm}^T = -\rho_{\mp}$, where T means transposition.

To present further results in a concise manner, we introduce a unifying notation

$$J_n^{\alpha\beta} = \mathrm{Tr}(\mathrm{S}^{\alpha\beta}\mathscr{W}^n)\,, \tag{3.6.3}$$

where $\mathscr{W}$ should be identified with $\mathscr{W}^+ = BA^{-1}$ or with $\mathscr{W}^- = A^{-1}B$. The Poisson brackets between the entries of $\mathscr{W}^\pm$ is them

$$\frac{1}{\varkappa}\{\mathscr{W}_1^\pm, \mathscr{W}_2^\pm\} \;=\; -r_\mp\,\mathscr{W}_1^\pm\mathscr{W}_2^\pm - \mathscr{W}_1^\pm\mathscr{W}_2^\pm\,r_\pm + \mathscr{W}_1^\pm\,r_\mp\,\mathscr{W}_2^\pm + \mathscr{W}_2^\pm\,r_\pm\,\mathscr{W}_1^\pm\,. \tag{3.6.4}$$

By straightforward computation we then find the following result

$$\begin{aligned}\frac{1}{\varkappa}\{J_n^{\alpha\beta}, J_m^{\gamma\delta}\} \;=&\; \frac{1}{\varkappa}\big(\delta^{\beta\gamma}J_{n+m}^{\alpha\delta} - \delta^{\alpha\delta}J_{n+m}^{\gamma\beta}\big)\\ &\pm\Big[\rho_{\alpha\mu,\gamma\nu}J_n^{\mu\beta}J_m^{\nu\delta} + J_n^{\alpha\mu}J_m^{\gamma\nu}\rho_{\mu\beta,\nu\delta} - J_m^{\gamma\nu}\rho_{\pm\alpha\mu,\nu\delta}J_n^{\mu\beta} - J_n^{\alpha\mu}\rho_{\mp\mu\beta,\gamma\nu}J_m^{\nu\delta}\Big]\\ &\pm\Big[-\frac{1}{2}\big(J_n^{\alpha\delta}J_m^{\gamma\beta} - J_m^{\alpha\delta}J_n^{\gamma\beta}\big) + \sum_{p=0}^{m}\big(J_{n+m-p}^{\alpha\delta}J_p^{\gamma\beta} - J_{m-p}^{\alpha\delta}J_{n+p}^{\gamma\beta}\big)\Big]\\ &+\frac{1\mp 1}{2}\big(J_{n+m}^{\alpha\delta}J_0^{\gamma\beta} - J_0^{\alpha\delta}J_{n+m}^{\gamma\beta}\big)\,.\end{aligned} \tag{3.6.5}$$

Here the signs "±" in the second line of this formula originate from that of (3.6.2) and they are associated to the choice of the oscillator manifold $\Sigma_{N,\ell}^\pm$. The different signs on the third and fourth lines have different origin and they are related to the choice of $\mathscr{W}$, namely, the upper sign corresponds to $\mathscr{W}^+$ and the lower one to $\mathscr{W}^-$. The bracket (3.6.5) is not manifestly anti-symmetric, but its anti-symmetry can be seen from the following identity

$$\sum_{p=0}^{m}\big(J_{n+m-p}^{\alpha\delta}J_p^{\gamma\beta} - J_{m-p}^{\alpha\delta}J_{n+p}^{\gamma\beta}\big) = \sum_{p=0}^{n}\big(J_{n+m-p}^{\alpha\delta}J_p^{\gamma\beta} - J_{n-p}^{\alpha\delta}J_{m+p}^{\gamma\beta}\big) + J_n^{\alpha\delta}J_m^{\gamma\beta} - J_m^{\alpha\delta}J_n^{\gamma\beta}\,.$$

Further, we note that the zero modes $J_0^{\alpha\beta}$ form a Poisson subalgebra

$$\begin{aligned}&\{J_0^{\alpha\beta}, J_0^{\gamma\delta}\} = \delta^{\beta\gamma}J_0^{\alpha\delta} - \delta^{\alpha\delta}J_0^{\gamma\beta}\\ &\quad\pm\varkappa\Big[\rho_{\alpha\mu,\nu\rho}J_0^{\mu\beta}J_0^{\nu\delta} + J_0^{\alpha\mu}J_0^{\gamma\nu}\rho_{\mu\beta,\nu\delta} - J_0^{\gamma\nu}\rho_{\pm\alpha\mu,\nu\delta}J_0^{\mu\beta} - J_0^{\alpha\mu}\rho_{\mp\mu\beta,\gamma\nu}J_0^{\nu\delta}\Big]\,.\end{aligned}$$

Define for both choices of the sign in the last formula the quantity

$$\varpi^{\alpha\beta} = \delta^{\alpha\beta} + \varkappa J_0^{\alpha\beta}\,. \tag{3.6.6}$$

We then see that the Poisson bracket for the entries of ϖ is nothing else but the Semenov-Tian-Shansky bracket in the spin space

$$\{\varpi_1, \varpi_2\}_\pm = \pm(\rho\,\varpi_1\varpi_2 + \varpi_1\varpi_2\rho - \varpi_2\rho_\pm\varpi_1 - \varpi_1\rho_\mp\varpi_2). \tag{3.6.7}$$

We therefore recognize that ϖ is the non-abelian moment map for the Poisson actions (3.2.13) of the spin Poisson-Lie group (3.2.14) on $\Sigma_{N,\ell}^\pm$. Thus, $J_0^{\alpha\beta}$ generates infinitesimal spin transformations, while the conserved quantities $J_n^{\pm\alpha\beta}$ generate higher symmetries arising from conjunction of spin transformations with abelian symmetries generated by H_k.

Since on $\mathscr{P}$ the passage from J_n^- to J_n^+ can be understood as a redefinition of invariant spin variables, it is enough to consider one of these families. As is clear from (3.6.5), the Poisson algebra of $J_n^{+\alpha\beta}$ is simpler because a distinguished contribution of zero modes in the last line of (3.6.5) decouples. Introducing a generating function of the corresponding modes

$$J(\lambda) = \sum_{n=0}^{\infty} J_n^+ \lambda^{-n-1}\,, \tag{3.6.8}$$

we then convert (3.6.5) into the Poisson bracket between the currents. In the matrix notation this bracket reads as

$$\begin{aligned}\{J_1(\lambda), J_2(\mu)\}_\pm &= \frac{1}{\lambda-\mu}[C_{12}^{\rm s}, J_1(\lambda) + J_2(\mu)] \\ &\pm \varkappa\Big[\rho_\pm(\lambda,\mu)J_1(\lambda)J_2(\mu) + J_1(\lambda)J_2(\mu)\rho_\mp(\lambda,\mu) - J_2(\mu)\rho_\pm J_1(\lambda) - J_1(\lambda)\rho_\mp J_2(\mu)\Big]\,.\end{aligned} \tag{3.6.9}$$

Here we have introduce two spectral dependent r-matrices in the spin space

$$\rho_\pm(\lambda,\mu) = \rho \pm \frac{1}{2}\frac{\lambda+\mu}{\lambda-\mu}C_{12}^{\rm s} = \frac{\lambda\rho_\pm \mp \mu\rho_\mp}{\lambda-\mu}\,, \tag{3.6.10}$$

which are the standard solutions of the trigonometric[5] Yang-Baxter equation with properties

$$\rho_\pm(\mu,\lambda) = \rho_\mp(\lambda,\mu)\,, \quad P\rho_\pm(\lambda,\mu)P = -\rho_\pm(\mu,\lambda)\,,$$

where $P = C^{\rm s}$ is the permutation in the spin space. Note also that $\rho_\pm(\lambda, 0) = \rho_\pm$.

Formula (3.6.9) is the symmetry algebra of non-abelian integrals of the hyperbolic spin RS model. In the rational limit $\varkappa \to 0$ the bracket linearises and coincides with the defining relations of the positive-frequency part of the $\mathrm{GL}(\ell)$-current algebra [69]. The quadratic piece of (3.6.9) is the affine version of the Semenov-Tian-Shansky bracket that extends the Poisson algebra of zero modes, while the whole bracket is the Poisson pencil of the linear and quadratic structures. The algebra (3.6.9) has an abelian subalgebra spanned by $\mathrm{Tr}J(\lambda)^n$, $n \in \mathbb{Z}_+$, where the trace is taken over the spin space.

Finally, we note that the superintegrable structure of the model is ultimately responsible for the possibility to solve the equations of motion for invariant spins. Indeed, the equations of motion on $\mathscr{P}$ triggered by H_1 are

$$\dot{A} = -B\,, \quad \dot{B} = -BA^{-1}B\,, \quad \dot{a} = 0 = \dot{b}\,.$$

These equations imply that $BA^{-1} = I$ is an integral of motion and also $a = \text{const}$, $b = \text{const}$. Thus, equations for A and B are elementary integrated

$$A(\tau) = e^{-I\tau}A(0)\,, \quad B(\tau) = Ie^{-I\tau}A(0)\,. \tag{3.6.11}$$

[5] In the difference parametrization.

We assume that at the initial moment of time $\tau = 0$ the system is represented by a point on the reduced phase space $\mathscr{P}$. In particular, at this moment of time coordinates of particles constitute a diagonal matrix $A(0) \equiv \mathcal{Q}$ and the variables $a_{i\alpha}(0) \equiv a_{i\alpha}$ obey the Frobenius condition $\sum a_{i\alpha} = 1$ for any i. With this assumption, it is easy to see that $I = L(0)$, where L is the Lax matrix containing the dependence on the initial data. Then, the positions of particles at time τ are given by the solution $\mathcal{Q}(\tau)$ of the factorization problem $e^{-L(0)\tau}\mathcal{Q} = T(\tau)\mathcal{Q}(\tau)T(\tau)^{-1}$, where $T(\tau)$ is the Frobenius matrix satisfying the initial condition $T(0) = \mathbb{1}$. Equations of motion for invariant spins $\mathbf{a}_{i\alpha}(\tau)$ are then solved with the help of $T(\tau)$

$$\mathbf{a}_{i\alpha}(\tau) = \frac{T(\tau)^{-1}_{ij} a_{j\alpha}}{\sum\limits_{\beta} T(\tau)^{-1}_{ij} a_{j\beta}} = T(\tau)^{-1}_{ij} a_{j\alpha} \,.$$

A similar solution can be given for invariant spins $\mathbf{c}_{\alpha i}$. While oscillators $a_{i\alpha}$ mix under the time evolution with respect to their "particle" index i, the "spin" index α remains essentially untouched and the solution above is written for the whole ℓ-dimensional vector. This situation is, of course, a consequence of the spin symmetry commuting with the evolution flow.

Part II

Exactly solvable correlators in the fishnet Conformal Field Theory

Chapter 1
The Double-Scaling limit of γ-deformed $\mathcal{N} = 4$ SYM

1.1 Introduction

Quantum conformal field theories in various space-time dimensions attracted recently a considerable attention, not only due to their phenomenological importance in physics, for subjects ranging from the description of critical phenomena to the fundamental interactions beyond the Standard Model, but also due to their beautiful mathematical structure allowing to get a deeper insight into the fundamental structures of Quantum Field Theory and, via AdS/CFT duality, of Quantum Gravity. In spite of the considerable simplifications in the properties of CFTs in comparison with the massive QFTs, the non-perturbative structure of strongly interacting CFTs in $d > 2$ dimension is very complicated and in general not very well studied analytically.

A considerable progress in this direction has been achieved due to the conformal bootstrap methods [75, 76] based on the basic properties of CFTs following from the conformal symmetry, such as crossing symmetry in various channels for the four-point correlation functions. But this approach stays to a great extent "experimental", based on heavy numerical computations rather than on explicit analytic formulation of the final results.

A great progress in our understanding of analytic structure of CFTs in $d > 2$ dimensions has been achieved for various superconformal QFTs, often due to the AdS/CFT correspondence. In a special case – the $\mathcal{N} = 4$ SYM– the analytic study of the OPE data was greatly advanced due to the planar integrability of the theory [13][27]. In particular, the spectral problem – exact, all-loop calculation of anomalous dimensions of local operators – found its ultimate formulation in terms of the Quantum Spectral Curve (QSC) [77, 78] – a system of algebraic relations on Baxter-type Q-functions, supplied by analyticity properties and Riemann-Hilbert monodromy conditions (see recent reviews [79, 80]).

The integrability appears to persist - at least in some sectors - for a class of 3-parameter γ-deformations of the R-symmetry of $\mathcal{N} = 4$ SYM [81–83] if one tunes

	ϕ_1	ϕ_2	ϕ_3	ψ_1	ψ_2	ψ_3	ψ_4
Q_1	$+1$	0	0	$+\frac{1}{2}$	$-\frac{1}{2}$	$-\frac{1}{2}$	$+\frac{1}{2}$
Q_2	0	$+1$	0	$-\frac{1}{2}$	$+\frac{1}{2}$	$-\frac{1}{2}$	$+\frac{1}{2}$
Q_3	0	0	$+1$	$-\frac{1}{2}$	$-\frac{1}{2}$	$+\frac{1}{2}$	$+\frac{1}{2}$

Table 1.1: Charges of scalar and fermionic fields under the Cartan charges of R-symmetry $SU(4)$. These charges generate the symmetry group $U(1)\otimes U(1)\otimes U(1)$ left over after the breaking of R-symmetry by twisting. The $SU(N)$ gauge field A_μ has zero R-charges.

the so-called double-trace terms, generated by the RG of the model, to their critical, in general complex values [36, 84]. This γ-deformation of $\mathcal{N}=4$ SYM describes a family of non-sypersymmetric and non-unitary four-dimensional CFTs labeled by 't Hooft coupling g and three γ-deformation angles $\gamma_j,\ j=1,2,3$. The Lagrangian of such theory reads (see e.g.[85])

$$\mathcal{L}=N_c\mathrm{Tr}\left[-\frac{1}{4}F_{\mu\nu}F^{\mu\nu}-\frac{1}{2}D^\mu\phi_i^\dagger D_\mu\phi^i+i\bar{\psi}_{\dot{\alpha}\ A}D^{\dot{\alpha}\alpha}\psi^A_\alpha\right]+\mathcal{L}_{\text{int}}\,, \tag{1.1.1}$$

where $i=1,2,3\ \ A=1,2,3,4,\ D^{\dot{\alpha}\alpha}=D_\mu(\bar{\sigma}^\mu)^{\dot{\alpha}\alpha}$ and

$$\begin{aligned}\mathcal{L}_{\text{int}}=N_cg\ \mathrm{Tr}\ \Big[&\frac{g}{4}\{\phi_i^\dagger,\phi^i\}\{\phi_j^\dagger,\phi^j\}-g\,e^{-i\epsilon^{ijk}\gamma_k}\phi_i^\dagger\phi_j^\dagger\phi^i\phi^j\\ &-e^{-\frac{i}{2}\gamma_j^-}\,\bar{\psi}_j\phi^j\bar{\psi}_4+e^{+\frac{i}{2}\gamma_j^-}\,\bar{\psi}_4\phi^j\bar{\psi}_j+i\epsilon_{ijk}e^{\frac{i}{2}\epsilon_{jkm}\gamma_m^+}\psi^k\phi^i\psi^j\\ &-e^{+\frac{i}{2}\gamma_j^-}\,\psi_4\phi_j^\dagger\psi_j+e^{-\frac{i}{2}\gamma_j^-}\,\psi_j\phi_j^\dagger\psi_4+i\epsilon^{ijk}e^{\frac{i}{2}\epsilon_{jkm}\gamma_m^+}\bar{\psi}_k\phi_i^\dagger\bar{\psi}_j\Big]\,.\end{aligned} \tag{1.1.2}$$

where the summation is assumed w.r.t. doubly and triply repeating indices, and we use the standard notations for scalar, fermionic fields, covariant derivative and $F_{\mu\nu}$ tensor. We suppress the Lorentz indices of fermions, assuming the contractions $\psi_i^\alpha\psi_{j,\alpha}$ and $\bar{\psi}_{i,\dot{\alpha}}\bar{\psi}_j^{\dot{\alpha}}$. We also use the notations

$$\gamma_1^\pm=-\frac{\gamma_3\pm\gamma_2}{2},\quad\gamma_2^\pm=-\frac{\gamma_1\pm\gamma_3}{2},\quad\gamma_3^\pm=-\frac{\gamma_2\pm\gamma_1}{2}\,. \tag{1.1.3}$$

The parameters of the γ-deformation $q_j=e^{-\frac{i}{2}\gamma_j}\ j=1,2,3$ are related to the Cartan subalgebra $\mathfrak{u}(1)^3\subset\mathfrak{su}(4)\cong\mathfrak{so}(6)$ and the value of such charges for the fields are represented in Tab.1.1.

As regards the conformal data, for the non-deformed $\mathcal{N}=4$ SYM several OPE have been studied in numerous papers, using the integrability properties, as well as AdS/CFT correspondence for the strong coupling regime $g\to\infty$, or a direct Feynman graph calculus at weak coupling $g\to 0$. Apart from the spectral problem, an impressive progress has been achieved in a more difficult problem of computation of structure constants and correlation functions [86–89], as well as of $1/N_c^2$ corrections [90]. However, the efficient all-loop solution of these problems is still hindered by outstanding technical complexity. We also have to admit that integrability of $\mathcal{N}=4$ SYM is still a somewhat mysterious phenomenon, not very well understood, especially on the CFT side of this AdS_5/ CFT_4 duality.

In 2015, Ö. Gürdogan and V. Kazakov proposed a family of non-unitary, non-supersymmetric CFTs [32], based on a special double scaling limit of γ-deformed $\mathcal{N}=4$ SYM combining weak coupling limit of small 't Hooft coupling, $g\to 0$, and strong imaginary twist, $\gamma_j \to i\infty$, with three finite effective couplings $\xi_j = ge^{-i\gamma_j/2}$. The gauge field A_μ and the gaugino ψ_4 decouple in this limit and one is left with three complex scalars and three complex fermions with certain chiral structure of interactions (see the Lagrangian of the theory (1.2.1),(1.2.2)). These CFTs, on the one hand, helps to shed some light on the origins of integrability in $\mathcal{N}=4$ SYM, and on the other hand, the double scaling limit significantly facilitates the computations of interesting physical properties, such as the OPE data and certain multi-loop Feynman graphs, revealing rich and instructive dynamical properties of the theory. These dynamical properties were further studied in [91], in particular, by the asymptotic Bethe ansatz methods. This full three-couplings double scaled version of $\mathcal{N}=4$ SYM was dubbed in [91] the chiral CFT, or, shortly, χCFT. We will employ this name in what follows.

In the single coupling reduction, $\xi_1=\xi_2=0$, $\xi_3\neq 0$, the theory reduces to two interacting complex scalar matrix fields (see eq.(1.2.6)). The planar Feynman graphs for typical physical quantities in such a bi-scalar theory appear to have, at least in the bulk, the fishnet structure where the massless scalar propagators form a regular quadratic lattice [32]. This theory will be called in what follows the bi-scalar, or fishnet CFT. The fishnet graphs of simple topology, such as a torus, appear to represent an integrable statistical mechanical system [92]. Remarkably, there exists also an integrable generalization of the Fishnet CFT to any dimension d [28], presented extensively in the next chapter of this thesis.

Many results recently obtained for the bi-scalar fishnet CFT, would be utterly difficult to achieve for the analogous quantities in the full γ-deformed $\mathcal{N}=4$ SYM. First of them, the anomalous dimensions of the operators Tr $[\phi_1^L]$ – dominated by wheel-type fishnet Feynmann diagrams – were computed explicitly, in terms of multiple zeta values (MZV), at two wrappings (up to $2L$ loops for any L [32, 93]) and, iteratively, to any loop order for $L=3$. Another remarkable example of exact computations, unique in $d>2$ CFTs, are the all-loop four-point correlation functions of the shortest protected operators [36, 37, 80]. The biscalar fishnet CFT gives a unique opportunity for the study of single-trace multi-point correlators and of the related exact planar scalar amplitudes, revealing their Yangian symmetry [94, 95]. One is even able to compute exactly, using the above mentioned exact four-point correlators, the simplest non-planar ($\sim 1/N_c^2$) scattering amplitude [96] (see also [97] for the perturbative study of this amplitude).

All this shows that this integrable theory resulting from the double-scaling limit of planar γ-deformed $\mathcal{N}=4$ SYM allows a unique insight into the non-perturbative structure of strongly interacting CFTs and a closer look at them could reveal many general properties of CFTs in $d > 2$ dimensions. It is also worth mentioning the existence of 3 dimensional analogues of these CFTs, obtained by a similar limit from the three-dimensional γ-deformed ABJM model [91] dominated by fishnet graphs with regular triangular structure, as well as the 6d version of fishnet CFT [98], where the fishnet graphs have a regular hexagonal structure. The "bulk" integrability of all three cases of regular fishnet planar graphs was predicted in [92].

In this thesis we attempt to extend the study of some of the questions already explored in the case of bi-scalar fishnets, to the full double-scaling limit of $\mathcal{N} = 4$ SYM theory. First of all, we will give the complete description of the bulk structure of Feynman graphs (far from their boundaries defined by the particular underlying physical quantities). It appears to be much richer than in the fishnet CFT, though much simpler than in the full $\mathcal{N} = 4$ SYM conserving a certain lattice regularity. A pictorious way to describe these graphs is to introduce the regular triangular lattice and then to do all possible Baxter moves of all three types of lines, as shown on Fig.1.2. These lines should represent sequences of bosonic and fermionic propagators and the mixed intersections (where both bosonic and fermionic propagators meet) should be disentangled, in a unique way, into pairs of Yukawa vertices). These configurations should be summed up, so that the collection of such graphs could be called the "dynamical fishnet". The integrability of these graphs, or the sum of them, remains to be proved, though we demonstrate it in this chapter in a simpler case of the two-coupling reduction of χCFT (see eq.(1.2.4)), with two bosonic and one Yukawa coupling.

In the next chapters we will compute exactly the 4-point correlation functions of certain short, protected scalar operators, similar those obtained in fishnet CFT [36, 37, 80], for its d-dimensional generalization and for the full χCFT_4. For that we identify all the graphs contributing these quantities and sum them up using the Bethe-Salpeter approach helped by the conformal invariance. In comparison to the fishnet CFT, the two-coupling dependence of these correlators in the full double-scaled CFT will reveal a rich phase structure in the coupling space. In the remaining sections of this chapter we provide details about the theory under study, its reductions, its conformality and the bulk topology of large Feynmann diagrams in the planar limit.

1.2 Feynman graphs and correlators of χCFT

In this section, we will study the generic structure of planar Feynman graphs and discuss their integrability properties, in the full three-coupling chiral CFT (χCFT) proposed in [32] (see also [91] for more details).

This CFT was obtained as a double scaling limit of γ-twisted $\mathcal{N} = 4$ SYM described above. It is defined by the Lagrangian for three complex scalars and three complex fermions transforming in the adjoint representation of $SU(N_c)$:

$$\mathcal{L}_{\phi\psi} = N_c \mathrm{Tr}\left(-\frac{1}{2}\partial^\mu \phi_j^\dagger \partial_\mu \phi^j + i\bar{\psi}_j^{\dot{\alpha}} (\tilde{\sigma}^\mu)^\alpha_{\dot{\alpha}} \partial_\mu \psi^j_\alpha\right) + \mathcal{L}_{\rm int}\,, \tag{1.2.1}$$

where the sum is taken with respect to all doubly repeated indices, including $j = 1,2,3$, and the interaction part is

$$\mathcal{L}_{\rm int} = N_c\,\mathrm{Tr}\Big[\xi_1^2\,\phi_2^\dagger\phi_3^\dagger\phi^2\phi^3 + \xi_2^2\,\phi_3^\dagger\phi_1^\dagger\phi^3\phi^1 + \xi_3^2\,\phi_1^\dagger\phi_2^\dagger\phi^1\phi^2 + i\sqrt{\xi_2\xi_3}(\psi^3\phi^1\psi^2 + \bar{\psi}_3\phi_1^\dagger\bar{\psi}_2) + i\sqrt{\xi_1\xi_3}(\psi^1\phi^2\psi^3 + \bar{\psi}_1\phi_2^\dagger\bar{\psi}_3) + i\sqrt{\xi_1\xi_2}(\psi^2\phi^3\psi^1 + \bar{\psi}_2\phi_3^\dagger\bar{\psi}_1)\Big]. \tag{1.2.2}$$

We suppressed in the last equation the spinorial indices assuming the scalar product of both fermions in each term. We will refer to this theory as χCFT theory.
The double scaling procedure and the derivation of this action from γ-deformed $\mathcal{N}=4$ SYM can be found in papers [85],[91]. In the next sections, we will study the four-point functions obtained by point splitting of fields in coinciding points, in the two-point correlation functions of local operators of the type:

$$\mathrm{Tr}[\phi_j^2(x)] \quad (j=1,2,3)\,. \tag{1.2.3}$$

Since the Lagrangian (1.2.2) depends on three arbitrary couplings, one can tune their values to obtain interesting reductions of this χCFT. For example, in the limit $\xi_1 \to 0$, one fermion decouples and we obtain the following action [91]

$$\mathcal{L}_{\rm int} = N_c\,\mathrm{Tr}\left(\xi_3^2\,\phi_1^\dagger\phi_2^\dagger\phi^1\phi^2 + \xi_2^2\,\phi_3^\dagger\phi_1^\dagger\phi^3\phi^1 + i\sqrt{\xi_2\xi_3}(\psi^2\phi^1\psi^3 + \bar{\psi}_2\phi_1^\dagger\bar{\psi}_3)\right). \tag{1.2.4}$$

We will refer to this theory as χ_0CFT theory. Another interesting case of (1.2.2) occurs when all three couplings are equal $\xi_1 = \xi_2 = \xi_3 = \xi$ and corresponds to the doubly-scaled β-deformed SYM [99, 100]. It has the following interaction Lagrangian [91]

$$\begin{aligned}\mathcal{L}_{\rm int} &= \xi^2 N_c\,\mathrm{Tr}\left(\phi_2^\dagger\phi_3^\dagger\phi^2\phi^3 + \phi_3^\dagger\phi_1^\dagger\phi^3\phi^1 + \phi_1^\dagger\phi_2^\dagger\phi^1\phi^2\right)\\ &+ i\xi N_c \mathrm{Tr}\left(\psi^3\phi^1\psi^2 + \bar{\psi}_3\phi_1^\dagger\bar{\psi}_2 + \psi^1\phi^2\psi^3 + \bar{\psi}_1\phi_2^\dagger\bar{\psi}_3 + \psi^2\phi^3\psi^1 + \bar{\psi}_2\phi_3^\dagger\bar{\psi}_1\right).\end{aligned} \tag{1.2.5}$$

In this case, one supersymmetry is left unbroken, as in the original β-deformed $\mathcal{N}=1$ SYM.

Most of the papers on this relatively young subject were devoted to the above-mentioned single coupling reduction of this model: $\xi_1 = \xi_2 = 0, \quad \xi_3 \equiv \xi \neq 0$, i.e. the *bi-scalar*, fishnet CFT defined by the action [32]:

$$\mathcal{L}_\phi = \frac{N_c}{2}\mathrm{Tr}\left(\partial^\mu\phi_1^\dagger\partial_\mu\phi^1 + \partial^\mu\phi_2^\dagger\partial_\mu\phi^2 + 2\xi^2\,\phi_1^\dagger\phi_2^\dagger\phi^1\phi^2\right)\,. \tag{1.2.6}$$

In the following we will describe the general bulk structure of the planar Feynman diagrams of (1.2.1). Indeed, one interesting feature of those models is the drastic

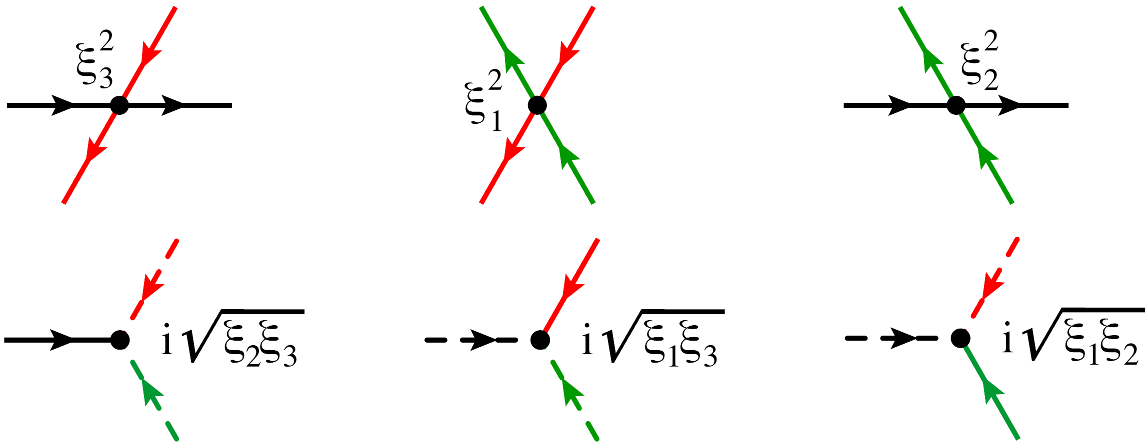

Figure 1.1: The chiral vertices of the doubly scaled theory (1.2.2). The graphs of the first line represent the quartic scalar interactions and the ones in the second line are the Yukawa interactions. Tick solid lines and dashed lines represent scalar and fermionic propagators respectively. Colors stand for the various "flavour" of the particles ϕ^i and ψ^i: black for $i=1$, red for $i=2$ and green for $i=3$. Arrows symbolize the fixed orientation (chirality) of the vertices and, according to our notation, they point always to the fields with bars or daggers. The second chirality of Yukawa interactions *i.e.* the one with $\bar{\psi}_i \to \psi^i$ and $\phi_i^\dagger \to \phi^i$ with $i=1,2,3$, can be represented as the second line of vertices with flipped arrows.

simplification of their weak coupling expansions in terms of Feynman diagrams in the planar limit. In general, any diagram of χCFT can be built as a collection of the vertices in Fig.1.1, connected by scalar and fermionic propagators[1]. The arrows indicate the fixed orientation (chirality) of the interactions, i.e. in a propagator it is directed from a field to its hermitian conjugate. An essential feature of (1.2.2) is the absence of the hermitian conjugate of every interaction vertex. The chirality of this theory makes it non-unitary and plays a crucial role for the underlying conformality and integrability in the 't Hooft limit. In fact, in the absence of the hermitian conjugate vertices, all the graphs which could renormalize the couplings and the mass are non-planar. As a consequence, we will see in sec.1.2.2 that the planar weak coupling expansion of physical quantities w.r.t. interactions (1.2.2) in χCFT is dominated, at least in the bulk and for high enough perturbative order, by a specific class of planar diagrams having a kind of a lattice structure, much more rigid than the structure of graphs in the original $\mathcal{N}=4$ SYM. This lattice structure is, however, richer and more "dynamical" than in the bi-scalar theory where the unique regular square fishnet structure dominates at any order in perturbation theory. In the full χCFT, due to the presence of Yukawa interactions and quartic scalar vertices, there are more planar graphs contributing at each perturbative order, but the chirality still dramatically reduces their number. We can dubb the structure of full χCFT graphs as "dynamical fishnet".

[1]Apart from the double-trace vertices [101, 102] whose role will be discussed below.

1.2.1 Double-trace interactions and conformal symmetry

The γ-deformed $\mathcal{N}=4$ SYM theory and its doubly-scaled version are not conformal invariant, not even in the planar limit [85]. Indeed, the renormalization group calculations show [103] that the new, scalar double-trace interactions are generated

$$\mathcal{L}_{\rm dt} = (4\pi)^2 \sum_{j=1}^{3} \Big[\alpha_{1,j}^2 \,\mathrm{Tr}[\phi_j\phi_j]\mathrm{Tr}[\phi_j^\dagger\phi_j^\dagger] + \alpha_{2,j}^2\,\mathrm{Tr}[\phi_j\phi_{j_+}^\dagger]\mathrm{Tr}[\phi_j^\dagger\phi_{j_+}] + \alpha_{3,j}^2\,\mathrm{Tr}[\phi_j\phi_{j_+}]\mathrm{Tr}[\phi_j^\dagger\phi_{j_+}^\dagger]\Big] \,, \tag{1.2.7}$$

where in our notation $j_+ = j+1$ with the constraint $3_+ = 1$. The double-trace couplings $\alpha_{k,j}$ generically flow with the scale. They are needed to renormalise the 2-point correlators of the local operators $\mathrm{Tr}[\phi_j\phi_j]$, $\mathrm{Tr}[\phi_j\phi_{j_+}^\dagger]$ and $\mathrm{Tr}[\phi_j\phi_{j_+}]$ respectively. For any of these planar correlators only one double-trace term contributes, that is the β-function of each $\alpha_{k,j}$ depends only on couplings $\{\xi_1,\xi_2,\xi_3\}$ and $\alpha_{k,j}$ itself. Due to permutation symmetry of flavour indices $j=1,2,3$ in the Lagrangian (1.2.1), the functions $\beta_{\alpha_{k,j}}$ show the same symmetry in the coupling dependence, namely

$$\beta_{\alpha_{k,j}}(\alpha_{k,j},\xi_j,\xi_{j_+},\xi_{j_-}) \;=\; \beta_{\alpha_{k,j'}}(\alpha_{k,j'},\xi_{j'},\xi_{j'_+},\xi_{j'_-})\,, \tag{1.2.8}$$

thus will drop in what follows the specification of subscript j in double-trace couplings. The double-trace terms (1.2.7) appear in the theory already at one-loop renormalization and the β-functions associated to the couplings α_k^2 are not zero. In γ-deformed $\mathcal{N}=4$ SYM the one-loop β-function associated to the double-trace interaction $\alpha_1^2\,\mathrm{Tr}[\phi_j\phi_j]\mathrm{Tr}[\phi_j^\dagger\phi_j^\dagger]$ of (1.2.7) is [103]

$$\beta_{\alpha_k} = \frac{g^4}{\pi^2}\sin^2\gamma_k^+\sin^2\gamma_k^- + 4^3\pi^2\alpha_k^4 + \mathcal{O}(g^6,\alpha_k^6)\,, \tag{1.2.9}$$

where $\gamma_k^\pm$ are linear combinations of the deformation parameters γ_j of the theory defined in (1.1.3). Let us turn to the theory (1.2.2) with the double-trace terms (1.2.7). In contrast to the bi-scalar theories, where the invariance under exchange

$$\begin{cases} \phi_j \longrightarrow \phi_{j_+} \\ \phi_{j_+} \longrightarrow \phi_j^\dagger \end{cases} \tag{1.2.10}$$

allows to identify α_2 and α_3, the presence of Yukawa interactions in χCFT specifically breaks this symmetry, and operators $\mathrm{Tr}[\phi_j\phi_{j_+}^\dagger]$ and $\mathrm{Tr}[\phi_j\phi_{j_+}]$ show different behaviour. When only one α_k coupling is running, the corresponding β-function has the following form

$$\beta_{\alpha_k} = a(\xi) + b(\xi)\,\alpha_k^2 + c(\xi)\,\alpha_k^4\,, \tag{1.2.11}$$

where a,b,c are functions of the couplings $\xi=\{\xi_1,\xi_2,\xi_3\}$. This quadratic behavior of β as a function of α_k^2 was encounter for the first time in [102] as an example of non-supersymmetric orbifold theories with double-trace interactions and established in [104] for a generic deformed theory in the 't Hooft limit. If the running coupling α_k is associated to the double trace interaction $\mathrm{Tr}\mathcal{O}\mathrm{Tr}\mathcal{O}^\dagger$ of length-two scalar operators

$\mathcal{O}$, the functions a, b and c are related to the normalization coefficient of the two-point function of $\mathcal{O}$, the contribution of the single-traces to the anomalous dimension of $\mathcal{O}$ and the coefficient of the induced double-trace terms.

To make the theory conformal at the quantum level, one needs to tune the double-trace couplings to a fixed point. In the original γ-deformed $\mathcal{N}=4$ SYM , the 't Hooft coupling g^2 is not running, so the critical (conformal) point for double-trace couplings can be computed imposing the vanishing of their β-functions. In the case of a single running coupling, (1.2.9) has the following fixed points

$$\alpha^2_{k\star} = \pm \frac{ig^2}{8\pi^2} \sin\gamma_k^+ \sin\gamma_k^- + \mathcal{O}(g^4)\,. \tag{1.2.12}$$

Similarly, the coupling constants ξ_i of the theory (1.2.2) are not running in the 't Hooft limit and one can fine-tune the double-trace couplings α_i^2 to critical values in terms of their ξ_i dependence, imposing the vanishing of the underlying β-function (1.2.11) as follows

$$\beta_{\alpha_k} \stackrel{!}{=} 0 \qquad \Rightarrow \qquad (4\pi)^2\alpha^2_{k\star} = -\frac{b \pm \sqrt{b^2-4ac}}{2c}\,. \tag{1.2.13}$$

At the two fixed points (1.2.13), it is possible to write the anomalous dimension $\gamma_\star$ of the operator $\mathcal{O}$ in terms of the discriminant of $\beta_{\alpha_k}=0$ [104]

$$4\gamma^2_{\mathcal{O}\star} = b^2 - 4ac\,. \tag{1.2.14}$$

At the fixed points for all double-trace couplings (1.2.7) of γ-deformed $\mathcal{N}=4$ SYM , the theory becomes a genuine non-supersymmetric CFT. This conformal theory appears also to be integrable [36, 82, 83] and its spectrum of anomalous dimensions can be treated by such a powerful tool as quantum spectral curve (QSC) [77, 78, 83]. The same statements hold for the double-scaling limit of the $4D$ χCFT theory (1.2.2), to which we have to add the double-trace Lagrangian (1.2.7). Integrability of the full χCFT is still a conjecture, as it is for the full γ-deformed $\mathcal{N}=4$ SYM . It was demonstrated explicitly only for the simplest reduction of χCFT – the bi-scalar CFT (1.2.6), where the fishnet planar graphs have an iterative regular lattice structure [32], shown to be integrable long ago by A.Zamolodchikov [92] (see also [39]). We extended the proof of integrability to a larger, two-coupling sector of χCFT in Sec.4.1.1, by methods of conformal $SU(2,2)$ quantum spin chain. In the case of χCFT we also have good chances to prove full integrability on the level of planar Feynman graphs since, as we show below, these graphs preserve a certain rigid lattice structure.

The obvious physical defect of such CFTs is the loss of unitarity. Indeed, as it will be clear with the explicit example below, the discriminant of the equation $\beta_{\alpha_i}=0$ is negative, inducing complex values for the fixed points (1.2.13) and anomalous dimension (1.2.14). Moreover in the AdS/CFT context, this fact can be interpreted as the presence of true tachyons in the bulk on the string theory side [104].

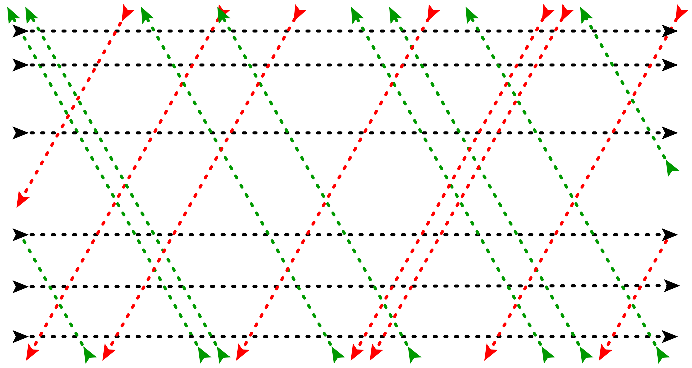

Figure 1.2: General "dynamical" fishnet bulk structure of a planar graph for 3-coupling chiral CFT (1.2.2). Dotted lines represent scalar or fermionic propagators (the rules for the choice of propagators will be explained below and demonstrated in Fig.1.3) The colors and directions of the lines stand for the three "flavours" of the particles $i = 1, 2, 3$ with the same notation as we used in Fig.1.1. The intersections correspond to six different effective vertices that can be written in terms of the usual ones following the map given in Tab.1.2.

The one-loop anomalous dimension of the length-two operator $\mathrm{Tr}[\phi_j \phi_j]$ in γ-deformed $\mathcal{N} = 4$ SYM at the fixed point is [103]

$$\gamma_{\phi_j \phi_{j\star}} = \mp \frac{ig^2}{2\pi^2} \sin \gamma_j^+ \sin \gamma_j^- + \mathcal{O}(g^4). \tag{1.2.15}$$

Notice that both the fixed points (1.2.12) and the anomalous dimensions (1.2.15) are complex conjugate, as expected. Those relations are actually valid in the full γ-deformed $\mathcal{N} = 4$ SYM theory, but in the double-scaling limit under analysis it is simple to obtain some predictions for the one-loop β, the associated critical points and the anomalous dimensions. In particular we have

$$\gamma_{\phi_j \phi_{j\star}} \overset{\text{DS limit}}{=} \mp 2i(\xi_{j+}^2 - \xi_{j-}^2) + \dots \qquad \text{and} \qquad \alpha_{1\star}^2 \overset{\text{DS limit}}{=} \pm i \frac{\xi_{j+}^2 - \xi_{j-}^2}{2} + \dots . \tag{1.2.16}$$

In Sec.4.3.3 we will verify these results computing the exact spectrum of the operator $\mathrm{Tr}[\phi_j \phi_j]$ with the Bethe-Salpeter method, and the first order of the fixed point $\alpha_{1\star}^2$ using Feynman diagrams.

Non-unitary CFTs are usually logarithmic [105], i.e. with an interesting, logarithmic behavior of certain correlators. The γ-deformed $\mathcal{N} = 4$ SYM and its double-scaled version – the χCFT (1.2.2) (and its reductions mentioned above) are not exceptions: they show the same logaritmic properties due to the non-hermiticity of their dilatation operators [38, 39].

1.2.2 Bulk structure of large planar graphs

Let us try to describe the general structure of an arbitrarily big Feynman graph in the bulk, far from the boundaries. The generic picture is illustrated on Fig.1.2. The theory (1.2.2) contains 3 complex scalars ϕ^i and 3 complex fermions ψ^i labelled by $i = 1, 2, 3$. We chose to represent scalar propagators with thick solid lines and fermionic propagators with dashed lines (see Fig.1.1), while the label denoting their $U(1)^{\otimes 3}$ flavour (see App.(1.1)) is mapped into colours: $(1, 2, 3) \equiv (black, red, green)$. In Fig.1.2, coloured dotted[2] lines in a particular direction represent a generic propagator, both scalar or fermionic. In this framework, a set of parallel lines represents any combination of fermionic and scalar propagators of a given flavour.

This system of three dotted lines forms a lattice which combines the features of both regularity and irregularity. Any such lattice can be obtained from the regular triangular lattice (or a more general Kagomé lattice) by arbitrary Baxter moves of all lines: displacements in the direction orthogonal to the line, i.e. conserving its direction.

The links of the resulting lattice are propagators while nodes are quartic *effective interactions*. These interactions are of three kinds, depending on which lines are crossing and which propagators enter the corresponding crossing (effective vertex). They can represent a set of ϕ^4 or various Yukawa vertices, according to the rules listed in Tab.1.2. Indeed in this framework, a quartic vertex involving fermions can be though of as a couple of Yukawa vertices, or similarly, as a split quartic vertex in which we have added a propagator in the remaining direction, according to the rules in Tab.1.2. The quartic interaction can involve four scalars, four fermions or two of each. Moreover, we chose the directions of the arrows to be consistent with the Feynman rules in Fig.1.1. Depending on the orientation of the mixed interactions we will refer to them as *crossing* or *scattering* interactions as in Tab.1.2.

Given three sets of parallel lines crossing each other with quartic interactions, the resulting irregular lattice is formed by a finite set of convex polygons. The smallest possible n-gon is a triangle and the largest one is a hexagon. Those convex polygons can be constructed locally by the abovementioned moves of lines in two or three different directions:

- *2 directions (colors)*: We can discard the lines in one of the directions. The local interaction of lines with only two directions (colors) forms a square lattice as in [32, 92]. Since we are considering three colors, we can have three different squares depending on their directions.
- *3 directions (colors)*: In this case there are more possibilities to build convex polygons. Indeed let's start with the crossing of three lines with three different directions. Locally, they form a triangle that can have two different orientations. Adding another line, parallel to one of the previous three, and cutting the triangle, we will end up with a square. Since we can add a line of any color and there are two possible triangle orientations, we can draw 6 different squares. Iterating this cutting procedure by adding one and two lines we obtain pentagons and the hexagon.

[2]The reader should distinguish between dashed lines, representing fermionic propagators, and dotted lines representing the lattice based on effective vertices.

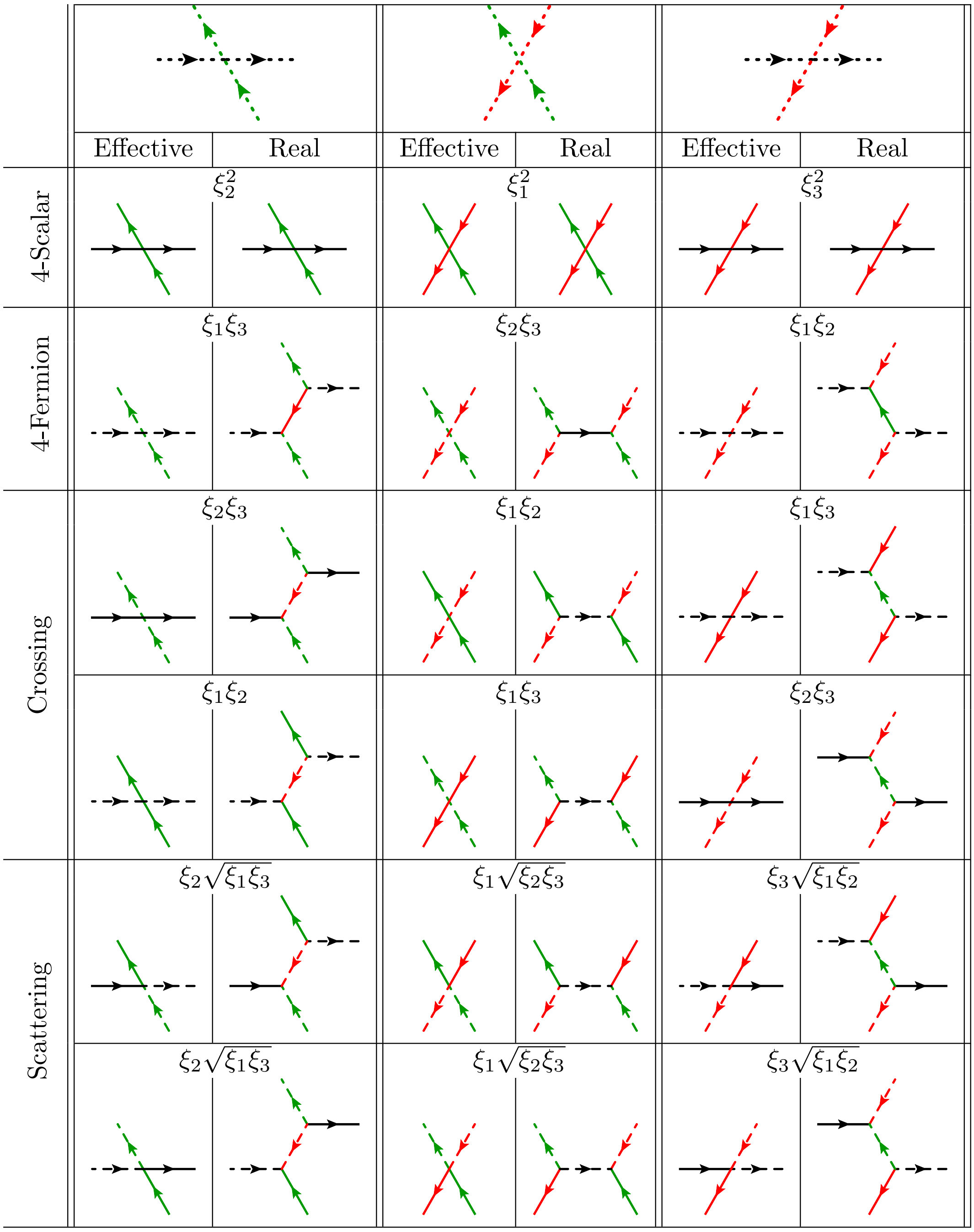

Table 1.2: Substitution rules for the effective vertices appearing in the fishnet bulk structure of Fig.1.2 in terms of the Feynman rules of Fig.1.1. Any effective vertices is associated with a combination of the coupling constants ξ_i with $i = 1, 2, 3$ of order ξ^2.

In the following table we recap all the possible n-gons and their multiplicity, that is the number of different ways (i.e.: not superposable by simple translation and scaling) the same polygon can appear in the graph.

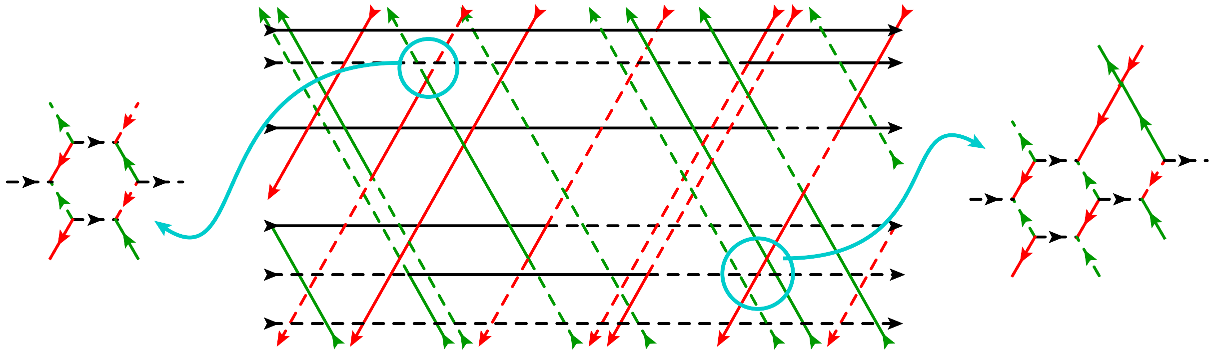

Figure 1.3: One of the possible configurations in terms of effective vertices of Tab.1.2 for the bulk topology represented in Fig.1.2. The diagrams at the two sides of the figure represents the parts of the graph in the light-blue circles in terms of real vertices of Fig.1.1 according with the rules given in Tab.1.2. We stress that given a set of effective vertices, the translation in real vertices is unique.

n-gon	△	□	⬠	⬡
Multiplicity	2	9	6	1

It follows that for a given set of lines, the resulting lattice can be seen as a tiling of the plane with 18 different tiles.

The structure of the fishnet bulk is very rich, indeed once the topology of the lattice is defined as in Fig.1.2, some information is lost, as any quartic effective vertex can be associated to six different physical vertices, as listed in Tab.1.2. The number of possible Feynman diagrams N_d which can be associated to a given close n-gon, defined by n quartic effective vertices, can be computed considering first all possible combinations of fermionic and scalar propagators for the edges of the polygon and then cancel out those vertices which does not fit in any configuration. After this tedious combinatorics we obtain the following table

n-gon	△	□	⬠	⬡
N_d	28	82	244	730

This result can be written in the following compact formula

$$N_d(n) = 1 + 3^n \,. \tag{1.2.17}$$

Now we can estimate the number of Feynman diagrams for a given topology of the effective fishnet bulk. This number has the sum of all the N_d's for all the polygons as an upper bound and we can estimate its order of magnitude. Then the number of possible Feynman diagrams for the topology of the fishnet bulk given in Fig.1.2 is around 1.5×10^4. Moreover, since any vertex is associated with a combination of the couplings ξ_i with $i = 1, 2, 3$ of order 2, we know that the diagram in Fig.1.2 is of order ξ^{234}. One of those configurations is represented in Fig.1.3.

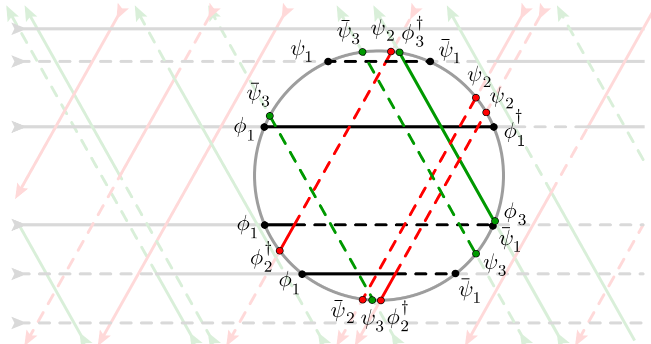

Figure 1.4: The result of drawing a disc on the lattice of Fig.1.3 can be interpreted as one planar graph contributing to an n-point functions of the kind (1.2.18), drawn in terms of *effective* vertices. In this example we present Tr $[\phi_1\bar{\psi}_3\psi_1\bar{\psi}_3\psi_2\phi_3^\dagger\bar{\psi}_1\psi_2\psi_2\phi_1^\dagger\phi_3\bar{\psi}_1\psi_3\bar{\psi}_1\phi_2^\dagger\psi_3\bar{\psi}_2\phi_1\phi_2^\dagger\phi_1](x_1\dots x_{20})$, and the graph is of order ξ^{42}. As it results from Tab.1.2, each effective vertex can be replaced in a univocal way in terms of structure made of real vertices.

1.2.3 Single-trace correlation functions

We can realize the above mentioned bulk graphs (with fixed coordinates of external legs) as a single-trace operator of the form:

$$K(x_1,x_2,\dots,x_M) = \text{Tr}\ [\chi(x_1)\chi(x_2)\dots\chi(x_M)]\,, \tag{1.2.18}$$

$$\chi \in \{\phi_j,\phi_j^\dagger,\psi_j^\alpha,\bar{\psi}_j^{\dot\alpha}\}, \qquad (j=1,2,3;\ \alpha,\dot\alpha=1,2\,), \tag{1.2.19}$$

i.e. each $\chi(x)$ under the trace is one of 18 fields of the χCFT model (1.2.1)-(1.2.2). Of course (1.2.18) must have zero overall R-charge, to have a non-zero answer. This implies a condition on the elementary fields under trace, namely if we define n_j and m_j as the differences between the number of ϕ_j, respectively ψ_j and the conjugated fields, the mentioned condition reads

$$n_j + 2m_j - \sum_{k\neq j} n_k = 0\,, \qquad j=1,2,3\,. \tag{1.2.20}$$

To describe the Feynman graph content of this quantity, let us remind that a similar single-trace correlator in bi-scalar fishnet CFT [94, 95], consisting only of scalar fields, was given by a single fishnet graph of the disc topology where the disc was cut out across the edges of a regular square lattice. The ends of the cut edges represented external fixed coordinates and the integrals were taken over all vertices inside the disc. Similarly, for each of the quantities (1.2.18) there exist a collection of graphs of the disc shape cut out of the lattice of the type drawn on Fig. 1.3. The types of external legs – the cut edges along the boundary – define the species of fields from the set χ following in the same order under the trace in (1.2.18). We present an example in Fig.1.4, where the disc is drawn on the concrete realization of the lattice as given in Fig.1.3. A big difference w.r.t. the bi-scalar single-trace correlators is that in the full χCFT such a quantity is defined by the sum of all graphs with the same order of fields on the boundary (same sequence of external legs) which are related to each other

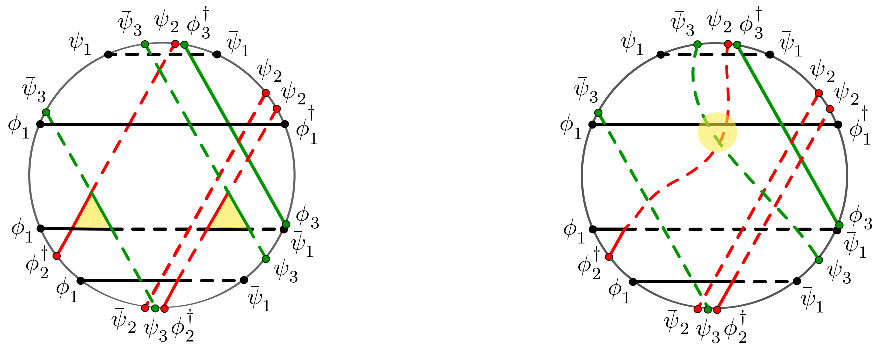

Figure 1.5: Other possible planar graphs for the same 20-point function of Fig.1.4 at order ξ^{48}. On the left, the yellow triangles have different edges w.r.t. Fig.1.4. On the right, one red-dashed line has been moved down-right, changing the topology w.r.t. Fig.1.4 in the highlighted region.

by the orthogonal moves of three types of parallel lines described in the previous subsection (as example, see Fig.1.5 (right)). Furthermore, even at fixed topology, one can change the interaction vertices inside the graph, namely switching some dashed (fermionic) lines to solid (scalar) lines and vice-versa (Fig.1.5 (left)). This corresponds to different realizations of a disc segment of the dotted-lattice in Fig.1.2 with boundary conditions fixed by the external legs. The number of possible graphs can be estimated by considerations of the previous subsection. This single-trace correlator can be used to define the scattering amplitudes via Lehmann-Symanzik-Zimmerman procedure, by going to the dual momentum space and taking on-shell external momenta, in the spirit of the papers [94, 95]. It is worth noticing that not all the planar single-trace correlators are obtained out of this procedure. Indeed certain external states can be cut out only drawing a circle on the actual Feynman graph (see Tab.1.2) where all propagators are explicitly drawn. Moreover, for given correlation functions, there are lower order graphs in the coupling which cannot be cut out of the planar lattice, but from two or more sheets of such lattice as explained in [94].

1.3 Conclusions

We found here the complete description of possible Feynman graphs of χCFT_4 in the "bulk" – i.e. far from the boundaries of the graph defined by a particular physical quantity. These graphs can be dubbed as "dynamical fishnet", since, unlike the usual regular fishnet of the bi-scalar model (1.2.6) they have a certain dynamics (summation over many of such graphs) preserving at the same time a kind of irregular fishnet structure shown on Figs. 1.2,1.3. Interestingly, this bulk structure is neatly realized as Feynman graphs describing arbitrary single-trace correlation functions of all elementary fields, as shown on Figs. 1.4,1.5. It would be very interesting to find the realisation of the Yangian symmetry of these correlators, and of the related planar amplitudes (with disc topology), generalizing the results of [94, 95] for the bi-scalar

CFT. It would be the neatest demonstration of the integrability of the full model. In Sec.1.2 we have shown such integrability in the two-coupling reduction of the full χCFT, having a much simpler fishnet structure (combination of regular "brick wall" graphs with Yukawa vertices and regular square lattice fishnets). A considerably more involved analysis of the integrability of the full dynamical fishnet of χCFT, in particular, via the Yangian symmetry of single-trace correlators, is underway. We believe that it will be another important step to the understanding of integrability of the mother theory – the $\mathcal{N} = 4$ SYM. It is worth noticing here that γ-deformation represents a rather mild, "topological" modification of the planar graphs of original $\mathcal{N} = 4$ SYM, altering only the boundaries of these graphs, and not the bulk.

Chapter 2
Fishnets in a d-dimensional sea

2.1 Introduction

Conformal field theories (CFT) are ubiquitous in two dimensions [17], and quite a few super-symmetric CFTs in $d = 3, 4, 6$ dimensions are known. But well defined and not super-symmetric CFTs in $d > 2$, such as 3D Ising or Potts models, or Banks-Zaks model [106], are rare species, in spite of their rich potential applications ranging from the theory of phase transitions to fundamental interactions. The CFTs at $d > 2$ which in addition are integrable, such as 4D $\mathcal{N} = 4$ SYM and Aharony-Bergman-Jafferis-Maldacena (ABJM) theories in the 't Hooft limit, are true exceptions [13] [1]. That's why a new family of planar integrable CFTs obtained in [32] as a special double scaling limit of γ-deformed $\mathcal{N} = 4$ SYM seems to be an important and instructive example. This theory can be studied via quantum spectral curve (QSC) formalism [83, 107, 108] or using the integrability of its dominant Feynman graphs via the conformal, $SU(2,2)$ non-compact spin chain. A nice particular case of this family is the $4D$ bi-scalar theory, whose planar limit is dominated by"fishnet" type Feynman graphs [32, 91].

A rather exceptional feature of the fishnet theory is that it can be defined in any space-time dimension. This provides an interesting laboratory for studying the properties of higher dimensional CFTs, and its connection to other known conformal and integrable models. Let us define the d-dimensional generalization of the $4D$ bi-scalar theory introduced in [32] as follows

$$\mathcal{L}_\phi = N_c \,\mathrm{tr}[\phi_1^\dagger \,(-\partial_\mu \partial^\mu)^\omega \,\phi_1 + \phi_2^\dagger \,(-\partial_\mu \partial^\mu)^{\frac{d}{2}-\omega} \,\phi_2 + (4\pi)^{\frac{d}{2}} \xi^2 \phi_1^\dagger \phi_2^\dagger \phi_1 \phi_2]\,, \tag{2.1.1}$$

where both scalar fields transform under the adjoint representation of $SU(N_c)$; ξ^2 is the coupling constant and $\omega \in \left(0, \frac{d}{2}\right)$ is a deformation parameter. The non-local (for general d, ω) operators in kinetic terms should be understood as an integral kernel

$$(\partial_\mu \partial^\mu)^\beta f(x) \equiv \frac{(-4)^\beta \,\Gamma(\frac{d}{2}+\beta)}{\pi^{\frac{d}{2}} \Gamma(-\beta)} \int \frac{d^d y \, f(y)}{|x-y|^{d+2\beta}}. \tag{2.1.2}$$

[1] The integrability of such theories emerges due to their duality to string sigma models on specific cosets, having an infinite number of quantum conservation lows for their world-sheet dynamics, or due to the analogy between the planar Feynman diagram technique and integrable $(1 + 1)$ dimensional quantum spin chains [13].

The propagator of scalar fields is its functional inverse:

$$(-\partial_\mu\partial^\mu)^\beta D(x) = \delta^{(d)}(x)\,, \quad D(x-y) = \frac{\Gamma(\frac{d}{2}-\beta)}{4^\beta\,\pi^{\frac{d}{2}}\Gamma(\beta)\,|x-y|^{d-2\beta}}. \tag{2.1.3}$$

The typical structure in the bulk of sufficiently big planar Feynman graphs in this theory is that of the regular square lattice ("fishnet" graphs, proposed in [92] as an integrable lattice spin model), by the same reasons as in $4D$ case [32, 91], namely, due to the presence of the single chiral interaction vertex in the Lagrangian, and the absence of its hermitian conjugate. For example, the graphs renormalizing local "vacuum" operator $\mathrm{tr}(\phi_j)^L$ are those of the "wheel" type and they can be studied via the integrable conformal $SO(2,d)$ spin chain [2], as was suggested for $4D$ case in [39]. The dimensions of operators of the type $\mathrm{tr}[\phi_1^3(\phi_2^\dagger\phi_2)^k]$ have been also studied in $4D$ [39] by QSC methods. It is not clear whether this method can be generalized to our d dimensional model. But the spin chain methods certainly can.

In general, the propagators of the fishnet graphs of the model (2.1.1) are different for the two different fields: $|x-y|^{-d+2\omega}$ for ϕ_1 fields and $|x-y|^{-2\omega}$ for ϕ_2 fields. Let us concentrate here on the "isotropic" case $\omega = d/4$. In order to maintain the renormalizability we should add to (2.1.1) the following double-trace counter-terms [85, 103]

$$\mathcal{L}_{\mathrm{dt}}/(4\pi)^{\frac{d}{2}} = \alpha_1^2\sum_{i=1}^{2}\mathrm{tr}(\phi_i\phi_i)\,\mathrm{tr}(\phi_i^\dagger\phi_i^\dagger) - \alpha_2^2\,\mathrm{tr}(\phi_1\phi_2)\mathrm{tr}(\phi_2^\dagger\phi_1^\dagger) - \alpha_2^2\mathrm{tr}(\phi_1\phi_2^\dagger)\mathrm{tr}(\phi_2\phi_1^\dagger)\,, \tag{2.1.4}$$

Notice that the first term disappears in the "non-isotropic" case $\omega \neq \frac{d}{4}$ since the couplings of two terms in the first line of (2.1.4) would become dimensionful.

As it was suggested in [84] and explicitly shown in [36] for the 4D case, the "isotropic" bi-scalar theory with Lagrangian $\mathcal{L}_\phi + \mathcal{L}_{\mathrm{dt}}$ has two fixed points. We generalize here this result to any dimension, up to two loops, computing the corresponding Feynman graphs (Fig.2.1) contributing to the β_{α_1}-function. Its two zeroes are

$$\alpha_1^2(\xi) = \mp\frac{i\,\xi^2}{2} - J^{(d)}\xi^4 + O(\xi^6) \tag{2.1.5}$$

where the real coefficient $J^{(d)}$ depends on the ϵ^{-1} coefficient of the down-left graph of Fig.2.1 in dimensional regularization. For example: $J^{(4)} = 1/2$, $J^{(2)} = 2\ln 2$, $J^{(1)} = \frac{\pi+4\ln 2}{2\sqrt{\pi}}$ [3]. At this critical coupling $\alpha_1(\xi)$ the bi-scalar theory becomes a genuine non-unitary CFT at any coupling ξ. The operators $\mathrm{tr}(\phi_1\phi_2)$, and $\mathrm{tr}(\phi_1\phi_2^\dagger)$ are protected in the planar limit as in [36].

[2] in the rest of the chapter we will use its Euclidean version $SO(1,d+1)$ instead of the Minkowskian $SO(2,d)$.

[3] This term can be computed at any d by means of Integration by Parts and Mellin-Barnes transformation, according to [109]

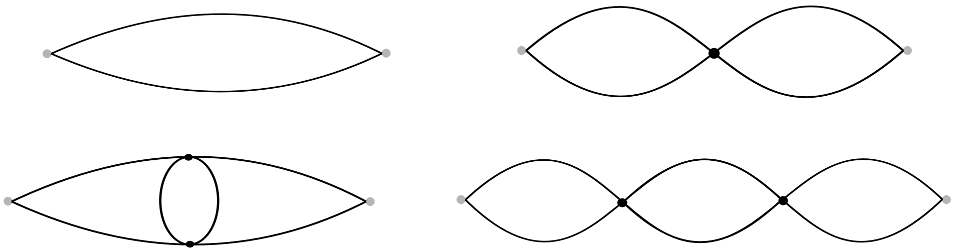

Figure 2.1: Loop expansion of $\langle \mathrm{tr}(\phi_1^2)(x)\mathrm{tr}(\phi_1^2)^\dagger(0)\rangle$ planar graphs up to 2-loops.

Generalizing the $4D$ results of [36] to any d, we will compute exactly a particular four-point function and read off from it the exact scaling dimensions and certain OPE structure constants of operators of the type $\mathrm{tr}(\phi_1\partial_+^S\phi_1(\phi_2^\dagger\phi_2)^k)$+permutations. Their dimensions are encoded in a remarkably simple exact relation

$$h_{\Delta,S} \equiv \frac{\Gamma\left(\frac{3d}{4}-\frac{\Delta-S}{2}\right)}{\Gamma\left(\frac{d}{4}-\frac{\Delta-S}{2}\right)}\frac{\Gamma\left(\frac{d}{4}+\frac{\Delta+S}{2}\right)}{\Gamma\left(-\frac{d}{4}+\frac{\Delta+S}{2}\right)} = \xi^4\,, \tag{2.1.6}$$

which reduces of course at $4D$ to the result of [36]. For even d it gives d different solutions $\Delta(\xi) = \Delta_0 + \gamma(\xi)$. At odd (or non-integer) d there are infinitely many, in general complex, solutions. At weak coupling the two complex conjugate solutions at $S = 0$ [4]

$$\gamma = \pm i\frac{2\xi^2}{\Gamma\left(\frac{d}{2}\right)} \pm \frac{i}{6}\frac{\xi^6}{\Gamma\left(\frac{d}{2}\right)^3}\left(\pi^2 - 6\,\psi^{(1)}\left(\frac{d}{2}\right)\right) + O(\xi^{10})$$

describe anomalous dimensions of the operator $\mathrm{tr}(\phi_1\phi_1)$ at the two fixed points. In a similar way, for any $S \in 2\mathbb{Z}$ the real weak coupling solution

$$\begin{aligned}\gamma =& -2\frac{\xi^4\Gamma(S)}{\Gamma\left(\frac{d}{2}\right)\Gamma\left(\frac{d}{2}+S\right)}+\\ &+\frac{2\,\xi^8\Gamma(S)^2}{\Gamma\left(\frac{d}{2}\right)^2\Gamma\left(\frac{d}{2}+S\right)^2}\left(\psi^{(0)}\left(\frac{d}{2}\right)-\psi^{(0)}\left(\frac{d}{2}+S\right)+\psi^{(0)}(S)+\gamma_E\right)+O(\xi^{10}).\end{aligned}$$

describes the operators of the type $\mathrm{tr}(\phi_1\partial_+^S\phi_1)$, where $\partial_+^S = (\hat{n}\cdot\partial)^S$ with $\hat{n}$ being an auxiliary light-like vector.

For $d = 2m,\ m \in \mathbb{N}$ the l.h.s. of (2.1.6) factorizes into a polynomial of degree $2m$ and $2m$ roots of eq.(2.1.6) describe the scaling dimension of the exchanged operators in the OPE channel $x_3 \to x_4$ of (2.3.1) together with their shadows $\tilde{\Delta} = d - \Delta$. At $\xi = 0$ we get for the bare dimensions of physical operators (i.e., excluding "shadow" operators)

$$\Delta_0 - S = \{m, m+2, \cdots, 3m-2\},$$

[4]Here and in the following we adopt the notation $\psi^{(k-1)}(x) = \frac{d^k}{dx^k}\log\Gamma(x)$ for polygamma functions.

At $d=2$ there is a single solution with the dimension $\Delta = 1+\sqrt{S^2-4\xi^4}$ of the local twist-2 operators of the type $\mathrm{tr}(\phi_1\partial_+^S\phi_1)$, while at $4D$ the additional $\Delta_0 - S = 4$ describes twist-4 operators [36]. As an example, at $d=6$ and $S=0$ the possible non-shadow solutions for (2.1.6) are $\Delta_0 = 3,5,7$. They can be realized as $\mathrm{tr}(\phi_1^2)$ for $\Delta_0 = 3$, linear combinations of $\mathrm{tr}(\phi_1\Delta\phi_1)$, $\mathrm{tr}(\partial_\mu\phi_1\partial^\mu\phi_1)$ for $\Delta_0 = 5$ and of $\mathrm{tr}(\phi_1\Delta^2\phi_1)$, $\mathrm{tr}(\Delta\phi_1\Delta\phi_1)$, $\mathrm{tr}(\partial_\mu\phi_1\partial^\mu\Delta^2\phi_1)$, $\mathrm{tr}(\partial_\mu\partial_\nu\phi_1\partial^\mu\partial^\nu\phi_1)$ for $\Delta_0 = 7$.

Diagonalizing the mixing matrix of these operators at $\xi \neq 0$ we would obtain operators with non-trivial, ξ-dependent anomalous dimensions, as well as the so called log-multiplets [38, 39], omnipresent in this non-unitary theory [105, 110], containing the operators with zero anomalous dimension. Eq.(2.1.6) predicts that all the exchange operators from this set acquire non-trivial anomalous dimensions, whereas the operators belonging to log-multiplets never appear among them. This appears to be true at any even dimension d.

As a general rule, according to the eq.(2.1.6) the operators of the type

$$\{\mathrm{tr}(\phi_1\partial_+^S\phi_1(\phi_2\phi_2^\dagger)^k) + \text{permutations}\}\,, \tag{2.1.7}$$

appear in the multiplets only at $d/4 \in \mathbb{N}$, $k=1$. We will find below from the exact 4-point function the conformal structure constants of these operators with two scalar fields.

2.2 Integrability of d-dimensional bi-scalar CFT

As it was noticed in [32] and further developed in [36, 39, 91], the $4D$ case of the theory (2.1.1), with $\omega = 1$, is integrable in the planar limit. On the one hand, this integrability is the direct consequence of integrability of γ-twisted planar $\mathcal{N}=4$ SYM theory, from which it was obtained in the double scaling limit combining strong imaginary twist and weak coupling. On the other hand, this integrability was explicitly related in [32, 39] to the fact that the bi-scalar theory was dominated by the integrable "fishnet" Feynman graphs [92][5].

Apart from $4D$ case, for arbitrary d our bi-scalar model (2.1.1) does not have any integrable SYM origin. But the arguments of equivalence to the integrable conformal $SO(1,d+1)$ spin chain do work. Namely, let us introduce the d-dimensional analogue of the $4D$ "graph-building" operator [32] at general ω-deformation

$$\mathcal{H}_L\Phi(x_1,\dots,x_L) = \frac{1}{\pi^{\frac{dL}{2}}}\int \frac{d^dx_{1'}\dots d^dx_{L'}\,\Phi(x_{1'},\dots,x_{L'})}{|x_{11'}|^{d-2\omega}\dots|x_{LL'}|^{d-2\omega}\times|x_{1'2'}|^{2\omega}\dots|x_{L'1'}|^{2\omega}} \tag{2.2.1}$$

[5] This terminology for the graphs of regular square lattice shape was introduced by B.Sakita and M.Virasoro in 1970.

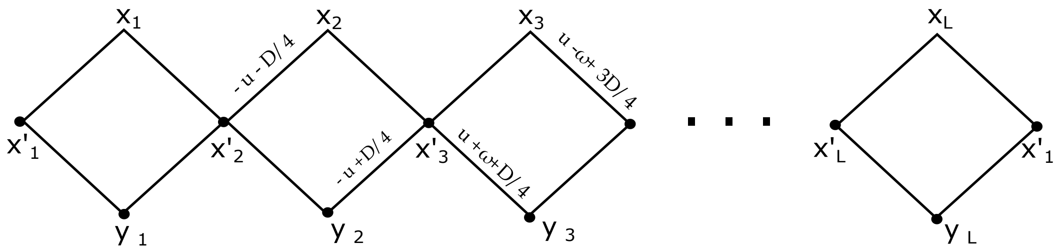

Figure 2.2: Graphical representation of the transfer matrix as a convolution of R-kernels according to formulas (2.2.2)and (2.2.3). Black dots are integration points and the weights of propagators are written in the second and third R-kernel. The primed points x'_i belong to the auxiliary space.

schematically presented on Fig.2.3. It is easy to see that a power of this operator $\mathcal{H}_L^M$ generates a fishnet Feynman graph with topology of a cylinder of length M with the circumference L. Now, in analogy with the $4D$ observation of [39], we notice that this operator can be related to the transfer-matrix of integrable $SO(1, d+1)$ conformal Heisenberg spin chain [111] presented on Fig.2.2:

$$\mathbb{T}(u) = \mathrm{Tr}_0\left(R_{01}(u)\, R_{02}(u) \ldots R_{0L}(u)\right) \tag{2.2.2}$$

where u is the spectral parameter and the R-matrix acts as an integral operator

$$[R_{12}\Phi](x_1, x_2)(u) = c(u, d, \omega) \int \frac{d^d x_{1'} d^d x_{2'}\, \Phi(x_{1'}, x_{2'})}{(x_{12}^2)^{-u-\frac{d}{4}} (x_{21'}^2)^{\frac{d}{4}+u+\omega} (x_{12'}^2)^{\frac{3d}{4}+u-\omega} (x_{1'2'}^2)^{-u+\frac{d}{4}}}, \tag{2.2.3}$$

with the normalization constant

$$c(u, d, \omega) = \frac{4^{2u}}{\pi^d} \frac{\Gamma\left(u + \frac{d}{4} + \omega\right) \Gamma\left(u + \frac{3d}{4} - \omega\right)}{\Gamma\left(-u - \frac{d}{4} + \omega\right) \Gamma\left(-u + \frac{d}{4} - \omega\right)}.$$

Indeed, in analogy with $4D$ case [39], at a particular value of spectral parameter this transfer matrix becomes the graph-building operator (2.2.1) at any d

$$\mathcal{H}_L = \pi^{-\frac{dL}{2}} \left[(4\pi^2)^{\frac{d}{2}} \Gamma\left(\frac{d}{2}\right)\right]^L \lim_{\epsilon \to 0} \epsilon^L\, \mathbb{T}\left(-\frac{d}{4} + \epsilon\right). \tag{2.2.4}$$

presented on Fig. 2.3. Thus this operator is one of the conserved charges of the equivalent spin chain: $[\mathbb{T}(u), \mathbb{T}(u')] = [\mathbb{T}(u), \mathcal{H}_L] = 0$.

2.3 Exact 4-points correlation function

In analogy with $4D$ results of [36], employing the d-dimensional conformal symmetry of the theory (2.1.1),(2.1.4) we will compute exactly the four-point correlation function

$$G = \langle O(x_1, x_2) \bar{O}(x_3, x_4) \rangle = \frac{\mathcal{G}(u, v)}{(2\pi)^d (x_{12}^2 x_{34}^2)^{\frac{d}{4}}}, \tag{2.3.1}$$

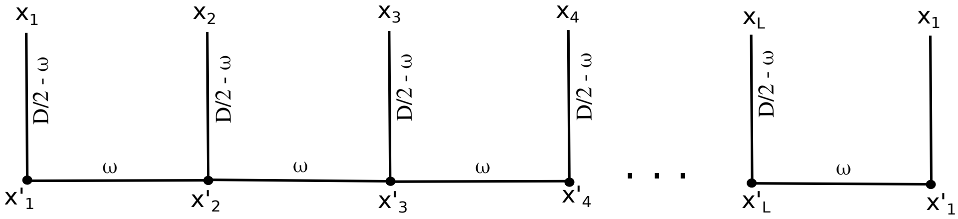

Figure 2.3: Graphical representation of the kernel of the graph-building operator for generic d and ω. It is obtained by setting $u = -\frac{d}{4}$ in the transfer matrix (2.2.2) presented on Fig. 2.2, so that $x_{jj'+1}$ –type type propagators disappear while $x_{j'+1} - y_j$ -type propagators are replaced by $\delta^{(d)}(x_{j'+1} - y_j)$ factors. After that, integration over the points y_j is equivalent to setting $y_j = x_{j'+1}$.

where the notation is introduced for the operators $O(x, y) = \mathrm{tr}[\phi_1(x)\phi_1(y)]$ and $\bar{O}(x, y) = \mathrm{tr}[\phi_1^\dagger(x)\phi_1^\dagger(y)]$.

Here $\mathcal{G}(u, v)$ is a finite function of cross-ratios $u = x_{12}^2 x_{34}^2/(x_{13}^2 x_{24}^2)$ and $v = x_{14}^2 x_{23}^2/(x_{13}^2 x_{24}^2)$, invariant under the exchange of points $x_1 \leftrightarrow x_2$ and $x_3 \leftrightarrow x_4$. The OPE expansion leads to the formula

$$\mathcal{G}(u, v) = \sum_{\Delta} \sum_{S/2 \in \mathbb{Z}_+} C_{\Delta,S}^2 \, u^{(\Delta - S)/2} g_{\Delta,S}(u, v), \tag{2.3.2}$$

where the sums run over operators with scaling dimensions Δ and even Lorentz spin S. Here $C_{\Delta,S}$ is the corresponding OPE coefficient (structure constant) and $g_{\Delta,S}(u, v)$ is the known d dimensional conformal block (see (2.9) and sections 4,5 in [112]). If we compute (2.3.1) we will identify the conformal data for the operators emerging in the OPE of $O(x_1, x_2)$.

In the planar limit G is given by the set of fishnet Feynman diagrams presented in Fig. 2.4. Summing up the corresponding perturbation series we encounter a geometric progression involving the combination of operators $\alpha^2\mathcal{V} + \xi^4\mathcal{H}_2$, where $\alpha^2 = \alpha_\pm^2$ is the double-trace coupling at the fixed point, $\mathcal{V}$ is the operator inserting the double-trace vertex

$$\mathcal{V}\ \Phi(x_1, x_2) = \frac{2}{\pi^{\frac{d}{2}}} \int \frac{d^d x_{1'} d^d x_{2'}\, \delta^{(d)}(x_{1'2'})\, \Phi(x_{1'}, x_{2'})}{|x_{11'}|^{d/2} |x_{22'}|^{d/2}},$$

which is the d-dimensional version of (11) in [36], and the operator $\mathcal{H}_2$ defined by (2.2.1) adds a scalar loop inside the diagram. Hence we obtain the following representation

$$G = \frac{1}{(2\pi)^d} \int \frac{d^4 x_{3'} d^4 x_{4'}}{(x_{33'}^2 x_{44'}^2)^{\frac{d}{4}}} \langle x_1, x_2 | \frac{1}{1 - \alpha^2\mathcal{V} - \xi^4\mathcal{H}_2} | x_3', x_4' \rangle + (x_1 \leftrightarrow x_2). \tag{2.3.3}$$

where $x_{ij} \equiv x_i - x_j$.[6]

[6]The operators $\mathcal{V}$ and $\mathcal{H}$ are not well-defined separately, e.g. for an arbitrary $\Phi(x_i)$ the expressions for $\alpha^4\mathcal{V}^2\Phi(x_i)$ and $\xi^4\mathcal{H}\Phi(x_i)$ are given by divergent integrals. However, at the fixed point, their sum is finite by virtue of conformal symmetry.

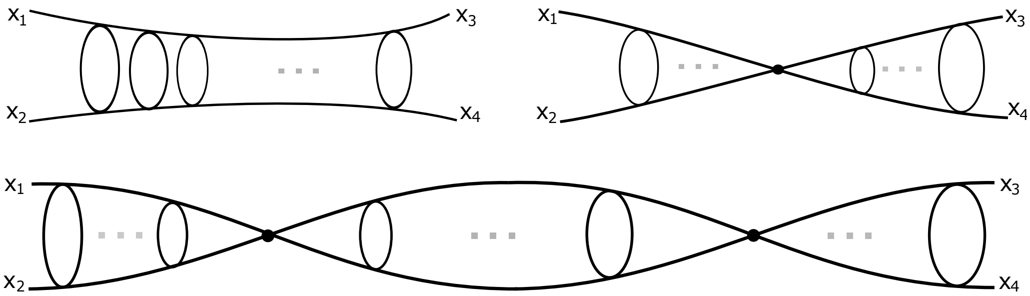

Figure 2.4: General fishnet graphs up to α_1^2 order in the expansion of four point function (2.3.3).

Remarkably, the operators $\mathcal{V}$ and $\mathcal{H}_2$ commute with the generators of the conformal group, as in the particular $4D$ case [36]. This fixes the form of their eigenstates

$$\Phi_{\Delta,S,n}(x_{10},x_{20}) = \frac{1}{(x_{12}^2)^{\frac{d}{4}}}\left(\frac{x_{12}^2}{x_{10}^2x_{20}^2}\right)^{(\Delta-S)/2}\left(\partial_0 \ln\frac{x_{20}^2}{x_{10}^2}\right)^S, \tag{2.3.4}$$

where $\Delta = \frac{d}{2}+2i\nu$ and $\partial_0 \equiv (\hat{n}\cdot\partial_{x_0})$. The state $\Phi_{\Delta,S,n}$ belongs to the principal series of the conformal group and can be represented in the form of a conformal three-point correlation function

$$C_{\Delta,S}\,\Phi_{\Delta,S,n}(x_{10},x_{20}) = \langle\, \mathrm{tr}[\phi_1(x_1)\phi_1(x_2)]O_{\Delta,S,n}(x_0)\,\rangle\,,$$

where the operator $O_{\Delta,S,n}(x_0)$ carries the scaling dimension Δ and Lorentz spin S, and $C_{\Delta,S}$ is the 3-points structure constant. The states (2.3.4) satisfy the orthogonality condition [113, 114]

$$\int \frac{d^dx_1d^dx_2}{(x_{12}^2)^{\frac{d}{2}}}\,\overline{\Phi_{\Delta',S',n'}}(x_{10'},x_{20'})\,\Phi_{\Delta,S,n}(x_{10},x_{20})$$
$$= c_1(\nu,S)\delta(\nu-\nu')\,\delta_{S,S'}\delta^{(d)}(x_{00'})(nn')^S + c_2(\nu,S)\delta(\nu+\nu')\delta_{S,S'}Y^S(x_{00'})/(x_{00'}^2)^{\frac{d}{2}-S-2i\nu},$$

where $\Delta' = \frac{d}{2}+2i\nu'$, $Y(x_{00'}) = (n\partial_{x_0})(n'\partial_{x_{0'}})\ln x_{00'}^2$, and

$$c_1(\nu,S) = \frac{2^{S+1}\,S!\,|\Gamma(2i\nu)|^2\left(4\nu^2+(\frac{d}{2}+S-1)^2\right)^{-1}}{\pi^{-(3d/2+1)}\left|\Gamma\left(\frac{d}{2}-1+2i\nu\right)\right|^2\Gamma(\frac{d}{2}+S)}, \tag{2.3.5}$$
$$c_2(\nu,S) = \frac{2(-1)^S\,\Gamma^2\left(\frac{d}{4}+\frac{S}{2}-i\nu\right)}{\pi^{-(d+1)}\,\Gamma^2\left(\frac{d}{4}+\frac{S}{2}+i\nu\right)}\frac{\Gamma(2i\nu)}{\Gamma(\frac{d}{2}+2i\nu-1)}\times\frac{\Gamma(\frac{d}{2}+S+2i\nu-1)\,S!}{\Gamma(\frac{d}{2}+S-2i\nu)\Gamma(\frac{d}{2}+S)}\,.$$

Calculating the corresponding eigenvalues of the operators $\mathcal{V}$ and $\mathcal{H}$ we find

$$\mathcal{V}\,\Phi_{\Delta,S,n}(x_1,x_2) = \delta(\nu)\delta_{S,0}\Phi_{\Delta,S,n}(x_1,x_2),$$
$$\mathcal{H}\,\Phi_{\Delta,S,n}(x_1,x_2) = h_{\Delta,S}^{-1}\Phi_{\Delta,S,n}(x_1,x_2), \tag{2.3.6}$$

where the function $h(\Delta,S)$ is given by (2.1.6). Applying (2.3.5)–(2.3.6) we can expand the correlation function (2.3.3) over the basis of states (2.3.4). This yields the expansion of G over conformal partial waves defined by the operators $O_{\Delta,S}(x_0)$ in the OPE channel $O(x_1, x_2)$

$$\mathcal{G}(u,v) = \sum_{S/2\in\mathbb{Z}_+} \int_{-\infty}^{\infty} d\nu \mu_{\Delta,S} \frac{u^{(\Delta-S)/2} g_{\Delta,S}(u,v)}{h_{\Delta,S} - \xi^4}, \tag{2.3.7}$$

where $\Delta = \frac{d}{2} + 2i\nu$, and $\mu_{\Delta,S} = 2\pi^d / c_2(\nu, S)$ is related to the norm of the state (2.3.5). The fact that the dependence on α^2 disappears from (2.3.7) can be understood as follows. Viewed as a function of S, $\xi^4/h_{\Delta,S}$ develops poles at $\nu = \pm iS$ which pinch the integration contour in (2.3.7) for $S \to 0$. The contribution of the operator $\mathcal{V}$ is needed to make a perturbative expansion of (2.3.7) well-defined. For finite ξ^4, these poles provide a vanishing contribution to (2.3.7) but generate a branch-cut $\sqrt{-\xi^4}$ singularity of $\mathcal{G}(u,v)$, as in $4D$ case [36].

At small u, we close the integration contour in (2.3.7) to the lower half-plane and pick up residues at the poles located at solutions of (2.1.6) and satisfying the unitarity bound $\mathrm{Re}\,\Delta > S$. The resulting expression for $\mathcal{G}(u,v)$ takes the expected form (2.3.2) with the OPE coefficients given by

$$C^2_{\Delta,S} = \frac{\Gamma(\frac{d}{2}+S)}{S!} \frac{\Gamma(\Delta-1)}{\Gamma(\Delta-\frac{d}{2})} \mathrm{Res}\left(\frac{d\Delta}{h_{\Delta,S}-\xi^4}\right) \frac{\Gamma(S-\Delta+d)\,\Gamma^2\left(\frac{1}{2}(S+\Delta)\right)}{\Gamma^2\left(\frac{1}{2}(S-\Delta+d)\right)\Gamma(S+\Delta-1)}. \tag{2.3.8}$$

where the residue is computed w.r.t. the appropriate solution of (2.1.6) for each relevant operator. For instance, we can consider $\mathrm{tr}(\phi_1^2)^\dagger$, which is exchanged for any even d; then the perturbative expansion of (2.3.8) is

$$C^2_{\mathrm{tr}\phi^2} = 2 + \frac{4i\xi^2}{\Gamma\left(\frac{d}{2}\right)} \left(2\psi^{(0)}\left(\frac{d}{4}\right) - \psi^{(0)}\left(\frac{d}{2}\right) + \gamma_E\right) + O(\xi^4) \tag{2.3.9}$$

The relations (2.1.6) and (2.3.8) define exact conformal data of operators propagating in the OPE channel $x_1 \to x_2$.

Finally, we discuss an interesting $d \to \infty$ limit of the theory. We should then rescale the coupling $\xi = \xi_\infty \sqrt{\Gamma(d/2)}$, where ξ_∞ is fixed. Anomalous dimension γ_∞ of $\mathrm{tr}(\phi_1^2)$ has finite limit since for $S = 0$ in eq.(2.1.6) it is given by

$$-\gamma_\infty \sin\left(\frac{\pi\gamma_\infty}{2}\right) = 2\pi\xi_\infty^4$$

while γ_∞ vanishes for operators with higher spin $S \neq 0$. As concerns the expansion (2.3.2), the number of exchanged operators becomes a countable infinity, diverging linearly in d. Finally, the OPE structure constant (2.3.9) for $\mathrm{tr}(\phi_1^2)$ trivially reduces to its bare value in this limit.

2.4 Conclusions

We showed that the strongly γ-deformed $\mathcal{N} = 4$ SYM theory proposed in [32] is just the 4-dimensional representative of a wider, d-dimensional family of theories of two complex scalar fields obtained by modifying the propagators of fields in a d-dependent way. Similarly to the $4D$ case [36], they turn out to be conformal and integrable at any d, at least in the planar limit, if we add to the action certain double-trace terms with specific couplings. The conformality of our theory at finite N_c remains an open question, though it is quite plausible that the planar conformal point simply shifts to some other complex values of couplings. There are two such complex conjugate values of these couplings and we compute them perturbatively up to two loops. The integrability is explicit due to the domination of sufficiently large orders of perturbation theory by the "fishnet" Feynman diagrams. The cylindric fishnet graphs, related to the renormalization of "vacuum" $\mathrm{tr}(\phi_1^L)$ operators, can be created by multiple application of a "graph-building" operator which appears to be an integral of motion of the integrable conformal $SO(1, d+1)$ spin chain. We also generalize the bi-scalar model to a CFT with different propagators for the fields ϕ_1 and ϕ_2, leading to "non-isotropic" fishnet Feynman graphs. The underlying graph building operator has representations with different conformal spins in two directions on the fishnet graph. In the 2D case the fishnet graphs are described by the same $SL(2, \mathbb{C})$ chain as used for the dynamics of generalized Lipatov's reggeized gluons [115] but with different value of spin, $s = 1/4$ in isotropic case, instead of the Balitski-Kuraeev-Fadin-Lipatov reggeized gluon spin $s = 0$. This spin chain, extensively studied in the literature [116, 116–121], is restored in the singular limit $\omega \to 0$ of our bi-scalar model (2.1.1). In the spirit of [36], we computed here the exact four point correlator at any d as an expansion into conformal blocks with explicit OPE coefficients and dimensions of exchange operators in one of the channels. In $1d$ case, our results are similar to the scalar version of conformal Sachdev-Ye-Kitaev fermionic theory [122] at $q = 4$. For even d we found a finite, d-dependent number of local exchange operators at a given spin and dimension. It would be very interesting to compute some of the discussed quantities (dimensions, structure constants) in the next $1/N_c^2$ approximation, similarly to [97, 123, 124], if the conformality of the theory holds at any N_c. The explicit form of this operators can be obtained by the analysis of the mixing matrix for their quantum multiplets [38, 39]. This becomes more complicated as the dimension grows due to growing rank of the multiplets and the number of transitions, together with log-CFT effects which arise starting from $4D$, due to the chirality.

Although the Lagrangian (2.1.1) of our theory is non-local at general d (apart from the sequence $d \in 4\mathbb{N}$ in "isotropic" case), it does not prevent the existence of standard OPE data in this theory, which is more important for the physical interpretation of this CFT. Moreover it would be interesting to generalize to any d the results for fishnet graphs of the type considered in [125] and to the correlation functions for operators involving more than two scalars. Finally, an important question remains, as in $4D$, whether these theories have any string dual at any d, according to the original proposal of G .'t Hooft [126].

Chapter 3
Four-point functions of Basso-Dixon type

3.1 Introduction

Recently, B. Basso and L. Dixon obtained an elegant explicit expression for a specific, conformal planar Feynman graph of fishnet type [35], having N rows and L columns, and thus $(N+1)(L+1)-4$ loops. This graph is presented on Fig.3.1. It has four external fixed coordinates and, similarly to the conformal 4-point functions, has a non-trivial dependence on two cross-ratios u, v. This Basso-Dixon (BD) formula takes the form of an $N \times N$ determinant of explicitly known "ladder" integrals [34, 127]. It is one of very few examples of explicit results for Feynman graphs with arbitrary many loops.

The BD formula appeared in the context of its application to the previously introduced bi-scalar fishnet theory in $4D$ which emerged as a specific double scaling limit of γ-deformed $\mathcal{N}=4$ SYM theory combining weak coupling and strong imaginary γ-twists [32, 91]. In particular, in the bi-scalar theory, the BD integral represents indeed a particular single-trace correlation function (described in the following). In general, the bulk structure of planar graphs in fishnet CFT is that of the regular square lattice of massless propagators. Such a graph represents an integrable two-dimensional statistical mechanical system [92] which can be studied via integrable quantum spin chain with the symmetry of 4D conformal group $SU(2,2)$ [32, 39, 91, 128].

3.2 Two-dimensional case

In the chapter 2 we introduced the d-dimensional generalization of bi-scalar fishnet theory [28]. The Basso-Dixon type integral corresponds to the following single-trace correlation function:

$$I^{BD}_{L,N}(z_0, z_1, w_0, w_1) = \left\langle \operatorname{tr}\left(\phi_1^L(z_0)\phi_2^N(z_1)\phi_1^{\dagger L}(w_0)\phi_2^{\dagger N}(w_1)\right)\right\rangle . \qquad (3.2.1)$$

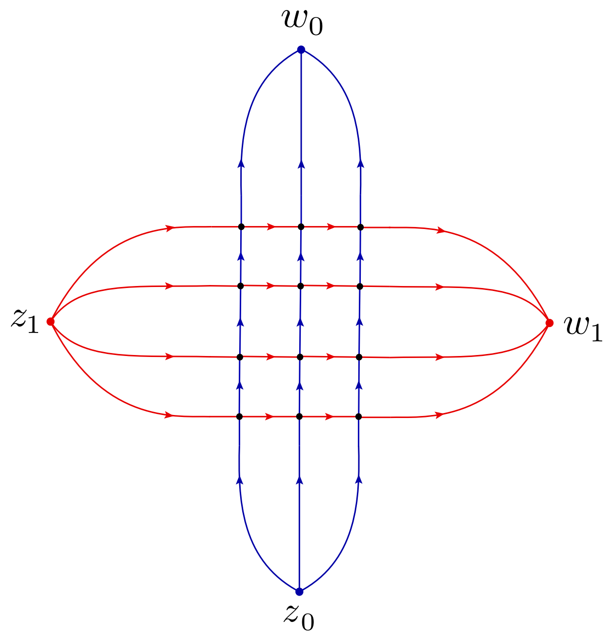

Figure 3.1: Basso-Dixon type Feynman diagram for $N = 4$, $L = 3$. The propagators have the form $[w - z]^{-\alpha}$ where $\alpha = 1/2 \pm \omega$ for vertical and horizontal lines, respectively.

It is easy to see that, due to the chiral nature of interaction of two scalars, this correlation function is given in the planar limit by a single, fishnet-type planar graph of BD-type drawn in Fig.3.1. Explicitly, this Feynman graph is given by expression

$$I^{BD}_{L,N}(z_0, z_1, w_0, w_1) = \int \prod_{(l,n)\in\mathcal{L}_{L,N}} d^d z_{l,n} \times$$
$$\times \left(\prod_{(l,n)\in\mathcal{L}_{L,N+1}} \frac{1}{|z_{l,n-1} - z_{l,n}|^{d/2+2\omega}} \right) \left(\prod_{(l,n)\in\mathcal{L}_{L+1,N}} \frac{1}{|z_{l-1,n} - z_{l,n}|^{d/2-2\omega}} \right), \quad (3.2.2)$$

where we have $N \cdot L$ integration variables belonging to the $L \times N$ lattice of positive integers $\mathcal{L}_{L,N} = \{1 \le L \le L, 1 \le n \le N\}$, and we take equal coordinates at each of the four boundaries of this rectangular lattice: $\{z_{j,0} = z_0,\ z_{j,N+1} = w_0,\ z_{0,k} = z_1,\ z_{L+1,k} = w_1\}$ are imposed for $j = 1, ..., L$ and $k = 1, ..., N$.

This integral was computed explicitly in $d = 4$, for "isotropic" case $\omega = 0$, in [35]. The derivation is based on certain assumptions, typical for the S-matrix bootstrap methods inherited from the integrability of planar $\mathcal{N} = 4$ SYM [13]. It would be important to derive this formula from the first principles, based on the conformal spin chain interpretation of fishnet graphs, but in four dimensions such a derivation is so far missing.

In the first part of this chapter we will derive from the first principles the explicit expression for the two-dimensional analogue, $d = 2$, of Basso-Dixon formula for the

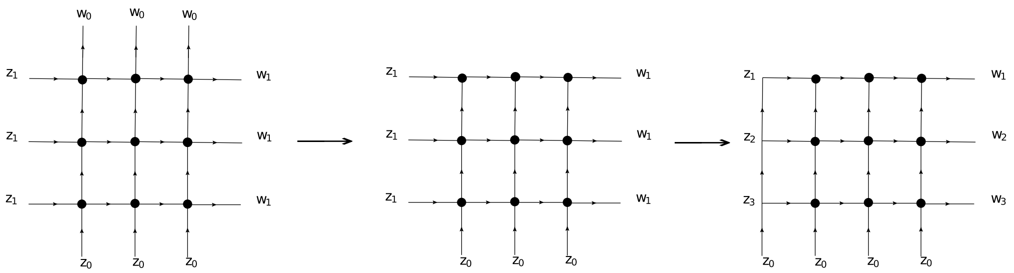

Figure 3.2: Basso-Dixon type diagram $I^{BD}_{L,N}(z_0, z_1, w_0, w_1)$ (on the left), its reduction $G_{L,N}(\mathbf{z}|\mathbf{w})$ (in the middle) and generalization $D_{L,N}(\mathbf{z}|\mathbf{w})$ (on the right) described in sec.3.2.1. We integrate only the coordinates in the vertices marked by black blobs. Sending $w_0 \to \infty$ in the original Basso-Dixon type diagram, we remove the upper row of propagators and obtain the reduced diagram (in the middle). Using conformal invariance of the original graph (on the left), we can always restore it from the graph on the right, by inversion and shift of coordinates w_1, z_1, z_0. Further on, we generalize the middle diagram by splitting the end point coordinates of left and right columns of external propagators, to separate coordinates $z_1 \to (z_1, z_2, \ldots, z_N)$ and $w_1 \to (w_1, w_2, \ldots, w_N)$, and then add at the left a column of vertical propagators $[z_i - z_{i+1}]^{-\gamma}$, thus getting the generalized configuration (on the right).

"fishnet" Feynman integral[1]

$$I^{BD}_{L,N}(z_0, z_1, w_0, w_1) = \tag{3.2.3}$$
$$= \int \prod_{(l,n)\in\mathcal{L}_{L,N}} d^d z_{l,n} \left(\prod_{(l,n)\in\mathcal{L}_{L,N+1}} \frac{1}{[z_{l,n-1} - z_{l,n}]^{\gamma}} \right) \left(\prod_{(l,n)\in\mathcal{L}_{L+1,N}} \frac{1}{[z_{l-1,n} - z_{l,n}]^{1-\gamma}} \right),$$

where the coordinates (z_0, z_1, w_0, w_1) are defined as after the eq.(3.2.2). We took here propagators transforming in the spinless complementary series of representations ($\bar{\gamma} = \gamma \in (0, 1)$) under $SL(2, \mathbb{C})$ group action (3.2.10). The propagators for $d = 2$, $\omega = \gamma - 1/2$ are $[w - z]^{-1/2 \mp \omega}$, where $\mp$ is chosen for vertical and horizontal lines, i.e. for the fields ϕ_1, ϕ_2, respectively.

Our derivation will be based on integrable $SL(2, \mathbb{C})$ spin chain methods worked out in [117, 129, 130], using the Sklyanin separation of variables (SoV) method [131–133]. The result can be presented in explicit form, in terms of $N \times N$ determinant of a matrix with the elements which are explicitly computed in terms of hypergeometric functions of cross-ratios[2]. Our main formula looks as follows:

$$I^{BD}_{L,N}(z_0, z_1, w_0, w_1) = \frac{[z_1 - z_0]^{(\gamma-1)N} [w_1 - w_0]^{(\gamma-1)N}}{[z_0 - w_0]^{(\gamma-1)N + \gamma L}} [\eta]^{\frac{\gamma-1}{2}N} B^{(\gamma)}_{L,N}(\eta) \tag{3.2.4}$$

where

$$B^{(\gamma)}_{L,N}(\eta, \bar{\eta}) = (2\pi)^{-N} \pi^{-N^2} \det_{1\le j,k\le N} \left[(\eta\partial_\eta)^{i-1} (\bar{\eta}\partial_{\bar{\eta}})^{k-1} I^{(\gamma)}_{N+L}(\eta, \bar{\eta}) \right], \quad \eta = \frac{z_0 - w_1}{w_1 - w_0} \frac{z_1 - w_0}{z_0 - z_1}, \tag{3.2.5}$$

[1]Here and in the following we adopt the notation $[z - w]^{\alpha} \equiv (z - w)^{\alpha} (z^* - w^*)^{\bar{\alpha}}$ for propagators, see App.B.1 for details.

[2]Or alternatively, due to the obvious $L \leftrightarrow N$ symmetry of the integral, in terms of the $(L-1) \times (L-1)$ determinant of the same matrix elements, which will depend only on $L + N$ combination.

and

$$I_M^{(\gamma)}(\eta,\bar\eta) = \frac{2\pi^{M+1}}{(M-1)!\,[\eta]^{\frac{\gamma-1}{2}}}\frac{\Gamma^M(\gamma)}{\Gamma^M(1-\gamma)} \times$$
$$\times\, \partial_\varepsilon^{M-1}\big|_{\varepsilon=0}\left[\frac{\Gamma^M(1-\gamma-\varepsilon)}{\Gamma^M(\gamma+\varepsilon)}\frac{\Gamma^M(1+\varepsilon)}{\Gamma^M(1-\varepsilon)}[\eta]^{-\varepsilon}\left|{}_{M+1}F_M\left(\begin{matrix}1-\gamma-\varepsilon & \cdots & 1-\gamma-\varepsilon & 1\\ 1-\varepsilon & \cdots & 1-\varepsilon & \end{matrix}\middle|\,\eta\right)\right|^2\right].$$

Formula (3.2.5) is also generalized in sections 3.2.2, 3.2.4 to the principal series representations of $SL(2,\mathbb{C})$, see (3.2.10).

In the next section, we will define the basic building blocks for construction of the Basso-Dixon configuration in the operatorial way. In section 3.2.2, we will introduce the generalized "graph-building" operator related to the transfer-matrix of the integrable open $SL(2,\mathbb{C})$ quantum spin chain. We will diagonalize there this operator by means of the SoV method and describe the full system of its eigenfunctions. In section 3.2.2 the result for 2d Basso-Dixon-like $N\times L$ graph will be presented in terms of an $N\times N$ determinant of the matrix constructed from ladder graph, that is the $1\times M$ case of Basso-Dixon diagram. In section 3.2.4, the ladder graph will be computed explicitly, in terms of the hypergeometric functions and their derivatives, thus completing the explicit result for the full two-dimensional Basso-Dixon-like $N\times L$ graph presented above. The ladder graph is employed to compute the so-called simple wheel graph in two dimensions. A particular case of $N=L=1$ (the two-dimensional "cross" graph) will be explicitly given in terms of the elliptic functions of the cross ratio.

3.2.1 Transformations of Basso-Dixon type graph and $L\leftrightarrow N$ duality

In order to apply the powerful methods of $SL(2,\mathbb{C})$ spin chain integrability, such as the separation of variables (SoV), we will use the conformal symmetry to reduce the BD graph on Fig.3.1 to a more convenient quantity for our purposes. First of all, we send $w_0\to\infty$ and drop the corresponding propagators containing this variable:

$$I^{BD}_{L,N}(z_0,z_1,w_0,w_1) \underset{w_0\to\infty}{\to} [w_0]^{-\gamma L} G_{L,N}(z_1,w_1|z_0)$$
$$\text{where}\quad G_{L,N}(z_1,w_1|z_0) =$$
$$= \int \prod_{l=1}^{L}\prod_{n=1}^{N} d^2 z_{ln}\left(\prod_{\substack{1\le l\le L\\ 1\le n\le N}} \frac{1}{[z_{l,n-1}-z_{l,n}]^{\gamma}\times[z_{l,n}-z_{l+1,n}]^{1-\gamma}}\right)\prod_{n=0}^{N-1}\frac{1}{[z_{0,n}-z_{1,n}]^{1-\gamma}},$$

where we take $\{z_{j,0}=z_0,\ z_{0,k}=z_1,\ z_{L+1,k}=w_1\}$ for $j=1,\dots,L$ and $k=1,\dots,N$. We can always restore the original quantity $I^{BD}_{L,N}(z_0,z_1,w_0,w_1)$ from $G_{L,N}(z_1,w_1|z_0)$, presented on Fig.3.2(middle), using the conformal symmetry of $I^{BD}_{L,N}$, i.e. by applying the inversion+shift transformation and thus getting the original quantity (3.2.4) (see Appendix B.2 for derivation and examples).

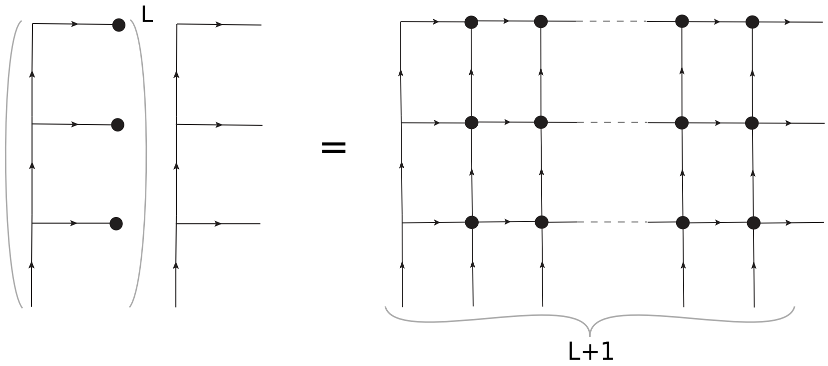

Figure 3.3: The "comb" transfer matrix for an open spin chain of length N ($N = 3$ on the picture) is applied L times to itself as an integral kernel. The resulting structure is a fishnet of the type of fig.3.2(right) with $L+1$ vertical and 3 horizontal lines.

Now we are going to generalize the quantity $G_{L,N}(z_1, w_1|z_0)$, in order to apply the integrability techniques. Therefore, we introduce a more general quantity drawn on Fig.3.2(right):

$$D_{L,N}(z_0)(\boldsymbol{z}|\boldsymbol{w}) = \int \prod_{l=1}^{L}\prod_{n=1}^{N} d^2 z_{ln} \left(\prod_{(l,n)\in\mathcal{L}_{L+1,N}} \frac{1}{[z_{l-1,n-1} - z_{l-1,n}]^{\gamma} \times [z_{l-1,n} - z_{l,n}]^{1-\gamma}} \right), \tag{3.2.6}$$

where all the external legs on the left and on the right of Fig.3.2(left) have different coordinates: $\{z_{j,0} = z_0,\ z_{0,k} = z_k,\ z_{L+1,k} = w_k\}$ for $j = 0, 1, ..., L$ and $k = 1, ..., N$. We introduced in the r.h.s. of (3.2.6) the vector notations: $\boldsymbol{z} = \{z_1, z_2, \ldots, z_N\}$, $\boldsymbol{w} = \{w_1, w_2, \ldots, w_N\}$. Notice that, after point-splitting, we multiplied, for the future convenience, the middle diagram of Fig.3.2 by the vertical propagators on the left, without altering the essential part of the quantity, since the coordinates in the left column are exterior and they are not integrated.

The last expression (3.2.6), representing the diagram on the right of Fig.3.2, is the most appropriate for the application of integrability methods. Namely, we can represent it as a consecutive action of a "comb" transfer matrix "building" the graph, as shown on the Fig.3.3. In the next section, we will define yet a more general transfer matrix $\Lambda_N(x)(\boldsymbol{z}|\boldsymbol{w})$ depending on a spectral parameter x and diagonalize it by means of eigenfunctions using separation of variable (SoV) method of Sklyanin. The lattice of propagators can be inhomogeneous in L-direction, since each transfer matrix, corresponding to an open spin chain of length N "building" the BD configuration by L consecutive applications, as on Fig.3.3, can have its own spectral parameter. Its particular, homogeneous case will give the explicit formula for $2D$ BD graph. [3]

Now we will comment on the obvious $L \leftrightarrow N$ duality of the original BD diagram:

$$I^{BD}_{L,N}(z_0, z_1, w_0, w_1; \gamma) = I^{BD}_{N,L}(z_1, w_0, z_0, w_1, 1-\gamma), \tag{3.2.7}$$

[3] Still containing the anisotropy parameter γ.

where we explicitly introduced among the arguments the anisotropy parameter γ. It is useful to represent the same quantity in a more explicitly conformally symmetric way:

$$I^{BD}_{L,N}(z_0, z_1, w_0, w_1; \gamma) = [w_0 - z_0]^{-L\gamma}[w_1 - z_1]^{N(\gamma-1)} [\eta]^{N\frac{\gamma-1}{2}} [1-\eta]^{N(1-\gamma)} B^{(\gamma)}_{L,N}(\eta). \tag{3.2.8}$$

Then the $L \leftrightarrow N$ duality reads as follows:

$$B^{(1-\gamma)}_{N,L}(1/\eta) = [\eta]^{\frac{\gamma}{2}(N+L)-\frac{N}{2}}[1-\eta]^{-(N+L)\gamma+N} B^{(\gamma)}_{L,N}(\eta). \tag{3.2.9}$$

3.2.2 "Graph building" operator

Our main goal in this chapter is the computation of the quantity $B^{(\gamma)}_{L,N}(\eta)$ directly related to the BD integral by (3.2.8). To that end, we define a more general transfer matrix of an open $SL(2,\mathbb{C})$ spin chain, building the generalized BD graph. The explicit computations will be carried out for values of γ corresponding to the principal series of representations of $SL(2,\mathbb{C})$. Then the original quantity (3.2.3) is obtained by analytic continuation to real $\gamma = \frac{1}{2} + \omega$ in the final result.
First of all, we fix our parameters:

- Definition of the conformal spin:

$$s = \frac{1+n_s}{2} + i\nu_s \ , \ \bar{s} = \frac{1-n_s}{2} + i\nu_s \tag{3.2.10}$$

  where $n_s \in \mathbb{Z}$ is the $SO(2)$ spin and $\nu_s \in \mathbb{R}$, so that $1 + 2i\nu_s$ is the scaling dimension in the principal series of representations [113].

- Definition of the x_k-parameters which will play the role of spin chain inhomogeneities in spectral parameter, and then also of Sklyanin separated variables:

$$x_k = \frac{n_k}{2} + i\nu_k \ , \ \bar{x}_k = -\frac{n_k}{2} + i\nu_k \tag{3.2.11}$$

  where $n_k \in \mathbb{Z}$ and $\nu_k \in \mathbb{R}$.

- The spin s and the parameter x (or y) will enter almost everywhere in special combinations [4], so that for simplicity we shall use the shorthand notations and define the $\alpha\,,\beta\,,\gamma$-parameters

$$\alpha = 1 - s - y \ , \ \beta = 1 - s + y \ , \ \gamma = 2s - 1 \tag{3.2.12}$$

$$\bar{\alpha} = 1 - \bar{s} - \bar{y} \ , \ \bar{\beta} = 1 - \bar{s} + \bar{y} \ , \ \bar{\gamma} = 2\bar{s} - 1 \tag{3.2.13}$$

Now let us define the integral operator $\Lambda_N(y|z_0)$ by its explicit action on a function $\Phi(z_1\,,\ldots,z_N)$ by the formula

$$[\Lambda_N(y|z_0)\Phi](z_1\,,\ldots,z_N\,,z_0) = \prod_{k=1}^{N}[z_k - z_{k+1}]^{-\gamma}\times \tag{3.2.14}$$

[4] In what follows, we will always use the notation y,y_k when the separated variables appear as spectral parameters of an operator, while x,x_k when they label an eigenfunction. Both notations refer to objects of the kind (3.2.11).

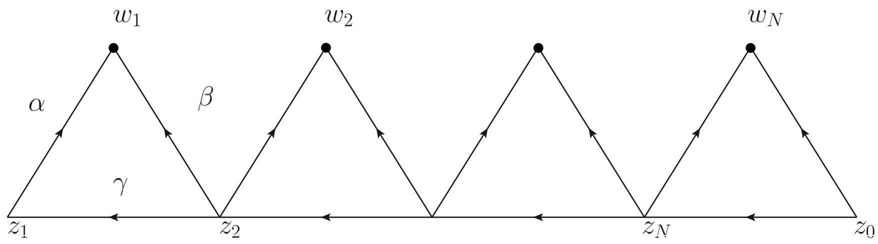

Figure 3.4: The diagrammatic representation for the kernel of $\Lambda_N(y|z_0)$. The arrow with index α from z to w stands for $[w-z]^{-\alpha}$. The indices are given by the following expressions: $\alpha = 1-s-y$, $\beta = 1-s+y$, $\gamma = 2s-1$.

$$\times \int d^2w_1 \cdots d^2w_N \prod_{k=1}^{N} [w_k - z_k]^{-\alpha} [w_k - z_{k+1}]^{-\beta}\, \Phi(w_1\,, \ldots\,, w_N, z_0)\,,$$

where by definition $z_{N+1} = z_0$, and we introduced the symbol $[z]^\alpha \equiv z^\alpha (z^*)^{\bar{\alpha}}$ (see the details for this notation in App. B.1). Note that the operator $\Lambda_N(y|z_0)$ maps the function of N variables to the function of $N+1$ variables, but the last variable z_0 plays some special role of an external variable. The diagrammatic representation for the kernel of the integral operator $\Lambda_N(y|z_0)$ is shown schematically on the Fig.3.4. The operators $\Lambda_N(y|z_0)$ form a commutative family and the proof of the commutation relation

$$\Lambda_N(y_1|z_0)\,\Lambda_N(y_2|z_0) = \Lambda_N(y_2|z_0)\,\Lambda_N(y_1|z_0) \tag{3.2.15}$$

is equivalent to the proof of the corresponding relation for the kernels which is demonstrated on the Fig.3.5. The proof is presented there diagrammatically, with the help of cross relation (B.1.7). In this way, we proved the integrability of our open spin chain since both operators on each side of the last relation contain different spectral parameter, y_1 or y_2. We shall use the similar notations $\Lambda_k(y)$ for $k = 2\,, \ldots\,, N-1$ for operators whose action on a function $\Phi(z_1\,, \ldots\,, z_k)$ is defined in a similar way

$$[z_i - z_{i+1}]^{-\gamma} \times \tag{3.2.16}$$
$$\times \int d^2w_1 \cdots d^2w_k \prod_{i=1}^{k} [w_i - z_i]^{-\alpha} [w_i - z_{i+1}]^{-\beta}\; \Phi(w_1\,, \ldots\,, w_k)\,,$$

The variable z_{k+1} plays here a special role and the diagrammatic representation for the kernel of $\Lambda_k(y)$ is the same as for $\Lambda_N(y|z_0)$ with the evident substitutions $N \to k$ and $z_0 \to z_{k+1}$.

Eigenfunctions of the operator $\Lambda_N(y|z_0)$

The eigenfunctions of the operator $\Lambda_N(y|z_0)$ are constructed explicitly and they admit the following representation

$$\Psi(\boldsymbol{x}|\boldsymbol{z}) = \tilde{\Lambda}_{N-1}\,(x_1)\; \tilde{\Lambda}_{N-2}\,(x_2) \cdots \tilde{\Lambda}_1\,(x_{N-1})\; [z_1 - z_0]^{-s+x_N} \tag{3.2.17}$$

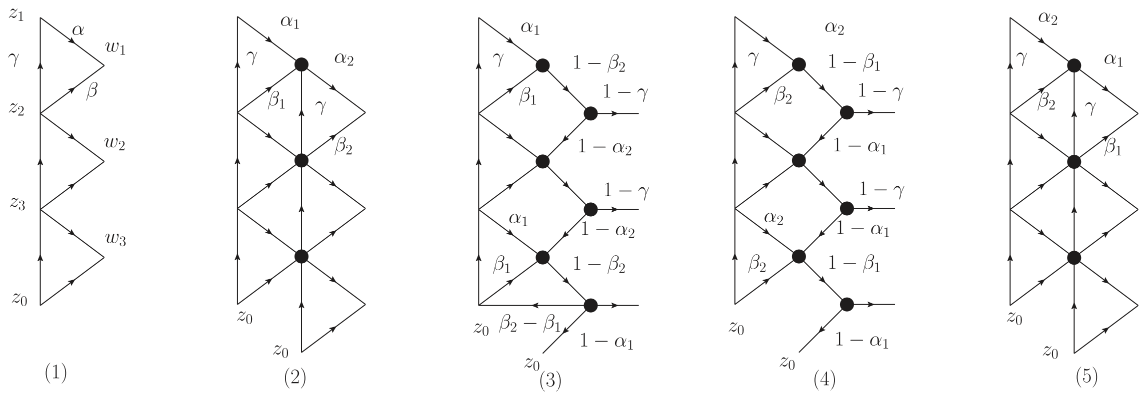

Figure 3.5: The proof of commutation relation (3.2.15) for two operators $\Lambda_N(y|z_0)$: (1) The diagram for the kernel of $\Lambda_3(y|z_0)$. (2) The diagram for $\Lambda_3(y_1|z_0)\,\Lambda_3(y_2|z_0)$: $\alpha_1 = 1-s-y_1$, $\alpha_2 = 1-s-y_2$, $\beta_1 = 1-s+y_1$, $\beta_2 = 1-s+y_2$, $\gamma = 2s-1$. (3) Triangle-star transformations inside the right column of triangles, leading to $\Lambda_3(y_2)$ (4) Movement of the line with index $\beta_2-\beta_1$ upstairs using cross relations. (5) Star-triangle transformations back to $\Lambda_3(y_2|z_0)\,\Lambda_3(y_1|z_0)$.

where the operators $\tilde{\Lambda}_{N-k}\,(x_k)$ differ from the operators $\Lambda_{N-k}\,(x_k)$ by a simple factor

$$\tilde{\Lambda}_{N-k}\,(x_k) = [z_{N-k}-z_0]^{-s+x_k}\, r_{N-k}(x_k,\bar{x}_k)\,\Lambda_{N-k}\,(x_k)\;, \qquad (3.2.18)$$

with r_{N-k} defined according to

$$r_k(x,\bar{x}) = \left(\frac{\Gamma(1-\bar{s}+\bar{x})\Gamma(1-s+x)}{\Gamma(s+x)\Gamma(\bar{s}-\bar{x})}\right)^{k-1}\;. \qquad (3.2.19)$$

and where we introduce a shorthand vector notation for the whole set of variables

$$\begin{aligned} \boldsymbol{x} &= \{\boldsymbol{x}_1,\dots,\boldsymbol{x}_N\}, \qquad \boldsymbol{x}_k = \left(x_k = \frac{n_k}{2}+i\nu_k\;,\;\bar{x}_k = -\frac{n_k}{2}+i\nu_k\right) \\ \boldsymbol{z} &= \{z_1,\dots,z_N\}, \qquad z_k\;\in\;\mathbb{C} \end{aligned} \qquad (3.2.20)$$

The presence of the pre-factor (3.2.19) in the definition of $\tilde{\Lambda}_{N-k}(x)$ operators (3.2.18) is crucial to prove the exchange relation

$$\tilde{\Lambda}_n(x_1)\,\tilde{\Lambda}_{n-1}(x_2) = \tilde{\Lambda}_n(x_2)\,\tilde{\Lambda}_{n-1}(x_1)\,, \qquad (3.2.21)$$

from which follows that $\Psi(\boldsymbol{x}|\boldsymbol{z})$ are symmetric functions of the $\boldsymbol{x}$-variables

$$\Psi(\boldsymbol{x}|\boldsymbol{z}) \;=\; \Psi(x_1,\dots x_k,\dots x_h,\dots,x_N|\boldsymbol{z}) \;=\; \Psi(x_1,\dots x_h,\dots x_k,\dots,x_N|\boldsymbol{z})\,. \qquad (3.2.22)$$

The vector of variables $\boldsymbol{x}$ is used as quantum numbers (separated variables) to label the eigenfunction and $\boldsymbol{z}$ is the set of complex coordinates in our initial representation. We will prove that

$$\Lambda_N(y|z_0)\,\Psi(\boldsymbol{x}|\boldsymbol{z}) = \lambda(y,x_1)\cdots\lambda(y,x_N)\,\Psi(\boldsymbol{x}|\boldsymbol{z})\,, \qquad (3.2.23)$$

where

$$\lambda(y, x_k) = \pi\, a(1-s-y, s+x_k, 1+y-x_k)\,(-1)^{[y+x_k]}\,. \tag{3.2.24}$$

and the function $a(\alpha,\beta,\gamma)$ is defined in App. B.1. We should note that functions $\Psi(\boldsymbol{x}|\boldsymbol{z})$ are generalized eigenfunctions of the operator $A + z_0 B$ where A, B are standard matrix elements of the monodromy matrix [6, 133].

Note that the detailed notation for the eigenfunction should be $\Psi_N(\boldsymbol{x}|\boldsymbol{z})$ but we shall skip N almost everywhere for sake of brevity.

In the simplest case $N = 1$ we have

$$\begin{aligned} \Psi(x_1|z_1) &= [z_1 - z_0]^{-s+x_1}\,, \\ \Lambda_1(y|z_0)\,[z_1 - z_0]^{-s+x_1} &= \lambda(y, x_1)[z_1 - z_0]^{-s+x_1}\,. \end{aligned} \tag{3.2.25}$$

The relation (3.2.25) can be derived by using the chain integration rule (B.1.4). The general proof of the relations (3.2.23)-(3.2.24) is based on the exchange relation

$$\Lambda_N(y|z_0)\,\tilde{\Lambda}_{N-1}(x_1) = \lambda(y, x_1)\,\tilde{\Lambda}_{N-1}(x_1)\,\Lambda_{N-1}(y|z_0) \tag{3.2.26}$$

The proof of the relation (3.2.26) for $N = 3$ is shown in Fig.3.6 and the generalization is obvious. Notice that after exchange, the operator defining the eigenfunction enters with the reduced length N of the effective spin chain. Using the exchange relation step by step it is easy to derive the formula

$$\begin{aligned} &\Lambda_N(y|z_0)\tilde{\Lambda}_{N-1}(x_1)\;\tilde{\Lambda}_{N-2}(x_2)\cdots\tilde{\Lambda}_1(x_{N-1}) = \\ &\lambda(y, x_1)\,\lambda(y, x_2)\cdots\lambda(y, x_{N-1})\,\tilde{\Lambda}_{N-1}(x_1)\;\tilde{\Lambda}_{N-2}(x_2)\cdots\tilde{\Lambda}_1(x_{N-1})\;\Lambda_1(y|z_0)\,. \end{aligned} \tag{3.2.27}$$

Then the proof that $\Psi(\boldsymbol{x}|\boldsymbol{z})$ from (3.2.17) is eigenfunction of the operator $\Lambda_N(x|z_0)$ with the eigenvalues given by (3.2.23) is reduced to the relation (3.2.25) in the form[5]

$$\Lambda_1(y|z_0)\,[z_1 - z_0]^{-s+x_N} = \lambda(y, x_N)[z_1 - z_0]^{-s+x_N}\,.$$

We will see that these eigenfunctions form the complete orthonormal basis. Using them, as well as the explicit eigenvalues of $\Lambda_N(y|z_0)$ give above, we will compute the Basso-Dixon type two-dimensional integral.

Orthogonality and completeness

The functions $\Psi(\boldsymbol{x}|\boldsymbol{z})$ form a complete orthonormal basis in the Hilbert space $\mathbb{H}_N$. Any function $\Phi \in \mathbb{H}_N$ can be expanded w.r.t. this basis as follows

$$\Phi(\boldsymbol{z}) = \int \mathcal{D}_N\boldsymbol{x}\,\boldsymbol{\mu}(\boldsymbol{x})\,C(\boldsymbol{x})\,\Psi(\boldsymbol{x}|\boldsymbol{z})\,. \tag{3.2.28}$$

The symbol $\mathcal{D}_N\boldsymbol{x}$ stands for the measure in the principal series representation of $SL(2,\mathbb{C})$ group

$$\mathcal{D}_N\boldsymbol{x} = \prod_{k=1}^{N}\left(\sum_{n_k=-\infty}^{\infty}\int_{-\infty}^{\infty} d\nu_k\right)\,. \tag{3.2.29}$$

[5] This computation, based on uniqueness relation, can also be checked at $n_k = 0, 1$ conwith the software [134].

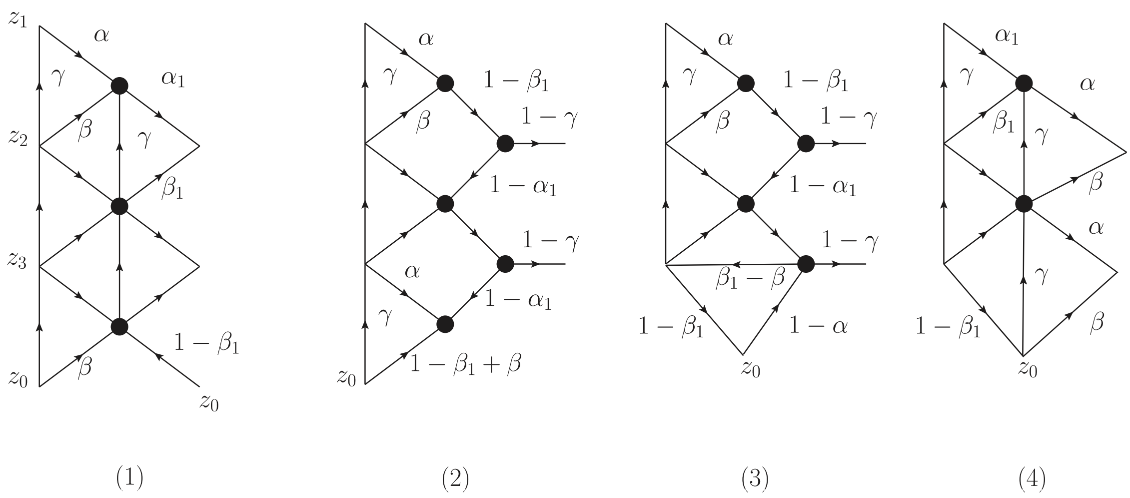

Figure 3.6: The proof of diagonalization procedure for the operator $\Lambda_N(y|z_0)$ for $N=3$, pushing the operator through the first row of the eigenfunction: (1) The diagram for $\Lambda_3(y|z_0)\,\tilde{\Lambda}_2(x_1)$: $\alpha = 1-s-y$, $\alpha_1 = 1-s-x_1$, $\beta = 1-s+y$, $\beta_1 = 1-s+x_1$, $\gamma = 2s-1$. (2) Star-triangle transformations inside $\tilde{\Lambda}_2(x_1)$ and two lines β and $1-\beta_1$ ending at z_0 joint to the one line (3) Movement of the line with index $\beta_1-\beta$ upstairs using cross relations leads to $\tilde{\Lambda}_2(x_1)\,\Lambda_2(y|z_0)$, (4).

Depending on the value of spin in the quantum space, $n_s = s-\bar{s}$, the sum over n_k goes over all integers (integer n_s) or half-integers (half-integer n_s). The coefficient function $C(\boldsymbol{x})$ is given by the scalar product

$$C(\boldsymbol{x}) = \int \mathrm{d}^{2N}\boldsymbol{z}\,\overline{\Psi(\boldsymbol{x}|\boldsymbol{z})}\,\Phi(\boldsymbol{z})\,. \tag{3.2.30}$$

The weight function $\boldsymbol{\mu}(\boldsymbol{x})$

$$\boldsymbol{\mu}(\boldsymbol{x}) = \frac{(2\pi)^{-N}\pi^{-N^2}}{N!}\prod_{k<j}[x_k-x_j] \tag{3.2.31}$$

is the so-called Sklyanin measure [131, 132]. It is related to the scalar product of the eigenfunctions

$$\int \mathrm{d}^{2N}\boldsymbol{z}\,\overline{\Psi(\boldsymbol{x}'|\boldsymbol{z})}\,\Psi(\boldsymbol{x}|\boldsymbol{z}) = \boldsymbol{\mu}^{-1}(\boldsymbol{x})\,\delta_N(\boldsymbol{x}-\boldsymbol{x}')\,. \tag{3.2.32}$$

Here the delta function $\delta_N(\boldsymbol{x}-\boldsymbol{x}')$ is defined as follows:

$$\delta_N(\boldsymbol{x}-\boldsymbol{x}') = \frac{1}{N!}\sum_{s\in S_N}\delta(\boldsymbol{x}_1-\boldsymbol{x}'_{s(1)})\ldots\delta(\boldsymbol{x}_N-\boldsymbol{x}'_{s(N)})\,, \tag{3.2.33}$$

where summation goes over all permutations of N elements and we define

$$\delta(\boldsymbol{x}-\boldsymbol{x}') \equiv \delta_{nn'}\delta(\nu-\nu')\,. \tag{3.2.34}$$

These formulae were obtained in [117, 130] and the corresponding diagrammatic calculations are discussed at length in these papers. The completeness condition for the functions $\Psi(\boldsymbol{x}|\boldsymbol{z})$ has the following form

$$\frac{(2\pi)^{-N}\pi^{-N^2}}{N!}\int \mathcal{D}_N\boldsymbol{x}\prod_{k<j}[x_k - x_j]\,\Psi(\boldsymbol{x}|\boldsymbol{z})\,\overline{\Psi(\boldsymbol{x}|\boldsymbol{z}')} = \prod_{k=1}^{N}\delta^2(\vec{z}_k - \vec{z}^{\,\prime}_k)\,. \quad (3.2.35)$$

A similar formula was proven in the case of $SL(2,\mathbb{R})$ Toda spin chain by [135], in the case of modular XXZ magnet in [136] and for b-Whittaker functions in [137]. It is commonly believed to work for our $SL(2,\mathbb{C})$ spin chain as well, though the proof is still missing.

SoV representation of generalized Basso-Dixon diagrams

We have now the necessary instruments to reduce the Basso-Dixon type Feynman integrals to the SoV form. First we present the most general, inhomogeneous generalization of our construction and then reduce it to homogeneous anisotropic, or even isotropic case. The last one will be the $2D$ analogue of the standard fishnet graph considered in $d = 4$ dimensions in [35]. We will suggest for it an explicit determinant representation.

3.2.3 SoV representation for general inhomogeneous lattice

Using the completeness (3.2.35) and the relation (3.2.23) we can represent the most general "graph-generating" kernel, operator

$$\hat{B}(y_1, y_2, \cdots, y_L, y_{L+1}; z_0) = \Lambda_N(y_1|z_0)\,\Lambda_N(y_2|z_0)\cdots\Lambda_N(y_{L+1}|z_0), \quad (3.2.36)$$

which "builds" a lattice formed by a repeated action of the operator (3.2.14). The integral kernel of the operator (3.2.36) in coordinate representation looks as follows

$$\hat{B}(y_1, y_2, \cdots, y_L, y_{L+1}; z_0)(\boldsymbol{z}|\boldsymbol{w}) = \\ = \frac{(2\pi)^{-N}\pi^{-N^2}}{N!}\int \mathcal{D}_N\boldsymbol{x}\prod_{k<j}[x_k - x_j]\prod_{k=1}^{N}\prod_{l=1}^{L+1}\lambda(y_l, x_k)\,\Psi(\boldsymbol{x}|\boldsymbol{z})\,\overline{\Psi(\boldsymbol{x}|\boldsymbol{w})} \quad (3.2.37)$$

The graphical representation for the left hand side (3.2.37) for this general case is given in the left picture on Fig.3.7. This operator is represented there in the form of a lattice with inhomogeneities defined by spectral parameters $y_1, y_2, \ldots, y_{L+1}$. Later in this section we will perform the reduction of this formula to the homogeneous lattice of propagators as in the Basso-Dixon integral (3.2.2) by taking equal spectral parameters in each column: $y_1 = y_2 = \cdots = y_{L+1} = y$, or even a more particular case of homogeneous but anisotropic lattice of propagators (different powers in two directions), putting $y = s-1$. But so far we consider the most general configuration.

The diagram in Fig.3.7 (right) can be reduced to a generalized Basso-Dixon diagram. First, we have to perform amputation of the most left vertical lines, then the reduction of all $z_k \to z_1$ in the function $\Psi(\boldsymbol{x}|\boldsymbol{z})$ and finally the reduction of all $w_k \to w_1$ in the function $\overline{\Psi(\boldsymbol{x}|\boldsymbol{w})}$ in the right hand side of (3.2.37). We will see

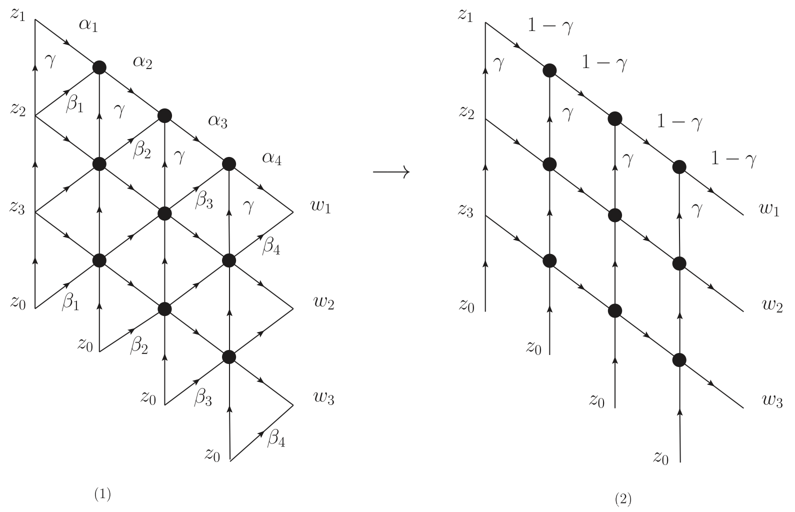

Figure 3.7: (1) The diagram for $\Lambda_3(y_1|z_0)\Lambda_3(y_2|z_0)\Lambda_3(y_3|z_0)\Lambda_3(y_4|z_0)$: $\alpha_k = 1-s-y_k$, $\beta_k = 1-s+y_k$, $\gamma = 2s-1$. (2) Reduction of the diagram for $y_k \to s-1$, or $\beta_k \to 0$.

that such a reduction leads to a significant simplification of the eq. (3.2.37), allowing to perform at the end all the integrations and summations over separated variables explicitly.

Let us start from the function $\Psi_N(x_1\,, x_2 \dots x_N|\boldsymbol{z})$. All the needed steps are illustrated in the Fig. 3.8 for $N=3$. Before the reduction $z_k \to z_1$ we have to perform the amputation of the factors

$$[z_0 - z_1]^{-\gamma}\,[z_1 - z_2]^{-\gamma} \cdots [z_{N-1} - z_N]^{-\gamma}\,.$$

After amputation and reduction $z_k \to z_1$ we obtain the diagram for the action of the operator $\Lambda_N(x)$ for $x = s-1$ on the function $\Psi^{(N-1)}(x_2\,, x_3 \dots x_N|\boldsymbol{z})$. It is an eigenfunction for this operator, with the eigenvalue $\lambda(y_1,x_2)\,\lambda(y_1,x_3)\cdots\lambda(y_1,x_N)\,$. The next step is similar but for a reduced chain $N \to N-1$ and we obtain the next eigenvalue which is $\lambda(y_2,x_3)\,\lambda(y_2,x_4)\cdots\lambda(y_2,x_N)\,$, etc.

After all these manipulations we obtain the following formula for the reduction of the amputated eigenfunction

$$\prod_{k=0}^{N-1}[z_k - z_{k+1}]^{\gamma}\,\Psi(\boldsymbol{x}|\boldsymbol{z}) \to [z_0 - z_1]^{-\alpha_1 - \ldots - \alpha_N}\prod_{k=1}^{N} r_{N-k+1}(x_k, \bar{x}_k)\,\lambda(x_k)^{k-1}\,, \tag{3.2.38}$$

where we introduced

$$\lambda(x_k) = \pi a(2-2s, s+x_k, s-x_k)\,(-1)^{[s+x_k]}\,, \tag{3.2.39}$$

and used the factor $r_n(x_k, \bar{x}_k)$ defined in (3.2.19).

The reduction $z_k \to z_1$ for the eigenfunction $\Psi(\boldsymbol{x}|\boldsymbol{z})$ without amputations of the lines is shown step by step in the Fig.3.9. First of all we use the star-triangle

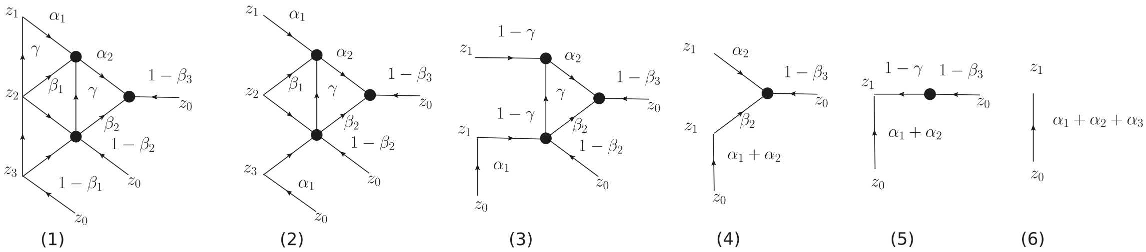

Figure 3.8: Amputation of propagators from the eigenfunction $\Psi(x_1, x_2, x_3|z_1, z_2, z_3)$ and then reduction in the limit $z_k \to z_1$ to the simple power $[z_0 - z_1]^{-\alpha_1-\alpha_2-\alpha_3}$. We perform amputation of $[z_1 - z_2]$ and $[z_2 - z_3]$ lines in (1), then (2) we reduce the first row $z_2, z_3 \to z_1$ leading to (3). We can open the triangle in (3) to a star, so that integrations in upper-left, and then lower-left vertex are performed using chain relation and star-triangle relation. At the next step (4) we join propagators with coinciding coordinates on the left, and performing the last integration (5) via chain relation, the eigenfunction is reduced to a simple line (6).

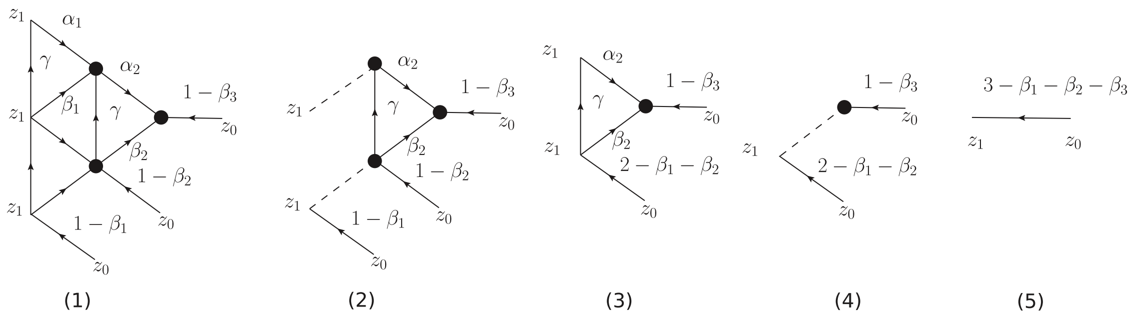

Figure 3.9: Reduction of the eigenfunction $\Psi(x_1, x_2, x_3|z_1, z_2, z_3)$ in the limit $z_k \to z_1$ to simple power $[z_0 - z_1]^{\beta_1+\beta_2+\beta_3-3}$. Dashed lines stand for $\delta^{(2)}(z)$, see also (B.1.5). We reduce $z_3, z_2 \to z_1$ in (1). By applying triangle-star relations to the first row of triangles (1) we obtain δ function kernels. We integrate out δ functions (2) and we open the triangle in (3) to a a star and put together the points z_1 obtaining (4). The δ function is integrated (4), leading to the full reduction of the eigenfunction to a simple line (5).

relation and reduce the triangle to the corresponding delta-function. This elementary reduction

$$[z_2 - z_1]^{-\gamma}\,[w - z_1]^{-\alpha}\,[w - z_2]^{-\beta} \to -\frac{\pi^2}{\gamma\bar{\gamma}}\frac{1}{\lambda(x)}\,\delta^2(z_1 - w)$$

is shown on the right in Fig.3.2. Using this elementary reduction it is possible to reduce the first layer of the diagram for the general eigenfunction $\Psi(\boldsymbol{x}|\boldsymbol{z})$ to the product of the corresponding delta-functions and $[z_0 - z_1]^{\beta_1-1}$ with the coefficient $\left(-\frac{\pi^2}{\gamma\bar{\gamma}}\frac{1}{\lambda(x_1)}\right)^{N-1}$. After integrations in the corresponding vertices in the second layer all delta-functions disappear so that it is possible to repeat the same procedure. After all iterations one obtains the following expression for the reduced eigenfunction

$$\Psi(\boldsymbol{x}|\boldsymbol{z}) \to \prod_{k=1}^{N}\left(r_{N-k+1}(x_k)\left(-\frac{\pi^2}{\gamma\bar{\gamma}}\frac{1}{\lambda(x_k)}\right)^{N-k}\right)\,[z_0 - z_1]^{\beta_1+\ldots+\beta_N-N}\,.$$

Note that we have to perform such reduction also in the function $\overline{\Psi(\boldsymbol{x}|\boldsymbol{w})}$ so that it remains to perform the complex conjugation and evident substitution $\boldsymbol{z} \to \boldsymbol{w}$. Using the rules of the complex conjugation

$$s^* = 1 - \bar{s}\,, (x_k)^* = -\bar{x}_k \quad ; \quad \alpha^* = 1 - \bar{\alpha}\,, \beta^* = 1 - \bar{\beta}\,, \gamma^* = -\bar{\gamma} \tag{3.2.40}$$

$$r_k(x_h)^* = r_k(x_h)^{-1} \;;\; \left([z]^{\beta}\right)^* = [z]^{1-\beta} \quad ; \quad , \lambda^*(x) = -\frac{\pi^2}{\gamma\bar{\gamma}}\frac{1}{\lambda(x)} \tag{3.2.41}$$

and substituting $\boldsymbol{z} \to \boldsymbol{w}$ we obtain

$$\overline{\Psi(\boldsymbol{x}|\boldsymbol{w})} \to \prod_{k=1}^{N} \left(\lambda^{N-k}(x_k)\,/\,r_{N-k+1}(x_k)\right)\, [z_0 - w_1]^{-\beta_1 - \ldots - \beta_N}\,. \tag{3.2.42}$$

Finally, as a result of amputation-reduction on $\Psi(\boldsymbol{x}|\boldsymbol{z})$ and reduction of $\overline{\Psi(\boldsymbol{x}|\boldsymbol{w})}$, by the use of (3.2.38) and (3.2.42) the projector $\Psi(\boldsymbol{x}|\boldsymbol{z})\overline{\Psi(\boldsymbol{x}|\boldsymbol{w})}$ is transformed into

$$\prod_{k=1}^{N} \lambda^{N-1}(x_k)\, [z_0 - z_1]^{-\alpha_1 - \ldots - \alpha_N}\, [z_0 - w_1]^{-\beta_1 - \ldots - \beta_N}\,. \tag{3.2.43}$$

We point out that the way we reduce the N coordinates $\boldsymbol{z} = \{z_k\}$ to a single point in the functions $\Psi(\boldsymbol{x}|\boldsymbol{z})$ and $\overline{\Psi(\boldsymbol{x}|\boldsymbol{z})}$ can be alternatively obtained by inserting the complete basis (3.2.35) between two Λ-kernels in (3.2.36), and repeating their diagonalization after the reduction of the last kernel $\Lambda_N(y_{L+1}|z_0)$ and the amputation and reduction of the first $\Lambda_N(y_1|z_0)$.
From formula (3.2.43) we obtain the following representation for the two-dimensional analogue of generalized Basso-Dixon diagram:

$$G^{\boldsymbol{y}}_{N,L}(z_1\,, w_1\,, z_0) = \frac{(2\pi)^{-N}\pi^{-N^2}}{N!} \int \mathcal{D}_N\boldsymbol{x} \prod_{k<j}[x_k - x_j] \times \tag{3.2.44}$$

$$\times \prod_{k=1}^{N} \left(\lambda^{N-1}(x_k) \prod_{l=1}^{L+1} \lambda(y_l, x_k)\right) [z_0 - z_1]^{-\alpha_1 - \ldots - \alpha_N}\, [z_0 - w_1]^{-\beta_1 - \ldots - \beta_N}\,.$$

We recall that $\alpha_k = 1 - s - x_k\,,\ \beta_k = 1 - s + x_k$ and $x_k = \frac{n_k}{2} + i\nu_k\ ,\ \bar{x}_k = -\frac{n_k}{2} + i\nu_k$.

Introducing the amputated cross ratio

$$\eta|_{w_0 \to \infty} = \frac{z_0 - w_1}{z_0 - z_1} \tag{3.2.45}$$

we rewrite the last expression for inhomogeneous and anisotropic 2D Basso-Dixon type integral in a concise form

$$G^{\boldsymbol{y}}_{L,N}(z_1\,, w_1\,, z_0) = \left([z_0 - z_1]\,[z_0 - w_1]\right)^{N(s-1)}\, B^{\boldsymbol{y}}_{L,N}(\eta) \tag{3.2.46}$$

where

$$B^{\boldsymbol{y}}_{L,N}(\eta) = \frac{(2\pi)^{-N}\pi^{-N^2}}{N!} \int \mathcal{D}_N\boldsymbol{x} \prod_{k=1}^{N} \left([\eta]^{-x_k}\lambda^{N-1}(x_k) \prod_{l=1}^{L+1} \lambda(y_l, x_k)\right) \prod_{k<j}[x_k - x_j]\,.$$

and by superscript $\boldsymbol{y}$ we mean the vector of inhomogeneity parameters $\boldsymbol{y} = (y_1, y_2, \ldots, y_N)$.

Determinant representation

We notice that in (3.2.47) we deal with the multiple integral of a special type which can be transformed, similarly to the eigenvalue reduction of the hermitian one-matrix integral [138, 139], to the determinant form

$$B^{\boldsymbol{y}}_{L,N}(\eta) = \frac{(2\pi)^{-N}\pi^{-N^2}}{N!} \int \mathcal{D}_N \boldsymbol{x} \prod_{k<j} [x_k - x_j] \prod_{k=1}^{N} f_{\{y\}}(x_k) = N!\det M \tag{3.2.47}$$

where we introduced the momenta

$$M_{ij} = \int \mathcal{D}x \; x^{i-1}\bar{x}^{j-1} f_{\{y\}}(x) \; ; \; i,j = 1\,,\dots\,,N \tag{3.2.48}$$

with the weight function given in our case by the expression

$$f_{\{y\}}(x) = [\eta]^{-x}\lambda^{N-1}(x) \prod_{l=1}^{L+1} \lambda(y_l, x) = \eta^{-x}\bar{\eta}^{-\bar{x}}\lambda^{N-1}(x) \prod_{l=1}^{L+1} \lambda(y_l, x) \tag{3.2.49}$$

where $\lambda(x)$ and $\lambda(y,x)$ are defined in eqs.(3.2.39),(3.2.24). So for any pair of integers L, N the problem is reduced to the computation of momenta (3.2.48), which we will do explicitly in the section 3.2.4 after the reduction to Basso-Dixon configuration of the general formula (3.2.46).

Reductions

In particular case, leading to the homogenous Basso-Dixon lattice configuration, we put $y_1 = y_2 = \cdots = y_L = y$ and obtain for the reduced quantity

$$B^{\boldsymbol{y}}(z_0)(\boldsymbol{z}|\boldsymbol{w})\,|_{y_1=y_2=\cdots=y_L=y} \equiv B(y;z_0)(\boldsymbol{z}|\boldsymbol{w}) = \Lambda^L(y|z_0)(\boldsymbol{z}|\boldsymbol{w}) \tag{3.2.50}$$

the following SoV representation:

$$B(y;z_0)(\boldsymbol{z}|\boldsymbol{w}) = \frac{(2\pi)^{-N}\pi^{-N^2}}{N!} \int \mathcal{D}_N \boldsymbol{x} \prod_{k<j} [x_k - x_j] \prod_{k=1}^{N} \lambda^L(y, x_k)\, \Psi(\boldsymbol{x}|\boldsymbol{z})\, \overline{\Psi(\boldsymbol{x}|\boldsymbol{w})}\,.$$

The further reduction of this expression, $\beta_k \to 0$, or $y_k = y \to s-1$, will lead to anisotropic Basso-Dixon type $d = 2$ integral (3.2.3) with parameters $\gamma = 2s-1$, $\bar{\gamma} = 2\bar{s}-1$. After this reduction we obtain the second diagram in Fig.3.7, with the different propagators $[z-z']^{1-2s}$ and $[z-z']^{2s-2}$ in vertical and horizontal directions of the lattice. In this case, we have to substitute into the formula (3.2.37) representing this diagram the reduced eigenvalues

$$\begin{aligned} \lambda(y,x_k) &= \pi a(1-s-y, s+x_k, 1+y-x_k)\,(-1)^{[y+x_k]} \quad \xrightarrow{y=s-1} \\ \longrightarrow \lambda(x_k) &= \pi a(2-2s, s+x_k, s-x_k)\,(-1)^{[s+x_k]}\,. \end{aligned} \tag{3.2.51}$$

This leads, after the identification of external coordinates: $z_k \to z_1$, $w_k \to w_1$, described above, to the following representation for the two-dimensional analog of (anisotropic) Basso-Dixon diagram $B_{L,N}(\eta)$ in terms of the multiple integral over N separated variables

$$B_{L,N}(\eta) = \frac{(2\pi)^{-N}\pi^{-N^2}}{N!} \int \mathcal{D}_N \boldsymbol{x} \prod_{k=1}^{N} [\eta]^{-x_k} \lambda^{N+L}(x_k) \prod_{k<j} [x_k - x_j]\,. \quad (3.2.52)$$

Notice that the parameters of the representation $(s, \bar{s})$ can be chosen in the principal series (3.2.10), or even in the imaginary strip $\nu^{(s)} \in (-i/2\,, 0)$ by analytic continuation. With the choice of parameters $n_s = 0$ and $\nu^{(s)} = -i/4 \pm i\,\omega/2$ in (3.2.10) we describe the 2D Basso-Dixon type integral with real propagators $|z - z'|^{-1\mp\omega}$, where $\pm$ signs corresponds to two different axis of the square lattice shaped Feynman graph, according to the bi-scalar Lagrangian (2.1.3). The isotropy of the lattice is restored at $s = \bar{s} = 3/4$, that is $\omega = 0$.

The determinant formula (3.2.47) reads for this reduction as follows

$$B^{(\gamma,\bar{\gamma})}_{L,N}(\eta) = (2\pi)^{-N}\pi^{-N^2} \det_{1\le j,k\le N} m_{jk}\,, \quad (3.2.53)$$

where

$$m_{ij} = \int \mathcal{D}x \; x^{i-1}\bar{x}^{j-1} f(x) \;;\; i, j = 1\,, \ldots\,, N \quad (3.2.54)$$

and

$$f(x) = [\eta]^{-x}\lambda^{N+L}(x) = \eta^{-x}\bar{\eta}^{-\bar{x}}\lambda^{N+L}(x) \quad (3.2.55)$$

where $\lambda(x)$ is defined in eqs.(3.2.39).

3.2.4 Explicit computation of ladder integral

In this section, we will explicitly compute the momenta m_{ij} given by (3.2.54) in terms of hypergeometric functions, which leads to explicit expressions of Basso-Dixon type integrals via the determinant representation (3.2.53). Some details of the derivation can be found in Appendix B.3. In particular this leads to the computation of the class of ladder integrals in $2D$, that are defined as the Basso-Dixon diagram for $N = 1$ and generic L (or viceversa).

Noticing that

$$m_{ij} = (\eta\partial_\eta)^{i-1}(\bar{\eta}\partial_{\bar{\eta}})^{j-1} I_{N+L}\;, \quad \text{where} \quad I_M = \int \mathcal{D}x\, \eta^{-x}\bar{\eta}^{-\bar{x}}\lambda^M(x) \quad (3.2.56)$$

we are led to compute the following sum and integral[6]:

$$
\begin{aligned}
&I_M = \int \mathcal{D}x\, \eta^{-x}\bar{\eta}^{-\bar{x}}\lambda^M(x) = \\
&= \pi^M a^M(2-2s)(-1)^{M[s]} \int \mathcal{D}x\, a^M(s+x,s-x)\,(-1)^{M[x]}\eta^{-x}\bar{\eta}^{-\bar{x}} = \\
&= \pi^M a^M(2-2s)\times \\
&\times \sum_{n\in Z}\int_{-\infty}^{+\infty} d\nu\, \frac{\Gamma^M(1-\bar{s}-\frac{n}{2}+i\nu)\Gamma^M(1-\bar{s}+\frac{n}{2}-i\nu)}{\Gamma^M(s-\frac{n}{2}-i\nu)\Gamma^M(s+\frac{n}{2}+i\nu)}(-1)^{M(n+n_s)}\eta^{-\frac{n}{2}-i\nu}\bar{\eta}^{\frac{n}{2}-i\nu}\,,
\end{aligned}
\tag{3.2.57}
$$

where in the last line we substituted explicit parameters. We will compute the integral over ν by residues. The structure of the poles and zeroes is shown in the Fig. 3.10. We can close the integration contour on the upper/lower half-plane under the condition $|\eta| < 1$, respectively $|\eta| > 1$, ensuring the exponential suppression of the integrand at $\pm i\infty$. Consider first the case $|\eta| < 1$. In the upper half-plane there is one infinite sequence of poles of the order M. After the change of variables $n \to -n+n_s+1$ in the sum over n and $\nu \to \nu+\nu_s$ in the integral over ν, the integral (3.2.57) reads

$$
\begin{aligned}
I_M = &\frac{\pi^M a^M(2-2s)(-1)^M}{\eta^s\bar{\eta}^{\bar{s}-1}}\times \\
\times &\sum_{n\in Z}\int_{-\infty}^{+\infty} d\nu\, \frac{\Gamma^M(2-2\bar{s}-\frac{n}{2}-i\nu)\Gamma^M(\frac{n}{2}+i\nu)}{\Gamma^M(2s-\frac{n}{2}+i\nu)\Gamma^M(\frac{n}{2}-i\nu)}(-1)^{Mn}\eta^{\frac{n}{2}-i\nu}\bar{\eta}^{-\frac{n}{2}-i\nu}
\end{aligned}
$$

We close the contour in the upper half-plane and calculate the ν-integral as the sum of residues. Due to the mechanism illustrated in fig.3.10, this is equivalent to take residues at the points $\nu = \frac{in}{2}+ik\,, k = 0\,,1\,,2\,,\ldots$, i.e. the series of the poles created by the function $\Gamma^M(\frac{n}{2}+i\nu)$. The residue at the point $\nu = \frac{in}{2}+ik$ can be represented in the following form

$$
\begin{aligned}
\mathrm{Res}_{\nu=\frac{in}{2}+ik} = -\frac{i}{(M-1)!}\,\partial_\varepsilon^{M-1}\big|_{\varepsilon=0}\Bigg[&\frac{\Gamma^M(1+\varepsilon)\Gamma^M(1-\varepsilon)}{\Gamma^M(2s+\varepsilon)\Gamma^M(1-2s-\varepsilon)}\,[\eta]^{-\varepsilon}\times \\
\times&\frac{\Gamma^M(1-2s+n+k-\varepsilon)}{\Gamma^M(n+k-\varepsilon)}\frac{\Gamma^M(2-2\bar{s}+k-\varepsilon)}{\Gamma^M(1+k-\varepsilon)}\,\eta^{n+k}\,\bar{\eta}^k\Bigg]\,.
\end{aligned}
$$

Using this formula one obtains the following relation

$$
\begin{aligned}
&\sum_{n\in Z}\int_{-\infty}^{+\infty} d\nu\, \frac{\Gamma^M(2-2\bar{s}-\frac{n}{2}-i\nu)\Gamma^M(\frac{n}{2}+i\nu)}{\Gamma^M(2s-\frac{n}{2}+i\nu)\Gamma^M(\frac{n}{2}-i\nu)}(-1)^{Mn}\eta^{\frac{n}{2}-i\nu}\bar{\eta}^{-\frac{n}{2}-i\nu} = \\
&\qquad = \frac{2\pi}{(M-1)!}\,\partial_\varepsilon^{M-1}\big|_{\varepsilon=0}\Bigg[\frac{\Gamma^M(1+\varepsilon)\Gamma^M(1-\varepsilon)}{\Gamma^M(2s+\varepsilon)\Gamma^M(1-2s-\varepsilon)}\,[\eta]^{-\varepsilon}\,\times
\end{aligned}
$$

[6] We use here and in the following the notation $(-1)^{[\alpha]}$, see (B.1.2).

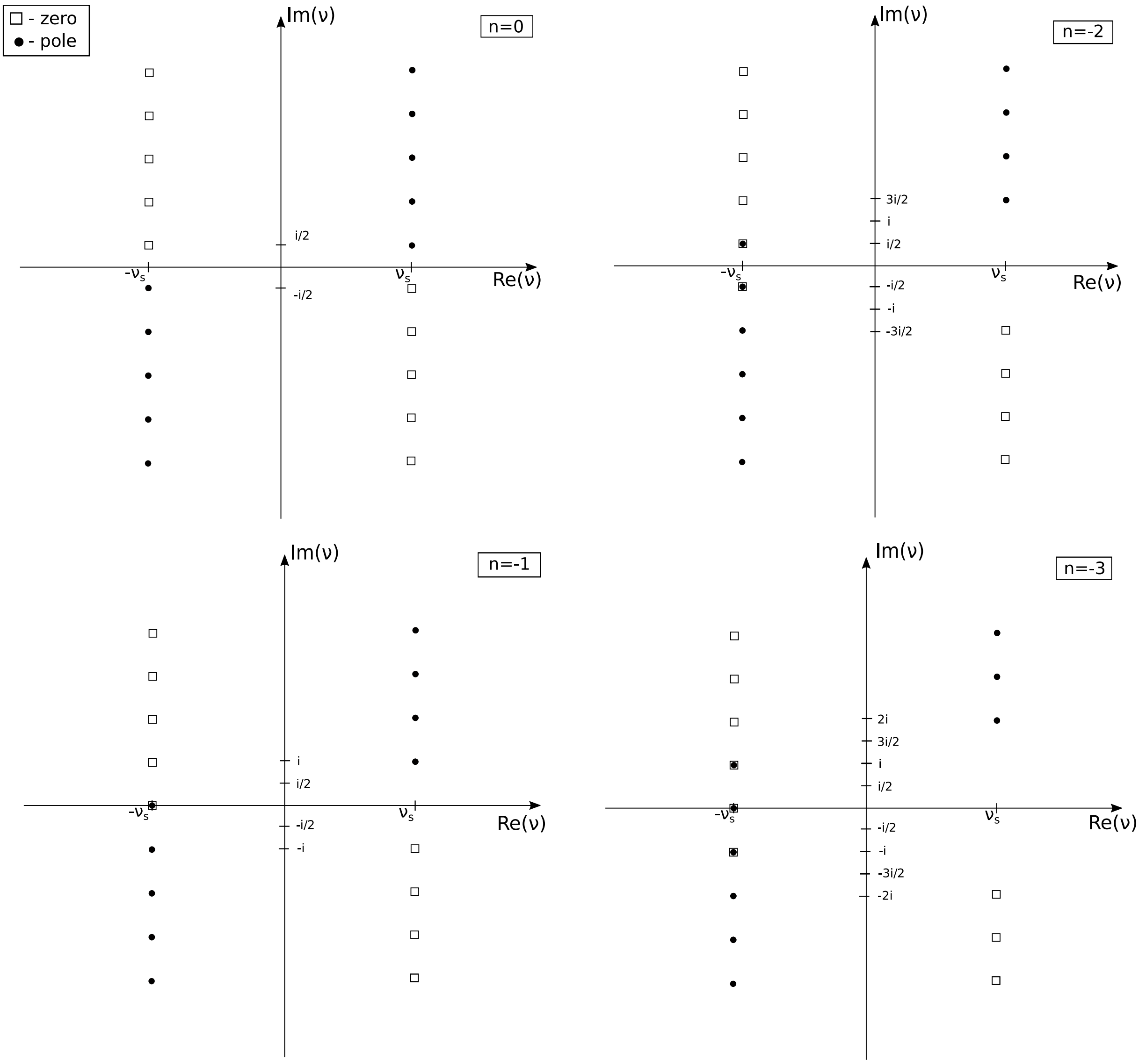

Figure 3.10: Structure of poles and zeroes of the integrand in (3.2.57), at different values of the discrete variable n, for $n_s = 0$. Superposition of zeroes and poles occurs in such a way that there is only one semi-infinite series of poles (and zeroes) in upper- and lower- half-planes.

$$\times \sum_{n \in Z} \sum_{k=0}^{+\infty} \frac{\Gamma^M(1-2s+n+k-\varepsilon)}{\Gamma^M(n+k-\varepsilon)} \frac{\Gamma^M(2-2\bar{s}+k-\varepsilon)}{\Gamma^M(1+k-\varepsilon)} \eta^{n+k} \bar{\eta}^k \Bigg] \, .$$

Remarkably enough, since we take derivative at $\varepsilon = 0$ the last double sum can be equivalently rewritten in a factorized form, setting $p = n + k - 1$

$$\eta \sum_{p=0}^{+\infty} \frac{\Gamma^M(2-2s+p-\varepsilon)}{\Gamma^M(1+p-\varepsilon)} \eta^p \sum_{k=0}^{+\infty} \frac{\Gamma^M(2-2\bar{s}+k-\varepsilon)}{\Gamma^M(1+k-\varepsilon)} \bar{\eta}^k \, ,$$

and we obtain the following expression for the ladder integral

$$\int \mathcal{D}x\lambda^M(x)[\eta]^{-x} = \frac{2\pi^{M+1}a^M(1-\gamma)(-1)^M}{(M-1)!\,[\eta]^{\frac{\gamma-1}{2}}} \times \\ \times\, \partial_\varepsilon^{M-1}\big|_{\varepsilon=0} \frac{\Gamma^M(1+\varepsilon)\Gamma^M(1-\varepsilon)}{\Gamma^M(\gamma+1+\varepsilon)\Gamma^M(-\gamma-\varepsilon)}\,[\eta]^{-\varepsilon}\,F_M(1-\gamma\,,\varepsilon|\eta)\,F_M(1-\bar\gamma\,,\varepsilon|\bar\eta)\,, \tag{3.2.58}$$

where $\gamma = 2s-1$ and the function $F_M(\lambda\,,\varepsilon|\eta)$ is given by the hypergeometric series

$$F_M(\lambda\,,\varepsilon|\eta) = \sum_{k=0}^{\infty}\frac{\Gamma^M(\lambda+k-\varepsilon)}{\Gamma^M(1+k-\varepsilon)}\,\eta^k = \frac{\Gamma(\lambda-\epsilon)^M}{\Gamma(1-\epsilon)^M}\times \\ \times\ {}_{M+1}F_M(1,\underbrace{\lambda-\epsilon,\ldots,\lambda-\epsilon}_{M};\underbrace{1-\epsilon,\ldots,1-\epsilon}_{M};\eta)\,. \tag{3.2.59}$$

Therefore we can write in a more compact notation, for $|\eta|<1$:

$$I_M = \frac{2\pi^{M+1}a^M(1-\gamma)}{(M-1)!\,[\eta]^{\frac{\gamma-1}{2}}}\ \partial_\varepsilon^{M-1}\big|_{\varepsilon=0}\frac{a^M(\gamma+\varepsilon)\Gamma^M(1+\varepsilon)}{\Gamma^M(1-\varepsilon)}\,[\eta]^{-\varepsilon}\,\mathcal{F}_M^{\gamma,\bar\gamma}(\eta,\bar\eta|\varepsilon),$$

where

$$\mathcal{F}_M^{\gamma,\bar\gamma}(\eta,\bar\eta|\varepsilon) = \\ = {}_{M+1}F_M\left(\begin{matrix}1-\gamma-\varepsilon & \cdots & 1-\gamma-\varepsilon & 1\\ 1-\varepsilon & \cdots & 1-\varepsilon & \end{matrix}\middle|\,\eta\right)\,{}_{M+1}F_M\left(\begin{matrix}1-\bar\gamma-\varepsilon & \cdots & 1-\bar\gamma-\varepsilon & 1\\ 1-\varepsilon & \cdots & 1-\varepsilon & \end{matrix}\middle|\,\bar\eta\right). \tag{3.2.60}$$

In the opposite case of $|\eta|>1$ the same kind of computation can be repeated picking residues in the lower half plane. After redefinition $n\to -n+2n_s+2$, this is equivalent to pick the series of poles $\nu = 2is+\frac{in}{2}-ik\,,k=0\,,1\,,2\,,\ldots$, and the residues are

$$\mathrm{Res}_{\nu=2is+\frac{in}{2}-ik} = \frac{i}{(M-1)!}\eta^{2s}\bar\eta^{2\bar s-2}\,\partial_\varepsilon^{M-1}\big|_{\varepsilon=0}\frac{\Gamma^M(1+\varepsilon)\Gamma^M(1-\varepsilon)}{\Gamma^M(2s+\varepsilon)\Gamma^M(1-2s-\varepsilon)}\,[\eta]^{\varepsilon}\times \\ \times\frac{\Gamma^M(1-2s+n+k-\varepsilon)}{\Gamma^M(n+k-\varepsilon)}\frac{\Gamma^M(2-2\bar s+k-\varepsilon)}{\Gamma^M(1+k-\varepsilon)}\,\eta^{-n-k}\,\bar\eta^{-k}\,.$$

It follows from (3.2.61) that the final expression of the ladder for $|\eta|>1$ is the same as (3.2.60) after replacing η with $1/\eta$. For a generic cross-ratio $|\eta|\lessgtr 1$ the M-ladder is, respectively

$$I_M = \frac{2\pi^{M+1}a^M(1-\gamma)}{(M-1)!\,[\eta]^{\pm(\frac{\gamma-1}{2})}}\ \partial_\varepsilon^{M-1}\big|_{\varepsilon=0}\frac{a^M(\gamma+\varepsilon)\Gamma^M(1+\varepsilon)}{\Gamma^M(1-\varepsilon)}\,[\eta]^{\mp\varepsilon}\,\mathcal{F}_M^{\gamma,\bar\gamma}(\eta^{\pm1},\bar\eta^{\pm1}|\varepsilon)\,, \tag{3.2.61}$$

and it shows explicitly the invariance under exchange $z_1\leftrightarrow w_1$; in fact

$$I_M(\eta) = I_M\left(\frac{1}{\eta}\right)\,. \tag{3.2.62}$$

The result (3.2.61), obtained under the assumption of $(s, \bar{s})$ in the principal series of $SL(2,\mathbb{C})$, can be remarkably extended by analytic continuation to $s = \bar{s} \in (1/2\,,1)$, that is setting $\gamma = \bar{\gamma} \in (0,1)$ in (3.2.61). The direct computation of ladder integrals is more involved in this last case, since analytic continuation leads to the failure of the cancellation of poles by zeros presented on Fig.3.10, and integration in (3.2.57) must be carried out under an appropriate contour deformation prescription. The explicit result for the particular choice of weights $\gamma = \bar{\gamma} = 1/2$, corresponding to the isotropic fishnet theory (the case considered by Basso and Dixon in [35] for $d = 4$) reads:

$$I_M = \frac{2\pi^{M+1}}{(M-1)!\,|\eta|^{\pm\frac{1}{2}}}\; \partial_\varepsilon^{M-1}\Big|_{\varepsilon=0} \frac{a^M\left(\frac{1}{2}+\varepsilon\right)\Gamma^M(1+\varepsilon)}{\Gamma^M(1-\varepsilon)}\,[\eta]^{\mp\varepsilon}\,\mathcal{F}_M^{\frac{1}{2},\frac{1}{2}}(\eta^{\pm 1},\bar{\eta}^{\pm 1}|\varepsilon), \tag{3.2.63}$$

$$\mathcal{F}_M^{\frac{1}{2},\frac{1}{2}}(\eta,\bar{\eta}|\varepsilon) \;=\; {}_{M+1}F_M\left(\begin{matrix}\frac{1}{2}-\varepsilon & \cdots & \frac{1}{2}-\varepsilon & 1\\ 1-\varepsilon & \cdots & 1-\varepsilon & \end{matrix}\,\middle|\,\eta\right)\,{}_{M+1}F_M\left(\begin{matrix}\frac{1}{2}-\varepsilon & \cdots & \frac{1}{2}-\varepsilon & 1\\ 1-\varepsilon & \cdots & 1-\varepsilon & \end{matrix}\,\middle|\,\bar{\eta}\right).$$

Moreover in the isotropic case $\gamma = 1-\gamma$, and for the simple "cross" $N = 1$, $L = 1$ diagram (computed below in terms of elliptic functions), the duality (3.2.9) is a mere consequence of (3.2.62)

$$B_{1,1}^{(1/2)}(\eta) = I_2^{(1/2)}(\eta) = I_2^{(1/2)}\left(\frac{1}{\eta}\right) = B_{1,1}^{(1/2)}\left(\frac{1}{\eta}\right).$$

For the sake of duality in the more involved anisotropic case we will need also the relation between ladders with exchange of $\gamma \leftrightarrow 1-\gamma$. This relation can be easily checked and looks as follows

$$I_2^{(1-\gamma)}\left(\frac{1}{\eta}\right) \;=\; [\eta]^{\gamma-\frac{1}{2}}[1-\eta]^{1-2\gamma}\,I_2^{(\gamma)}(\eta)\,,$$

and due to $B_{1,1}^{(\gamma)} = I_2^{(\gamma)}$ the duality (3.2.9) is also proved.
In the simplest particular case $M = 1$ we can simply put $\varepsilon = 0$ everywhere and then reduce to the simple power

$$F_1(\lambda\,,0|\eta) = \sum_{k=0}^{\infty}\frac{\Gamma(\lambda+k)}{k!}\,\eta^k = \frac{\Gamma(\lambda)}{(1-\eta)^\lambda}\,,$$

so that

$$\begin{aligned} G_{L=0,N=1}(z_1\,,w_1\,,z_0) &= (2\pi^2)^{-1}\left([z_0-z_1]\,[z_0-w_1]\right)^{\frac{\gamma-1}{2}}\,B_{0,1}^{(\gamma,\bar{\gamma})}(\eta) = \\ &= \left([z_0-z_1]\,[z_0-w_1]\right)^{\frac{\gamma-1}{2}}\,\frac{a(1-\gamma,\gamma)}{[\eta]^{\frac{\gamma-1}{2}}[1-\eta]^{1-\gamma}} = \frac{1}{[w_1-z_1]^{1-\gamma}}\,, \end{aligned} \tag{3.2.64}$$

which is precisely the single propagator in the trivial case of the Basso-Dixon type formula, with no integrations.

In order to get a better feeling of the structure of our result (3.2.60) at generic $N+L$, it is instructive to compute the first non-trivial graph $G_{L=1,N=1}(z_1,w_1,z_0)$ - the two-dimensional "cross" integral. In four dimensions, the cross integral can be computed in terms of the Bloch-Wigner function (di-logarithm function) [34]. We will see that in our two-dimensional case the answer for the cross integral can be expressed through elliptic functions. Since it involves only $N=1$ separated variable, it is simply related to the ladder I_2:

$$G_{L=1,N=1}(z_1,w_1,z_0) \;=\; (2\pi^2)^{-1}([z_0-z_1][z_0-w_1])^{\frac{\gamma-1}{2}} I_2(\eta). \tag{3.2.65}$$

For $M=2$ the ladder integral (3.2.60) reads:

$$\frac{2\pi^3 a^2(1-\gamma)}{[\eta]^{\frac{\gamma-1}{2}}}\times$$
$$\times\, \partial_\varepsilon|_{\varepsilon=0}\, a^2(\gamma+\varepsilon)\frac{\Gamma^2(1+\varepsilon)}{\Gamma^2(1-\varepsilon)}[\eta]_3^{-\varepsilon}F_2\left(\begin{matrix}1-\gamma-\varepsilon & 1-\gamma-\varepsilon & 1\\ 1-\varepsilon & 1-\varepsilon & \end{matrix}\middle|\,\eta\right){}_3F_2\left(\begin{matrix}1-\gamma-\varepsilon & 1-\gamma-\varepsilon & 1\\ 1-\varepsilon & 1-\varepsilon & \end{matrix}\middle|\,\bar\eta\right).$$

Choosing the conformal weights for isotropic fishnets $\gamma=\bar\gamma=1/2$, the ladder simplifies to

$$2\pi^3\,\partial_\varepsilon|_{\varepsilon=0}\frac{\Gamma^2(1+\varepsilon)\Gamma^2(1/2-\varepsilon)}{\Gamma^2(1-\varepsilon)\Gamma^2(1/2+\varepsilon)}[\eta]_2^{\frac14-\varepsilon}F_1\left(\frac12-\varepsilon,\frac12-\varepsilon;1-2\varepsilon\middle|\,\eta\right)_2F_1\left(\frac12-\varepsilon,\frac12-\varepsilon;1-2\varepsilon\middle|\,\bar\eta\right). \tag{3.2.66}$$

We can recall the expression of the $2D$ conformal cross integral [140] (e.g. see the formula (1.7) of [141]); after amputation of one line by sending w_0 to infinity, we get

$$\tilde G_{h,\bar h}=\int\frac{d^2\rho}{[w_1-\rho]^h[z_0-\rho]^h[z_1-\rho]^{1-h}}=\frac{{}_2F_1(h,h;2h|\eta)\,{}_2F_1(\bar h,\bar h;2\bar h|\bar\eta)[\eta]^h}{[w_1-z_0]^hB(1-h)}+(h\leftrightarrow 1-h); \tag{3.2.67}$$

$$B(h)=\frac{2^{-2i\sigma}(-2i\sigma)}{\pi}\frac{\Gamma\left(\frac12+i\sigma\right)\Gamma\left(-i\sigma\right)}{\Gamma\left(\frac12-i\sigma\right)\Gamma\left(i\sigma\right)};\qquad h=\frac12+i\sigma. \tag{3.2.68}$$

In order to compare with (3.2.65) we should set $h=1/2$, that is $\sigma=0$. Due to the vanishing of $B(1/2)$, this expression is an ill-defined sum of two divergent terms. The issue is solved by taking the limit $\sigma\to0$ in (3.2.67), which gives the well defined function

$$\frac{\pi}{2\,|w_1-z_0|}\lim_{\sigma\to0}\left[\frac{\Gamma\left(\frac12+i\sigma\right)^2\Gamma\left(1-i\sigma\right)^2}{\Gamma\left(\frac12-i\sigma\right)^2\Gamma\left(1+i\sigma\right)^2}[\eta]^{i\sigma}F\left(\sigma|\eta\right)\,F\left(\sigma|\bar\eta\right)\;+\;(\sigma\leftrightarrow-\sigma)\right],$$
$$\text{where}\;\; F\left(\sigma|x\right)\;=\;{}_2F_1\left(\frac12+i\sigma,\frac12+i\sigma;1+2i\sigma\,\middle|\,x\right)$$

and reproduces the result of plugging (3.2.66) into (3.2.65). The problem reduces to computing $F\left(\sigma|\eta\right)$ and $\partial_\sigma|_{\sigma=0}F\left(\sigma|\eta\right)$ which reduce to elliptic integrals. Then the cross integral can be presented in explicit form:

$$I^{BD}_{1,1}(z_0,z_1,w_0,w_1)\;\equiv\;\int\frac{d^2\rho}{|z_0-\rho||w_0-\rho||z_1-\rho||w_1-\rho|}\;=$$

$$= \frac{4\,|1-\eta|}{|w_1 - z_1||w_0 - z_0|}\left[K(\eta)K(1-\bar{\eta}) + K(\bar{\eta})K(1-\eta)\right], \qquad |\eta| < 1 \tag{3.2.69}$$

where here:

$$\eta = \frac{z_0 - w_1}{w_1 - w_0}\frac{z_1 - w_0}{z_0 - z_1}$$

and $K(x)$ is the elliptic integral of the first kind:

$$K(x) = \int_0^1 \frac{dt}{\sqrt{(1-t^2)(1-x\,t^2)}}.$$

This result for the cross integral suggests that even for any L, N the formula for two-dimensional Basso-Dixon integral can be presented in terms of elliptic polylogarithms encountered in various Feynman graph calculations [142].

3.2.5 Ladders and the wheel integrals

The computation of 2-dimensional ladders carried out in the previous sections has other interesting applications in the context of the theory (2.1.3). The simplest observables in this theory are single trace operators $\mathrm{tr}(\phi_1^l)(z)$, $\mathrm{tr}(\phi_2^l)(z)$. As explained in [28, 32], the perturbative expansions of their correlators

$$\langle \mathrm{tr}\phi_1^l(z)\mathrm{tr}(\phi_1^\dagger)^l(w)\rangle \qquad \langle \mathrm{tr}\phi_2^l(z)\mathrm{tr}(\phi_2^\dagger)^l(w)\rangle \tag{3.2.70}$$

consist, for $l > 2$, of only of the "globe"-shaped fishnet Feynman integrals:

$$F_{l,N}(x,y) = \int \prod_{j=1}^{l} \frac{1}{|z_{0,j} - z_{j,1}|^{1+2\omega}|z_{j,N} - z_{j,N+1}|^{1+2\omega}} \prod_{k=1}^{N} \frac{d^2 z_{j,k}}{|z_{j,k} - z_{j,k+1}|^{1+2\omega}|z_{j,k} - z_{j+1,k}|^{1-2\omega}}, \tag{3.2.71}$$

where we set $z_{j,0} \equiv z$, $z_{j,N+1} \equiv w$, and the expansion itself reads:

$$G_l(z-w) = \sum_{N=0}^{\infty} \xi^{2Nl}\, F_{l,N}(z,w)\,, \tag{3.2.72}$$

where G_l is one of the correlation functions (3.2.70). For any value of the coupling ξ^2 the correlators (3.2.70) are conformal, thus it is possible to define the scaling dimension of the fields X and Z as:

$$\Delta(\xi^2) = -\lim_{|z-w|\to\infty} \frac{\log(G_l(z-w))}{\log(z-w)^2} = \frac{l}{2} + \gamma(\xi^2) \tag{3.2.73}$$

where the anomalous dimension γ is an expansion in the log-divergence of $F_{l,N}$ graphs, i.e. its coefficient of $\frac{1}{\varepsilon}$ in dimensional regularization. Since this divergence is the same for the corresponding wheel graph, obtained after amputation of $|z_{j,N} - z_{j,N+1}|$ propagators:

$$W_{l,N}(z) = \int \prod_{j=1}^{l} \frac{1}{|z_{0,j} - z_{j,1}|^{1+2\omega}} \prod_{k=1}^{N} \frac{d^2 z_{j,k}}{|z_{j,k} - z_{j,k+1}|^{1+2\omega}|z_{j,k} - z_{j+1,k}|^{1-2\omega}}, \tag{3.2.74}$$

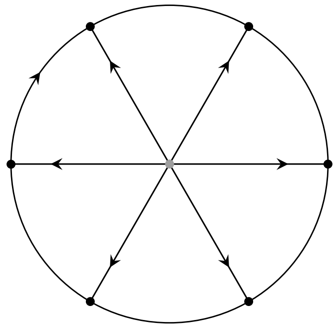

Figure 3.11: Simple wheel at $l = 6$. The black blobs are integrated over, while the gray blob in the center of the figure is the external point of $F_{l,N}(z, w)$ left over after amputation.

we can write

$$-\gamma(\xi^2) = \sum_{N=1}^{\infty} \xi^{2Nl} W_{l,N}^{(1)}$$

where $W_{l,N}^{(1)}$ stands for the $1/\varepsilon$-divergence coefficient in the expansion of the (l, N) wheel in dimensional regularization.[7] The simple case $N = 1$ can be worked out explicitly, since the integral (3.2.74) can be regarded as a ladder with periodic boundary conditions and $L = l-1$, see Fig.3.11. In the formalism of integral operators (3.2.14) we can write:

$$W_{l,1}(z) = \int \prod_{j=1}^{l} \frac{d^2 z_j}{[z_0 - z_j]^{2s-1}[z_j - z_{j+1}]^{2-2s}} = \text{Tr}\left[\Lambda_1^l(x|z_0)\right], \tag{3.2.75}$$

where $x = s - 1$, $s = \bar{s} = 3/2 - \omega$. We can insert inside the trace in (3.2.75) a complete basis (3.2.32) in order to get an integral over one separated variable:

$$\frac{1}{2\pi^2} \sum_{n=-\infty}^{\infty} \int_{-\infty}^{+\infty} d\nu \, \text{Tr}\left[\Lambda_1^l(x|z_0)\Psi(x|z)\overline{\Psi(x|z')}\right] =$$
$$= \frac{1}{2\pi^2}\left(\sum_{n=-\infty}^{\infty} \int_{-\infty}^{+\infty} d\nu \, \lambda_1^l(x)\right) \int d^2 z \, \Psi(x|z)\overline{\Psi(x|z)}. \tag{3.2.76}$$

The integration over z is the scalar product of two eigenfunctions with the same weights x, thus carrying the log-divergence of (3.2.75), or the $\frac{1}{\epsilon}$ divergence which is the leading one at $N = 1$ in the ϵ-regularization. We can easily extract it:

$$\int_{UV} d^{2+\epsilon} z \, \Psi(x|z)\overline{\Psi(x|z)} = 2\pi \int_0^1 \frac{dr}{r^{1-\epsilon}} = \frac{2\pi}{\varepsilon},$$

and the resulting $W_{l,1}^{(1)}$ reads:

$$W_{l,1}^{(1)} = \frac{1}{2\pi^2} \sum_{n=-\infty}^{\infty} \int_{-\infty}^{+\infty} d\nu \, \lambda_1^l(x) = \frac{1}{\pi} I_l(\eta)|_{\eta=1}$$

[7] In general, the following wheel integral has $\frac{1}{\epsilon^N}$ divergence, so one has to extract the sub-leading $\frac{1}{\epsilon}$ term.

The L-ladder at $\eta = 1$ is a finite quantity only for $L = l-1 > 1$, and it isn't otherwise possible to close the integration contour in (3.2.57). Indeed the asymptotic expansion of λ_1 in ν is

$$\lambda_1^{L+1}(n,\nu) \;=\; (-i\nu)^{-L-1} + O(\nu^{-L})\,.$$

The divergence of the wheel diagram at $l = L+1 = 2$ is in agreement with our expectations: in order to renormalize correlators (3.2.70) at $l = 2$ the specific double-trace counter-terms are needed [28, 36, 37, 84, 85, 103]. More explicitly, fixing the propagators along the frames and spokes to be the same ($\omega = 0$), we get:

$$W^{(1)}_{l,1} \;=\; \frac{2\pi^l}{(l-1)!}\;\frac{d^{l-1}}{d\varepsilon^{l-1}}\bigg|_{\varepsilon=0}\;\frac{\Gamma^l(1+\varepsilon)\Gamma^l(1-\varepsilon)}{\Gamma^l(3/2+\varepsilon)\Gamma^l(-1/2-\varepsilon)}\;\left(\sum_{k=0}^{\infty}\frac{\Gamma^l(1/2+k-\varepsilon)}{\Gamma^l(1+k-\varepsilon)}\right)^2 \tag{3.2.77}$$

The quantity (3.2.77) can be computed numerically and, hopefully, expressed in terms of Elliptic Multiple Zeta Values.

3.2.6 Conclusions

In the first part of this chapter we derived an explicit formula for the two-dimensional analogue of Basso-Dixon integral given by conformal fishnet Feynman graph represented by regular square lattice of rectangular $L \times N$ shape, presented on Fig.3.1 and Fig.3.2 (left). The definition of this integral and the result are presented at the end of Introduction (sec.3.2). Our result represents a slightly more general quantity then Basso-Dixon graph: it concerns the anisotropic fishnet, i.e. with different powers for vertical and horizontal propagators, corresponding to arbitrary spins $s, \bar{s}$ of principal series representation of $SL(2,\mathbb{C})$ group, or for the analytic continuation to $s = \bar{s}$ belonging to the real interval $\left(\frac{1}{2}, 1\right)$. The particular case of isotropic fishnet, a-la Basso-Dixon, corresponds to the case $s = \bar{s} = 3/4$. In two-dimensional case the fishnet graph is built from propagators $\frac{1}{|z_1-z_2|}$. Such graph is a particular case of single-trace correlators introduced in [94, 95] for the study of planar scalar scattering amplitudes in the bi-scalar fishnet CFT [28, 32]. In the simplest case $N = L = 1$ (cross integral) we managed to present the result in terms of elliptic functions. It seems plausible that even for general L, N the result can be expressed in terms of elliptic functions. A probable full basis of such functions, in terms of which our quantity could be presented, are the so-called multiple elliptic poly-logarithmic functions (see [143] and references therein). It would be interesting to obtain it for a few smallest N, L.

Interestingly, in the case $s \to 1/2$ (or, alternatively, $s \to 1$, which is an equivalent $SL(2,\mathbb{C})$ representation for the graph's propagators) this fishnet corresponds to one of the conservation laws of Lipatov integrable (open) spin chain hamiltonian [144, 145] describing the system of reggeized gluons for the Regge (BFKL) limit of QCD

[115, 117, 118, 146]. It would be interesting to understand what kind of BFKL physics it can describe.

The Basso-Dixon type configuration represents only one set of possible physical quantities which can be, in principle, analyzed and computed in the planar bi-scalar fishnet CFT due to integrability. To fix the OPE rules in such a theory, we have to compute the spectrum of anomalous dimensions and the structure constants of all local operators. Some of them have been analyzed and even computed in the literature. In particular, the so-called wheel graphs, corresponding to operators $\mathrm{tr}X^L$, have been computed in $d = 4$ dimensions in [32, 93] up to two wrappings at any L. In [39] they have been computed in particular cases of $L = 2, 3$ ($L = 4$ case is to appear [147]) to any reasonable loop order (for any wrapping there exists an iterative analytic procedure) or numerically with a great precision, by means of the Quantum Spectral Curve method [77–79, 148]. We think that, to give a more general result for any L in rather explicit form, we have to employ a powerful technique of separated variables, similarly to the one we employed here in two dimensions for Basso-Dixon type graphs. The first step would be to compute the wheel graphs in two dimensions using the techniques of this chapter. An interesting task would be to advance to $d > 2$ dimensions by integrable spin chain methods. This is done in the rest of the chapter for the remarkable case of $d = 4$ fishnet theory. It would be also good to generalize our techniques, at least in two dimensions, to the computation of multi-magnon operators related to "multi-spiral" Feynman graphs [91].

The computation of structure constants is an even more complicated task. Certain explicit results for OPE of short protected operators have been obtained for fishnet CFT in [28, 36, 37] (see also [120, 121] in BFKL limit) using solely the conformal symmetry. The calculation of more complicated structure constant is a difficult task demanding the most sophisticated techniques, such as SoV method. Since for the $2D$ case the SoV formalism is well developed it would be interesting to apply the methods of this chapter to computations of more complicated structure constants at least in two dimensions.

Finally, it would be good to understand the role of separated variables in the non-perturbative structure of the bi-scalar fishnet CFT. A good beginning would be to understand in terms of SoV the strong coupling limit for long operators of the theory and to relate it to the classical limit of the dual non-compact sigma model which will probably arise in two-dimensional case similarly to the one which was observed in four-dimensional bi-scalar fishnet CFT in [149].

3.3 Four-dimensional case

The exactly solvable spin magnets [5, 9] constitute a class of condensed matter models of wide interest throughout theoretical and mathematical physics. In particular, the integrable chains of nearest-neighbors interacting spins [150, 151] serve as a tool to encode the symmetries of local or non-local operators in quantum field theory, providing a rich amount of non-perturbative results ranging from the scattering spectrum of high-energy gluons in QCD [115, 152, 153] to the conformal data of the supersymmetric $\mathcal{N}=4$ SYM and $\mathcal{N}=6$ ABJM theories [13]. The archetype model of this class is the $SU(2)$ Heisenberg magnet of spin $\frac{1}{2}$, which for open boundary conditions is described by the Hamiltonian

$$H_{SU(2)} = \sum_{a=1}^{N-1} \vec{\sigma}_a \cdot \vec{\sigma}_{a+1} \,, \tag{3.3.1}$$

being $\vec{\sigma}_a$ the vector of Pauli matrices acting on the space $\mathbb{V}_a = \mathbb{C}^2$. Generalizations of (3.3.1) to other symmetry groups are known, including the non-compact $SO(1,5)$ spin chain [8]. The latter model is relevant for the study of covariant quantities in a four-dimensional conformal field theory (CFT) [17]. We consider the homogeneous model in the irreducible unitary representation defined by the scaling dimension $\Delta = 2 - i\lambda,\ \lambda \in \mathbb{R}$, and the $SO(4)$ spins $\ell = \dot{\ell} = 0$ [154]. The Hamiltonian operator acts on the Hilbert spaces $\mathbb{V}_a = L^2(x_a, d^4x_a)$ as

$$\begin{aligned} \mathbb{H} = \sum_{a=1}^{N-1} \left[2\ln x_{aa+1}^2 + (x_{aa+1}^2)^{-i\lambda} \ln(\hat{p}_a^2 \hat{p}_{a+1}^2)(x_{aa+1}^2)^{i\lambda}\right] + \\ + 2\ln x_{N0}^2 + \ln(\hat{p}_1^2) + (x_{N0}^2)^{-i\lambda} \ln(p_N^2)(x_{N0}^2)^{i\lambda} \,, \end{aligned} \tag{3.3.2}$$

where $x_{aa+1} = x_a - x_{a+1}$, $\hat{p}_a^2 = -\partial_a \cdot \partial_a$ and $x_{N+1} = x_0$. The point x_0 is effectively a parameter for the model, and we will always omit it from the set of coordinates. The spin chain (3.3.2) is the four-dimensional version of the open $SL(2,\mathbb{C})$ Heisenberg magnet which describes the scattering amplitudes of high energy gluons in the Regge limit of QCD [115, 155]. In the rest of this chapter we will indeed try to translate the methods of the first part of the chapter - based on the $SL(2,\mathbb{C})$ spin chain - to the four dimensional situation. The integrability of (3.3.2) is realized by the commutative family of normal operators[9]

$$\mathbb{Q}_N(u) = \mathrm{Q}_{12}(u) \cdot \mathrm{Q}_{23}(u) \cdots \mathrm{Q}_{N0}(u) \,, \tag{3.3.3}$$

labeled by the spectral parameter $u \in \mathbb{R}$ and where

$$\mathrm{Q}_{ij}(u) = (x_{ij}^2)^{-i\lambda} (\hat{p}_i^2)^u (x_{ij}^2)^{u+i\lambda} \,.$$

By the introduction of the operator

$$\widehat{\mathbb{Q}}_N(u) = [\mathbb{Q}_N(u - i\lambda)]^\dagger \mathbb{Q}_N(-i\lambda) \,,$$

the Hamiltonian $\mathbb{H}$ is recovered from the expansion

$$\mathbb{Q}_N(u) + \widehat{\mathbb{Q}}_N(u) = 2 \cdot \mathbb{1} + u\,\mathbb{H} + o(u) \,. \tag{3.3.4}$$

[8]We consider an Euclidean space-time in the chapter, without loss of generality respect to the Minkowskian case.
[9]We recall that a linear operator of an Hilbert space is called normal if it commutes with its hermitian conjugate.

It follows from (3.3.4) and from the commutation relation $[\mathbb{Q}_N(u), \mathbb{Q}_N(v)] = 0$ at generic u and v, that the eigenfunctions of $\mathbb{Q}_N$ diagonalize the Hamiltonian (3.3.2) as well. The spectra of these operators are labeled by the quantum numbers

$$Y_a = 1 + \frac{n_a}{2} + i\nu_a, \quad Y_a^* = 1 + \frac{n_a}{2} - i\nu_a, \quad \nu_a \in \mathbb{R}\,, \; n_a \in \mathbb{N}\,, \tag{3.3.5}$$

for $a = 1, \ldots, N$, and we use to write $\mathbf{Y} = (Y_1, \ldots, Y_N)$. The spectral equation for the operator (3.3.3) reads

$$\mathbb{Q}_N(u) \cdot \Psi^{\boldsymbol{\alpha\beta}}(\mathbf{x}|\mathbf{Y}) = \tau_N(u, \mathbf{Y})\, \Psi^{\boldsymbol{\alpha\beta}}(\mathbf{x}|\mathbf{Y})\,,$$

where we denote $\mathbf{x} = (x_1, \ldots, x_N)$ and $\boldsymbol{\alpha}$,$\boldsymbol{\beta}$ stand for $2N$ auxiliary complex spinors

$$|\alpha_1\rangle, \ldots, |\alpha_N\rangle \;\text{ and }\; |\beta_1\rangle, \ldots, |\beta_N\rangle \in \mathbb{C}^2.$$

The eigenfunctions form an orthogonal set respect to the quantum numbers $(\mathbf{Y}, \boldsymbol{\alpha}, \boldsymbol{\beta})$, and the eigenvalue is factorized respect to the labels (3.3.5) into equal contributions

$$\tau_N(u, \mathbf{Y}) = \prod_{a=1}^{N} \tau_1(u, Y_a)\,, \tag{3.3.6}$$

$$\tau_1(u, Y_a) = 4^u \frac{\Gamma\left(Y_a - \frac{i}{2}\lambda\right) \Gamma\left(Y_a^* + u + \frac{i}{2}\lambda\right)}{\Gamma\left(Y_a^* + \frac{i}{2}\lambda\right) \Gamma\left(Y_a - u - \frac{i}{2}\lambda\right)}\,.$$

As a consequence of (3.3.4) and (3.3.6) we obtained the spectrum of the Hamiltonian $\mathbb{H}$ as a sum of N independent terms

$$\eta_N(\mathbf{Y}) = \sum_{a=1}^{N} \left[\psi\left(Y_a - \frac{i}{2}\lambda\right) + \psi\left(Y_a + \frac{i}{2}\lambda\right) + \ln 4\right] + \text{c.c.} \tag{3.3.7}$$

Formulas (3.3.6),(3.3.7) show that the N-body system defined in (3.3.2) gets separated into N one-particle systems over the quantum numbers (3.3.5). In other words, the quantities $(Y_a, |\alpha_a\rangle, |\beta_a\rangle)$ are the separated variables of the system in the sense of [7, 132, 156**?**], and the spectrum of (3.3.2) and (3.3.3) is degenerate in the spinors due to rotation invariance.

The representation over the separated variables $(\mathbf{Y}, \boldsymbol{\alpha}, \boldsymbol{\beta})$ is defined for a generic function $\phi(\mathbf{x}) = \phi(x_1, \ldots, x_N)$ by the linear transform

$$\widetilde{\phi}(\mathbf{Y}, \boldsymbol{\alpha}, \boldsymbol{\beta}) = \int d\mathbf{x}\, \Psi^{\boldsymbol{\alpha\beta}}(\mathbf{x}|\mathbf{Y})^*\, \phi(\mathbf{x})\,. \tag{3.3.8}$$

The inverse transform of (3.3.8) provides the expansion of $\phi(\mathbf{x})$ over the basis of eigenfunctions

$$\phi(\mathbf{x}) = \sum_{\mathbf{n}} \int d\boldsymbol{\nu}\; \mu(\mathbf{Y}) \int D\boldsymbol{\alpha} D\boldsymbol{\beta}\;\; \Psi^{\boldsymbol{\alpha\beta}}(\mathbf{x}|\mathbf{Y})\, \widetilde{\phi}(\mathbf{Y}, \boldsymbol{\alpha}, \boldsymbol{\beta})\,, \tag{3.3.9}$$

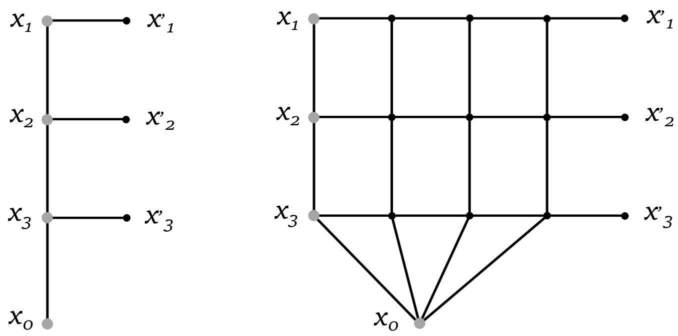

Figure 3.12: On the left the graph-building kernel $\mathbb{B}_3(\mathbf{x}|\mathbf{x}')$, where the lines are propagators $1/x_{ij}^2$, grey dots are external points and the black ones are integrated. On the right the portion of fishnet $(\mathbb{B}_3)^4$ with two fixed points x_0 (down) and ∞ (up).

where the sum runs over the non-negative integers $\mathbf{n} = (n_1, \ldots, n_N)$, the integrations $d\boldsymbol{\nu} = d\nu_1 \cdots d\nu_N$ are on the real line and the integration in the space of spinors $D\boldsymbol{\alpha} = D\alpha_1 \cdots D\alpha_N$ is defined as

$$\int D\alpha = \int_{\mathbb{C}^2} d\alpha\, e^{-\langle\alpha|\alpha\rangle}\,, \quad \langle\alpha|\alpha\rangle = |\alpha^{(1)}|^2 + |\alpha^{(2)}|^2\,.$$

The spectral measure in (3.3.9) can be extracted from the scalar product of eigenfunctions and it is given by

$$\mu(\mathbf{Y}) = \frac{1}{N!}\prod_{a=1}^{N}(n_a+1)\prod_{b\neq a}^{N}\left[\nu_{ab}^2 + \frac{n_{ab}^2}{4}\right]\left[\nu_{ab}^2 + \frac{(n_a+n_b+2)^2}{4}\right]\,, \tag{3.3.10}$$

in the notation $\nu_{ab} = \nu_a - \nu_b$ and $n_{ab} = n_a - n_b$.

All considerations done so far can be extended by an accurate analytic continuation of the parameter λ to the imaginary strip $(-2i, +2i)$. In particular, at $\lambda = -i$ each site of the chain carries the representation $\Delta = 1$, $\ell = \dot{\ell} = 0$ of a bare scalar field in four dimensions. In this case at the point $u = -1$ the operator $\mathbb{Q}_N(u)$ becomes proportional to the graph-building integral operator for a Feynman diagram of square lattice topology

$$\mathbb{B}_N\,\phi(\mathbf{x}) = \frac{1}{(2\pi)^{4N}}\int d\mathbf{x}'\phi(\mathbf{x}')\prod_{a=1}^{N}\frac{1}{x_{aa+1}^2\,x_{aa'}^2}\,, \tag{3.3.11}$$

with $\mathbf{x} = (x_1, \ldots, x_N)$, $\mathbf{x}' = (x_1', \ldots, x_N')$. Throughout the rest of the chapter we denote $x_{ab'} = x_a - x_b'$. According to (3.3.6) the representation of the operator $(\mathbb{B}_N)^L$ over the separated variables factorizes completely a portion of size $N \times L$ of the planar fishnet diagram [92] in Fig.3.12, extending to a $4D$ space-time the analogue result in two-dimensions of [29].

As a direct application of our results, we computed a specific set of four-point functions of fishnet CFT [32], providing a direct check to formula (14) of [125], obtained via arguments of AdS/CFT correspondence [157–159].

In the next two sections we present the explicit construction of the eigenfunctions of the model (3.3.2) by means of newly found integral identities.

3.3.1 Generalized Star-triangle identity

Our construction of a basis of eigenfunctions for $\mathbb{Q}_N(u)$ follows the logic outlined in [160] for the two-dimensional model, and requires the formulation of certain conformal integral identities in $4D$.

First we consider a positive integer $M \leq N$ and set $x_0^\mu = 0$ without loss of generality. We will denote $\mathbf{x} = (x_1, \dots, x_M)$, $\mathbf{x}' = (x'_1, \dots, x'_{M-1})$. Let us introduce the tensors

$$C^{\alpha\beta}_{\mu_1\mu_{1'}\mu_2\dots\mu_M} = \langle\alpha|\bar{\boldsymbol{\sigma}}_{\mu_1}\boldsymbol{\sigma}_{\mu'_1}\bar{\boldsymbol{\sigma}}_{\mu_2}\cdots\bar{\boldsymbol{\sigma}}_{\mu_M}|\beta\rangle\,, \tag{3.3.12}$$

where the symbols $\boldsymbol{\sigma}$ and $\bar{\boldsymbol{\sigma}}$ are defined in terms of Pauli matrices

$$\boldsymbol{\sigma}_0 = \bar{\boldsymbol{\sigma}}_0 = \mathbb{1}, \;\; \boldsymbol{\sigma}_k = -\bar{\boldsymbol{\sigma}}_k = i\sigma_k, \quad k = 1,2,3\,.$$

The tensors (3.3.12) satisfy the light-cone condition

$$t^{\mu_1\dots\mu_a}\, t^{\nu_1\dots\nu_a}\, C^{\alpha\beta}_{\mu_1\dots\mu_a\,\rho\dots\mu_M} C^{\alpha\beta}_{\nu_1\dots\nu_a}{}^{\rho}{}_{\dots\nu_M} = 0\,,$$

where $t^{\mu_1\cdots\mu_a}$ are arbitrary tensors and $a = 1, 1', \dots, M$. This property allows to define a family of degree-n homogeneous harmonic polynomials

$$C^{\alpha\beta}_M(\mathbf{x}|\mathbf{x}')^n = \langle\alpha|\bar{\mathbf{x}}_{11'}\mathbf{x}_{1'2}\bar{\mathbf{x}}_{22'}\dots\bar{\mathbf{x}}_{M0}|\beta\rangle^n\,, \tag{3.3.13}$$

where $\mathbf{x}_{ij} = \boldsymbol{\sigma}_\mu x^\mu_{ij}/|x_{ij}|$ and $\bar{\mathbf{x}}_{ij} = \bar{\boldsymbol{\sigma}}_\mu x^\mu_{ij}/|x_{ij}|$. Under a coordinate inversion $x^\mu \to x^\mu/x^2$ such harmonic polynomials transform covariantly and it follows that using (3.3.13) it is possible to generalize the uniqueness - "star-triangle" - relation for a conformal invariant vertex of three scalar propagators [161] (see also [162, 163] and references therein) to any symmetric traceless representation.

The core of the generalized identity we are going to derive is the mixing operator acting on a pair of symmetric spinors $|\alpha,\alpha'\rangle = |\alpha\rangle^{\otimes n}\otimes|\alpha'\rangle^{\otimes n'}$ of degrees n and n' as

$$\begin{aligned}&\langle\alpha,\alpha'|\mathbf{R}_{n,n'}\,(z)\,|\beta,\beta'\rangle = \\ &= \frac{\Gamma(z+\frac{n-n'}{2})\Gamma(z+\frac{n'-n}{2})}{\Gamma^2(z+\frac{n+n'}{2})}\,\partial_s^n\partial_t^{n'}(1+s\langle\alpha|\beta\rangle+t\langle\alpha'|\beta'\rangle+st\langle\alpha|\beta'\rangle\langle\alpha'|\beta\rangle)^{z+\frac{n+n'}{2}}\,,\end{aligned} \tag{3.3.14}$$

where upon differentiation we set $s = t = 0$. The operator defined by (3.3.14) is a unitary solution of the Yang-Baxter equation and can be obtained via the fusion procedure [164] applied to the Yangian R-matrix $\mathbf{R}_{1,1}(z)$.

Under the uniqueness constraint $a+b+c=4$ and for any $n,n'\in\mathbb{N}$ the following identity holds

$$\int d^4x_4\,\frac{\langle\alpha|\bar{\mathbf{x}}_{\mathbf{14}}\mathbf{x}_{\mathbf{43}}|\beta\rangle^n\langle\alpha'|\bar{\mathbf{x}}_{\mathbf{34}}\mathbf{x}_{\mathbf{42}}|\beta'\rangle^{n'}}{(x_{14}^2)^a\,(x_{24}^2)^b\,(x_{34}^2)^c}=$$
$$=\pi^2\frac{(-1)^n\,A_{n,n'}(a,b,c)}{(x_{12}^2)^{(2-c)}(x_{13}^2)^{(2-b)}(x_{23}^2)^{(2-a)}}\,\frac{\langle\alpha\,\bar{\mathbf{x}}_{\mathbf{12}}\mathbf{x}_{\mathbf{23}},\alpha'|\mathbf{R}_{n,n'}\,(c-2)\,|\beta,\bar{\mathbf{x}}_{\mathbf{31}}\mathbf{x}_{\mathbf{12}}\,\beta'\rangle}{\left(c-1+\frac{n+n'}{2}\right)\left(2-c+\frac{n'-n}{2}\right)}\,. \quad (3.3.15)$$

with the coefficient

$$A_{n,n'}(a,b,c)=\frac{\Gamma\left(2-a+\frac{n}{2}\right)\Gamma\left(2-b+\frac{n'}{2}\right)\Gamma\left(3-c+\frac{n'-n}{2}\right)}{\Gamma\left(a+\frac{n}{2}\right)\Gamma\left(b+\frac{n'}{2}\right)\Gamma\left(c-1+\frac{n'-n}{2}\right)}\,.$$

Setting $n'=0$, the identity (3.3.15) is equivalent to (A.11) of [111], and setting further $n=0$ it degenerates to the scalar identity [161].

We point out that (3.3.15) is the four-dimensional versions of the $2D$ star-triangle relation which underlies the solution of the $SL(2,\mathbb{C})$ Heisenberg magnet as in [117, 160].

3.3.2 Eigenfunctions construction

The eigenfunctions of the open conformal chain (3.3.2) can be obtained by a recursive procedure in the number of sites of the system. First of all we introduce the integral operators $\hat{\Lambda}^{\alpha\beta}_{M,Y_a}=\langle\alpha|\hat{\Lambda}_{M,Y_a}|\beta\rangle$

$$\hat{\Lambda}^{\alpha\beta}_{M,Y_a}\cdot\phi(\mathbf{x})=\int d\mathbf{x}'\,\Lambda^{\alpha\beta}_{M,Y_a}(\mathbf{x}|\mathbf{x}')\,\phi(\mathbf{x}')\,, \quad (3.3.16)$$

through its kernel $\Lambda^{\alpha\beta}_{M,Y_a}(\mathbf{x}|\mathbf{x}')=\langle\alpha|\Lambda_{M,Y_a}(\mathbf{x}|\mathbf{x}')|\beta\rangle=$

$$=\frac{C^{\alpha\beta}_M(\mathbf{x}|\mathbf{x}')^{n_a}}{(x_{M0}^2)^{1+i\nu_a+i\lambda/2}}\prod_{a=1}^{M-1}\frac{(x^2_{a'a+1})^{-1+i\nu_a+i\lambda/2}}{(x^2_{aa'})^{1+i\nu_a-i\lambda/2}(x^2_{aa+1})^{i\lambda}}\,,$$

which at $M=1$ reduces to a conformal propagator of scaling dimension $\Delta=1+i\lambda/2+i\nu_a$ and tensor rank n_a

$$\Lambda^{\alpha\beta}_{1,Y_a}(x_1)=\frac{\langle\alpha|\bar{\mathbf{x}}_1|\beta\rangle^{n_a}}{(x_1^2)^{1+i\nu_a+i\lambda/2}}\,.$$

Making use of (3.3.15) at $n=n_a$, $n'=0$ we verify that

$$\mathbb{Q}_M(u)\,\hat{\Lambda}^{\alpha\beta}_{M,Y_a}=\tau_1(u,Y_a)\,\hat{\Lambda}^{\alpha\beta}_{M,Y_a}\,\mathbb{Q}_{M-1}(u)\,, \quad (3.3.17)$$

for any $M>1$, moreover

$$\mathbb{Q}_1(u)\,\Lambda^{\alpha\beta}_{1,Y_a}(x_1)=\tau_1(u,Y_a)\,\Lambda^{\alpha\beta}_{1,Y_a}(x_1)\,. \quad (3.3.18)$$

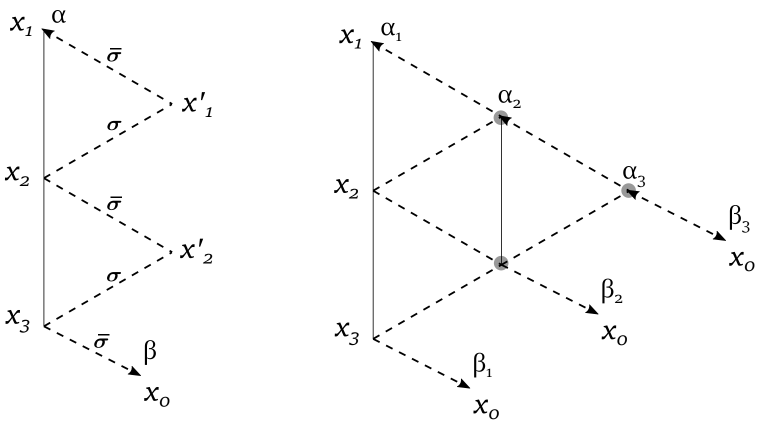

Figure 3.13: Graphic representation of the integral kernel $\Lambda^{\alpha,\beta}_{3,Y}(x_1,x_2,x_3|x_1',x_2')$ (left) and of the eigenfunction $\Psi^{\boldsymbol{\alpha\beta}}(\mathbf{Y}|x_1,x_2,x_3)$ (right). Solid lines denote $(x_{ij}^2)^{-i\lambda}$, while the dashed ones stand for the polynomials (3.3.13) together with the denominators of type $(x_{i,i'}^2)$ and $(x_{i',i+1}^2)$ carrying the variables $\boldsymbol{\nu}$ in the power. The external arrows indicate symmetric spinors and the grey blobs are integrated points.

The iterative application of (3.3.17) for the length M going from N to 2, together with the initial condition (3.3.18), provides a recursive definition of the eigenfunctions of the model with N sites

$$\Psi^{\boldsymbol{\alpha\beta}}(\mathbf{Y}|\mathbf{x}) = \hat{\Lambda}^{\alpha_N\beta_N}_{N,Y_N}\cdots\hat{\Lambda}^{\alpha_2\beta_2}_{2,Y_2}\cdot\Lambda^{\alpha_1\beta_1}_{1,Y_1}\prod_{a=1}^{N}\frac{r(Y_a)^{a-1}}{\sqrt{2\pi^{2N+1}}}\,, \tag{3.3.19}$$

where the last factor is a suitable normalization and

$$r(Y) = \frac{\Gamma\left(Y - i\frac{\lambda}{2}\right)\Gamma\left(Y^* - i\frac{\lambda}{2}\right)}{\Gamma\left(Y + i\frac{\lambda}{2}\right)\Gamma\left(Y^* + i\frac{\lambda}{2}\right)}\,.$$

Such a function has a simple behavior in the permutation of two separated variables (Y,α,β), (Y',α',β'), encoded by the exchange property

$$\begin{aligned}\hat{\Lambda}^{\alpha'\beta'}_{M,Y'}\cdot\hat{\Lambda}^{\alpha\beta}_{M-1,Y} &= \langle\alpha',\alpha|\hat{\Lambda}_{M,Y'}\cdot\hat{\Lambda}_{M-1,Y}|\beta',\beta\rangle = \\ &= \frac{r(Y)}{r(Y')}\langle\alpha,\alpha'|\mathbf{R}(z)^\dagger\,\hat{\Lambda}_{M,Y}\cdot\hat{\Lambda}_{M-1,Y'}\mathbf{R}(z)|\beta,\beta'\rangle\,,\end{aligned} \tag{3.3.20}$$

where $z = i(\nu'-\nu)$ and $\mathbf{R} = \mathbf{R}_{n,n'}$. Any permutation of the separated variables in (3.3.19) can be decomposed into elementary steps of type (3.3.20), defining a representation of the symmetric group generators

$$s_k\,\mathbf{Y} = (Y_1,\ldots,Y_{k+1},Y_k,\ldots Y_N)\,,$$

on the space of symmetric spinors

$$\mathbf{s}_k|\boldsymbol{\alpha}\rangle = \mathbf{R}_{n_k,n_{k+1}}(i\,\nu_{k+1,k})\,|\alpha_1,\ldots,\alpha_{k+1},\alpha_k,\ldots,\alpha_N\rangle\,,$$

and allowing to state the exchange symmetry

$$\Psi^{\boldsymbol{\alpha\beta}}(\mathbf{Y}|\mathbf{x}) = \Psi^{s_k(\boldsymbol{\alpha},\boldsymbol{\beta})}(s_k\mathbf{Y}|\mathbf{x})\,. \tag{3.3.21}$$

The scalar product of two eigenfunctions can be written according to (3.3.19) in operatorial form, so that it can be reduced to N factorized single-site contributions of the type

$$(\Lambda^{\alpha'\beta'}_{1,Y'})^\dagger \cdot \Lambda^{\alpha\beta}_{1,Y} = \frac{2\pi^3}{n+1}\,\delta_{n,n'}\delta(\nu-\nu')\langle\alpha|\alpha'\rangle^n\langle\beta|\beta'\rangle^n\,,$$

by the iterative application of the property

$$(\hat{\Lambda}^{\alpha'\beta'}_{M,Y'})^\dagger \cdot \hat{\Lambda}^{\alpha\beta}_{M,Y} = \langle\beta',\alpha|\hat{\Lambda}^\dagger_{M,Y'}\cdot\hat{\Lambda}_{M,Y}|\alpha',\beta\rangle = \frac{r(Y')}{r(Y)}\times$$
$$\times\,\pi^4\frac{\mathrm{Tr}_{n'}[\langle\alpha|\mathbf{R}(z)|\alpha'\rangle\,\hat{\Lambda}_{M-1,Y}\,\langle\beta'|\mathbf{R}^\dagger(z)|\beta\rangle\,\hat{\Lambda}^\dagger_{M-1,Y'}]}{\left((\nu-\nu')^2+\frac{(n-n')^2}{4}\right)\left((\nu-\nu')^2+\frac{(n+n'+2)^2}{4}\right)}\,,$$

valid under the assumption $Y \neq Y'$ and where the trace means the cyclic contraction of indexes in the space of primed spinors. As result the scalar product of two functions (3.3.19) takes the form of an orthogonality relation

$$\frac{\mu(\mathbf{Y})^{-1}}{N!}\sum_{\pi\in\mathbb{S}_N}\delta(\mathbf{Y}-\pi(\mathbf{Y}'))\langle\boldsymbol{\alpha}|\boldsymbol{\pi}|\boldsymbol{\alpha}'\rangle\langle\boldsymbol{\beta}'|\boldsymbol{\pi}|\boldsymbol{\beta}\rangle\,, \tag{3.3.22}$$

where $\mathbb{S}_N$ are the permutations of N objects and we introduced the compact notation

$$\delta(\mathbf{Y}-\mathbf{Y}') = \prod_{a=1}^{N}\delta_{n_a,n'_a}\,\delta(\nu_a-\nu'_a)\,.$$

3.3.3 Conformal fishnet Integrals

In analogy with the $2D$ results of [29], employing the results of the previous sections we will compute exactly the four-point correlation function

$$G_{N,L} = \langle\mathrm{Tr}[\phi_1^N(x_1)\phi_2^L(x_2)\phi_1^{\dagger N}(x_3)\phi_2^{\dagger L}(x_4)]\rangle\,, \tag{3.3.23}$$

for any N and L, where $\phi_1(x)\,,\phi_2(x)$ are the two complex scalar $N_c\times N_c$ fields which appear in the Lagrangian of the conformal fishnet theory [32] in four dimensions. In the planar limit [126] $N_c\to\infty$ the only Feynman diagram which contributes to the perturbative expansion in the coupling ξ^2 of $G_{N,L}$ is given by the integral

$$\int\frac{d\mathbf{z}}{(4\pi^2)^{NL}}\left(\prod_{a=0}^{N}\frac{1}{(z_{a,b}-z_{a+1,b})^2}\right)\left(\prod_{b=0}^{L}\frac{1}{(z_{a,b}-z_{a,b+1})^2}\right)\,, \tag{3.3.24}$$

where the integration measure is $d\mathbf{z} = \prod_{a,b=1}^{N,L} d^4z_{a,b}$ and we set $z_{0b} = x_1$, $z_{N+1b} = x_3$, $z_{a0} = x_4$, $z_{aL+1} = x_2$. Such a square-lattice integral can be expressed via the

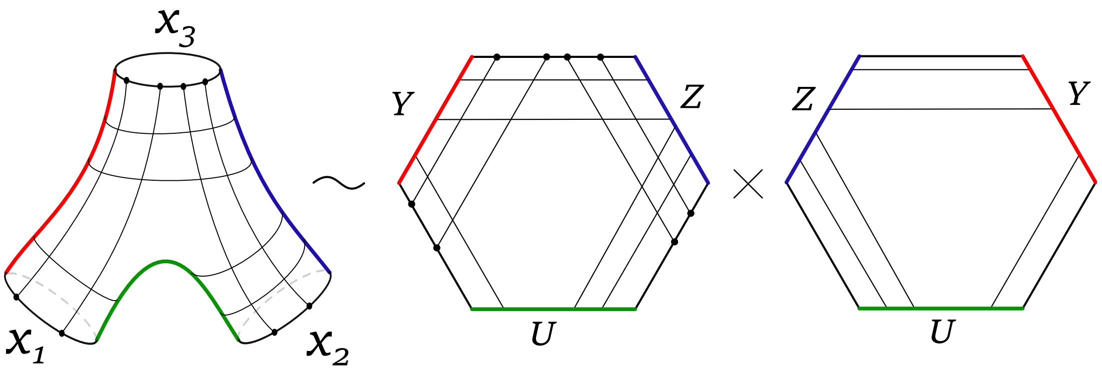

Figure 3.14: A Feynman diagram contributing to the planar limit of $\langle \mathrm{Tr}(\phi_1^2)(x_1)\mathrm{Tr}(\phi_1^2)(x_2)\mathrm{Tr}(\phi_1^{\dagger\,4})(x_3)\rangle$ at order ξ^{28} and its decomposition into hexagons. Here $M_1 = 1$, $M_2 = 2$, $M_3 = 2$. Each color of a cut corresponds to the insertion of a different set of separated variables, as indicated on the hexagons.

graph-building operator (3.3.11). Indeed, starting from the fishnet diagram

$$F_{N,L} = \left(\prod_{a=1}^{N} z_{aa+1}^2\right) (\mathbb{B}_N)^{L+1} \left(\prod_{a=1}^{N} \delta^{(4)}(z'_a - z_a)\right) , \tag{3.3.25}$$

one can transform it to (3.3.24) by the reductions of external points $z_a \to x_1$, $z'_a \to x_3$ followed by a conformal transformation. Therefore, as a functions $\mathcal{G}_{N,L}(u,v)$ of the cross-ratios $u = x_{12}^2 x_{34}^2/(x_{13}^2 x_{24}^2)$ and $v = x_{14}^2 x_{23}^2/(x_{13}^2 x_{24}^2)$, the planar limit of (3.3.23) is equal to $F_{N,L}$ with reduced external points. According to (3.3.6) the integral kernel of $(\mathbb{B}_N)^L$ in the space of separated variables is factorized as

$$\widetilde{\mathbb{B}_N^L}(Y_1, \dots, Y_N) = \frac{1}{\pi^{2NL}} \prod_{a=1}^{N} \left[\frac{1}{4\nu_a^2 + (1+n_a)^2}\right]^L . \tag{3.3.26}$$

In order to restore the (u,v)-dependence of (3.3.24) one has first to expand the r.h.s. of (3.3.25) over the eigenfunctions via the inverse transform (3.3.9). Then, by the appropriate reduction of the external points and upon integration of spinors and normalization by the bare correlator, we get

$$\mathcal{G}_{N,L}(u,v) = \sum_{\boldsymbol{n}\in\mathbb{Z}} \int d\boldsymbol{\nu}\ \mu(\mathbf{Y}) \prod_{k=1}^{N} \frac{|x|^{-2i\nu_k} (\bar{x}/x)^{(n_k+1)/2}}{(\nu_k^2 + (n_k+1)^2/4)^{L+N}} ,$$

where $u/v = x\bar{x}$, $v = 1/\sqrt{(1-x)(1-\bar{x})}$. After the redefinition $n_k \to a_k - 1$, $\nu_k \to u_k$, $x \to z$ it coincides with the result of [125].

We shall conjecture further applications of the separated variables transform (3.3.9) to the computation of planar fishnet integrals. An interesting example in this sense is provided by the three-point function of "vacuum" operators

$$\langle \mathrm{Tr}(\phi_1^N)(x_1)\mathrm{Tr}(\phi_1^L)(x_2)\mathrm{Tr}(\phi_1^{\dagger\,N+L})(x_3)\rangle . \tag{3.3.27}$$

In the planar limit the perturbative expansion of (3.3.27) in the coupling constant consist of regular square lattice diagrams drawn on a three-punctured sphere $S^2\backslash\{x_1, x_2, x_3\}$ as explained in [165] and exemplified in Fig.3.14. In the same spirit of "hexagonalisation" techniques [158, 159, 165, 166] we perform three cuts on the diagram connecting the punctures, and insert along each cut a sum over the basis (3.3.19), labeled by the separated variables

$$(\mathbf{Y}, \boldsymbol{\alpha}, \boldsymbol{\beta})\,, \quad (\mathbf{Z}, \boldsymbol{\lambda}, \boldsymbol{\chi})\,, \quad (\mathbf{U}, \boldsymbol{\kappa}, \boldsymbol{\omega}),$$

where $Y_a = [\nu_a, n_a]$, $Z_a = [\mu_a, m_a]$, $U_a = [\tau_a, t_a]$. Let M_i be the number of $\phi_2\phi_2^\dagger$ wrappings around the puncture x_i (see Fig.3.14). The representation of the two hexagons over the separated variables reads

$$|H|^2 \sim |\mathcal{A}|^2 \prod_{a=1}^{M_1+M_3} \left[\frac{1}{\nu_a^2 + \frac{(n_a+1)^2}{4}}\right]^N \prod_{b=1}^{M_2+M_3} \left[\frac{1}{\mu_b^2 + \frac{(m_b+1)^2}{4}}\right]^L,$$

and the form factor $\mathcal{A}$ is given by the overlapping of three eigenfunctions of type (3.3.19) at different values of x_0

$$\mathcal{A} = \int d\mathbf{z}\, d\mathbf{z}'\, d\mathbf{z}'' \quad \Psi_{\mathbf{Y}}^{\boldsymbol{\alpha}\boldsymbol{\beta}}(\mathbf{z}, \mathbf{z}')\, \Psi_{\mathbf{Z}}^{\boldsymbol{\lambda}\boldsymbol{\chi}}(\mathbf{z}, \mathbf{z}'')\, \Psi_{\mathbf{U}}^{\boldsymbol{\kappa}\boldsymbol{\omega}}(\mathbf{z}', \mathbf{z}'')\,, \tag{3.3.28}$$

for $\mathbf{z} = (z_1, \ldots, z_{M_3})$, $\mathbf{z}' = (z_1', \ldots, z_{M_1}')$, and $\mathbf{z}'' = (z_1'', \ldots, z_{M_2}'')$. Finally, the Feynman integral is recovered by gluing the two hexagons via completeness sums

$$\sim \sum_{\mathbf{n},\mathbf{m},\mathbf{t}} \int d\boldsymbol{\nu}\, d\boldsymbol{\mu}\, d\boldsymbol{\tau}\, \mu(\mathbf{Y})\, \mu(\mathbf{Z})\, \mu(\mathbf{U}) \int D\boldsymbol{\alpha} \cdots D\boldsymbol{\omega}\, |H|^2\,.$$

An interesting reduction of the correlator (3.3.27) is obtained setting $L = 0$ and degenerating it to the two-point function $\langle \mathrm{Tr}(\phi_1^N)(x_1)\mathrm{Tr}(\phi_1^{\dagger\,N})(x_3)\rangle$, for which the planar fishnet lies on a cylinder and it is conformally equivalent to a "wheel" diagram [32, 39, 167, 168].

As a general fact the diagrams describing the planar limit of (3.3.27) develop UV divergences, which in our representation should be contained in the form factor (3.3.28). The elaboration of a regularization technique at this level is an intriguing task as it would enable the direct computation of several conformal data in the fishnet CFT at finite order in the coupling.

3.3.4 Conclusions

In this second part of the chapter we formulated and solved the spin chain of $SO(1, 5)$ conformal spins for any number of sites N and for open boundary conditions, in the principal series representation of zero spin [154]. Its integrability is realized by a commuting family of spectral parameter-dependent operators $\mathbb{Q}_N(u)$ which generate the conserved charges of the model. The spectrum of the model is separated into N symmetric contributions, each depending on quantum numbers which for this reason we call separated variables. We explained how to construct the eigenfunctions and prove their orthogonality, extending the logic of [160] to a four dimensional space-time by means of new integral indentities which generalize the star-triangle relation [161] to symmetric traceless tensors.

Our results can be analytically continued from the representation of the principal series to real scaling dimensions, recovering the graph-building operator - introduced in $2D$ by the authors and V. Kazakov [29] - for the Feynman diagrams of fishnet CFT [32, 91]. The variant of this graph-builder with periodic boundary was first introduced in [32] and coincides with the $\hat{B}$-operator of the fishchain holographic model [169–171]. Following the same steps as [29], we computed the planar limit of the fishnet correlator studied by B. Basso and L. Dixon providing a direct check of the formula (14) of [125].

The separation of variables (SoV) for non-compact spin magnets is a topic which recently attracted great attention [172–177], and SoV features appear in remarkable results of AdS/CFT integrability, for instance [178, 179]. It has not escaped our notice that the properties of the proposed eigenfunctions immediately suggest their role in the SoV of the periodic $SO(1,5)$ spin chain [111], in full analogy with [117]. Moreover it would be interesting to apply our methods to the computation of other classes of Feynman integrals, for example introducing fermions as in [31, 180], or considering any space-time dimension and extending our results to the theory proposed in [28]. In the latter context, the functions (3.3.19) for $N = 2$ sites have been derived in a somewhat different form and applied to the formulation of the Thermodynamic Bethe Ansatz equations [181].

Finally we have conjectured how, by means of a cutting-and-gluing procedure inspired by [165], certain planar two- and three-point functions of the fishnet CFT at finite coupling get factorized into simple contributions over the separated variables. This observation puts as a compelling future task the regularization of such formulas, in order to compare the results based on the AdS/CFT correspondence to a direct computation.

Chapter 4
Four-point functions in Chiral CFT$_4$

4.1 Introduction

Whereas a big progress already in the study of the bi-scalar fishnet CFT has been done, little is known about the most general version of the double-scaled γ-deformed $\mathcal{N}=4$ SYM. Until very recently, apart from the original formulation [32] and the study, in [91], of asymptotic Bethe Ansatz equations for anomalous dimensions in certain sectors of this theory, as well as the computations of related unwrapped and single-wrapped Feynman graphs, no serious attempts had been undertaken to understand the physical properties and the Feynman graph structure of the full χCFT. It is worth noticing that, unlike the bi-scalar fishnet CFT, the reasons for the (hypothetical) integrability of this model remains quite mysterious.

The non-unitarity of the χCFT represents an obvious drawback from the point of view of the physical interpretation: the presence of complex OPE data violates basic quantum-mechanical axioms and standard analyticity constraints. On the other hand, non-unitary theories are curious objects by themselves, having interesting OPE properties, such as a logarithmic behavior of certain correlators (χCFT is an example of logarithmic CFTs). In addition, they share many basic common features with unitary CFTs and help to understand their general features.

4.1.1 Integrability of Wheel graphs in χCFT

A statement of integrability, milder than the lattice integrability of the bulk of large planar graphs, can be made for the scaling dimension of Tr $[\phi_j^L]$ operators at any L. These operators, protected in the original $\mathcal{N}=4$ SYM due to super-symmetry, are described in the planar limit of bi-scalar theory by a perturbative expansion in globe-like fishnet graphs [32] with an integrable square-lattice bulk [92]. These graphs can be built up by the action of an integral "graph-building" kernel $\hat{\mathcal{H}}_B^{(L)}$

$$[\hat{\mathcal{H}}_B^{(L)}\Phi](x_1,\cdots,x_L) = \frac{1}{\pi^{2L}}\int\prod_{k=1}^{L}\frac{d^4y_k}{(x_k-y_k)^2(y_k-y_{k+1})^2}\Phi(y_1,\cdots,y_L), \quad y_{L+1}\equiv y_1\,. \tag{4.1.1}$$

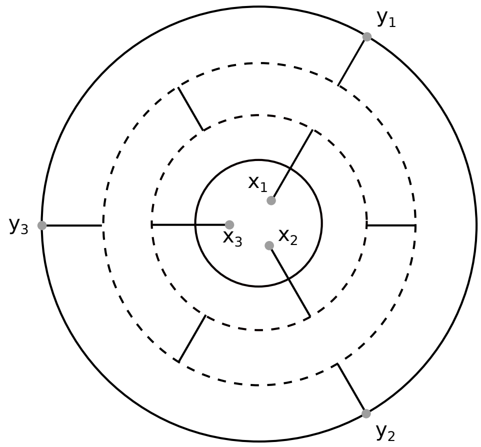

Figure 4.1: An example of bulk of a planar diagram appearing in the perturbative expansion of $\langle \text{Tr } [\phi_j^3](x)\text{Tr } [\phi_j^3]^\dagger(y)\rangle$. It mixes together a square lattice structure of quartic scalar interactions and the "brick-wall" domain made by Yukawa interactions. This case corresponds to the operatorial expression $\hat{\mathcal{H}}_B^{(3)}(\hat{\mathcal{H}}_F^{(3)})^2\,\mathcal{H}_B^{(3)}(x_1,x_2,x_3|y_1,y_2,y_3)$.

It represents one of the conserved charges generated by the transfer matrix of the integrable quantum $SU(2,2)$ spin chain of L sites in the scalar $(\Delta, J_1, J_2) = (1,0,0)$ representation [39]. Similarly, in the two-coupling version (1.2.4) of χCFT the perturbative expansion can be described by graphs which, in spite of more complicated structure (see Fig.4.1), can be still built by integrals of motion of the conformal spin chain. Namely, every planar graph in the ξ_j expansion is a certain permutation of multiple action of operators $\hat{\mathcal{H}}_B^{(L)}$ and $\hat{\mathcal{H}}_F^{(L)}$, where the latter operator is responsible for fermionic loops contribution. As we will see, the order in the permutation doesn't matter, since any fermionic loop can be moved through scalar wrappings, due to their commutativity, and this fact lays at the basis of integrability of these graphs. The action of $\hat{\mathcal{H}}_F^{(L)}$ reads

$$[\hat{\mathcal{H}}_F^{(L)}\Phi](x_1,\cdots,x_L) = \int \prod_{k=1}^{L} d^4y_k\, d^4z_k\ \mathcal{H}_F^{(L)}(x_1\cdots x_L|y_1\cdots y_L)\Phi(y_1,\cdots,y_L)\,,$$
$$\mathcal{H}_F^{(L)}(x_1\cdots x_L|y_1\cdots y_L) = \frac{\text{tr}[\sigma_{\mu_1}\bar{\sigma}_{\nu_1}\cdots\sigma_{\mu_L}\bar{\sigma}_{\nu_L}]}{(4\pi^3)^{2L}}\times \tag{4.1.2}$$
$$\times\int\prod_{k=1}^{L}\frac{d^4z_k}{(x_k-z_k)^2}\frac{(z_k-y_k)^{\mu_k}(y_k-z_{k+1})^{\nu_k}}{|z_k-y_k|^4|z_{k+1}-y_k|^4}\,,$$

and it builds up an integrable "brick-wall" domain [95]. Its commutation with $\hat{\mathcal{H}}_B^{(L)}$ can be proven directly by star-triangle relation (3.3.15), as shown in Fig.4.2. In order to show that $\hat{\mathcal{H}}_F^{(L)}$ is a conserved charge of the conformal scalar spin chain, we should prove its commutation with the transfer matrix at any value of the spectral

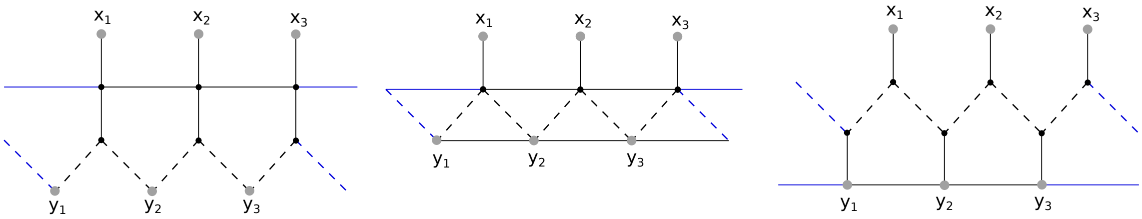

Figure 4.2: Proof of the commutation relation $[\hat{\mathcal{H}}_B^{(L)}, \hat{\mathcal{H}}_F^{(L)}] = 0$ at $L = 3$. Gray blobs are external coordinates, black dots are integration points and we denoted lines which coincide due to periodic b.c. with blue. Left: $\hat{\mathcal{H}}_B^{(L)}\mathcal{H}_F^{(L)}(x_1, x_2, x_3|y_1, y_2, y_3)$. In the middle: the result of integration over Yukawa vertices. Right: $\hat{\mathcal{H}}_F^{(L)}\mathcal{H}_B^{(L)}(x_1, x_2, x_3|y_1, y_2, y_3)$ as result of opening triangles with single y_j vertex in the middle figure.

parameter u,

$$[\hat{\mathcal{H}}_F^{(L)}, \mathbb{T}^{(L)}(u)] = 0\,. \tag{4.1.3}$$

For this purpose, we rewrite the kernel integrating out z_k variables

$$\mathcal{H}_F^{(L)}(x_1 \cdots x_L|y_1 \cdots y_L) = \frac{\mathrm{tr}[\sigma_{\mu_1}\bar{\sigma}_{\nu_1} \cdots \bar{\sigma}_{\nu_L}]}{(2\pi)^{4L}} \prod_{k=1}^{L} \frac{(y_k - x_k)^{\mu_k}(x_k - y_{k+1})^{\nu_k}}{(x_k - y_k)^2(x_k - y_{k+1})^2(y_k - y_{k+1})^2}\,,$$

and we recall the definition of $\mathbb{T}^{(L)}(u)$

$$\mathbb{T}^{(L)}(u) = \mathrm{Tr}\,_0[R_{10}(u)\,R_{20}(u)\cdots R_{L0}(u)], \qquad R_{j0}(u) \in \mathrm{End}(L^2(x_j)\otimes L^2(x_0)) \tag{4.1.4}$$

$$[R_{ij}(u)\Phi](x_i, x_j) = \frac{4^{2u}}{\pi^4}\frac{\Gamma(u+2)^2}{\Gamma(-u-1)\,\Gamma(-u+1)}\int \frac{d^4x_{i'}d^4x_{j'}\,\Phi(x_{i'}, x_{j'})}{(x_{ij}^2)^{-u-1}(x_{ji'}^2)^{1+u}(x_{ij'}^2)^{3+u}(x_{i'j'}^2)^{-u+1}},$$

where $R_{ij}(u)$ is the R-operator of the scalar conformal chain. It satisfies the Yang-Baxter equation [182]

$$R_{ij}(u)R_{ik}(v)R_{jk}(v-u) = R_{jk}(v-u)R_{ik}(v)R_{ij}(u)\,.$$

Then operator (4.1.1) coincides with $4^{-2L}\mathbb{T}^{(L)}$ in the limit $u \to -1$, as pointed out in [39], since the first propagator under the integral in (4.1.4) disappears and the last one effectively becomes a δ-function.
Now we introduce the transfer matrix for the brick-wall domain[1]

$$\mathbb{T}_F^{(L)}(u) = \mathrm{Tr}\,_0[\tilde{R}_{10}(u)\tilde{R}_{20}(u)\cdots\tilde{R}_{L0}(u)], \quad \tilde{R}_{j0}(u) \in \mathrm{End}(L^2(x_j)\otimes L^2(x_0)\otimes\mathbb{C}^2) \tag{4.1.5}$$

$$[(\tilde{R}_{ij})^{\alpha}_{\beta}(u)\Phi](x_i, x_j) = \frac{4^{2u}}{\pi^4}\frac{\Gamma(u+2)^2}{\Gamma(-u)\,\Gamma(-u+1)}\times \tag{4.1.6}$$
$$\times \int d^4x_{i'}d^4x_{j'}\frac{(\sigma_\mu)^{\alpha\dot{\alpha}}(\bar{\sigma}_\nu)_{\dot{\alpha}\beta}\;x_{ij'}^{\mu}\,x_{i'j}^{\nu}\;\Phi(x_i', x_j')}{(x_{ij}^2)^{-u}(x_{ji'}^2)^{1+u}(x_{ij'}^2)^{3+u}(x_{i'j'}^2)^{-u+1}},$$

[1]Here we implicitly mean the trace over spinorial indices of the fermionic loop.

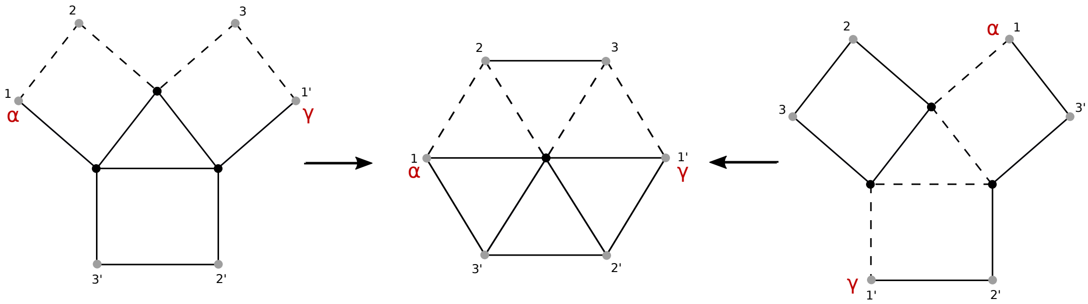

Figure 4.3: Graphical representation of relation (4.1.8) of Yang-Baxter type. The squares represent the kernels of $R(v-u)_{23}$ (solid lines) and $(\tilde{R}_{12})^{\alpha}_{\beta}(u)$, $(\tilde{R}_{13})^{\beta}_{\gamma}(v)$ (solid and dashed lines). Black dots are integration points, while gray blobs are external coordinates. Figures on the left and on the right are respectively the L.H.S. and R.H.S. of (4.1.8). Both sides can be transformed in the hexagonal object in the middle. First the triangle is opened into a star integral using the star-triangle relation. Doing so, each of the three black dots will become the end of only three lines. Then integration can be performed again by star-triangle and leads to the hexagon.

and we check, similarly to the above scalar case, that $\lim_{u\to -1}\mathbb{T}_F^{(L)}(u) = \hat{\mathcal{H}}_F^{(L)}$. The final step to prove (4.1.3) is to show that

$$[\mathbb{T}^{(L)}(u), \mathbb{T}_F^{(L)}(v)] = 0 \qquad \forall u, v \;, \tag{4.1.7}$$

which will be done by means of a Yang-Baxter type relation

$$\tilde{R}_{ij}^{\alpha}{}_{\beta}(u)\tilde{R}_{ik}^{\beta}{}_{\gamma}(v)R_{jk}(v-u) = R_{jk}(v-u)\tilde{R}_{ik}^{\alpha}{}_{\beta}(v)\tilde{R}_{ij}^{\beta}{}_{\gamma}(u)\,. \tag{4.1.8}$$

graphically represented in Fig.4.3. Indeed (4.1.7) follows immediately from (4.1.8). First of all we can introduce the monodromy operators

$$\tilde{\Omega}_0^{(L)}{}_{\beta}^{\alpha}(u) = \left[\tilde{R}_{01}(u)\cdots\tilde{R}_{0L}(u)\right]^{\alpha}_{\beta} \qquad \text{and} \quad \Omega_0^{(L)}(u) = R_{01}(u)\cdots R_{0L}(u)\,, \tag{4.1.9}$$

then iterating (4.1.8) we can write

$$\left[\tilde{R}_{00'}(u)\tilde{\Omega}_0^{(L)}(v)\right]^{\alpha}_{\beta}\Omega_{0'}^{(L)}(u-v) = \Omega_{0'}^{(L)}(u-v)\left[\tilde{\Omega}_0^{(L)}(v)\tilde{R}_{00'}(u)\right]^{\alpha}_{\beta}\,, \tag{4.1.10}$$

and we finally trace over space $L^2(x_0)\otimes L^2(x_{0'})$ and over spinorial indices getting

$$\begin{aligned}\mathrm{Tr}_{\,0,0'}\left(\tilde{\Omega}_0^{(L)}(v)\Omega_{0'}^{(L)}(v-u)\right) &= \mathrm{Tr}_{\,0,0'}\left(\tilde{R}_{00'}(u)^{-1}\Omega_{0'}^{(L)}(v-u)\tilde{\Omega}_0^{(L)}(v)\tilde{R}_{00'}(u)\right)\\ \mathrm{Tr}_{\,0}\left(\tilde{\Omega}_0^{(L)}(v)\right)\mathrm{Tr}_{\,0'}\left(\Omega_{0'}^{(L)}(v-u)\right) &= \mathrm{Tr}_{\,0'}\left(\Omega_{0'}^{(L)}(v-u)\right)\mathrm{Tr}_{\,0}\left(\tilde{\Omega}_0^{(L)}(v)\right)\,,\end{aligned} \tag{4.1.11}$$

which is equivalent to (4.1.7). Our derivation straightforwardly shows that from the point of view of integrability the regular square lattice and the brick-wall lattice built by Yukawa vertices can be combined into the same integrable structure and form a mixed lattice. This concludes the demonstration of integrability of the two-coupling model (1.2.4). The proof of integrability of the full χCFT (1.2.2) is a more tricky exercise and we leave it for the future.

4.2 Bethe-Salpeter equation correlators and conformal data

In this and the next sections of this paper, we will exploit conformal symmetry and the Bethe-Salpeter method to obtain the exact 4-point correlation function of the type

$$G_{\mathcal{O}_1\mathcal{O}_2}(x_1,x_2|x_3,x_4) = \langle \mathrm{Tr}[\mathcal{O}_1(x_1)\mathcal{O}_2(x_2)]\mathrm{Tr}[\mathcal{O}_1^\dagger(x_3)\mathcal{O}_2^\dagger(x_4)]\rangle\,, \tag{4.2.1}$$

where the operators $\mathcal{O}_i$ are protected operators in the planar limit of χCFT. Then we will extract from it the OPE data (anomalous dimensions and structure constants) for length-2 unprotected operators exchanged in the s-channel of (4.2.1). In the current section, we present the generalities of conformal Bethe-Salpeter approach, generalizing the one applied in [28, 36, 37] to the bi-scalar fishnet CFT, to sum up the Feynman graphs for these quantities in χCFT.

At the fixed point (1.2.13) and in the planar limit, the correlation function (4.2.1) is a finite function of the couplings ξ_i with $i = 1, 2, 3$. The correlation functions can be written as a geometric sum of primitive divergences in the perturbative expansion. For this reason, we will study those diagrams with the help of the Bethe-Salpeter equation. In the following we will review the Bethe-Salpeter method pointing out how to extract the spectrum and the OPE data from a four-point function (4.2.1).

In Sec.1.2.2, we presented the *bulk* fishnet structure of large planar diagrams in the general double-scaled γ deformed $\mathcal{N} = 4$ SYM theory. In this section we will focus on the correlation functions defined by (4.2.1) for matrix (untraced) operators with bare dimensions $\Delta_{\mathcal{O}_1}$ and $\Delta_{\mathcal{O}_2}$. In order to preserve renormalizability of the theory we have to add double-trace counter-terms (1.2.7), so that the diagrams in the perturbative expansion of (4.2.1) will take the following *chain* structure

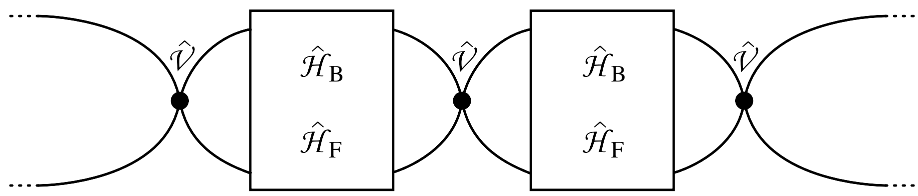

where the black dots are insertions of the double-trace operator[2] and the links of the chain are periodically repeating configurations of propagators (a special case of the topologies presented in Sec.1.2.2) generated by kernels of integral operators. We will refer to this set of operators as *Hamiltonians* or *graph-building operators* $\hat{\mathcal{H}}_i$. In the family of theories we are considering, $\hat{\mathcal{H}}_i$ can be of three different kind: the double trace operator $\hat{\mathcal{V}}$, the bosonic operator $\hat{\mathcal{H}}_B$ and the fermionic operator $\hat{\mathcal{H}}_F$. The operators $\hat{\mathcal{V}}$, $\hat{\mathcal{H}}_B$ and $\hat{\mathcal{H}}_F$ separately produce divergent integrals. However, at the fixed point, their combination is finite due to conformal symmetry (see Sec.4.4). These integral operators commute among themselves and they are diagonalized by the same basis of conformal triangles – the 3-point correlators of the two protected operators with one unprotected operator described below.

[2]Such insertions should always split a graphs, and its color structure, into two disconnected pieces.

In general, the correlation function (4.2.1) can be written in general as a geometric series of a linear combination of the Hamiltonian graph-building operators as follows

$$\begin{aligned}\hat{G}_{\mathcal{O}_1\mathcal{O}_2} &= \left(\frac{c_B}{x_{34}^2}\right)^{\Delta_{\mathcal{O}_1}+\Delta_{\mathcal{O}_2}-d} \sum_{\ell=0}^{\infty} \hat{\mathcal{H}}_B(\chi_{\mathcal{V}}\hat{\mathcal{V}} + \chi_B\hat{\mathcal{H}}_B + \chi_F\hat{\mathcal{H}}_F)^\ell \\ &= \left(\frac{c_B}{x_{34}^2}\right)^{\Delta_{\mathcal{O}_1}+\Delta_{\mathcal{O}_2}-d} \frac{\hat{\mathcal{H}}_B}{1-\chi_{\mathcal{V}}\hat{\mathcal{V}}-\chi_B\hat{\mathcal{H}}_B-\chi_F\hat{\mathcal{H}}_F}\,,\end{aligned} \tag{4.2.2}$$

where $c_B = 1/(4\pi^2)$ is the normalization factor of the free scalar propagator, $\chi_{\mathcal{V}}$, χ_B an χ_F are combinations of the couplings α_i and ξ_i with $i = 1, 2, 3$, which will be introduced later (see Sec.4.3). The space-time dimension d in this paper is always taken to be $d = 4$. [3] The correlation function (4.2.1) can be obtained from the operator $\hat{G}_{\mathcal{O}_1\mathcal{O}_2}$ as follows

$$G_{\mathcal{O}_1\mathcal{O}_2}(x_1, x_2|x_3, x_4) = \langle x_1, x_2|\hat{G}_{\mathcal{O}_1\mathcal{O}_2}|x_3, x_4\rangle\,, \tag{4.2.3}$$

where the Hamiltonian operators are represented by the corresponding integration kernels such that

$$\langle x_1, x_2|\hat{\mathcal{H}}_i^n|x_3, x_4\rangle = \int\prod_{k=1}^{2n} d^4y_k \mathcal{H}_i(x_1, x_2|y_1, y_2)\mathcal{H}_i(y_1, y_2|y_3, y_4)...\mathcal{H}_i(y_{2n-1}, y_{2n}|x_3, x_4)\,. \tag{4.2.4}$$

In order to compute the correlators $G_{\mathcal{O}_1\mathcal{O}_2}$, given the set of Hamiltonian graph-building operators $\hat{\mathcal{H}}_i$, we need to compute their eigenvalues and decompose $\hat{G}_{\mathcal{O}_1\mathcal{O}_2}$ over a complete basis of their eigenfunctions.

To compute the eigenvalues of $\hat{\mathcal{H}}_i$, we can use the fact that these integral operators transform covariantly with respect to the $(1, 0, 0) \otimes (1, 0, 0)$ conformal spin chain generators.[4] This property completely fixes their eigenstates to be the *conformal triangle* $\Phi_{\Delta,S,x_0}(x_1, x_2)$, the three-point function of two (scalar) operators in x_1 and x_2 with an operator $O_{\Delta,S}(x_0)$ with scaling dimension Δ, spin S at the position x_0

$$\begin{aligned}\Phi_{\Delta,S,x_0}(x_1, x_2) &= \langle \mathrm{Tr}\,[\mathcal{O}_1(x_1)\mathcal{O}_2(x_2)]O_{\Delta,S}(x_0)\rangle \\ &= (x_{12}^2)^{p-\frac{\Delta_{\mathcal{O}_1}+\Delta_{\mathcal{O}_2}}{2}}(x_{10}^2)^{\frac{\Delta_{\mathcal{O}_2}-\Delta_{\mathcal{O}_1}}{2}-p}(x_{20}^2)^{\frac{\Delta_{\mathcal{O}_1}-\Delta_{\mathcal{O}_2}}{2}-p}\left(\frac{2(nx_{02})}{x_{02}^2}-\frac{2(nx_{01})}{x_{01}^2}\right)^S\,,\end{aligned} \tag{4.2.5}$$

where $p = \frac{\Delta-S}{2}$ and n^μ an auxiliary light-cone vector. In the case $S = 0$, the conformal triangle is composed by simply three scalar propagators that we can graphically

[3] It is possible to generalize the bi-scalar fishnet theory to any integer dimension d, as in [28], at the cost of losing locality. It is not evident that such a generalization is possible for the full χCFT.

[4] In particular, defining the inversion $I[x_i^\mu] = x_i^\mu/x_i^2$, we have, for a conformal triangle $\Phi_{x_0}(x_1, x_2)$in the representation $(1, 0, 0) \otimes (1, 0, 0)$, $I[\Phi_{x_0}(x_1, x_2)] = \Phi_{x_0}(x_1/x_1^2, x_2/x_2^2) = U\Phi_{x_0}(x_1/x_1^2, x_2/x_2^2)$, and $U = x_1^2x_2^2x_0^{\Delta-S}$. We can check that for every integral operator: $I[\hat{\mathcal{H}}_i] = U\hat{\mathcal{H}}_iU^{-1}$.

represents as follows

$$\Phi_{\Delta,0,x_0}(x_1,x_2) \;\equiv \tag{4.2.6}$$

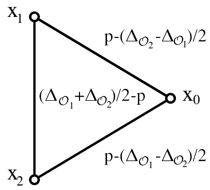

Finally, given the eigenstate (4.2.5), we can compute the spectrum of the Hamiltonian operators $\hat{\mathcal{H}}_i$ as follows

$$\int d^4y_1 d^4y_2\, \mathcal{H}_i(x_1,x_2|y_1,y_2)\,\Phi_{\Delta,S,x_0}(y_1,y_2) = h_{i\Delta,S}\,\Phi_{\Delta,S,x_0}(x_1,x_2), \tag{4.2.7}$$

where $h_{i\Delta,S}$ is the eigenvalue. More specifically, given the Hamiltonians operators defined in (4.2.2), we have

$$\left[\hat{\mathcal{V}}\;\Phi_{\Delta,S,x_0}\right](x_1,x_2) = h_{\mathcal{V}\Delta,S}\;\Phi_{\Delta,S,x_0}(x_1,x_2), \tag{4.2.8}$$

$$\left[\hat{\mathcal{H}}_B\;\Phi_{\Delta,S,x_0}\right](x_1,x_2) = h_{B\Delta,S}\;\Phi_{\Delta,S,x_0}(x_1,x_2), \tag{4.2.9}$$

$$\left[\hat{\mathcal{H}}_F\;\Phi_{\Delta,S,x_0}\right](x_1,x_2) = h_{F\Delta,S}\;\Phi_{\Delta,S,x_0}(x_1,x_2). \tag{4.2.10}$$

In Sec.4.3, we will verify that (4.2.5) diagonalizes these Hamiltonians and perform a direct computation of the eigenvalues. The scaling dimension appearing in (4.2.5) is defined as [183]

$$\Delta = 2 + 2i\nu\,, \tag{4.2.11}$$

with ν a non-negative real number. For such values of Δ, the state Φ_{Δ,S,x_0} belongs to the principal series of type-I irreducible representations $(\Delta,S,0)$ of the conformal group labeled by ν and the discrete spin S and satisfies the orthogonality condition [183, 184]

$$\begin{aligned}&\int \frac{d^4x_1 d^4x_2\overline{\Phi_{\Delta',S',x_{0'}}}(x_1,x_2)\Phi_{\Delta,S,x_0}(x_1,x_2)}{(x_{12}^2)^{4-\Delta_{\mathcal{O}_1}-\Delta_{\mathcal{O}_2}}} = \\ =\;& (-1)^S c_1(\nu,S)\delta(\nu-\nu')\,\delta_{S,S'}\delta^{(4)}(x_{00'})(nn')^S \\ &+(-1)^S c_2(\nu,S)\delta(\nu+\nu')\delta_{S,S'}((n\partial_{x_0})(n'\partial_{x_{0'}})\ln x_{00'}^2)^S/(x_{00'}^2)^{2-2i\nu-S},\end{aligned} \tag{4.2.12}$$

where the 4-dimensional coefficients c_1 and c_2 are given by

$$\begin{aligned}c_1 &= \frac{2^{S-1}\,\pi^7}{(S+1)\nu^2\,(4\nu^2+(S+1)^2)},\\ c_2 &= -\frac{i\pi^5(-1)^S\Gamma\left(\frac{S+\Delta_{\mathcal{O}_1}-\Delta_{\mathcal{O}_2}}{2}-i\nu+1\right)\Gamma\left(\frac{S-\Delta_{\mathcal{O}_1}+\Delta_{\mathcal{O}_2}}{2}-i\nu+1\right)\Gamma(S+2i\nu+1)}{\nu(S+1)\Gamma\left(\frac{S+\Delta_{\mathcal{O}_1}-\Delta_{\mathcal{O}_2}}{2}+i\nu+1\right)\Gamma\left(\frac{S-\Delta_{\mathcal{O}_1}+\Delta_{\mathcal{O}_2}}{2}+i\nu+1\right)\Gamma(S-2i\nu+1)}.\end{aligned} \tag{4.2.13}$$

The eigenfunctions Φ_{Δ,S,x_0} forms an orthonormal basis for $\nu \geq 0$ implying the following representation for the identity

$$\delta^{(4)}(x_{13})\delta^{(4)}(x_{24})=\sum_{S=0}^{\infty}\frac{(-1)^S}{(x_{34}^2)^{4-\Delta_{\mathcal{O}_1}-\Delta_{\mathcal{O}_2}}}\int_0^\infty \frac{d\nu}{c_1(\nu,S)}\int d^4x_0\Phi_{\Delta,S,x_0}(x_1,x_2)\overline{\Phi_{\Delta,S,x_0}}(x_3,x_4), \tag{4.2.14}$$

that, together with the definition (4.2.7), leads to the diagonalized representation

$$\mathcal{H}_i(x_1,x_2|x_3,x_4)=\sum_{S=0}^{\infty}\frac{(-1)^S}{(x_{34}^2)^{4-\Delta_{\mathcal{O}_1}-\Delta_{\mathcal{O}_2}}}\int_0^\infty \frac{d\nu h_{i\Delta,S}}{c_1(\nu,S)}\int d^4x_0\Phi_{\Delta,S,x_0}(x_1,x_2)\overline{\Phi_{\Delta,S,x_0}}(x_3,x_4), \tag{4.2.15}$$

where $\mathcal{H}_i$ stands for the set of Hamiltonians $\{\mathcal{V},\mathcal{H}_B,\mathcal{H}_F\}$ and $h_{i\Delta,S}$ for the set of eigenvalues $\{h_{\mathcal{V}\Delta,S},h_{B\Delta,S},h_{F\Delta,S}\}$ respectively.

Plugging the representation (4.2.15) for the graph-building operators $\mathcal{H}_i$ into (4.2.2), we obtain the representation of the 4-point function in terms of their eigenvalues $h_{i\Delta,S}$

$$\begin{aligned} G_{\mathcal{O}_1\mathcal{O}_2}(x_1,x_2|x_3,x_4) =& \sum_{S=0}^{\infty}\frac{(-1)^S}{(x_{34}^2)^{4-\Delta_{\mathcal{O}_1}-\Delta_{\mathcal{O}_2}}}\int_0^\infty \frac{d\nu}{c_1(\nu,S)}\times \\ &\times \frac{h_{B\Delta,S}}{1-\chi_{\mathcal{V}}h_{\mathcal{V}\Delta,S}-\chi_B h_{B\Delta,S}-\chi_F h_{F\Delta,S}}\int d^4x_0\Phi_{\Delta,S,x_0}(x_1,x_2)\overline{\Phi_{\Delta,S,x_0}}(x_3,x_4). \end{aligned} \tag{4.2.16}$$

The integral over the auxiliary point x_0 can be expressed in terms of the four-dimensional conformal blocks $g_{\Delta,S}$ [183, 185, 186]

$$\begin{aligned} &\int d^4x_0\Phi_{\Delta,S,x_0}(x_1,x_2)\overline{\Phi_{\Delta,S,x_0}}(x_3,x_4) \\ &=\left(\frac{1}{x_{12}^2x_{34}^2}\right)^{\frac{\Delta_{\mathcal{O}_1}+\Delta_{\mathcal{O}_2}}{2}}\left(\frac{x_{24}^2}{x_{13}^2}\right)^{\frac{\Delta_{\mathcal{O}_1}-\Delta_{\mathcal{O}_2}}{2}}\left(\frac{c_1(\nu,S)}{c_2(\nu,S)}g_{\Delta,S}(u,v)+\frac{c_1(-\nu,S)}{c_2(-\nu,S)}g_{4-\Delta,S}(u,v)\right), \end{aligned} \tag{4.2.17}$$

where the cross-ratios are $u = z\bar{z} = x_{12}^2x_{34}^2/(x_{13}^2x_{24}^2)$ and $v = (1-z)(1-\bar{z}) = x_{14}^2x_{23}^2/(x_{13}^2x_{24}^2)$ and we recall from [185] that

$$\begin{aligned} &g_{\Delta,S} = (-1)^S\frac{z\bar{z}}{z-\bar{z}}\left[k(\Delta+S,z)k(\Delta-S-2,\bar{z})-k(\Delta+S,\bar{z})k(\Delta-S-2,z)\right], \\ &\text{where}\quad k(\beta,x) = x^{\beta/2}\,{}_2F_1\left(\frac{\beta-(\Delta_1-\Delta_2)}{2},\frac{\beta+(\Delta_3-\Delta_4)}{2},\beta,x\right). \end{aligned} \tag{4.2.18}$$

Inserting (4.2.17) into (4.2.16), we obtain

$$G_{\mathcal{O}_1\mathcal{O}_2}(x_1,x_2|x_3,x_4) = \left(\frac{c_B^2}{x_{12}^2x_{34}^2}\right)^{\frac{\Delta_{\mathcal{O}_1}+\Delta_{\mathcal{O}_2}}{2}}\left(\frac{x_{24}^2}{x_{13}^2}\right)^{\frac{\Delta_{\mathcal{O}_1}-\Delta_{\mathcal{O}_2}}{2}}\mathcal{G}_{\mathcal{O}_1\mathcal{O}_2}(u,v)\,, \tag{4.2.19}$$

where we defined

$$\mathcal{G}_{\mathcal{O}_1\mathcal{O}_2}(u,v) = \frac{1}{c_B^4}\sum_{S=0}^{\infty}(-1)^S\int_{-\infty}^{\infty}\frac{d\nu}{c_2(\nu,S)}\frac{h_{B\Delta,S}\;g_{\Delta,S}(u,v)}{1-\chi_{\mathcal{V}}h_{\mathcal{V}\Delta,S}-\chi_B h_{B\Delta,S}-\chi_F h_{F\Delta,S}}\,. \tag{4.2.20}$$

Notice that we extended the integral over ν on the full real axis with the change of variable $\nu \to -\nu$ in the second term of (4.2.17). This is allowed by the symmetry of eigenvalues appearing in the spectral equation

$$h_{i\,4-\Delta,S} = h_{i\,\Delta,S}\,, \tag{4.2.21}$$

and can be interpreted as the fact that, for a given spin S, states with dimension Δ and $4-\Delta$ belong to unitary-equivalent representations of the conformal group. This symmetry is indeed satisfied for every studied case, (4.3.14) and (4.3.25).

Before studying the integral in (4.2.20), we want to focus on the role of the double-trace Hamiltonian and its eigenvalues in the perturbative and Bethe-Salpeter approaches. To find the correlation function (4.2.1), we have to sum up diagrams of the kind shown at the beginning of this section. These diagrams contain scalar and fermionic loops generated by the operators $\hat{\mathcal{H}}_B$ and $\hat{\mathcal{H}}_F$ interspersed with the contributions of the double-trace vertices introduced in (1.2.7). Since in general the integrals over the positions of the single-trace vertices develop ultraviolet (UV) divergences at short distances, one needs the double-trace interactions to produce other UV divergent contributions which cancels against them. Therefore, the weak coupling expansion of the four-point correlation function remains UV finite at any order as expected for protected $\mathcal{O}_1$ and $\mathcal{O}_2$.

In the context of the Bethe-Salpeter equation the story is slightly different. Indeed consider the Hamiltonian operator $\hat{\mathcal{V}}$ associated to the double-trace kernel defined as follows

$$\left[\hat{\mathcal{V}}\;\Phi\right](x_1,x_2) = 2c_B^2\int\frac{d^4y_1d^4y_2}{(x_1-y_1)^2(x_2-y_2)^2}\delta^{(4)}(y_{12})\,\Phi(y_1,y_2)\,, \tag{4.2.22}$$

where $\Phi(y_1,y_2)$ is a test function. We have to compute its spectrum by means of (4.2.8) that, when applied to (4.2.5), reads

$$\left[\hat{\mathcal{V}}\;\Phi_{\Delta,S,x_0}\right](x_1,x_2) = \frac{\delta^{(4)}(\nu)\delta_{S,0}}{(4\pi)^2}\,\Phi_{\Delta,S,x_0}(x_1,x_2) \qquad \Rightarrow \qquad h_{\mathcal{V}\Delta,S} = \frac{\delta^{(4)}(\nu)\delta_{S,0}}{(4\pi)^2}. \tag{4.2.23}$$

First of all, due to the form of the eigenvalue, the double-trace term can affect only the contribution to the sum in (4.2.20) with spin $S=0$. Then we expect that the contribution to (4.2.20) given by the Hamiltonian operators $\hat{\mathcal{H}}_B$ and $\hat{\mathcal{H}}_F$ are well-defined for $S\neq 0$ but in principle we have to take into account the double-trace term for $S=0$.

Since we want to write $\mathcal{G}_{\mathcal{O}_1\mathcal{O}_2}$ in the standard OPE form, we will consider the limit in which two of the external points are approaching, *i.e.* $|x_{12}|\to 0$ (or $u\to 0$

and $v \to 1$). Since the conformal block scales as $u^p(1-v)^S$ decaying exponentially for $\mathrm{Re}(i\nu) \to \infty$, one can close the contour in the integral over ν in the lower-half plane and then compute it by residues. At short distances, the eigenstate (4.2.5) scales as $\Phi_{\Delta,S,x_0}(x_1,x_2) \sim (x_{12}^2)^{\frac{\Delta-\Delta_{\mathcal{O}_1}-\Delta_{\mathcal{O}_2}}{2}}$ and thus it vanishes in the lower-half plane (which is true in our case, since $\Delta_{\mathcal{O}_1} = \Delta_{\mathcal{O}_2} = 1$ and $\Re(\Delta) > 2$). In this case, the bosonic and fermionic operators do not develop UV divergences (one can verify it in the two special cases that we study in detail in Sec.4.3). Moreover, given the definition (4.2.22) and the formula (4.2.23), the double-trace operator $\hat{\mathcal{V}}$ annihilates Φ_{Δ,S,x_0} with $\mathrm{Im}(\nu) < 0$ for any S and therefore, it does not contribute. With this argument, we are able to neglect the double-trace contributions when we compute the four-point function $G_{\mathcal{O}_1\mathcal{O}_2}$ with the Bethe-Salpeter method. Then we can rewrite (4.2.20) as follows

$$\mathcal{G}_{\mathcal{O}_1\mathcal{O}_2}(u,v) = \frac{1}{c_B^4}\sum_{S=0}^{\infty}(-1)^S \oint_{\mathcal{C}_-} \frac{d\nu}{c_2(\nu,S)} \frac{h_{B\Delta,S}}{1-\chi_B h_{B\Delta,S} - \chi_F h_{F\Delta,S}}\; g_{\Delta,S}(u,v)\,, \tag{4.2.24}$$

where $\mathcal{C}_-$ is the close path in the lower-half plane.

In order to compute the integral over ν in (4.2.24) with residues, we have to identify the poles of the integrand. The *physical poles* are given by the zeros of denominator of the integrand, i.e. by solutions of the equation

$$h_{B\Delta,S}{}^{-1} - \chi_F\, h_{F\Delta,S}\, h_{B\Delta,S}{}^{-1} = \chi_B\,. \tag{4.2.25}$$

We will refer to (4.2.25) as *spectral equation*: indeed given the eigenvalues $h_{i\Delta,S}$ and the constants χ_i, solving the equation we will obtain the scaling dimensions Δ as functions of the couplings ξ_i with $i = 1,2,3$ and the spin S. In the integrand of (4.2.24), two series of *spurious poles* are generated by the measure c_2 and the conformal block $g_{\Delta,S}$. In App.C.2 we will prove that the contribution of those poles cancel under the condition

$$h_{i\,3+S+k,S} - h_{i\,3+S,S+k} = 0 \qquad k = 0,2,4\ldots\ , \tag{4.2.26}$$

which happens to be satisfied.

Finally $\mathcal{G}_{\mathcal{O}_1\mathcal{O}_2}$ is given by the sum of only the residues at the physical pole (4.2.25). Then we can rewrite the correlation function in the standard form of a conformal partial wave expansion as follows

$$\mathcal{G}_{\mathcal{O}_1\mathcal{O}_2} = \sum_{\Delta,S\geq 0} C_{\Delta,S}\; g_{\Delta,S}(u,v)\,, \tag{4.2.27}$$

with the OPE coefficients $C_{\Delta,S}$ defined as

$$C_{\Delta,S} = \frac{(-1)^S}{c_B^4}\, 4\pi\, \mathrm{Res}_{\Delta}\left(\frac{1}{c_2(\nu,S)} \frac{h_{B\Delta,S}}{1-\chi_B h_{B\Delta,S} - \chi_F h_{F\Delta,S}}\right)\,. \tag{4.2.28}$$

The sum over Δ in (4.2.27) runs over the solutions of the spectral equation for scaling dimensions of exchanges operators with $\mathrm{Re}(\Delta) > 2$ [5].

In the following sections, we will focus on the computation of the point-split four-point correlation functions of the operators introduced in (1.2.3), establishing the Hamiltonian operators $\hat{\mathcal{H}}_i$ and the constants χ_i appearing in (4.2.1) from their Feynman diagram expansion. We closely follow in our analysis the logic of [37], but in contrast to this paper which treats the bi-scalar fishnet CFT, we have to introduce new types of diagrams into the Bethe-Salpeter procedure, reflecting a richer structure of the full three-coupling χCFT. To write the correlation function (4.2.1) in the standard OPE representation requires, as the only dynamical input, the knowledge of eigenvalues $h_{i\Delta,S}$ of the Hamiltonian operators. We will diagonalize $\hat{\mathcal{H}}_i$ to extract the conformal data, *i.e.* the scaling dimensions of the exchanged operators and the OPE coefficients. In what follows we consider only single scalar fields as protected external operators and then we should set $\Delta_{\mathcal{O}_1} = \Delta_{\mathcal{O}_2} = 1$. In the following sections we will concentrate with the sector $\phi_1\phi_1$ of the theory, and study its four-point correlator pointing out the richer OPE data which appear respect to the same correlator in the bi-scalar fishnet CFT.

4.3 Exact four-point correlation function $G_{\phi_1\phi_1}$

In this section we consider the four-point correlators associated to the first operator of (1.2.3), namely when $\mathcal{O}_1(x) = \mathcal{O}_2(x) = \phi_j(x)$ with $j = 1, 2, 3$. Since the computation of the correlators is the same for any j, we will consider the case $j = 1$ and then the four-point function we want to study takes the following form

$$G_{\phi_1\phi_1}(x_1, x_2|x_3, x_4) = \langle \mathrm{Tr}[\phi_1(x_1)\phi_1(x_2)]\mathrm{Tr}[\phi_1^\dagger(x_3)\phi_1^\dagger(x_4)]\rangle\,. \tag{4.3.1}$$

This correlation function was extensively studied in [36] in the simplest case of the family of theories we are inspecting, *i.e.* the bi-scalar theory (1.2.6).

In the planar limit $N_c \to \infty$, once chosen $j = 1$, the weak coupling expansion of (4.3.1) in terms of Feynman diagrams is given by a combination of the following bosonic vertices

$$\begin{gathered}(4\pi)^2\xi_3^2\mathrm{Tr}[\phi_1^\dagger\phi_2^\dagger\phi_2\phi_2](x)\,, \qquad (4\pi)^2\xi_2^2\mathrm{Tr}[\phi_3^\dagger\phi_1^\dagger\phi_3\phi_1](x)\,,\\ (4\pi)^2\alpha_1^2\,\mathrm{Tr}[\phi_1\phi_1](x)\,\mathrm{Tr}[\phi_1\phi_1]^\dagger(x)\,,\end{gathered} \tag{4.3.2}$$

and the following Yukawa vertices

$$4\pi i\sqrt{\xi_2\xi_3}\,\mathrm{Tr}[\overline{\psi}_3\phi_1^\dagger\,\overline{\psi}_2](x)\,, \qquad 4\pi i\sqrt{\xi_2\xi_3}\,\mathrm{Tr}[\psi_3\phi_1\,\psi_2](x)\,. \tag{4.3.3}$$

In the following we will study the correlation function (4.3.1) with the Bethe-Salpeter method.

[5] This condition in the OPE is equivalent to the restriction $\mathrm{Re}(i\nu) > 0$ in the contour integral in (4.2.24).

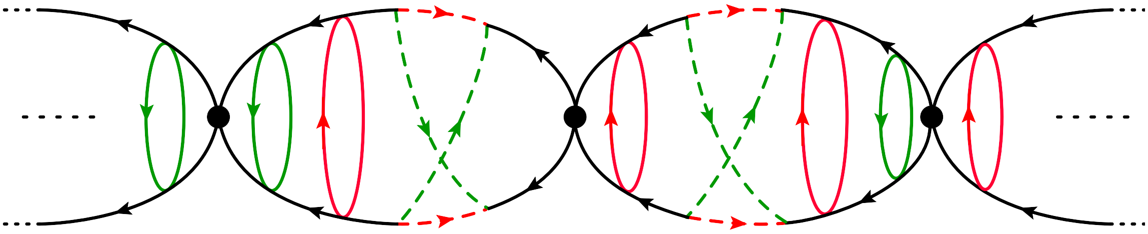

Figure 4.4: A Feynman diagram contributing to the perturbative expansion $G^{(\ell)}_{\phi_1\phi_1}$. The black dots stand for double-trace vertices and tick and dashed lines correspond to bosonic and fermionic propagators respectively. The colors represent different flavors j of the particles ϕ_j and ψ_j: in particular black for $j=1$, red for $j=2$ and green for $j=3$. The propagators are not crossing and are curved to stress the fact that they have a cylindrical topology.

4.3.1 Bethe-Salpeter method

The perturbative expansion of (4.3.1) can be written in the following form

$$G_{\phi_1\phi_1}(x_1,x_2|x_3,x_4) = \sum_{\ell=0}^{\infty}(4\pi)^{4\ell}\, G^{(\ell)}_{\phi_1\phi_1}(x_1,x_2|x_3,x_4)\,, \tag{4.3.4}$$

where $G^{(\ell)}_{\phi_1\phi_1}$ at any perturbative order ℓ contains contributions from the bosonic and fermionic integrals with different coupling dependencies. In Fig.4.4, we present an example of an arbitrary Feynman diagram contributing to $G^{(\ell)}_{\phi_1\phi_1}$. The black dots represents insertions of the double-trace vertex in the last line of (4.3.2) that in the Bethe-Salpeter picture are associated with the operator $\hat{\mathcal{V}}$ defined in (4.2.22). Then it is straightforward to fix the normalization of its coupling constant in (4.2.2) as follows

$$\chi_{\mathcal{V}} = (4\pi)^2\,\alpha_1^2\,. \tag{4.3.5}$$

In Sec.4.2, we discussed the role of the double-trace terms in the computation of the four-point function, discovering that they are not contributing to the spectral equation. Then, similarly to observations of [36, 37], as far as we consider the perturbative expansion (4.3.4) in the point-splitting $x_1 \neq x_2$ and $x_3 \neq x_4$, we need only to sum over the single trace contributions, namely the diagrams inside the chain link of Fig.4.4. In Sec.4.4 we will present in detail how the relation between single- and double-trace terms is crucial for the setting of the fixed point (1.2.13).

The first two orders of the perturbative expansion are given by the diagrams represented in Fig.4.5 and they can be written as follows

$$\begin{aligned} G^{(0)}_{\phi_1\phi_1} &= \frac{c_B^2}{x_{13}^2 x_{24}^2}\,,\\ G^{(1)}_{\phi_1\phi_1} &= c_B^6(\xi_2^4+\xi_3^4)\int \frac{d^4y_1 d^4y_2}{(x_1-y_1)^2(x_2-y_2)^2(y_{12}^2)^2(y_1-x_3)^2(y_2-x_4)^2}\\ &\quad - c_B^4 c_F^4 \xi_2^2\xi_3^2 \int \frac{\prod_{i=1}^{2} d^4y_i d^4y_{i'}\ \mathrm{Tr}\left[\sigma_\mu\bar{\sigma}_\rho\sigma_\eta\bar{\sigma}_\nu\right]\ y^\mu_{22'}y^\rho_{2'1}y^\eta_{11'}y^\nu_{1'2}}{(x_1-y_{1'})^2(x_2-y_{2'})^2 y^4_{22'}y^4_{2'1}y^4_{11'}y^4_{1'2}(y_1-x_3)^2(y_2-x_4)^2}\,, \end{aligned} \tag{4.3.6}$$

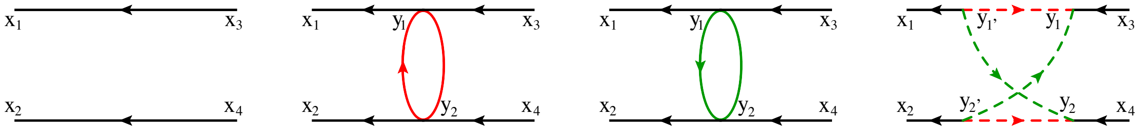

(a) $\xi_1^0\xi_2^0\xi_3^0$ (b) ξ_3^4 (c) ξ_2^4 (d) $\xi_2^2\xi_3^2$

Figure 4.5: First contribution to the four-point functions $G_{\phi_1\phi_1}$.

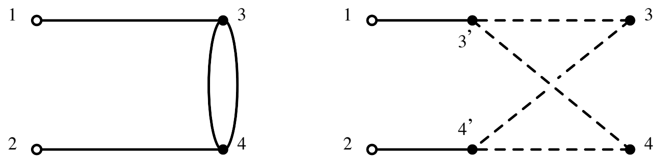

(a) $\mathcal{H}_B(x_1, x_2|x_3, x_4)$ (b) $\mathcal{H}_F(x_1, x_2|x_3, x_4)$

Figure 4.6: The kernels associated to the Hamiltonian graph-building operators $\hat{\mathcal{H}}_B$ and $\hat{\mathcal{H}}_F$ involved in the computation of the four-point function $G_{\phi_1\phi_1}$ with $j = 1, 2, 3$. White dots represent external points and black dots integration over the full space R^4.

where each scalar propagator brings in the factor c_B/x_{ij}^2 and each fermionic propagator the factor $c_F \not{x}_{ij}/x_{ij}^4$, where $\not{x}$ can be $\sigma_\mu x^\mu$ or $\bar{\sigma}_\mu x^\mu$. Since the fermionic propagator can also be written as $c_B \not{\partial}_{x_i} 1/x_{ij}^2$ we conclude that $c_F = -2c_B = -1/(2\pi^2)$. These functions can be expressed in terms of a combination of the Hamiltonian graph-building operators $\hat{\mathcal{H}}_i$. Indeed defining the following kernels

$$\begin{aligned} \mathcal{H}_B(x_1, x_2|x_3, x_4) &= \frac{c_B^4}{x_{13}^2 x_{24}^2 x_{34}^4}\,, \\ \mathcal{H}_F(x_1, x_2|x_3, x_4) &= -\,c_B^2\, c_F^4 \int \frac{d^4x_{3'} d^4x_{4'}\ \mathrm{Tr}\left[\sigma_\mu \bar{\sigma}_\rho \sigma_\eta \bar{\sigma}_\nu\right]\ x_{44'}^\mu x_{4'3}^\rho x_{33'}^\sigma x_{3'4}^\nu}{x_{13'}^2 x_{24'}^2 x_{44'}^4 x_{4'3}^4 x_{33'}^4 x_{3'4}^4}\,, \end{aligned} \tag{4.3.7}$$

represented in Fig.4.6, we can rewrite (4.3.6) as follows

$$\begin{aligned} G_{\phi_1\phi_1}^{(0)} &= \frac{x_{34}^4}{c_B^2} \mathcal{H}_B(x_1, x_2|x_3, x_4)\,, \\ G_{\phi_1\phi_1}^{(1)} &= \frac{x_{34}^4}{c_B^2} \int d^4y_1 d^4y_2 \Big[(\xi_2^4 + \xi_3^4)\ \mathcal{H}_B(x_1, x_2|y_1, y_2)\ \mathcal{H}_B(y_1, y_2|x_3, x_4) \\ &\qquad + \xi_2^2\xi_3^2\ \mathcal{H}_F(x_1, x_2|y_1, y_2)\ \mathcal{H}_B(y_1, y_2|x_3, x_4) \Big]\,. \end{aligned} \tag{4.3.8}$$

The kernels (4.3.7) transform covariantly under conformal transformations[6], then the corresponding Hamiltonian integral operators commute with the generators of the conformal group.

When carrying on the perturbative expansion, it becomes clear that an arbitrary

[6]The easiest way to prove it is to apply the inversion operator to (4.3.7). For the fermionic Hamiltonian it is convenient to use its representation after the two integrations will be performed later in (4.3.16).

diagram at order ℓ is given by

$$\hat{G}^{(\ell)}_{\phi_1\phi_1} = \frac{x_{34}^4}{c_B^2}\,\hat{\mathcal{H}}_B\left[(\xi_2^4+\xi_3^4)\hat{\mathcal{H}}_B + \xi_2^2\xi_3^2\hat{\mathcal{H}}_F\right]^\ell . \tag{4.3.9}$$

Then the correlator (4.3.4) can be presented in the following operatorial form

$$\hat{G}_{\phi_1\phi_1} = \sum_{\ell=0}^{\infty}(4\pi)^{4\ell}\hat{G}^{(\ell)}_{\phi_1\phi_1} = \frac{x_{34}^4}{c_B^2}\frac{\hat{\mathcal{H}}_B}{1-(4\pi)^4(\xi_2^4+\xi_3^4)\hat{\mathcal{H}}_B-(4\pi)^4\xi_2^2\xi_3^2\hat{\mathcal{H}}_F} . \tag{4.3.10}$$

Comparing it with the definition (4.2.2) we fix the values of the constants χ_i (in this case $\hat{\mathcal{V}}$ is not contributing)

$$\chi_B = (4\pi)^4(\xi_2^4+\xi_3^4)\,, \qquad \chi_F = (4\pi)^4\xi_2^2\xi_3^2\,. \tag{4.3.11}$$

4.3.2 Eigenvalues of the graph-building operators

Writing the four-point correlation function in the standard OPE form, as presented in detail in Sec.4.2, involves the computation of the spectrum of the graph-building operators (4.3.7). The eigenstate that diagonalize the Hamiltonians is defined in (4.2.5) for $\Delta_{\mathcal{O}_1} = \Delta_{\mathcal{O}_2} = 1$ and the eigenvalues are defined by means of equations (4.2.9) and (4.2.10). Substituting in the latter the kernels (4.3.7) and using the definition (4.2.7), we will end up with a set of integrals that can be computed with the help of the star-triangle relations (3.3.15). The fact that all the integrals that we have to compute can be computed by means of the star-triangle relations is a consequence of the underlying conformal symmetry.

Bosonic eigenvalue: The bosonic eigenvalue $h_{B\Delta,S}$ is defined in (4.2.9). Using the bosonic Hamiltonian (4.3.7), this relation can be written in the following integral form

$$c_B^4\int\frac{d^4y_1d^4y_2}{(x_1-y_1)^2(x_2-y_2)^2y_{12}^4}\Phi_{\Delta,S,x_0}(y_1,y_2) = h_{B\Delta,S}\Phi_{\Delta,S,x_0}(x_1,x_2)\,. \tag{4.3.12}$$

In the case of $S=0$, the function Φ_{Δ,S,x_0} reduces to (4.2.6) and the computation is straightforward. Indeed, one needs to apply the star-triangle relations two times as follows[7]

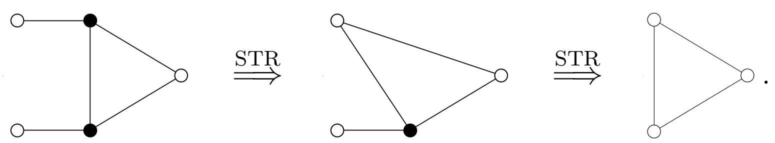

to obtain

$$h_{B\Delta,0} = \frac{16\pi^4c_B^4}{\Delta(\Delta-2)^2(\Delta-4)}\,. \tag{4.3.13}$$

The eigenvalue at $S\neq 0$ can be computed in the same way, using the generalization of star-triangle relation to any-spin case (3.3.15). The computation can be otherwise

[7]It is convenient to perform this and other similar computations, together with the pictures, with the `STR` package [134, 187].

done in a more tedious and explicit way as presented in detail in [37]. The result reads [36]

$$h_{B\Delta,S} = \frac{16\pi^4 c_B^4}{(\Delta+S)(\Delta+S-2)(\Delta-S-2)(\Delta-S-4)}\,. \tag{4.3.14}$$

The eigenvalue is invariant under $\Delta \to 4-\Delta$, as expected from (4.2.21).

Fermionic eigenvalue The fermionic eigenvalue $h_{F\Delta,S}$ is defined in (4.2.10). This is a new object, absent in the similar correlator of bi-scalar model treated in [36]. First of all we can simplify the fermionic Hamiltonian in (4.3.7) integrating the primed variables by means of the Yukawa star-triangle identity (3.3.15) as follows (red lines are spin-1/2 fermionic propagators)

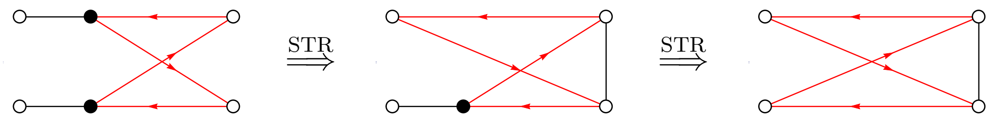

where the computation and figures are made with the `STR` package (see footnote 7). We obtain the following kernel

$$\mathcal{H}_F(x_1,x_2|x_3,x_4) = -\pi^4 c_B^2\, c_F^4 \frac{\mathrm{Tr}\left[\sigma_\mu \overline{\sigma}_\rho \sigma_\eta \overline{\sigma}_\nu\right]\, x_{42}^\mu x_{23}^\rho x_{31}^\eta x_{14}^\nu}{x_{42}^2 x_{23}^2 x_{31}^2 x_{14}^2 x_{34}^4}\,. \tag{4.3.15}$$

Using the formula for the trace of four σ-matrices (C.1.11) and simplifying the scalar products by means of (C.1.4), we can rewrite the fermionic Hamiltonian in the following form

$$\mathcal{H}_F(x_1,x_2|x_3,x_4) = \pi^4 c_B^2\, c_F^4 \tilde{\mathcal{H}}_F(x_1,x_2|x_3,x_4) - 2\mathcal{H}_B(x_1,x_2|x_3,x_4)\,. \tag{4.3.16}$$

where we used the symmetry $\mathcal{H}_B(x_1,x_2|x_3,x_4) = \mathcal{H}_B(x_2,x_1|x_3,x_4)$ of the bosonic Hamiltonian studied in the previous paragraph, and $\tilde{\mathcal{H}}_F$ is defined by

$$\tilde{\mathcal{H}}_F(x_1,x_2|x_3,x_4) \equiv \frac{x_{12}^2}{x_{42}^2 x_{23}^2 x_{31}^2 x_{14}^2 x_{34}^2}\,. \tag{4.3.17}$$

Then the fermionic eigenvalue $h_{F\Delta,S}$ consists of the bosonic eigenvalue (4.3.14) and the eigenvalue of $\tilde{\mathcal{H}}_F$ defined as follows

$$\left[\hat{\tilde{\mathcal{H}}}_F\, \Phi_{\Delta,S,x_0}\right](x_1,x_2) = \tilde{h}_{F\Delta,S}\, \Phi_{\Delta,S,x_0}(x_1,x_2)\,, \tag{4.3.18}$$

such that

$$h_{F\Delta,S} = \pi^4 c_B^2\, c_F^4\, \tilde{h}_{F\Delta,S} - 2\, h_{B\Delta,S}\,. \tag{4.3.19}$$

Let's focus on the relation (4.3.18). It can be written in the following integral form

$$\int \frac{d^4y_1 d^4y_2\; x_{12}^2}{(y_2-x_2)^2(x_2-y_1)^2(y_1-x_1)^2(x_1-y_2)^2 y_{12}^2}\Phi_{\Delta,S,x_0}(y_1,y_2) = \tilde{h}_{F\Delta,S}\Phi_{\Delta,S,x_0}(x_1,x_2). \tag{4.3.20}$$

In order to simplify the computation, we consider the limit in which $x_0 \to \infty$ on both sides of (4.3.20). In this limit the eigenvalue $\tilde{h}_{F\Delta,S}$ is given by the following integral

$$\tilde{h}_{F\Delta,S} = \int \frac{d^4y_1 d^4y_2\,(n\,y_{12})^S}{(y_2-x_2)^2(x_2-y_1)^2(y_1-x_1)^2(x_1-y_2)^2(y_{12}^2)^{2-p}}\,, \tag{4.3.21}$$

where $p = \frac{\Delta-S}{2}$ and we put $x_{12}^2 = (nx_{12}) = 1$ for convenience. Notice that the integrand is anti-symmetric in the exchange $y_1 \leftrightarrow y_2$ for odd S, then the eigenvalue $\tilde{h}_{F\Delta,S}$ is non-zero only for even S.

In the $S = 0$ case, the integral (4.3.21) is known as a massless two-loop self-energy Feynman integral, or *kite*. Its value is known for any power of the propagator $1/y_{12}^2$ in terms of an hypergeometric function [188], then

$$\tilde{h}_{F\Delta,0} = -2\pi^4\Gamma(\tfrac{\Delta}{2}-1)\Gamma(1-\tfrac{\Delta}{2})\left[\frac{{}_3F_2(1,2,\frac{\Delta}{2};\frac{\Delta}{2}+1,\frac{\Delta}{2}+1|1)}{\Delta/2\,\Gamma(\frac{\Delta}{2}+1)\Gamma(2-\frac{\Delta}{2})} + \pi\cot\pi(4-\tfrac{\Delta}{2})\right], \tag{4.3.22}$$

where $\Delta = 2 + 2i\nu$. Expanding (4.3.22) around $\nu = 0$, one can notice that the cotangent cancels all the odd terms of the hypergeometric functions. The analytic properties of (4.3.22) are more clear when writing it in the following equivalent form

$$\tilde{h}_{F\Delta,0} = \pi^4 \frac{\psi^{(1)}\left(\frac{\Delta}{4}\right) - \psi^{(1)}\left(\frac{\Delta}{4}-\frac{1}{2}\right)}{2-\Delta} + (\Delta \to 4-\Delta)\,, \tag{4.3.23}$$

where $\psi^{(1)}(x) = d\psi(x)/dx$ and $\psi(x)$ is the digamma function.

When $S \neq 0$, we can appeal to a similar computation made in [37]. In fact, the same integral of (4.3.21) appears in the study of the spectrum of the graph-building operator associated to the 2-magnon correlation function. The 2-magnon Hamiltonian is $\mathcal{H}_{\text{2-magnon}} = x_{34}^2/x_{12}^2\tilde{\mathcal{H}}_F$ but, when applied to the eigenstate Φ_{Δ,S,x_0}, that has in this case $\Delta_{\mathcal{O}_1} = \Delta_{\mathcal{O}_2} = 2$, it leads to an eigenvalue with the same integral representation as (4.3.21). The strategy to compute the eigenvalue is to write the following recursion relation for the integrals

$$\tilde{h}_{F\Delta,S} = \frac{1-S}{1+S}\,\tilde{h}_{F\Delta,S-2} + \frac{64\pi^4 S}{(S+1)[S^2-(\Delta-2)^2]^2}\,. \tag{4.3.24}$$

Solving the recurrence with the eigenvalue $\tilde{h}_{F\Delta,S=0}$, given by (4.3.23), as initial condition, we obtain

$$\tilde{h}_{F\Delta,S} = \pi^4 \frac{\psi^{(1)}\left(\frac{\Delta+S}{4}\right) - \psi^{(1)}\left(\frac{\Delta+S}{4}+\frac{1}{2}\right)}{(2-\Delta)(S+1)} + (\Delta \to 4-\Delta)\,. \tag{4.3.25}$$

We can conclude that the eigenvalue (4.3.19) is manifestly invariant under $\Delta \to 4-\Delta$, as expected from (4.2.21).

4.3.3 Spectrum of exchanged operators

In this section we will use the eigenvalues (4.3.14) and (4.3.19) to compute the scaling dimensions of the operators contributing to the correlation function (4.2.27) for $\mathcal{O}_1 = \mathcal{O}_2 = \phi_1$. The spectrum of the exchanged operators is defined by the solutions of the equation for the physical poles (4.2.25). Substituting in (4.2.25) the definition of bosonic and fermionic eigenvalues (4.3.14) and (4.3.19) and the constants χ_i computed in (4.3.11), we can rearrange the spectral equation in the following form

$$h_{B\Delta,S}{}^{-1} - (4\pi^2)^4\, c_B^2\, c_F^4\, \kappa^4\, \tilde{h}_{F\Delta,S}\, h_{B\Delta,S}{}^{-1} = (4\pi)^4\, \omega^4\,, \tag{4.3.26}$$

where we defined the new couplings

$$\kappa^4 = \xi_2^2 \xi_3^2\,, \qquad \text{and} \qquad \omega^4 = (\xi_2^2 - \xi_3^2)^2\,. \tag{4.3.27}$$

Plugging (4.3.14) and (4.3.25) into (4.3.26), we obtain the following spectral equation

$$\left(\tfrac{S^2}{4}+\nu^2\right)\!\left(\tfrac{(2+S)^2}{4}+\nu^2\right)\!\left[1+\frac{i\kappa^4}{2\nu(S+1)}\left(\psi^{(1)}\left(\frac{1}{2}\left(1+\tfrac{S}{2}-i\nu\right)\right)-\psi^{(1)}\left(\frac{1}{2}\left(2+\tfrac{S}{2}-i\nu\right)\right)+\right.\right.$$
$$\left.\left.+\,\psi^{(1)}\left(\frac{1}{2}\left(2+\tfrac{S}{2}+i\nu\right)\right)-\psi^{(1)}\left(\frac{1}{2}\left(1+\tfrac{S}{2}+i\nu\right)\right)\right)\right]=\omega^4, \tag{4.3.28}$$

with the additional constraint $\mathrm{Im}\,\nu < 0$. This equation can be studied perturbatively, for each individual anomalous dimension, expanding in ν around the value ν_0 corresponding to a bare dimension $\Delta_0 = 2 + 2i\nu_0$ at weak coupling, and in $1/\nu$ at strong coupling.

Weak coupling expansion: The small coupling limit suggests that the equation has solutions with bare dimensions $2+S$ and $4+S$, in analogy with the same quantity in the bi-scalar theory [36, 37]. There are six such solutions, but only half satisfies the physical requirement $\mathrm{Re}\,\Delta \geq 2$: one of them corresponds to the scaling dimensions of exchanged operator with bare dimension $\Delta_0 = 2 + S$ and two – to the scaling dimensions of operators with bare dimensions $\Delta_0 = 4 + S$. The remaining three solutions are related to the first ones b the transformation $\Delta \to 4 - \Delta$ and describe *shadow operators*, with $\mathrm{Re}\,\Delta < 2$. In addition to that, there is an infinite series of physical solutions around the bare dimensions $\Delta_0 = t + S$ with $t = 6, 8, \ldots$, due to the non algebraic eigenvalue $h_{F\Delta,S}$, similarly to the two-magnon case studied in [37]. For each value of the twist t there are two solutions; they describe the exchange of an infinite tower of local primary operators in the OPE of (4.3.5). Writing ν as a function of the two couplings (4.3.27) and expanding around the physical pole $\nu = -iS/2$ at weak coupling κ, $\omega \to 0$, we obtain the following expansion for the twist-two operator

$$\Delta^{(2)} = 2+S-\frac{2\omega^4}{S(S+1)}+\frac{2\omega^4}{3S^3(S+1)^3}\left[3(S(S-1)-1)\omega^4-6S(S+1)\kappa^4[2H_S^{(2)}-H_{S/2}^{(2)}]\right]+\ldots \tag{4.3.29}$$

and, around the physical pole $\nu = -i(S+2)/2$, the twist-four operators.

$$\begin{aligned}\Delta^{(4)} &= 4 + S + \frac{4\kappa^2}{\sqrt{(S+1)(S+2)}} + \frac{(S+2)\omega^4 - 8\kappa^4}{(S+1)(S+2)^2} + \\ &+ \frac{3\frac{\omega^8}{\kappa^2} - 48\frac{(6+S(S+6))}{(S+1)(S+2)}\kappa^2\omega^4 - 96\kappa^6\left[2H^{(2)}_{S+2} - H^{(2)}_{S/2} - \frac{12}{(S+2)^2}\right]}{24(S+1)^{3/2}(S+2)^{3/2}} + \dots \\ \Delta^{(4')} &= 4 + S - \frac{4\kappa^2}{\sqrt{(S+1)(S+2)}} + \frac{(S+2)\omega^4 - 8\kappa^4}{(S+1)(S+2)^2} + \\ &- \frac{3\frac{\omega^8}{\kappa^2} - 48\frac{(6+S(S+6))}{(S+1)(S+2)}\kappa^2\omega^4 - 96\kappa^6\left[2H^{(2)}_{S+2} - H^{(2)}_{S/2} - \frac{12}{(S+2)^2}\right]}{24(S+1)^{3/2}(S+2)^{3/2}} + \dots\end{aligned} \tag{4.3.30}$$

where $H^{(2)}_k$ are Harmonic numbers of order 2. Remarkably, the expressions in square brackets in (4.3.29), (4.3.30) are in fact rational numbers. In both cases, we present only the first few terms since the following ones are cumbersome. We notice that the weak coupling expansions of $\Delta^{(4)}$, $\Delta^{(4')}$ are divergent but, as it will be pointed out later in the analysis of Sec.4.3.5, the sum of the two corresponding OPE contributions has a well defined expansion[8]. Similar considerations can be made for the solutions at higher twist $t = \Delta_0 - S = 6, 8, \dots$

$$\Delta^{(t)}_{\pm} = t + S \pm \frac{4 i^{\frac{t}{2}}\kappa^2}{\sqrt{(S+1)(S+t-2)}} - \frac{(-1)^{\frac{t}{2}} 8\kappa^4}{(S+1)(S+t-2)^2} + \dots \,. \tag{4.3.31}$$

The twist-2 solution corresponds to the operator

$$\mathrm{Tr}\,[\phi_1\,\partial^S\phi_1] + \text{permutations}\,, \tag{4.3.32}$$

namely the traceless symmetric S-tensor obtained by insertion of light cone derivatives $\partial = n_\mu\partial^\mu$, $n^2 = 0$ into the operator $\mathrm{Tr}\,[\phi_1^2]$. At twist-4 the matter content of the theory allows to find several S-tensor operators satisfying the condition $\Delta_0 - S = 4$ and having the right $U(1)^{\otimes 3}$ quantum numbers (e.g. for $i = 1, j = 2$: $(2,0,0)$). Twist-4 operators start mixing with each other. We perform an introductory analysis of this phenomenon for the simple scalar case $S = 0$ in Appendix C.3. At this stage the log-CFT effects [105] due to chiral interaction vertices in (1.2.2) show up. The analysis suggests the presence at twist-4 of only two non-protected physical operators, which should be identified with the two solutions $\Delta^{(4)}$ and $\Delta^{(4')}$ at $S = 0$, in contrast to the bi-scalar fishnet CFT where only one type of twist-4 operators appears [36].Similar considerations apply to the higher twist operators $\Delta^{(t)}_{\pm}$. Indeed also for value of twist $t > 4$ it is possible to find several S-tensor primary operators with the correct set of Cartan's charges. The detailed study of these operators and their mixing would be an interesting insight in the structure of operator algebra of

[8] We are grateful to G. Korchemsky for the enlighting discussion about this point.

χCFT. We will restrict from here on most of our analysis to solution of twist two and four, whose contribution to the OPE expansion appears to be enough for complete description of the first non-trivial order of the weak coupling expansion, confirmed by direct computations in terms of Feynman diagrams.

Recalling the definition (4.3.27), the weak coupling expansion (4.3.29) for the twist-two operator goes in powers of ξ^4 of the original couplings which is exactly the expected behavior considering that the perturbative expansion in Fig.4.5 alternates bosonic and fermionic *wheels* attached to the diagrams with two quartic or four Yukawa single-trace vertices. On the contrary, the weak coupling expansions (4.3.30) for the twist-four operators go in power of ξ^2 of the original coupling. This fact can be understood looking at the expansion of (4.3.28) around the physical pole located at $\nu = -i(S+2)/2$. Indeed this expansion starts from $\kappa^4/(\nu + i(S+2)/2)^2$ and as a consequence the four-point correlation function (4.3.10) is convergent when $\nu \to -i(S+2)/2$ if κ is finite while it produces a divergence when we consider the weak coupling limit κ, $\omega \to 0$ such that $G_{\phi_1\phi_1} \sim \pm\kappa^2$.

The zero-spin case presents some peculiar behaviors. Indeed, expanding (4.3.28) for $S = 0$ around the physical poles $\nu = 0, -i$ at weak coupling, we obtain the following expansions for the solutions of (4.3.26)

$$\Delta^{(2)}\big|_{S=0} = 2 - 2i\omega + i\omega^2[\omega^4 - 6\kappa^4\zeta_3] + \frac{i}{4}\omega^2[7\omega^8 - 12\omega^4\kappa^4(3\zeta_3 + 5\zeta_5) + 108\kappa^8\zeta_3^2] + \dots$$

$$\Delta^{(4)}\big|_{S=0} = 4 + 2\sqrt{2}\kappa^2 + \frac{1}{2}[\omega^4 - 4\kappa^4] + \frac{16\kappa^6 - 48\kappa^2\omega^4 + \frac{\omega^8}{\kappa^2}}{16\sqrt{2}} + \dots \tag{4.3.33}$$

$$\Delta^{(4')}\big|_{S=0} = 4 - 2\sqrt{2}\kappa^2 + \frac{1}{2}[\omega^4 - 4\kappa^4] - \frac{16\kappa^6 - 48\kappa^2\omega^4 + \frac{\omega^8}{\kappa^2}}{16\sqrt{2}} + \dots \tag{4.3.34}$$

$$\Delta^{(t)}_{\pm}\big|_{S=0} = t \pm \frac{4i^{\frac{t}{2}}\kappa^2}{\sqrt{(t-2)}} - \frac{(-1)^{\frac{t}{2}}8\kappa^4}{(t-2)^2} + \dots \qquad t = 6, 4, 8 \dots \tag{4.3.35}$$

where the one-loop order of the scaling dimension $\Delta^{(2)}\big|_{S=0}$ is in agreement with the prediction (1.2.16). This twist-2 solution is the scaling dimension of the operator Tr $[\phi_1\phi_2^\dagger]$, while the two solutions of twist-4 arise from the operatorial mixing in a similar way as to $S = 0$ case analyzed in Appendix C.3.

Notice that the weak-coupling expansion of the twist-two operator is drastically different as compared to the $S \neq 0$ case, indeed it goes in powers of ξ^2. The same behavior was noticed in [37] and the reason is similar to the one explained above. We observe that, expanding around the physical pole $\nu = 0$, the spectral equation (4.3.28) goes as ω^4/ν^2. Then, when $\nu \to 0$, the correlation function (4.3.10) is convergent if μ is finite, but it produces a square-root divergence when we expand at weak coupling, as in the previous case. The fact that the weak-coupling and $S \to 0$ limits are not commutative is related to this divergence.

The divergence in the expansion of the scaling dimension of the twist-two operator is not a surprise. In fact, as noticed also in some different contexts in [36], in order to write the correlation function in the OPE form as in (4.2.27), we assumed that in the integral (4.2.24) no physical poles are located on the real ν-axes. However the poles that at weak coupling and when $S \neq 0$ are situated at $\nu = \mp iS/2$ pinch the integration contour at the origin when $S = 0$, thus producing a divergence. Hence, the contribution of the double-traces is needed in this case to produce a non-vanishing term that cancels this divergence at weak coupling. Again, we stress that at finite couplings the solutions of (4.3.28) are well-defined even at zero spin.

Strong coupling expansion: At strong coupling, $\kappa\,,\ \omega \to \infty$, we consider the four solutions of eq.(4.3.28) of lowest twist. The solutions are related to the physical poles of the spectral equation located at $\nu = e^{i\pi\frac{k}{2}}\sqrt[4]{\omega^4 + 2\kappa^4} + \dots$ with $k = 0, 1, 2, 3$ but only two of them satisfy the condition $\operatorname{Im}\nu < 0$, the remaining solutions being associated to the shadow operators. However we stress that we are neglecting all the infinite non-algebraic solutions of higher twist, purely generated by $h_{F\Delta,S}$. Then we have

$$\Delta_\infty = 2e^{i\pi\frac{k}{2}}\sqrt[4]{\omega^4 + 2\kappa^4} + 2 + \frac{[S(S+2)+2]\omega^4 + 2[S(S+2)-2]\kappa^4}{4e^{i\pi\frac{k}{2}}\left[\sqrt[4]{\omega^4 + 2\kappa^4}\,\right]^5} + \dots \quad (4.3.36)$$

Notice that, if all couplings scale as $\xi_j \sim \xi \gg 1$, the strong coupling expansion (4.3.36) is growing linearly with ξ. This becomes clear if one expands the eigenvalues appearing in (4.3.26). Indeed both of them decay at large ν as $h_{B\Delta,S}\,, \tilde{h}_{F\Delta,S} \sim\ 1/\nu^4$ then, since in the spectral equation the couplings appear in power of ξ^4, it is evident that the expansion will contain terms linear in ξ. The $S \to 0$ limit is not singular at strong coupling and one can compute $\Delta_\infty\big|_{S=0}$ directly from (4.3.36).

The spectrum of exchanged operators in reductions of χCFT In Sec.1.2.2, we presented the γ-deformed $\mathcal{N} = 4$ SYM theory in the double-scaling limit as a family of theories. In fact, playing with the three couplings ξ_j with $j = 1, 2, 3$ it is possible to describe different Lagrangians with different matter contents and symmetries. Thus we want to obtain the spectrum of exchanged operators for each theory of this family simply taking the limit on the couplings in the spectral equation (4.3.28) of the most general doubly-scaled theory. First of all, we recall the well-known result for the spectrum for the simplified Lagrangian (1.2.6) also known as $4D$ bi-scalar fishnet CFT. In this theory the only non-trivial four-point correlation function is $G_{\phi_1\phi_1}$, and it can be written in the same OPE form as the one we are considering as (4.2.27). By the Bethe-Salpeter method it is possible to compute the correlator at all-loops, since its perturbative expansion is generated only by a bosonic graph-building operator $\mathcal{H}_B$ of (4.3.7), then we can extract the non-perturbative scaling dimension of the exchanged operators in the OPE s-channel. The corresponding spectral equation is the same of (4.3.28) with $\omega^4 = \xi^4$ and $\kappa^4 = 0$ (indeed the bi-scalar theory has only one coupling ξ^2) and it has two solutions corresponding to the twist-two and -four

	limit	$\Delta^{(2)}$	$\Delta^{(4)}$	$\Delta^{(4')}$	$\Delta_\pm^{(t)}$
χ_0CFT	$\xi_1 \to 0$	$\Delta^{(2)}(\kappa,\omega)$	$\Delta^{(4)}(\kappa,\omega)$	$\Delta^{(4')}(\kappa,\omega)$	$\Delta_\pm^{(t)}(\kappa,\omega)$
	$\xi_2 \vee \xi_3 \to 0$	$\Delta_{\rm bi}^{(2)}(\xi_3^4 \vee \xi_2^4)$	$\Delta_{\rm bi}^{(4)}(\xi_3^4 \vee \xi_2^4)$		$t+S$
bi-scalar	$\xi_1 \wedge (\xi_2 \vee \xi_3) \to 0$	$\Delta_{\rm bi}^{(2)}(\xi_3^4 \vee \xi_2^4)$	$\Delta_{\rm bi}^{(4)}(\xi_3^4 \vee \xi_2^4)$		$t+S$
	$\xi_2 \wedge \xi_3 \to 0$	2+S	4+S		$t+S$
β-deformed	$\xi_1 = \xi_2 = \xi_3 = \xi$	2+S	$\Delta^{(4)}(\xi^4,0)$	$\Delta^{(4')}(\xi^4,0)$	$\Delta_\pm^{(t)}(\xi^4,0)$

Table 4.1: In this table we summarize the operator and dimension content of exchange operators in three reductions of χCFT.

operators with the following scaling dimensions

$$\begin{aligned}\Delta_{\rm bi}^{(2)}(\xi^4) &= 2+\sqrt{(S+1)^2+1-2\sqrt{(S+1)^2+4\xi^4}}\,,\\ \Delta_{\rm bi}^{(4)}(\xi^4) &= 2+\sqrt{(S+1)^2+1+2\sqrt{(S+1)^2+4\xi^4}}\,,\end{aligned} \tag{4.3.37}$$

together with two shadow solutions with $\Delta = 4-\Delta$ for $\mathrm{Re}\,\Delta < 2$. The analytic properties of those solution and their weak- and strong- coupling expansions have been studied in detail in [37].

The scaling dimensions of the exchanged operators in the correlation function $G_{\phi_1\phi_1}$ for theories defined as a reduction of χCFT as in Sec.1.2.2, can be computed as solutions of the spectral equation (4.3.28) in which we are applying some limits on the couplings, or even directly on the weak- and strong-coupling expansions. In the Tab.4.1 we present the summary of our results.

- χ_0CFT: since the spectrum of the exchanged operators for the four-point function $G_{\phi_1\phi_1}$ doesn't depend on ξ_1, the limit in which one of the couplings of the full χCFT is going to zero (reducing the theory to the χ_0CFT) is not unique. Indeed if we set $\xi_1 = 0$, the scaling dimensions of the exchanged operators in the χ_0CFT are the same of the full χCFT. On the contrary, if we set ξ_2 or ξ_3 to zero, the spectrum reduces to that of the bi-scalar theory (4.3.37) depending on a single coupling. Notice that in this case the number of solution of twist-four operators reduces to a single one, while the higher-twist operators get protected.

- bi-scalar theory: the reduction to bi-scalar theory corresponds to the limit in which two couplings of χCFT vanish. If one of the vanishing couplings is ξ_1, the spectrum is the usual one of the bi-scalar theory (4.3.37) while if $\xi_2 = \xi_3 = 0$ the operators are protected because the only remaining interaction vertex is not contributing.

- β-deformed theory: when all the couplings are equal we reduce the full theory to its β-deformation. In this case, due of the restoration of one super-symmetry, the operator of twist-two is protected as pointed out in [91] and confirmed by our computation (this reduction in terms of the new couplings κ and ω corresponds to $\kappa \to \xi$ and $\omega \to 0$). The symmetry doesn't constrain the operators of twist-four to be protected, as well as for higher twist $t > 4$. Indeed, their spectrum can be easily read applying the limit, for example at weak coupling, to the expansions (4.3.30),(4.3.31).

4.3.4 Structure constants of the exchanged operators

Once the spectrum of the exchanged operators is computed, in order to obtain the full set of conformal data for the four point function $G_{\phi_1\phi_1}$, one has to compute the OPE coefficients. From their definition (4.2.27), we get

$$C_{\Delta,S} = \frac{\pi}{c_B^4} \frac{(-1)^{S+1}}{c_2(\nu,S)\,\mathcal{R}_{\Delta,S}}\,, \tag{4.3.38}$$

where

$$\mathcal{R}_{\Delta,S} \;=\; \frac{d}{d\Delta}\left({h_{B\Delta,S}}^{-1} - \frac{\kappa^4}{\pi^4}\, \tilde{h}_{F\Delta,S}\, {h_{B\Delta,S}}^{-1} \right)\,. \tag{4.3.39}$$

Here c_2 is given in (4.2.13) and one puts $\Delta_{\mathcal{O}_1} = \Delta_{\mathcal{O}_2} = 1$. The eigenvalues $h_{B\Delta,S}$ and $\tilde{h}_{F\Delta,S}$ are presented in (4.3.14) and (4.3.25), and the constants $c_F = -2c_B = -1/(2\pi^2)$. Plugging these eigenvalues into (4.3.39) and performing the derivative, we obtain a rather cumbersome result that we will present in the next paragraph.

Weak coupling expansion Performing the derivative in (4.3.39) and substituting the weak coupling expansions of the scaling dimensions computed in (4.3.29) and (4.3.30), we obtain the following expansions for the structure constants associated to the exchanged operators for $S \neq 0$

$$\begin{aligned}
C_{\Delta^{(2)},S} &= \frac{S!^2}{(2S)!}\left(1+\frac{2\kappa^4[2H_S^{(2)}-H_{S/2}^{(2)}]-2\omega^4[\frac{1}{S(S+1)}+H_{S-1}-H_{2S-2}]}{S(S+1)}+\dots\right)\\
C_{\Delta^{(4)},S} &= \frac{(S+1)!^2}{\sqrt{(S+1)(S+2)}(2S+2)!}\left(-\frac{\kappa^2}{2}-\frac{\omega^4-8\kappa^4[\frac{9+S(11+3S)}{2(S+1)(S+2)}+H_{2S+2}-H_{S+1}]}{4\sqrt{(S+1)(S+2)}}+\dots\right)\\
C_{\Delta^{(4')},S} &= \frac{(S+1)!^2}{\sqrt{(S+1)(S+2)}(2S+2)!}\left(\frac{\kappa^2}{2}-\frac{\omega^4-8\kappa^4[\frac{9+S(11+3S)}{2(S+1)(S+2)}+H_{2S+2}-H_{S+1}]}{4\sqrt{(S+1)(S+2)}}+\dots\right)\\
C_{\Delta_\pm^{(t)},S} &= \frac{\pi\, i^t\, 2^{-2(t-4+S)}\Gamma\left(\frac{t}{2}-2\right)\Gamma\left(\frac{t}{2}-1+S\right)}{(t-2)(t+2S)\,\Gamma\left(\frac{t-3}{2}\right)\Gamma\left(\frac{t-1}{2}+S\right)}\kappa^4+\dots\,,
\end{aligned} \tag{4.3.40}$$

where $t = 6, 8, 10, \dots$ and H_k, $H_k^{(2)}$ are harmonic numbers. Again, the expressions in square brackets are in fact rational numbers. Similarly to the expansion of the scaling dimension, the OPE coefficient of the twist-two operator is singular for $S = 0$. Indeed, as discussed in Sec.4.3.3, due to the singularity arising at zero spin, the weak coupling and $S \to 0$ limits don't commute. In order to obtain the correct weak coupling expansion for the twist-two operator, one has to set $S = 0$ in (4.3.38) and then expand it in the coupling. The expansion the OPE coefficients of exchanged operators with spin $S = 0$ reads

$$\begin{aligned}
C_{\Delta^{(2)},0} =& 1 + 2i\omega^2 - 2[\omega^4 - 3\kappa^4\zeta_3] + i\omega^2[\omega^4(4\zeta_3 - 5) + 18\kappa^4\zeta_3] + \ldots \\
C_{\Delta^{(4)},0} =& -\frac{\kappa^2}{4\sqrt{2}} + \frac{22\kappa^4 - \omega^4}{16} - \frac{3[\frac{\omega^8}{\kappa^2} - 120\kappa^2\omega^4 + 912\kappa^6]}{256\sqrt{2}} + \ldots \\
C_{\Delta^{(4')},0} =& \frac{\kappa^2}{4\sqrt{2}} + \frac{22\kappa^4 - \omega^4}{16} + \frac{3[\frac{\omega^8}{\kappa^2} - 120\kappa^2\omega^4 + 912\kappa^6]}{256\sqrt{2}} + \ldots \\
C_{\Delta^{(t)}_{\pm},0} =& \frac{\pi\, i^t\, 2^{(8-2t)}\Gamma\left(\frac{t}{2} - 2\right)\Gamma\left(\frac{t}{2} - 1\right)}{(t-2)t\,\Gamma\left(\frac{t-3}{2}\right)\Gamma\left(\frac{t-1}{2}\right)}\kappa^4 + \ldots \qquad t = 6, 8, 10, \ldots .
\end{aligned} \tag{4.3.41}$$

In analogy with the spectrum analysis, the power counting shows that the twist-two operator goes in power of ξ^4 as expected if $S \neq 0$. In the $S = 0$ case it is going in powers of ξ^2, suggesting that the weak coupling expansion is sensitive to the double trace counterterms. Moreover in both cases (4.3.40) and (4.3.41), the twist-four OPE coefficients are suppressed by a factor of order ξ^2 as compared to those of the twist-2.

Strong coupling expansion Since we know from the expansion at strong coupling of the scaling dimension (4.3.36) that the scaling dimension becomes large, we can expand (4.3.38) in the limit $\Delta \to \infty$ and obtain

$$C_{\Delta,S} = \frac{2^{5-2\Delta}\,(S+1)}{\Delta}\tan\!\left(\pi\frac{\Delta - S}{2}\right)\left[1 + \frac{3}{2\Delta} + \frac{4(S+1)^2+25}{8\Delta^2} + \frac{36(S+1)^2+133}{16\Delta^3} + \mathcal{O}\!\left(\frac{1}{\Delta^4}\right)\right], \tag{4.3.42}$$

where we have to substitute Δ from the strong coupling spectrum Δ_∞ computed in (4.3.36) for low-twist operators. Naively, the expansion (4.3.42) looks the same as the one of the structure constant of the bi-scalar model [37], but actually it is not. Indeed, one can notice from the definition (4.3.38) that the OPE coefficient in our model depends explicitly on the coupling. Then in the expansion (4.3.42) some coefficients at higher order will start to depend on κ^4. The first contribution different from the bi-scalar expansion appear as κ^4/Δ^6 which, after the substitution Δ_∞, contributes at order $\mathcal{O}(1/\xi^2)$ in the inverse coupling expansion. Hence, it is convenient to write (4.3.42) as follows

$$\begin{aligned}
C_{\Delta_\infty,S} =& 2^5\frac{S+1}{2^{2\Delta_\infty}\Delta_\infty}\tan\!\left(\pi\frac{\Delta_\infty - S}{2}\right)\Bigg[1 + \frac{3}{4e^{i\pi k/2}(\omega^4 + 2\kappa^4)^{1/4}} + \\
&+ \left(\frac{4(S+1)^2+1}{32e^{i\pi k}(\omega^4 + 2\kappa^4)^{1/2}} - \frac{2(S+5)(2S+5)\kappa^4}{e^{i\pi k}(S+1)(\omega^4+2\kappa^4)^{3/2}}\right) + \ldots\Bigg],
\end{aligned} \tag{4.3.43}$$

where $k = 0, 1, 2, 3$ labels the four solutions of the spectral equation (4.3.28) and dots stand for higher orders in $1/\kappa$ and $1/\omega$. Thus, given the scaling dimension Δ_∞ (4.3.36), the OPE coefficient is exponentially small at strong coupling due to the factor $\frac{1}{2^{2\Delta_\infty}}$. The $S \to 0$ limit is not singular at strong coupling and one can compute $C_{\Delta_\infty,0}$ directly from (4.3.43).

4.3.5 Four-point correlation function

Once the conformal data in Secc.4.3.3 and 4.3.4 is computed, one can determine the four-point function (4.3.1) by means of (4.2.19). In the case $\mathcal{O}_1 = \mathcal{O}_2 = \phi_1$ we obtain

$$G_{\phi_1\phi_1}(x_1, x_2|x_3, x_4) = \frac{c_B^2}{x_{12}^2 x_{34}^2}\, \mathcal{G}_{\phi_1\phi_1}(u, v)\,, \tag{4.3.44}$$

with the cross-ratios defined as $u = x_{12}^2 x_{34}^2/(x_{13}^2 x_{24}^2)$ and $v = x_{14}^2 x_{23}^2/(x_{13}^2 x_{24}^2)$ and $\Delta_{\phi_1} = 1$. The function $\mathcal{G}_{\phi_1\phi_1}(u, v)$ can be written in terms of the OPE representation (4.2.27) as a sum over the non-negative integer Lorentz spin S and the states with scaling dimensions Δ. From the study of the spectrum of exchanged operators in Sec.4.3.3 it turns out that infinitely many operators are exchanged in the OPE channel. Then we have

$$\begin{aligned}\mathcal{G}_{\phi_1\phi_1}(u, v) =& \sum_{S=0}^{\infty} \left[C_{\Delta^{(2)},S}\, g_{\Delta^{(2)},S} + C_{\Delta^{(4)},S}\, g_{\Delta^{(4)},S} + C_{\Delta^{(4')},S}\, g_{\Delta^{(4')},S}\right] + \\ &+ \sum_{t=6,8,\ldots} \sum_{S=0}^{\infty} \left[C_{\Delta_+^{(t)},S}\, g_{\Delta_+^{(t)},S} + C_{\Delta_-^{(t)},S}\, g_{\Delta_-^{(t)},S}\right]\,,\end{aligned} \tag{4.3.45}$$

where the scaling dimensions $\Delta^{(i)}$ are defined by the spectral equation (4.3.28) and computed at weak coupling in (4.3.29), (4.3.30) and(4.3.31), and for low twist $t = 2, 4$ at strong coupling in (4.3.36). The structure constants $C_{\Delta^{(i)},S}$ associated to the exchanged operators are defined by (4.3.38) are computed at weak coupling in (4.3.40) and for low twist and strong coupling in (4.3.43). The four-dimensional conformal blocks $g_{\Delta,S}$ are defined in (4.2.18).

The proper definition of the four-point correlation function $G_{\phi_1\phi_1}$ takes into account the symmetrization $x_3 \leftrightarrow x_4$. Under this symmetry, the cross-ratios transform as $u \to u/v$ and $v \to 1/v$. Correspondingly, from the definition (4.2.18) the conformal blocks obey the symmetry $g_{\Delta,S}(u/v, 1/v) = (-1)^S g_{\Delta,S}(u, v)$. Combining together this relation with (4.3.45), it is easy to see that, imposing the symmetry $x_3 \leftrightarrow x_4$, the terms in (4.3.45) with odd S cancel out whereas those with even S get doubled.

Despite of the presence of singularities in the weak-coupling expansions of scaling dimensions and OPE coefficients, their combination in (4.3.45) is well defined. Indeed, plugging the conformal data into (4.3.45), we obtain an expansion in powers of the couplings that is compatible with the interpretation of the correlation function as a sum of Feynman diagrams in perturbation theory (see Sec.4.4 for an explicit example). In particular, since the first non-trivial order is fixed by the $S = 0$ conformal data, it is easy to write the very first contributions to $\mathcal{G}_{\phi_1\phi_1}$ in terms of the known functions, as follows

$$\mathcal{G}_{\phi_1\phi_1}(u, v) = u - i\kappa^2\, u\, \Phi^{(1)}(u, v) + \ldots\,. \tag{4.3.46}$$

where $\Phi^{(L)}$ is the ladder three-point function [189] that in the case $L = 1$ is given by the Bloch-Wigner dilogarithm function

$$\Phi^{(1)}(u,v) = \frac{1}{\theta}\left[2(\mathrm{Li}_2(-\rho u) + \mathrm{Li}_2(-\rho v)) + \log\frac{v}{u}\log\frac{1+\rho v}{1+\rho u} + \log\rho u\log\rho v + \frac{\pi^2}{3}\right], \tag{4.3.47}$$

with

$$\theta(u,v) \equiv \sqrt{(1-u-v)^2 - 4uv} \qquad \text{and} \qquad \rho(u,v) \equiv \frac{2}{1-u-v+\theta}. \tag{4.3.48}$$

4.4 Correlation functions at weak coupling from Feynman diagrams

In Sec.4.3 we have analyzed a four-point correlator computing the conformal data by means of the Bethe-Salpeter method. With this procedure we were able to diagonalize the graph-building operators and write exact equations for the spectrum of exchanged operators even though we ignored on the way the contribution of the double-trace interactions (1.2.7). The double-trace counterterms are necessary in the action to have a consistent description of the double-scaled theory (1.2.2) in the perturbative regime and in particular for the restoration of conformal symmetry.

In this section, we will study the weak coupling expansions of the four-point functions related to the operators (1.2.3) and clarify the role of the double-trace terms for this expansion. As we already mentioned, bosonic and fermionic wrappings in the related Feynman graphs develop UV divergences at short distances. Adding the double-trace vertices in the perturbative expansion we will be able to determine the conformal fixed points (1.2.13) canceling divergences generated by the single trace terms. However, they will not affect the finite coupling solutions computed in the section above.

The double-trace counterterms are given by the Lagrangian (1.2.7). In general, this action contains 9 terms but, due of the cylindric topology of Feynman diagrams for the observables we are computing. For any four-point function only one double-trace term is contributing generating a new local four-scalar vertex (see for instance Fig.4.4). This fact is crucial to ensure that conformal symmetry is restored. Indeed, in this case we know that the β-function can be written as (1.2.11) and it admits two fixed points $\alpha^2_{j\star}$ as in (1.2.13).

If we focus on the Feynman diagram expansion of the four point-functions we have to deal with divergent integrals. Then we have to introduce dimensional regularization setting $d = 4 - 2\epsilon$. One important observation is that the diagrams containing fermionic contributions produce the same divergence as the bosonic ones. In other words the fermionic kernels contains the divergent part of the bosonic one plus a remainder function that is finite in $d = 4$ which therefore does not require

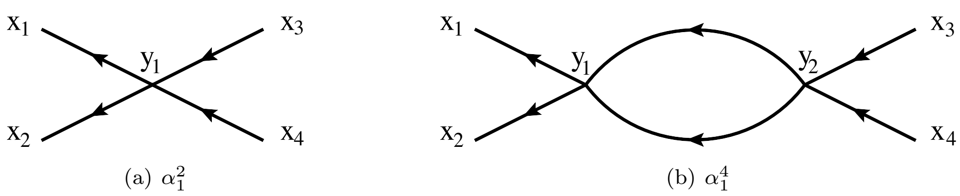

Figure 4.7: First two contributions of the double trace vertex $\mathrm{Tr}[\phi_1\phi_1]\mathrm{Tr}[\phi_1^\dagger\phi_1^\dagger]$ to the four-point functions $G_{\phi_1\phi_1}$.

regularization. Then the divergent operator can be written as

$$\begin{aligned}\left[\hat{\mathcal{V}}\ \Phi\right](x_1,x_2) =&2c_B^2\int\frac{d^{4-2\epsilon}y_1 d^{4-2\epsilon}y_2}{[(x_1-y_1)^2(x_2-y_2)^2]^{1-\epsilon}}\delta^{(4-2\epsilon)}(y_{12})\,\Phi(y_1,y_2)\\ \left[\hat{\mathcal{H}}_B\ \Phi\right](x_1,x_2) =&c_B^4\int\frac{d^{4-2\epsilon}y_1 d^{4-2\epsilon}y_2}{[(x_1-y_1)^2(x_2-y_2)^2y_{12}^4]^{1-\epsilon}}\,\Phi(y_1,y_2)\,,\end{aligned} \tag{4.4.1}$$

where $\Phi(x_1,x_2)$ is a test function.

Given the Hamiltonians (4.4.1) and the definition (4.2.2), the four-point correlation function is defined as follows

$$G(x_1,x_2|x_3,x_4)=\lim_{\epsilon\to0}\left(\frac{c_B}{x_{34}^2}\right)^{\Delta_{\mathcal{O}_1}+\Delta_{\mathcal{O}_2}-d}\langle x_1,x_2|\frac{\hat{\mathcal{H}}_B}{1-\chi^\star_{\mathcal{V}}\hat{\mathcal{V}}-\chi_B\hat{\mathcal{H}}_B-\chi_F\hat{\mathcal{H}}_F}|x_3,x_4\rangle\,, \tag{4.4.2}$$

where the effective coupling $\chi^\star_{\mathcal{V}}=\chi_{\mathcal{V}}|_{\alpha_j^2=\alpha_{j\star}^2}$, i.e. it is taken at the fixed point $\alpha_j^2=\alpha_{j\star}^2$. It is clear that for $\epsilon\neq0$ conformal symmetry is broken. However, expanding (4.4.2) at weak-coupling in terms of Feynman diagrams, one can demonstrate order-by-order how conformal symmetry is restored. In the following sections, we present some examples of this mechanism for the four-point correlation functions associated to the operators (1.2.3).

In Sec.4.3 we studied the contribution to the four-point function $G_{\phi_1\phi_1}$ of diagrams generated by the bosonic and fermionic Hamiltonians $\hat{\mathcal{H}}_B$ and $\hat{\mathcal{H}}_F$ but ignored the double-trace vertices, which works well for finite couplings. Since any diagram in Fig.4.5 (except for the trivial leading order diagram) is UV divergent, we will re-introduce in this section the double-trace counterterms in the perturbative expansion in order to make the weak-coupling expansion UV finite and to restore conformal symmetry.

Let us compute the first few orders of the weak coupling expansion of $G_{\phi_1\phi_1}$. In terms of Feynman diagrams, we have to compute the graphs given in Figg.4.5 and 4.7. Defining a function $G^{(a,b,c)}_{\phi_1\phi_1}$ where a counts the number of double-trace vertices, b the number of bosonic vertices (4.3.2) and c the number of fermionic vertices (4.3.3), we have

$$G_{\phi_1\phi_1}=G^{(0,0,0)}_{\phi_1\phi_1}+(4\pi)^2\alpha_1^2G^{(1,0,0)}_{\phi_1\phi_1}+(4\pi)^4[\alpha_1^4G^{(2,0,0)}_{\phi_1\phi_1}+(\xi_2^4+\xi_3^4)G^{(0,2,0)}_{\phi_1\phi_1}+\xi_2^2\xi_3^2G^{(0,0,4)}_{\phi_1\phi_1}]+\ldots\,. \tag{4.4.3}$$

The leading order $G^{(0,0,0)}_{\phi_1\phi_1}$ is already defined in (4.3.6), thus $G^{(0,0,0)}_{\phi_1\phi_1} = G^{(0)}_{\phi_1\phi_1}$. The first correction is given by the diagram in Fig.4.7(a). This contribution is finite and it can be written as follows

$$G^{(1,0,0)}_{\phi_1\phi_1} = \frac{2\pi^2 c_B^4}{x_{12}^2 x_{34}^2} u\Phi^{(1)}(u,v)\,, \tag{4.4.4}$$

where $\Phi^{(L)}$ is the ladder three-point function [189] that in the case $L = 1$ is given by the Bloch-Wigner dilogarithm function

$$\Phi^{(1)}(u,v) = \frac{1}{\theta}\left[2(\mathrm{Li}_2(-\rho u) + \mathrm{Li}_2(-\rho v)) + \log\frac{v}{u}\log\frac{1+\rho v}{1+\rho u} + \log\rho u \log\rho v + \frac{\pi^2}{3}\right]\,, \tag{4.4.5}$$

with

$$\theta(u,v) \equiv \sqrt{(1-u-v)^2 - 4uv} \qquad \text{and} \qquad \rho(u,v) \equiv \frac{2}{1-u-v+\theta}\,. \tag{4.4.6}$$

The cross-ratios are $u = x_{12}^2 x_{34}^2/(x_{13}^2 x_{24}^2)$ and $v = x_{14}^2 x_{23}^2/(x_{13}^2 x_{24}^2)$ and the constant $c_B = 1/(4\pi^2)$.

The bosonic part of the two-loop correction given by $G^{(2,0,0)}_{\phi_1\phi_1}$ and $G^{(0,2,0)}_{\phi_1\phi_1}$ comes from the diagrams in Figg.4.7(b), 4.5(b) and 4.5(c). The corresponding integrals are divergent and they need dimensional regularization, then we have

$$G^{(2,0,0)}_{\phi_1\phi_1} = 4c_B^6 \mathcal{I}(x_1,x_2|x_3,x_4)\,, \quad \text{and} \quad G^{(0,2,0)}_{\phi_1\phi_1} = c_B^6 \mathcal{I}(x_1,x_3|x_2,x_4)\,, \tag{4.4.7}$$

where we defined the short-hand notation

$$\mathcal{I}(x_1,x_2|x_3,x_4) = \int \frac{d^{4-2\epsilon}y_1 d^{4-2\epsilon}y_2}{[(x_1-y_1)^2(x_2-y_1)^2 y_{12}^4 (y_2-x_3)^2(y_2-x_4)^2]^{1-\epsilon}}\,. \tag{4.4.8}$$

This integral is UV divergent at short distances $y_{12}^2 \to 0$. By making use of the identity $1/(y_{12}^2)^{2-2\epsilon} = \pi^2\delta^{4-2\epsilon}(y_{12})/\epsilon + \mathcal{O}(\epsilon^0)$, one can compute the divergent part of the integral (4.4.8) that is proportional to the same one-loop function found in (4.4.4), as follows

$$\alpha_1^4 G^{(2,0,0)}_{\phi_1\phi_1} + (\xi_2^4 + \xi_3^4) G^{(0,2,0)}_{\phi_1\phi_1} = \frac{\pi^4 c_B^6}{x_{12}^2 x_{34}^2}\left(\frac{4\alpha_1^4 + \xi_2^4 + \xi_3^4}{\epsilon}\right) u\Phi^{(1)}(u,v) + \text{finite}\,, \tag{4.4.9}$$

where for the purpose of this section we are not interested in the finite part.

Let us finally consider the fermionic contribution $G^{(0,0,4)}_{\phi_1\phi_1}$. This term corresponds to the Feynman diagram in Fig.4.5(d) and its integral representation in four dimensions is given in the last line of (4.3.6). Since we are only interested in the computation of the UV divergent part of the diagram, we can avoid computing the whole integral (4.3.6) in dimensional regularization and proceed in a more naive way. Indeed, representing the integral as in the last line of (4.3.8) and considering that the fermionic Hamiltonian can be written as a combination of the bosonic one and some finite reminder function as in (4.3.16), we know that all the UV divergence is arising from $\mathcal{H}_B$. Then we can write

$$G^{(0,0,4)}_{\phi_1\phi_1} = -\frac{2\pi^4 c_B^6}{x_{12}^2 x_{34}^2}\,\frac{1}{\epsilon}\,u\,\Phi^{(1)}(u,v) + \text{finite}\,. \tag{4.4.10}$$

Combining this result with (4.4.9) and (4.4.4), we obtain that the expansion (4.4.3) takes the expected form (4.2.19) with the function $\mathcal{G}_{\phi_1\phi_1}(u,v)$ given by

$$\mathcal{G}_{\phi_1\phi_1}(u,v) = u + 2\alpha_1^2\,u\,\Phi^{(1)}(u,v) + \frac{4\alpha_1^4+\omega^4}{\epsilon}\,u\,\Phi^{(1)}(u,v) + \text{finite}(\kappa^4,\omega^4) + \dots\,, \tag{4.4.11}$$

where the new couplings κ and ω are defined in (4.3.27) and finite(κ^4,ω^4) stands for the finite part of $\mathcal{G}_{\phi_1\phi_1}$ at two-loop. Finally, imposing the UV finiteness of the correlation function we obtain the first order of the fixed point as follows

$$\alpha_{1\star}^2 = \pm\,i\,\frac{\omega^2}{2} + \dots\,, \tag{4.4.12}$$

and notice that it matches exactly the prediction given in (1.2.16). Replacing the double-trace coupling in (4.4.11) with its value[9] $\alpha_{1\star}^2 = -\,i\,\frac{\omega^2}{2}$ we obtain the one-loop expansion of the correlation function as follows

$$\mathcal{G}_{\phi_1\phi_1}(u,v) = u - i\omega^2\,u\,\Phi^{(1)}(u,v) + \dots\,. \tag{4.4.13}$$

This perfectly matches the same quantity computed via OPE, with conformal data fixed by the Bethe-Salpeter method (4.3.46).

4.5 Conclusions

This chapter represents an attempt of a deeper understanding of physical properties and analytic structure of the four-dimensional, three-coupling chiral CFT – the χCFT[10] – proposed in [32] as a double scaling limit of γ-deformed $\mathcal{N}=4$ SYM theory, combining the weak coupling with the strong imaginary γ-twist. We study here two aspects of this χCFT with three effective couplings, given by the Lagrangian (1.2.2): i) the explicit description of the Feynman graph content of the perturbative expansion, partially uncovering their integrability properties; ii) the exact computation, via conformal symmetry, of a four-point correlation functions of shortest protected scalar operators of the theory.

We managed to compute the four-point correlation functions of elementary fields ϕ_1 of the full three coupling χCFT, generalizing the bi-scalar fishnet CFT results of [36, 37]. As in these papers, we employed the Bethe-Salpeter method and the conformal symmetry to do the computations, but the procedure is more complicated

[9] This choice is coherent with the sign convention used in Sec.4.3.3.
[10] The name χCFT was suggested in [91].

and the corresponding analytic structures, both in coordinate and in the coupling spaces, are considerably richer, due to a more "dynamical" nature of the involved Feynman graphs. A new phenomenon presented in the correlators of the full theory is the non-perturbative behavior of certain individual OPE data – anomalous dimensions and structure constants of exchange operators, in the weak coupling limit. But the perturbative behavior of the four point correlator is restored in the sum over all OPE terms. The equations on the anomalous dimensions, obtained from the pole structure of integrands in spectral decomposition of these correlators, appear to have a few interesting singularities in the coupling space, whose physical significance for the theory is left to understand. We also demonstrate the relevance of the double-trace terms for the correct Feynman graph interpretation of our results obtained via Bethe-Salpeter conformally symmetric procedure.

To get a further insight to these interacting chiral CFTs, we have to compute more complicated correlation functions, involving the exchanged operators of higher R-charges, such as $\mathrm{tr}\phi_1^L$, or even more complicated multi-magnon operators. For the moment, only the exact anomalous dimensions of $L = 3$ case of such operators and of some related operators with the same R-charge have been computed for bi-scalar fishnet CFT in [39][11] via the double-scaling limit of the QSC equations. Similar results on $L = 4, 5$ and magnon operators will be reported in [147]. Not much is yet done in this direction for the full χCFT, apart from the Asymptotic Bethe Ansatz approach of [91] to long operators $L \gg 1$ and the one-loop study of [190], as well as the results of the current paper on the shortest exchange operators. As concerns the study of the structure constants, the first all-loop results for multi-magnon operators in bi-scalar fishnet CFT have been obtained in the very recent paper [191]. The generalization to four-point functions and to more complicated operators, and to the full χCFT, will necessitate a considerable new insight into integrability properties of these models.

The generalization of bi-scalar fishnet CFT to any dimension d [28] poses a natural question whether the D-dimensional generalization of the full 3-coupling χCFT exists. A related question: can we generalize the Basso-Dixon type fishnet integrals – the four-point single-trace correlators of scalar fields in bi-scalar CFT – explicitly computed in $d = 4$ [35] and $d = 2$ [29], to the case of dynamical fishnets of χCFT?

It would be also interesting to understand the behavior of large Feynman graphs in the full χCFT, in-line with the early results of [92] and the recent observations of [149] for the fishnet reduction of the χCFT. In particular, if the σ-model interpretation of the latter paper can be generalized to the full χCFT, it could be a big step in the explicit construction of the AdS dual of this chiral CFT, if such one exists at all after the double scaling limit of γ-deformed $\mathcal{N} = 4$ SYM theory.

As a final comment: it would be interesting to find a realization of these non-unitary theories in physical systems, if not in the fundamental quantum field theory

[11] In the sense that the exact Baxter equation, together with its quantization condition was obtained and studied perturbatively, to many loops, and numerically, to an arbitrary precision.

(at least as an effective theory) then maybe for certain non-equilibrium statistical-mechanical and condensed matter models. The beautiful mathematical structures behind the χCFT promises more of such applications in the future.

Acknowledgements

This thesis contains large part of the scientific contributions I have achieved during my doctoral studies. It is my duty to clarify here that such results are in a minor part due to my own abilities, while they are mostly the consequence of many great opportunities I have received from my teachers and collaborators.

First of all, I want to thank my supervisor Prof. Gleb Arutyunov for his teachings, his wise advice, and the long, honest and pressing scientific discussions always devoted to a deep and solid comprehension of the problems under study. I am infinitely grateful to Prof. Arutyunov for the large freedom he granted me, allowing me to work also on independent projects.

It is my pleasure to thank Prof. Vladimir Kazakov, for his will to work together on the fishnet theory, for the esteem he always showed to me, for having taught me his enthusiastic and intuitive approach to problems of theoretical physics. Thank you, Volodya, also for having introduced me to many amazing researchers.

My special thanks to Prof. Sergey Derkachov, for the long discussions and calls, for his numerous teachings and explanations and for the great availability to take into serious consideration any of my proposals or ideas. I greatly enjoyed working together and I hope there will be many other ideas to develop together.

Among the people I must thank, I want to specially mention the other co-authors of my papers, Dr. Rob Klabbers and Dr. Michelangelo Preti, for the precious time we spent together doing research and whipping each other in a muscovite banya.

Finally a special thank you to Dr. Sylvain Lacroix, Dr. Georgios Papathanasiou, Prof. Pedro Vieira, and all the people with whom I worked in the past and in the present and showed interest in my research. Your interest, your advice and demands, the task you set and the the ideas you share are a fuel for my enthusiasm. I deeply hope that the trust I have received will prove to be – at least partially – deserved.

Appendices

Appendix A
Details on the Ruijsenaars-Schneider model

A.1 Derivation of the Poisson structure

A.1.1 Lax matrix and its Poisson structure

Consider the following matrix function on the Heisenberg double

$$L = T^{-1}BT\,, \tag{A.1.1}$$

where T is the Frobenius solution of the factorisation problem (2.2.15). On the reduced space L turns into the Lax matrix of the hyperbolic RS model. For this reason we continue to call (A.1.1) the Lax matrix and below we compute the Poisson brackets between the entries of L considered as functions on the Heisenberg double. This will constitute the first step towards evaluation of the corresponding Dirac bracket.

The standard manipulations give

$$\begin{aligned}\{L_1, L_2\} &= \mathbb{T}_{12}L_1L_2 - L_1\mathbb{T}_{12}L_2 - L_2\mathbb{T}_{12}L_1 + L_1L_2\mathbb{T}_{12} \\ &\quad + T_1^{-1}T_2^{-1}\{B_1B_2\}T_1T_2 + \mathbb{B}_{21}L_2 - L_2\mathbb{B}_{21} - \mathbb{B}_{12}L_1 + L_1\mathbb{B}_{12}\,,\end{aligned} \tag{A.1.2}$$

where we defined the following quantities

$$\begin{aligned}\mathbb{T}_{12} &= T_1^{-1}T_2^{-1}\{T_1, T_2\}\,,\\ \mathbb{B}_{12} &= T_1^{-1}T_2^{-1}\{T_1, B_2\}T_2\,.\end{aligned}$$

By using (2.2.1), we get

$$T_1^{-1}T_2^{-1}\{B_1, B_2\}T_1T_2 = -\check{r}_-\,L_1L_2 - L_1L_2\check{r}_+ + L_1\check{r}_-L_2 + L_2\check{r}_+L_1\,.$$

Here we introduced the *dressed* r-matrices

$$\check{r}_\pm = T_1^{-1}T_2^{-1}r_\pm T_1T_2\,, \tag{A.1.3}$$

which have proved themselves to be a useful tool for the present calculation. The dressed r-matrices have essentially the same properties as their undressed counterparts, most importantly,

$$\check{r}_+ - \check{r}_- = C_{12}\,, \tag{A.1.4}$$

because C_{12} is an invariant element. Thus, for (A.1.2) we get

$$\begin{aligned}\{L_1, L_2\} &= (\mathbb{T}_{12} - \check{r}_-)L_1L_2 + L_1L_2(\mathbb{T}_{12} - \check{r}_+) + L_1(\check{r}_- - \mathbb{T}_{12})L_2 + L_2(\check{r}_+ - \mathbb{T}_{12})L_1 \\ &\quad + \mathbb{B}_{21}L_2 - L_2\mathbb{B}_{21} - \mathbb{B}_{12}L_1 + L_1\mathbb{B}_{12}\,. \end{aligned} \tag{A.1.5}$$

Now we proceed with evaluation of $\mathbb{T}$. Taking onto account that T satisfies (2.2.17), in components we have

$$\begin{aligned}\mathbb{T}_{ij,kl} &= T^{-1}_{ip}T^{-1}_{kq}\frac{\delta T_{pj}}{\delta A_{mn}}\frac{\delta T_{ql}}{\delta A_{rs}}\{A_{mn}, A_{rs}\} \\ &= \sum_{a\neq j}\sum_{b\neq l}\frac{1}{\mathcal{Q}_{ja}\mathcal{Q}_{lb}}(\delta_{ia}T_{nj}T^{-1}_{am} + \delta_{ij}T_{na}T^{-1}_{jm})(\delta_{kb}T_{sl}T^{-1}_{br} + \delta_{kl}T_{sb}T^{-1}_{lr})\{A_{mn}, A_{rs}\} \\ &= \sum_{a\neq j}\sum_{b\neq l}\frac{1}{\mathcal{Q}_{ja}\mathcal{Q}_{lb}}(\delta_{ia}\delta_{kb}\,\zeta_{aj,bl} + \delta_{ij}\delta_{kb}\,\zeta_{ja,bl} + \delta_{ia}\delta_{kl}\,\zeta_{aj,lb} + \delta_{ij}\delta_{kl}\,\zeta_{ja,lb})\,. \end{aligned} \tag{A.1.6}$$

Here $\mathcal{Q}_{ij} = \mathcal{Q}_i - \mathcal{Q}_j$ and we introduced the concise notation

$$\zeta_{12} = T_1^{-1}T_2^{-1}\{A_1, A_2\}T_1T_2\,.$$

Using (2.2.1) and the fact that $A = T\mathcal{Q}T^{-1}$, we find that

$$\zeta_{12} = -\check{r}_-\,\mathcal{Q}_1\mathcal{Q}_2 - \mathcal{Q}_1\mathcal{Q}_2\,\check{r}_+ + \mathcal{Q}_1\,\check{r}_-\mathcal{Q}_2 + \mathcal{Q}_2\,\check{r}_+\mathcal{Q}_1\,.$$

With the help of (A.1.4) we find in components

$$\zeta_{ij,kl} = -\mathcal{Q}_{ij}(\check{r}_{-ij,kl}\mathcal{Q}_{kl} + C_{ij,kl}\mathcal{Q}_k)\,,$$

where $C_{ij,kl} = \delta_{jk}\delta_{il}$ are the entries of C_{12}. Substitution of this tensor into (A.1.6) yields the following expression

$$\begin{aligned}\mathbb{T}_{ij,kl} &= \sum_{a\neq j}\sum_{b\neq l}\Big(- \delta_{ia}\delta_{kb}\check{r}_{-aj,bl} + \delta_{ij}\delta_{kb}\check{r}_{-ja,bl} + \delta_{ia}\delta_{kl}\check{r}_{-aj,lb} - \delta_{ij}\delta_{kl}\check{r}_{-ja,lb}\Big) \\ &\quad + \sum_{a\neq j}\sum_{b\neq l}\frac{1}{\mathcal{Q}_{lb}}\Big(\delta_{ia}\delta_{kb}C_{aj,bl}\mathcal{Q}_b - \delta_{ij}\delta_{kb}C_{ja,bl}\mathcal{Q}_b + \delta_{ia}\delta_{kl}C_{aj,lb}\mathcal{Q}_l - \delta_{ij}\delta_{kl}C_{ja,lb}\mathcal{Q}_l\Big)\,. \end{aligned}$$

In the first line the summation can be extended to all values of a and b, because the expression which is summed vanishes for $a = j$ and independently for $b = l$. For the same reason, we have extended the summation over a in the second line, where we also substitute the explicit value for $C_{ij,kl} = \delta_{jk}\delta_{il}$. In this way we find

$$\mathbb{T}_{ij,kl} = \sum_{ab}\Big(- \delta_{ia}\delta_{kb}\check{r}_{-aj,bl} + \delta_{ij}\delta_{kb}\check{r}_{-ja,bl} + \delta_{ia}\delta_{kl}\check{r}_{-aj,lb} - \delta_{ij}\delta_{kl}\check{r}_{-ja,lb}\Big)$$

$$+\sum_a \sum_{b\neq l} \frac{1}{\mathcal{Q}_{lb}}\Big(\delta_{ia}\delta_{kb}\delta_{al}\delta_{jb}\mathcal{Q}_b - \delta_{ij}\delta_{jl}\delta_{kb}\delta_{ab}\mathcal{Q}_b + \delta_{ia}\delta_{kl}\delta_{ab}\delta_{jl}\mathcal{Q}_l - \delta_{ij}\delta_{kl}\delta_{al}\delta_{jb}\mathcal{Q}_l\Big)\,.$$

This further yields the following expression

$$\begin{aligned}\mathbb{T}_{ij,kl} &= -\check{r}_{-ij,kl} + \delta_{ij}\sum_a \check{r}_{-ia,kl} + \delta_{kl}\sum_a \check{r}_{-ij,ka} - \delta_{ij}\delta_{kl}\sum_{ab}\check{r}_{-ia,kb} \\ &+ \sum_{b\neq l}\frac{1}{\mathcal{Q}_{lb}}\Big(\delta_{kb}\delta_{il}\delta_{jb}\mathcal{Q}_b - \delta_{ij}\delta_{jl}\delta_{kb}\mathcal{Q}_b + \delta_{kl}\delta_{ib}\delta_{jl}\mathcal{Q}_l - \delta_{ij}\delta_{kl}\delta_{jb}\mathcal{Q}_l\Big)\,.\end{aligned}$$

Here the second line can be written in the concise form as the matrix element $r_{\mathcal{Q}ij,kl}$ of the following matrix

$$r_{\mathcal{Q}} = \sum_{a\neq b}\frac{\mathcal{Q}_b}{\mathcal{Q}_{ab}}(E_{aa}-E_{ab})\otimes(E_{bb}-E_{ba}) \qquad \text{(A.1.7)}$$

Therefore,

$$\mathbb{T}_{ij,kl} = r_{\mathcal{Q}ij,kl} - \check{r}_{-ij,kl} + \delta_{ij}\sum_a \check{r}_{-ia,kl} + \delta_{kl}\sum_a \check{r}_{-ij,ka} - \delta_{ij}\delta_{kl}\sum_{ab}\check{r}_{-ia,kb}\,.$$

Hence,

$$\mathbb{T}_{12} = r_{\mathcal{Q}12} - \check{r}_{-12} + a_{12} + b_{12} - c_{12}\,. \qquad \text{(A.1.8)}$$

where we introduced three r-matrices, a, b and c with entries

$$a_{ij,kl} = \delta_{ij}\sum_a \check{r}_{-ia,kl}\,,\quad b_{ij,kl} = \delta_{kl}\sum_a \check{r}_{-ij,ka}\,,\quad c_{ij,kl} = \delta_{ij}\delta_{kl}\sum_{ab}\check{r}_{-ia,kb}\,. \text{(A.1.9)}$$

Needless to say, the bracket thus obtained is compatible with the Frobenius condition (2.2.17), which means that

$$\sum_a \mathbb{T}_{ia,kl} = 0\,,\qquad \sum_a \mathbb{T}_{ij,ka} = 0\,,$$

for any values of the free indices.

Now we turn our attention to $\mathbb{B}_{12}$, which in components reads as

$$\mathbb{B}_{ij,kl} = \sum_{a\neq j}\frac{1}{\mathcal{Q}_{ja}}(\delta_{ia}\eta_{aj,kl} + \delta_{ij}\eta_{ja,kl})\,,$$

where we introduced the notation

$$\eta_{12} = T_1^{-1}T_2^{-1}\{A_1, B_2\}T_1T_2\,.$$

With the help of (2.2.1) we get

$$\eta_{12} = -\check{r}_-\,\mathcal{Q}_1L_2 - \mathcal{Q}_1L_2\,\check{r}_- + \mathcal{Q}_1\,\check{r}_-L_2 + L_2\,\check{r}_+\mathcal{Q}_1\,,$$

and by using (A.1.4) obtain for components the following expression

$$\eta_{aj,kl} = \mathcal{Q}_{ja}(L_{ks}\check{r}_{-aj,sl} - \check{r}_{-aj,ks}L_{sl}) + L_{ks}C_{aj,sl}\mathcal{Q}_j\,.$$

With this expression at hand, we get

$$\begin{aligned}\mathbb{B}_{ij,kl} =& \sum_{a\neq j}\Big(\delta_{ia}(L_{ks}\check{r}_{-aj,sl} - \check{r}_{-aj,ks}L_{sl}) - \delta_{ij}(L_{ks}\check{r}_{-ja,sl} - \check{r}_{-ja,ks}L_{sl})\Big)\\ &+ L_{ks}\sum_{a\neq j}\frac{1}{\mathcal{Q}_{ja}}\Big(\delta_{ia}\delta_{al}\delta_{js}\mathcal{Q}_j + \delta_{ij}\delta_{jl}\delta_{as}\mathcal{Q}_a\Big)\,.\end{aligned}$$

Here the summation in the first line can be extended to include the term with $a = j$ because the latter vanishes. The second line can be conveniently written as a matrix element of some r-matrix. Namely,

$$\begin{aligned}\mathbb{B}_{ij,kl} =& L_{ks}\Big(\check{r}_{-ij,sl} - \delta_{ij}\sum_a \check{r}_{-ja,sl}\Big) - \Big(\check{r}_{-ij,ks} - \delta_{ij}\sum_a \check{r}_{-ja,ks}\Big)L_{sl}\\ &+ L_{ks}\sum_{a\neq b}\frac{\mathcal{Q}_b}{\mathcal{Q}_{ab}}(E_{aa} - E_{ab})_{ij}\otimes(E_{ba})_{sl}\,.\end{aligned}$$

In matrix form

$$\mathbb{B}_{12} = L_2(\check{r}_{-12} - a_{12}) - (\check{r}_{-12} - a_{12})L_2 + L_2 d_{12}\,, \qquad \text{(A.1.10)}$$

where a_{12} is the same matrix as in (A.1.8) and we introduced

$$d_{12} = \sum_{a\neq b}\frac{\mathcal{Q}_b}{\mathcal{Q}_{ab}}(E_{aa} - E_{ab})\otimes E_{ba}\,. \qquad \text{(A.1.11)}$$

We also need

$$\mathbb{B}_{21} = L_1(\check{r}_{-21} - a_{21}) - (\check{r}_{-21} - a_{21})L_1 + L_1 d_{21}\,,$$

Since $\check{r}_{-21} = -\check{r}_{+12}$, we have

$$\mathbb{B}_{21} = -L_1(\check{r}_{+12} + a_{21}) + (\check{r}_{+12} + a_{21})L_1 + L_1 d_{21}\,. \qquad \text{(A.1.12)}$$

Now everything is ready to obtain the bracket (A.1.5). Substituting in (A.1.5) expressions (A.1.8), (A.1.10) and (A.1.12), we conclude that (A.1.5) has the structure

$$\{L_1, L_2\} = k^+_{12}L_1L_2 + L_1L_2k^-_{12} + L_1s^-_{12}L_2 + L_2s^+_{12}L_1\,, \qquad \text{(A.1.13)}$$

where the coefficients are

$$\begin{aligned}k^+_{12} &= r_{\mathcal{Q}\,12} + C_{12} + (a_{21} + b_{12} - c_{12})\,,\\ k^-_{12} &= r_{\mathcal{Q}\,12} + d_{12} - d_{21} + (a_{21} + b_{12} - c_{12})\,,\\ s^+_{12} &= -r_{\mathcal{Q}\,12} - d_{12} - (a_{21} + b_{12} - c_{12})\,,\\ s^-_{12} &= -r_{\mathcal{Q}\,12} - C_{12} + d_{21} - (a_{21} + b_{12} - c_{12})\,.\end{aligned} \qquad \text{(A.1.14)}$$

First, we note that these coefficients satisfy

$$k^+ + k^- + s^+ + s^- = 0\,, \tag{A.1.15}$$

which guarantees that spectral invariants of L are in involution on the Heisenberg double. Second, in (A.1.14) the apparent dependence on the variable T occurs in the single combination $a_{21} + b_{12} - c_{12}$. To make further progress, consider

$$a_{21} = C_{12} a_{12} C_{12}\,,$$

as C_{12} acts as the permutation. We have, written in components,

$$\begin{aligned}(a_{21})_{ij,kl} &= C_{im,kn}(a_{12})_{mr,ns}C_{rj,sl} = \delta_{mk}\delta_{in}\Big(\delta_{mr}\sum_a \check{r}_{-ma,ns}\Big)\delta_{js}\delta_{rl} \\ &= \delta_{kl}\sum_a \check{r}_{-ka,ij} = -\delta_{kl}\sum_a \check{r}_{+ij,ka}\,.\end{aligned}$$

Therefore,

$$\begin{aligned}(a_{21}+b_{12})_{ij,kl} &= -\delta_{kl}\sum_a \check{r}_{+ij,ka} + \delta_{kl}\sum_a \check{r}_{-ij,ka} = -\delta_{kl}\sum_a C_{ij,ka} \\ &= -\sum_a \delta_{kl}\delta_{jk}\delta_{ia} = -\sum_{ab}(E_{ab})_{ij}\otimes(E_{bb})_{kl}\,.\end{aligned}$$

The dependence on T disappears and we find a simple answer

$$a_{21} + b_{12} = -\sum_{ab} E_{ab}\otimes E_{bb}\,. \tag{A.1.16}$$

The only T-dependence is in the coefficient c_{12}. This coefficient cannot be simplified or cancelled, so we leave it in the present form. Substituting in (A.1.14) the matrices (A.1.7), (A.1.11) and (A.1.16) and, performing necessary simplifications, we obtain our final result for the coefficients of the bracket (A.1.13)

$$\begin{aligned}k^+_{12} &= \sum_{a\neq b}\Big(\frac{\mathcal{Q}_b}{\mathcal{Q}_{ab}}E_{aa} - \frac{\mathcal{Q}_a}{\mathcal{Q}_{ab}}E_{ab}\Big)\otimes(E_{bb}-E_{ba}) - c_{12}\,,\\ k^-_{12} &= \sum_{a\neq b}\frac{\mathcal{Q}_a}{\mathcal{Q}_{ab}}E_{aa}\otimes E_{bb} - \sum_{a\neq b}\frac{\mathcal{Q}_a}{\mathcal{Q}_{ab}}E_{ab}\otimes E_{ba} - \mathbb{1}\otimes\mathbb{1} - c_{12}\,,\\ s^+_{12} &= -\sum_{a\neq b}\frac{\mathcal{Q}_a}{\mathcal{Q}_{ab}}(E_{aa}-E_{ab})\otimes E_{bb} + \mathbb{1}\otimes\mathbb{1} + c_{12}\,,\\ s^-_{12} &= -\sum_{a\neq b}\frac{\mathcal{Q}_b}{\mathcal{Q}_{ab}}E_{aa}\otimes(E_{bb}-E_{ba}) + c_{12}\,.\end{aligned} \tag{A.1.17}$$

In fact, the identity matrix $\mathbb{1}\otimes\mathbb{1}$ appearing in k^- and s^+ can be omitted as it cancels out in the expression (A.1.13). As was already mentioned, the only T-dependence left over is in the term c_{12}, namely,

$$(c_{12})_{ij,kl} = \delta_{ij}\delta_{kl}\sum_{ab}\check{r}_{-ia,kb} = \delta_{ij}\delta_{kl}T^{-1}_{im}T^{-1}_{kn}\sum_{ab} r_{-ma,nb}\,. \tag{A.1.18}$$

It is this term which violates the invariance of the bracket (A.1.13) under transformations from the Frobenius group.

To complete our discussion, we consider

$$(c_{21})_{ij,kl} = \delta_{ij}\delta_{kl} \sum_{ab} \check{r}_{-ka,ib} = -\delta_{ij}\delta_{kl} \sum_{ab} \check{r}_{+ia,kb} \,.$$

This gives

$$(c_{21} + c_{12})_{ij,kl} = -\delta_{ij}\delta_{kl} \sum_{ab} C_{ia,kb} = -\delta_{ij}\delta_{kl} \sum_{ab} \delta_{ib}\delta_{ka} = -\delta_{ij}\delta_{kl} = -(\mathbb{1} \otimes \mathbb{1})_{ij,kl} \,,$$

or in other words,

$$c_{21} + c_{12} = -\mathbb{1} \otimes \mathbb{1} \,. \tag{A.1.19}$$

Equation (A.1.19) leads to the following relations between the coefficients

$$k^+_{12} + k^+_{21} = C_{12} - 2\,(\mathbb{1} \otimes \mathbb{1}) \,, \qquad k^-_{12} + k^-_{21} = -C_{12} \,, \quad s^-_{12} = -s^+_{21} \,. \tag{A.1.20}$$

Notice that the fact that the right-hand side of the first two expressions is an invariant tensor. Relations (A.1.20) guarantee that the bracket (A.1.13) is skew-symmetric.

Following similar steps, we can derive the Poisson brackets involving other Frobenius invariants on the Heisenberg double, namely W_{ij} and P_i coordinates. Introducing the notations

$$r^{hg}_{\pm} = h_1^{-1} g_2^{-1} r_{\pm} h_1 g_2 \,, \qquad (c^{hg}_{12})_{ijkl} = \delta_{ij}\delta_{kl} \sum_{\alpha,\beta} (r^{hg}_{-})_{i\alpha k\beta} \,,$$

which, for Frobenius elements g, h satisfies

$$c^{hg}_{21} + c^{gh}_{12} \; = -\mathbb{1} \otimes \mathbb{1} \,,$$

we can write

$$\begin{aligned} \{W_1, W_2\} &= [r_{12}, W_1 W_2] + W_1\, c^{UT}_{12}\, W_2 + W_2\, c^{TU}_{12}\, W_1 - W_1 W_2\, c^{UU}_{12} - c^{TT}_{12}\, W_1 W_2 \\ \{W_1, P_2\} &= P_2[\bar{r}_{12}, W_1] + P_2 W_1 (c^{UT}_{12} - c^{UU}_{12}) + P_2 (c^{TU}_{12} - c^{TT}_{12}) W_1 \\ \{P_1, P_2\} &= P_1 P_2\, (c^{UT}_{12} + c^{TU}_{12} - c^{TT}_{12} - c^{UU}_{12}) \,, \end{aligned} \tag{A.1.21}$$

where matrices r_{12} and $\bar{r}_{12}$ are defined in (2.2.30). The c^{hg}-like terms in the brackets (A.1.21) are not Frobenius invariants, despite the arguments of the brackets are so, as it happens for (A.1.13). These terms disappear after imposing Dirac constraints in the reduced phase space, as it will explicitly shown for the LL-bracket in A.1.2.

A.1.2 Dirac bracket

Here we outline the construction of the Dirac bracket between the entries of the Lax matrix (A.1.1). We argue that the contribution to the Dirac bracket coming from the second class constraints has the same matrix structure as (A.1.13) and that this contribution precisely cancels all the terms c_{12} in (A.1.17), so that the resulting coefficients describing the Dirac bracket on the constraint surface are given by expressions (2.2.30) in the main text.

We start with the Poisson algebra of the non-abelian moment map

$$\{\mathcal{M}_1, \mathcal{M}_2\} = -r_+\mathcal{M}_1\mathcal{M}_2 - \mathcal{M}_1\mathcal{M}_2 r_- + \mathcal{M}_1 r_-\mathcal{M}_2 + \mathcal{M}_2 r_+\mathcal{M}_1 . \quad \text{(A.1.22)}$$

This is the Semenov-Tian-Shansky type bracket; it has N Casimir functions $\mathrm{Tr}(\mathcal{M}^k)$ with $k = 1, \dots, N$. On the constraint surface $\mathcal{S}$ the moment map is fixed to the following value

$$\mathcal{M} = \omega\mathbb{1} + \beta\mathbf{e}\otimes\mathbf{e}^{\tau} , \quad \text{(A.1.23)}$$

see (2.2.13). Substituting this expression into the right-hand side of (A.1.22) yields the following answer

$$\begin{aligned}\mathcal{M}_{ij,kl} \equiv \{\mathcal{M}_{ij}, \mathcal{M}_{kl}\}\Big|_{\mathcal{S}} = \beta\Big[&\big(\omega^{1-N} - \beta(i-\tfrac{1}{2})\big)\delta_{il} - \tfrac{\beta}{2}\delta_{jl} + \beta\,\Theta(l-j) \quad \text{(A.1.24)}\\ &- \big(\omega^{1-N} - \beta(j-\tfrac{1}{2})\big)\delta_{jk} + \tfrac{\beta}{2}\delta_{ik} - \beta\,\Theta(k-i)\Big] ,\end{aligned}$$

where Θ is the Heaviside step function

$$\Theta(j) = \begin{cases} 1, & j \geq 0 , \\ 0, & j < 0 \end{cases} . \quad \text{(A.1.25)}$$

For any $X \in \mathrm{Mat}(N, \mathbb{C})$ introduce the following quantities

$$\begin{aligned} t^{(0)}(X)_{ij} &= X_{ij} - \frac{1}{N}\sum_a X_{aj} - \frac{1}{N}\sum_a X_{ia} + \frac{1}{N^2}\sum_{ab} X_{ab} , \qquad i,j = 2,\dots,N,\\ t^{(1)}(X)_j &= \frac{1}{N^2}\sum_{ab} X_{ab} - \frac{1}{N}\sum_a X_{aj} , \qquad j = 2,\dots,N ,\\ t^{(2)}(X)_j &= \frac{1}{N^2}\sum_{ab} X_{ab} - \frac{1}{N}\sum_a X_{ja} , \qquad j = 2,\dots,N ,\\ t^{(3)}(X) &= \frac{1}{N^2}\sum_{ab} X_{ab} . \end{aligned} \quad \text{(A.1.26)}$$

From these quantities we construct the projectors $\pi^{(i)}$ that have the following action on X

$$\begin{aligned} \pi^{(0)}(X) &= \sum_{i,j=2}^{N} (E_{11} - E_{i1} - E_{1j} + E_{ij})\, t^{(0)}(X)_{ij} , \qquad & \pi^{(1)}(X) &= \sum_{j=2}^{N} a_j\, t^{(1)}(X)_j ,\\ \pi^{(2)}(X) &= \sum_{j=2}^{N} b_j\, t^{(2)}(X)_j , & \pi^{(3)}(X) &= \sum_{i,j=1}^{N} E_{ij}\, t^{(3)}(X) . \end{aligned} \quad \text{(A.1.27)}$$

where

$$a_j = \sum_{i=1}^{N}(E_{i1} - E_{ij}), \quad j = 2, \ldots, N,$$
$$b_j = \sum_{i=1}^{N}(E_{1i} - E_{ji}), \quad j = 2, \ldots, N.$$

In particular, $\pi^{(0)}$ projects on the Lie algebra of $\mathcal{F}$ and $\pi^{(3)}$ – on the one-dimensional dilatation subalgebra $\mathbb{C}^*$. The completeness condition is

$$X = \sum_{k=0}^{3} \pi^{(k)}(X).$$

From (A.1.24) it is readily seen that

$$\{t^{(3)}(\mathcal{M}), \mathcal{M}_{kl}\} = \frac{1}{N^2}\sum_{ab}\{\mathcal{M}_{ab}, \mathcal{M}_{kl}\} = 0.$$

Analogously, we find

$$\{t^{(0)}(M)_{ij}, \mathcal{M}_{kl}\} = \{\mathcal{M}_{ij} - \tfrac{1}{N}\textstyle\sum_a \mathcal{M}_{aj} - \tfrac{1}{N}\sum_a \mathcal{M}_{ia}, \mathcal{M}_{kl}\} = 0, \quad i, j = 2, \ldots, N.$$

Thus, projections $\pi^{(0)}(\mathcal{M})$ and $\pi^{(3)}(\mathcal{M})$ constitute $(N-1)^2 + 1 = N^2 - 2N + 2$ constraints of the first class. Projections $\pi^{(1)}$ and $\pi^{(2)}$ yield a non-degenerate matrix of Poisson brackets and, therefore, represent $2(N-1)$ constraints of the second class. This matrix should be inverted and used to define the corresponding Dirac bracket. Even simpler, the matrix (A.1.24) has rank $2(N-1)$ and we can use any non-degenerate submatrix of this rank to define the corresponding Dirac bracket.

Now we derive the Poisson relations between the moment map $\mathcal{M}$ and the Lax matrix given by (A.1.1). First, we compute

$$\begin{aligned}\{\mathcal{M}_{ij}, T_{kl}\} &= \frac{\delta T_{kl}}{\delta A_{rs}}\{\mathcal{M}_{ij}, A_{rs}\} = \\ &= -((r_+\mathcal{M}_1 - \mathcal{M}_1 r_-)T_2)_{ij,kl} + T_{kl}\sum_a (T_2^{-1}(r_+\mathcal{M}_1 - \mathcal{M}_1 r_-))_{ij,la}.\end{aligned} \tag{A.1.28}$$

Deriving this formula, we have used (2.2.7), as well as the fact that $T \in F$. Next, we obtain

$$\{\mathcal{M}_{ij}, L_{kl}\} = L_{kl}\sum_{sp}(T_{ls}^{-1} - T_{ks}^{-1})(r_+\mathcal{M}_1 - \mathcal{M}_1 r_-)_{ij,sp}. \tag{A.1.29}$$

It is clear that the diagonal entries from this expression of L commute with all the constraints: $\{\mathcal{M}_{ij}, L_{kk}\} = 0$, even without restricting to the constrained surface.

On the constrained surface where $\mathcal{M}$ is given by (A.1.23), we have

$$\{\mathcal{M}_{ij}, L_{kl}\}\Big|_{\mathcal{S}} = \omega^{1-N} L_{kl}(T_{lj}^{-1} - T_{kj}^{-1}) + \beta L_{kl}\sum_{sp}(T_{ls}^{-1} - T_{ks}^{-1})\Omega_{ijs}.$$

Here

$$\Omega_{ijs} \equiv \sum_p [r_+, (\mathbf{e}\otimes\mathbf{e}^t)_1]_{ij,sp} = -\tfrac{1}{2}\delta_{is} - (j-\tfrac{1}{2})\delta_{js} + \Theta(s-i)\,. \qquad \text{(A.1.30)}$$

From the explicit expression (A.1.30) and the fact that T is an element of the Frobenius group, we further deduce that

$$\{t^{(0)}(\mathcal{M})_{ij}, L_{kl}\}\Big|_{\mathcal{S}} = 0\,, \quad \{t^{(3)}(\mathcal{M})_{ij}, L_{kl}\}\Big|_{\mathcal{S}} = 0\,.$$

In other words, L commutes on the constraint surface with all constraints of the first class, independently on the value of T.

With the help of (A.1.30) we obtain

$$\{\mathcal{M}_{ij}, L_{kl}\}\Big|_{\mathcal{S}} = L_{kl}\Big[(\omega^{1-N} - \beta(j-\tfrac{1}{2}))(T^{-1}_{lj} - T^{-1}_{kj}) + \tfrac{\beta}{2}(T^{-1}_{li} - T^{-1}_{ki}) + \beta\sum_{s>i}(T^{-1}_{ls} - T^{-1}_{ks})\Big]\,.$$

Taking into account that

$$\sum_{s>i}^N (T^{-1}_{ls} - T^{-1}_{ks}) + \sum_{s<i}^N (T^{-1}_{ls} - T^{-1}_{ks}) + (T^{-1}_{li} - T^{-1}_{ki}) = 0\,,$$

we can write

$$\{\mathcal{M}_{ij}, L_{kl}\}\Big|_{\mathcal{S}} = L_{kl}\Big[(\omega^{1-N} - \beta(j-\tfrac{1}{2}))(T^{-1}_{lj} - T^{-1}_{kj}) + \tfrac{\beta}{2}\Big(\sum_{s>i}^N (T^{-1}_{ls} - T^{-1}_{ks}) - \sum_{s<i}^N (T^{-1}_{ls} - T^{-1}_{ks})\Big)\Big]\,.$$

Now we come to the Dirac bracket construction. By picking a non-degenerate submatrix Ψ of the matrix $\mathcal{M}_{ij,kl}$, we invert it and define the corresponding Dirac bracket

$$\{L_1, L_2\}_{\rm D} = \{L_1, L_2\} - \sum_{I,J=1}^{2N-2} \{L_1, \mathcal{M}_I\}\Psi^{-1}_{IJ}\{\mathcal{M}_J, L_2\}\,. \qquad \text{(A.1.31)}$$

Here $I = (ij)$ is a generalised index which we use to label matrix elements of $\mathcal{M}_{ij,kl}$ that comprise the non-degenerate matrix Ψ_{IJ}. To give an example, for $N = 3$ we can take as Ψ the following matrix

$$\Psi = \begin{pmatrix} \mathcal{M}_{11,11} & \mathcal{M}_{11,12} & \mathcal{M}_{11,13} & \mathcal{M}_{11,21} \\ \mathcal{M}_{12,11} & \mathcal{M}_{12,12} & \mathcal{M}_{12,13} & \mathcal{M}_{12,21} \\ \mathcal{M}_{13,11} & \mathcal{M}_{12,12} & \mathcal{M}_{13,13} & \mathcal{M}_{13,21} \\ \mathcal{M}_{21,11} & \mathcal{M}_{21,12} & \mathcal{M}_{21,13} & \mathcal{M}_{21,21} \end{pmatrix} = \beta \begin{pmatrix} 0 & -\omega-2\beta & -\omega-2\beta & -\omega-2\beta \\ \omega+2\beta & 0 & \frac{\beta}{2} & 0 \\ \omega+2\beta & -\frac{\beta}{2} & 0 & \omega+\frac{3}{2}\beta \\ \omega+2\beta & 0 & -\omega-\frac{3}{2}\beta & 0 \end{pmatrix}.$$

In particular $\det\Psi = \beta^4(\omega+\beta)^2(\omega+2\beta)^2$. Inverting Ψ, we find that

$$\sum_{I,J=1}^{2N-2} \{L_1, \mathcal{M}_I\}\Psi^{-1}_{IJ}\{\mathcal{M}_J, L_2\} = k^+_{\rm D12}L_1L_2 + L_1L_2k^-_{\rm D12} + L_1 s^-_{\rm D12}L_2 + L_2 s^+_{\rm D12}L_1\,,$$

that is, the contribution of the second class constraints has precisely the same structure as (A.1.13). Moreover, the corresponding coefficients are

$$k^+_{D12} = -c_{12}\,, \quad k^-_{D12} = -c_{12}\,, \quad s^+_{D12} = c_{12}\,, \quad s^-_{D12} = c_{12}\,, \tag{A.1.32}$$

where c_{12} is given by (A.1.18). Thus, in (A.1.31) all the terms c_{12} cancel out. We have also performed a similar computation for $N = 4, 5, 6, 7$ with the same result. An analytic derivation for arbitrary N is still missing, although our findings leave little doubt that it holds true.

In summary, on the reduced phase space the Dirac bracket between the components of the Lax matrix has the form (A.1.13) with the following coefficients

$$\begin{aligned} k^+_{12} &= \sum_{a\neq b}\Big(\frac{\mathcal{Q}_b}{\mathcal{Q}_{ab}}E_{aa} - \frac{\mathcal{Q}_a}{\mathcal{Q}_{ab}}E_{ab}\Big)\otimes(E_{bb}-E_{ba})\,,\\ k^-_{12} &= \sum_{a\neq b}\frac{\mathcal{Q}_a}{\mathcal{Q}_{ab}}E_{aa}\otimes E_{bb} - \sum_{a\neq b}\frac{\mathcal{Q}_a}{\mathcal{Q}_{ab}}E_{ab}\otimes E_{ba}\,,\\ s^+_{12} &= -\sum_{a\neq b}\frac{\mathcal{Q}_a}{\mathcal{Q}_{ab}}(E_{aa}-E_{ab})\otimes E_{bb}\,,\\ s^-_{12} &= -\sum_{a\neq b}\frac{\mathcal{Q}_b}{\mathcal{Q}_{ab}}E_{aa}\otimes(E_{bb}-E_{ba})\,. \end{aligned} \tag{A.1.33}$$

The coefficients have the following properties

$$k^\pm_{12} + k^\pm_{21} = \pm(C_{12} - \mathbb{1}\otimes\mathbb{1})\,, \quad s^-_{12} = -s^+_{21}\,, \tag{A.1.34}$$

which guarantee, in particular, skew-symmetry of (A.1.13). In addition, they satisfy the relation (A.1.15). In the main text we present the formula (A.1.13) in the r-matrix form (2.2.29) with the following identifications

$$k^+ = r\,, \quad s^+ = -\bar{r}\,, \quad k^- = -\underline{r}\,.$$

A.2 Derivation of the spectral-dependent r-matrices

To determine the r-matrices governing the structure (2.2.49), we start with computing the Poisson brackets between the components of $L(\lambda)$ given by (2.2.46). Applying the Poisson brackets (2.2.28) and (2.2.29), we obtain

$$\begin{aligned} \{L_1(\lambda), L_2(\mu)\} &= r_{12}L_1L_2 - L_1L_2\underline{r}_{12} + L_1\bar{r}_{21}L_2 - L_2\bar{r}_{12}L_1\\ &-\frac{1}{\lambda}\Big[\mathcal{Q}_1^{-1}r_{12}\mathcal{Q}_1L_1'L_2 - L_1'L_2(\mathcal{Q}_1^{-1}\underline{r}_{12}\mathcal{Q}_1 - \overline{C}_{12}) + L_1'\mathcal{Q}_1^{-1}\bar{r}_{21}\mathcal{Q}_1L_2 - L_2(\mathcal{Q}_1^{-1}\bar{r}_{12}\mathcal{Q}_1 + \overline{C}_{12})L_1'\Big]\\ &-\frac{1}{\mu}\Big[\mathcal{Q}_2^{-1}r_{12}\mathcal{Q}_2L_1L_2' - L_1L_2'(\mathcal{Q}_2^{-1}\underline{r}_{12}\mathcal{Q}_2 + \overline{C}_{12}) + L_1(\mathcal{Q}_2^{-1}\bar{r}_{21}\mathcal{Q}_2 + \overline{C}_{12})L_2' - L_2'\mathcal{Q}_2^{-1}\bar{r}_{12}\mathcal{Q}_2L_1\Big]\\ &+\frac{1}{\lambda\mu}\Big[\mathcal{Q}_1^{-1}\mathcal{Q}_2^{-1}r_{12}\mathcal{Q}_1\mathcal{Q}_2L_1'L_2' - L_1'L_2'\mathcal{Q}_1^{-1}\mathcal{Q}_2^{-1}\underline{r}_{12}\mathcal{Q}_1\mathcal{Q}_2\\ &\qquad + L_1'(\mathcal{Q}_1^{-1}\mathcal{Q}_2^{-1}\bar{r}_{21}\mathcal{Q}_1\mathcal{Q}_2 + \overline{C}_{12})L_2' - L_2'(\mathcal{Q}_1^{-1}\mathcal{Q}_2^{-1}\bar{r}_{12}\mathcal{Q}_1\mathcal{Q}_2 + \overline{C}_{12})L_1'\Big]\,. \end{aligned} \tag{A.2.1}$$

Further developments are based on the following observation about the properties of the r-matrices rotated by $\mathcal{Q}$'s. First, we find that

$$
\begin{aligned}
&\mathcal{Q}_1^{-1} r_{12} \mathcal{Q}_1 = r_{12} - \sigma_{12} - C_{12} + \mathbb{1} \otimes \mathbb{1}\,,\\
&\mathcal{Q}_2^{-1} r_{12} \mathcal{Q}_2 = r_{12} + \sigma_{21} + V_{12} - \mathbb{1} \otimes \mathbb{1}\,,\\
&\mathcal{Q}_1^{-1} \mathcal{Q}_2^{-1} r_{12} \mathcal{Q}_1 \mathcal{Q}_2 = r_{12} + \sigma_{21} - \sigma_{12}\,,
\end{aligned}
\tag{A.2.2}
$$

where σ_{12} is given by (2.2.50) and we introduced

$$
V_{12} = \sum_{i,j=1}^{N} \frac{\mathcal{Q}_i}{\mathcal{Q}_j} E_{ij} \otimes E_{ji}\,.
$$

Second,

$$
\begin{aligned}
&\mathcal{Q}_1^{-1} \underline{r}_{12} \mathcal{Q}_1 - \overline{C}_{12} = \underline{r}_{12} - C_{12}\,,\\
&\mathcal{Q}_2^{-1} \underline{r}_{12} \mathcal{Q}_2 + \overline{C}_{12} = \underline{r}_{12} + V_{12}\,,\\
&\mathcal{Q}_1^{-1} \mathcal{Q}_2^{-1} \underline{r}_{12} \mathcal{Q}_1 \mathcal{Q}_2 = \underline{r}_{12}\,.
\end{aligned}
\tag{A.2.3}
$$

Finally,

$$
\begin{aligned}
&\mathcal{Q}_1^{-1} \bar{r}_{12} \mathcal{Q}_1 + \overline{C}_{12} = \bar{r}_{12} - \sigma_{12} + \mathbb{1} \otimes \mathbb{1}\,,\\
&\mathcal{Q}_2^{-1} \bar{r}_{12} \mathcal{Q}_2 = \bar{r}_{12}\,,\\
&\mathcal{Q}_1^{-1} \mathcal{Q}_2^{-1} \bar{r}_{12} \mathcal{Q}_1 \mathcal{Q}_2 + \overline{C}_{12} = \bar{r}_{12} - \sigma_{12} + \mathbb{1} \otimes \mathbb{1}\,.
\end{aligned}
\tag{A.2.4}
$$

With the help of (A.2.2), (A.2.3) and (A.2.4) the bracket (A.2.1) turns into

$$
\begin{aligned}
\{L_1(\lambda), L_2(\mu)\} &= r_{12} L_1 L_2 - L_1 L_2 \underline{r}_{12} + L_1 \bar{r}_{21} L_2 - L_2 \bar{r}_{12} L_1\\
&- \frac{1}{\lambda}\Big[(r_{12} - \sigma_{12} - C_{12}) L_1' L_2 - L_1' L_2 (\underline{r}_{12} - C_{12}) + L_1' \bar{r}_{21} L_2 - L_2 (\bar{r}_{12} - \sigma_{12}) L_1'\Big]\\
&- \frac{1}{\mu}\Big[(r_{12} + \sigma_{21}) L_1 L_2' - L_1 L_2' \underline{r}_{12} + L_1 (\bar{r}_{21} - \sigma_{21}) L_2' - L_2' \bar{r}_{12} L_1\Big]\\
&+ \frac{1}{\lambda\mu}\Big[(r_{12} - \sigma_{12} + \sigma_{21}) L_1' L_2' - L_1' L_2' \underline{r}_{12}\\
&\qquad + L_1' (\bar{r}_{21} - \sigma_{21}) L_2' - L_2' (\bar{r}_{12} - \sigma_{12}) L_1'\Big]\,.
\end{aligned}
\tag{A.2.5}
$$

Notice that the element V_{12} totally decouples from from the right-hand side of (A.2.5), as it satisfies an identity

$$
V_{12} L_1 L_2' = L_1 L_2' V_{12}\,,
$$

which can be straightforwardly verified by computing its matrix elements,

$$
(V_{12} L_1 L_2')_{mn,kl} = \omega L_{ml} L_{kn} \mathcal{Q}_l \mathcal{Q}_k^{-1} = (L_1 L_2' V_{12})_{mn,kl}\,.
$$

The next progress relies on the identity (2.2.42), *i.e.*,

$$
L' = L - \frac{1 - \omega^N}{N} \mathbf{e} \otimes c^t L\,,
\tag{A.2.6}
$$

and the special (Frobenius) structure of the r-matrices. Indeed, from (A.2.6) it follows that

$$(E_{ii} - E_{ij})L' = (E_{ii} - E_{ij})L\,, \quad \forall\, i, j = 1\,, \dots, N\,.$$

This observation immediately shows that

$$\begin{aligned} \bar{r}_{12}L'_1 &= \bar{r}_{12}L_1\,, \quad & \bar{r}_{21}L'_2 &= \bar{r}_{21}L_2\,, \\ \sigma_{12}L'_1 &= \sigma_{12}L_1\,, \quad & \sigma_{21}L'_2 &= \sigma_{21}L_2\,. \end{aligned} \tag{A.2.7}$$

Analogously,

$$r_{12}L'_2 = r_{12}L_2\,, \qquad r_{21}L'_1 = r_{21}L_1\,. \tag{A.2.8}$$

Owing to the identity (2.2.35), we then have

$$r_{12}(L'_1 - L_1) = (-r_{21} + C_{12} - \mathbb{1}\otimes\mathbb{1})(L'_1 - L_1) = (C_{12} - \mathbb{1}\otimes\mathbb{1})(L'_1 - L_1)\,,$$

or, in other words,

$$r_{12}L'_1 = (C_{12} - \mathbb{1}\otimes\mathbb{1})L'_1 + (r_{12} - C_{12} + \mathbb{1}\otimes\mathbb{1})L_1\,. \tag{A.2.9}$$

Thus, to obtain an irreducible expression for the bracket (A.2.5), whenever its is possible we will use the reduction formulae (A.2.7), (A.2.8) and (A.2.9) to replace L' with L on the right-hand side of (A.2.5). This replacement leads to the following result

$$\begin{aligned} &\{L_1(\lambda), L_2(\mu)\} = \\ &= \Big(r_{12} - \frac{1}{\lambda}(r_{12} - \sigma_{12} - C_{12} + \mathbb{1}\otimes\mathbb{1}) - \frac{1}{\mu}(r_{12} + \sigma_{21}) + \frac{1}{\lambda\mu}(r_{12} - C_{12} + \mathbb{1}\otimes\mathbb{1})\Big)L_1L_2 \\ &- L_1L_2\underline{r}_{12} + \frac{1}{\lambda}L'_1L_2\underline{r}_{12} + \frac{1}{\mu}L_1L'_2\underline{r}_{12} - \frac{1}{\lambda\mu}L'_1L'_2\underline{r}_{12} \\ &+ L_1\Big(\bar{r}_{21} - \frac{1}{\mu}(\bar{r}_{21} - \sigma_{21})\Big)L_2 - L_2\Big(\bar{r}_{12} - \frac{1}{\lambda}(\bar{r}_{12} - \sigma_{12})\Big)L_1 \\ &- \frac{1}{\lambda}L'_1\Big(\bar{r}_{21} - \frac{1}{\mu}(\bar{r}_{21} - \sigma_{21})\Big)L_2 + \frac{1}{\mu}L'_2\Big(\bar{r}_{12} - \frac{1}{\lambda}(\bar{r}_{12} - \sigma_{12})\Big)L_1 \\ &+ \frac{1}{\lambda}\Big(\mathbb{1}\otimes\mathbb{1} + \frac{1}{\mu}(C_{12} + \sigma_{21} - \mathbb{1}\otimes\mathbb{1})\Big)L'_1L_2 - \frac{1}{\lambda}\Big(C_{12} + \frac{1}{\mu}\sigma_{12}\Big)L_1L'_2\,. \end{aligned} \tag{A.2.10}$$

We will now search for the spectral dependent r-matrices r^s that allow one to present the bracket above in the form

$$\begin{aligned} \{L_1(\lambda), L_2(\mu)\} = {}& r^s_{12}L_1(\lambda)L_2(\mu) - L_1(\lambda)L_2(\mu)\underline{r}^s_{12} \\ &+ L_1(\lambda)\bar{r}^s_{21}L_2(\mu) - L_2(\mu)\bar{r}^s_{12}L_1(\lambda)\,. \end{aligned} \tag{A.2.11}$$

An examination of this expression shows that it involves the following matrices r_{12}, $\bar{r}_{12}$, $\bar{r}_{21}$, σ_{12}, σ_{21} and C_{12}. There is also the identity matrix $\mathbb{1}\otimes\mathbb{1}$ but we ignore its presence for the moment. Thus, the structure of (A.2.10) motivates to try for the spectral-dependent r-matrices the following minimal ansatz

$$\begin{aligned} r^s_{12} &= r_{12} + \alpha\sigma_{12} + \beta\sigma_{21} + \delta C_{12} \\ \bar{r}^s_{12} &= \bar{r}_{12} + \delta_{12}\sigma_{12}\,, \\ \bar{r}^s_{21} &= \bar{r}_{21} + \delta_{21}\sigma_{21}\,, \\ \underline{r}^s_{12} &= \underline{r}_{12} + \delta C_{12}\,. \end{aligned}$$

This ansatz depends on five undermined parameters: $\alpha, \beta, \delta, \delta_{12}$ and δ_{21}, which should eventually be expressed via λ and μ. We then plug this ansatz together with the expression (2.2.46) for the spectral-dependent Lax matrix into (A.2.11) and, by using the reduction formulae (A.2.7), (A.2.8) and (A.2.9), bring the resulting expression to the following irreducible form

$$\begin{aligned} &\{L_1(\lambda), L_2(\mu)\} = \\ &= \Big[r_{12} + \alpha\sigma_{12} + \beta\sigma_{21} - \frac{1}{\lambda}(r_{12} - C_{12} + \mathbb{1}\otimes\mathbb{1} + \alpha\sigma_{12}) \\ &\qquad\qquad - \frac{1}{\mu}(r_{12} + \beta\sigma_{21}) + \frac{1}{\lambda\mu}(r_{12} - C_{12} + \mathbb{1}\otimes\mathbb{1})\Big] L_1 L_2 \\ &- L_1 L_2 \underline{r}_{12} + \frac{1}{\lambda} L'_1 L_2 \underline{r}_{12} + \frac{1}{\mu} L_1 L'_2 \underline{r}_{12} - \frac{1}{\lambda\mu} L'_1 L'_2 \underline{r}_{12} \\ &+ L_1\Big[(\bar{r}_{21} + \delta_{21}\sigma_{21}) - \frac{1}{\mu}(\bar{r}_{21} + \delta_{21}\sigma_{21})\Big] L_2 - L_2\Big[(\bar{r}_{12} + \delta_{12}\sigma_{12}) - \frac{1}{\lambda}(\bar{r}_{12} + \delta_{12}\sigma_{12})\Big] L_1 \\ &- \frac{1}{\lambda} L'_1\Big[(\bar{r}_{21} + \delta_{21}\sigma_{21}) - \frac{1}{\mu}(\bar{r}_{21} + \delta_{21}\sigma_{21})\Big] L_2 + \frac{1}{\mu} L'_2\Big[(\bar{r}_{12} + \delta_{12}\sigma_{12}) - \frac{1}{\lambda}(\bar{r}_{12} + \delta_{12}\sigma_{12})\Big] L_1 \\ &+ \Big[- \frac{1}{\lambda}(C_{12} - \mathbb{1}\otimes\mathbb{1} + \beta\sigma_{21} + \delta C_{12}) + \frac{1}{\mu}\delta C_{12} + \frac{1}{\lambda\mu}(C_{12} + \beta\sigma_{21} - \mathbb{1}\otimes\mathbb{1})\Big] L'_1 L_2 \\ &+ \Big[\frac{1}{\lambda}\delta C_{12} - \frac{1}{\mu}(\alpha\sigma_{12} + \delta C_{12}) + \frac{1}{\lambda\mu}\alpha\sigma_{12}\Big] L_1 L'_2\,. \end{aligned} \tag{A.2.12}$$

Comparison of the first lines of (A.2.10) and (A.2.12) yields a unique solution for α and β,

$$\alpha = \frac{1}{\lambda - 1}\,, \qquad \beta = -\frac{1}{\mu - 1}\,.$$

Comparison of third lines yields

$$\delta_{12} = \frac{1}{\lambda - 1}\,, \qquad \delta_{21} = \frac{1}{\mu - 1}\,,$$

which automatically makes the fourth lines of (A.2.10) and (A.2.12) equal. Finally, with α and β already determined, comparison of the terms in front of $L'_1 L_2$ or $L_1 L'_2$ gives an unambiguous solution for δ,

$$\delta = \frac{\mu}{\lambda - \mu}\,.$$

Thus, we end up with the following expressions for the spectral-dependent r-matrices realising the Poisson algebra (A.2.11)

$$\begin{aligned} r_{12}(\lambda,\mu) &= \frac{\lambda r_{12}+\mu r_{21}}{\lambda-\mu} + \frac{\sigma_{12}}{\lambda-1} - \frac{\sigma_{21}}{\mu-1} + \frac{\mu}{\lambda-\mu}\mathbb{1}\otimes\mathbb{1}\,, \\ \bar{r}_{12}(\lambda) &= \bar{r}_{12} + \frac{\sigma_{12}}{\lambda-1}\,, \\ \underline{r}_{12}(\lambda,\mu) &= r_{12}(\lambda,\mu) + \bar{r}_{21}(\mu) - \bar{r}_{12}(\lambda) = \frac{\lambda \underline{r}_{12}+\mu \underline{r}_{21}}{\lambda-\mu} + \frac{\mu}{\lambda-\mu}\mathbb{1}\otimes\mathbb{1}\,, \end{aligned} \tag{A.2.13}$$

where we used the relation (2.2.35) to bring the result to a more symmetric form. Finally, using the shift symmetry (2.2.57), we can omit in (A.2.13) the terms proportional to the identity matrix, obtaining a slightly simpler solution (2.2.51).

A.3 Poisson structures for the spin hyperbolic RS model

The Ruijsenaars-Schneider model with spins and hyperbolic potential has been realized as an Hamiltonian system for the first time by O.Chalykh and M.Fairon [48] providing an explicit Poisson bracket for the invariant spin variables. According to these Poisson brackets the $GL(\ell,\mathbb{C})$-invariant combinations of spins $f_{ij} = \mathbf{a}_{i\alpha}\mathbf{c}_j^\alpha$ (also called collective spins) satisfy the conjecture of [69]

$$\begin{aligned} \{f_{ij},f_{kl}\} &= \left(\frac{\mathcal{Q}_i+\mathcal{Q}_k}{\mathcal{Q}_i-\mathcal{Q}_k} + \frac{\mathcal{Q}_j+\mathcal{Q}_l}{\mathcal{Q}_j-\mathcal{Q}_l} + \frac{\mathcal{Q}_k+\mathcal{Q}_j}{\mathcal{Q}_k-\mathcal{Q}_j} + \frac{\mathcal{Q}_l+\mathcal{Q}_i}{\mathcal{Q}_l-\mathcal{Q}_i}\right) f_{ij}f_{kl} \\ &+ \left(\frac{\mathcal{Q}_i+\mathcal{Q}_k}{\mathcal{Q}_i-\mathcal{Q}_k} + \frac{\mathcal{Q}_j+\mathcal{Q}_l}{\mathcal{Q}_j-\mathcal{Q}_l} + \frac{\mathcal{Q}_k+\omega\mathcal{Q}_j}{\mathcal{Q}_k-\omega\mathcal{Q}_j} - \frac{\mathcal{Q}_i+\omega\mathcal{Q}_l}{\mathcal{Q}_i-\omega\mathcal{Q}_l}\right) f_{il}f_{kj} \\ &+ \left(\frac{\mathcal{Q}_k+\mathcal{Q}_i}{\mathcal{Q}_k-\mathcal{Q}_i} + \frac{\mathcal{Q}_i+\omega\mathcal{Q}_l}{\mathcal{Q}_i-\omega\mathcal{Q}_l}\right) f_{ij}f_{il} + \left(\frac{\mathcal{Q}_j+\mathcal{Q}_k}{\mathcal{Q}_j-\mathcal{Q}_k} - \frac{\mathcal{Q}_j+\omega\mathcal{Q}_l}{\mathcal{Q}_j-\omega\mathcal{Q}_l}\right) f_{ij}f_{jl} \\ &+ \left(\frac{\mathcal{Q}_k+\mathcal{Q}_i}{\mathcal{Q}_k-\mathcal{Q}_i} - \frac{\mathcal{Q}_k+\omega\mathcal{Q}_j}{\mathcal{Q}_k-\omega\mathcal{Q}_j}\right) f_{kj}f_{kl} + \left(\frac{\mathcal{Q}_i+\mathcal{Q}_l}{\mathcal{Q}_i-\mathcal{Q}_l} + \frac{\mathcal{Q}_l+\omega\mathcal{Q}_j}{\mathcal{Q}_l-\omega\mathcal{Q}_j}\right) f_{lj}f_{kl}\,. \end{aligned} \tag{A.3.1}$$

The Poisson brackets between invariant spins which realize (A.3.1) is given in components in [48] as

$$\begin{aligned} \{\mathbf{a}_{i\alpha},\mathbf{a}_{j\beta}\} &= \frac{1}{2}\delta_{i\neq j}\frac{\mathcal{Q}_i+\mathcal{Q}_j}{\mathcal{Q}_i-\mathcal{Q}_j}(\mathbf{a}_{i\alpha}\mathbf{a}_{j\beta}+\mathbf{a}_{j\alpha}\mathbf{a}_{i\beta}-\mathbf{a}_{i\alpha}\mathbf{a}_{i\beta}-\mathbf{a}_{j\alpha}\mathbf{a}_{j\beta}) + \frac{1}{2}\epsilon(\beta,\alpha)(\mathbf{a}_{i\alpha}\mathbf{a}_{j\beta}+\mathbf{a}_{j\alpha}\mathbf{a}_{i\beta}) \\ &+ \frac{1}{2}\mathbf{a}_{j\beta}\sum_{\gamma=1}^{\ell}\epsilon(\alpha,\gamma)(\mathbf{a}_{j\alpha}\mathbf{a}_{i\gamma}+\mathbf{a}_{i\alpha}\mathbf{a}_{j\gamma}) - \frac{1}{2}\mathbf{a}_{i\alpha}\sum_{\gamma=1}^{\ell}\epsilon(\beta,\gamma)(\mathbf{a}_{i\beta}\mathbf{a}_{j\gamma}+\mathbf{a}_{j\beta}\mathbf{a}_{i\gamma})\,, \\ \{\mathbf{a}_{i\alpha},\mathbf{c}_{\beta j}\} &= \mathbf{a}_{i\alpha}Z_{ij} - \delta_{\alpha\beta}Z_{ij} - \frac{1}{2}\delta_{i\neq j}\frac{\mathcal{Q}_i+\mathcal{Q}_j}{\mathcal{Q}_i-\mathcal{Q}_j}(\mathbf{a}_{i\alpha}-\mathbf{a}_{j\alpha})\mathbf{c}_{\beta j} + \mathbf{a}_{i\alpha}\sum_{\gamma=1}^{\beta-1}\mathbf{a}_{i\gamma}(\mathbf{c}_{\gamma j}-\mathbf{c}_{\beta j}) + \\ &- \delta_{\alpha\beta}\sum_{\gamma=1}^{\beta-1}\mathbf{a}_{i\gamma}\mathbf{c}_{\gamma j} - \frac{1}{2}\mathbf{c}_{\beta j}\sum_{\gamma=1}^{\ell}\epsilon(\alpha,\gamma)(\mathbf{a}_{i\gamma}\mathbf{a}_{j\alpha}+\mathbf{a}_{j\gamma}\mathbf{a}_{i\alpha}) + \delta_{\alpha<\beta}\mathbf{a}_{i\alpha}\mathbf{c}_{\beta j}\,, \\ \{\mathbf{c}_{\alpha i},\mathbf{c}_{\beta j}\} &= \frac{1}{2}\delta_{i\neq j}\frac{\mathcal{Q}_i+\mathcal{Q}_j}{\mathcal{Q}_i-\mathcal{Q}_j}(\mathbf{c}_{\alpha i}\mathbf{c}_{\beta j}+\mathbf{c}_{\alpha j}\mathbf{c}_{\beta i}) - \mathbf{c}_{\alpha i}Z_{ij} + \mathbf{c}_{\beta j}Z_{ji} + \frac{1}{2}\epsilon(\beta,\alpha)(\mathbf{c}_{\alpha i}\mathbf{c}_{\beta j}-\mathbf{c}_{\alpha j}\mathbf{c}_{\beta i}) \end{aligned}$$

$$- \mathbf{c}_{\alpha i} \sum_{\gamma=1}^{\beta-1} \mathbf{a}_{i\gamma}(\mathbf{c}_{\gamma j} - \mathbf{a}_{i\gamma}\mathbf{c}_{\beta j}) + \mathbf{c}_{\beta j} \sum_{\gamma=1}^{\alpha-1} \mathbf{a}_{j\gamma}(\mathbf{c}_{\gamma i} - \mathbf{c}_{\alpha i})\,, \tag{A.3.2}$$

where $\epsilon(\alpha,\beta) = \pm 1$ if $\alpha \lessgtr \beta$, and $\epsilon(\alpha,\alpha) = 0$. Here we recall that the Poisson structures of invariant spins that we found by Poisson reduction [192] and presented in (3.5.4) in matrix form, realize a different bracket for the variables $\{f_{ij}\}$. Despite that, the difference is given by the terms (3.5.6) which do not affect the equations of motion, showing that it is possible to define various Poisson structures for the hyperbolic spin RS model which differ in a non-trivial way. For the sake of comparison with (A.3.2), we express the brackets (3.5.4) with "-" in components:

$$\begin{aligned}
\{\mathbf{a}_{i\alpha}, \mathbf{a}_{j\beta}\} \;=\; & \frac{1}{2}\delta_{i\neq j}\frac{\mathcal{Q}_i + \mathcal{Q}_j}{\mathcal{Q}_i - \mathcal{Q}_j}(\mathbf{a}_{i\alpha}\mathbf{a}_{j\beta} + \mathbf{a}_{j\alpha}\mathbf{a}_{i\beta} - \mathbf{a}_{i\alpha}\mathbf{a}_{i\beta} - \mathbf{a}_{j\alpha}\mathbf{a}_{j\beta}) + \frac{1}{2}\epsilon(\beta,\alpha)\mathbf{a}_{j\alpha}\mathbf{a}_{i\beta} \\
& + \frac{1}{2}\mathbf{a}_{j\alpha}\mathbf{a}_{j\beta}\sum_{\gamma=1}^{\ell}\epsilon(\alpha,\gamma)\mathbf{a}_{i\gamma} - \frac{1}{2}\mathbf{a}_{i\alpha}\mathbf{a}_{i\beta}\sum_{\gamma=1}^{\ell}\epsilon(\beta,\gamma)\mathbf{a}_{j\gamma} + \frac{1}{2}\mathbf{a}_{i\alpha}\mathbf{a}_{j\beta}\sum_{\gamma=1}^{\ell}\epsilon(\gamma,\delta)\mathbf{a}_{i\gamma}\mathbf{a}_{j\delta}\,, \\
\{\mathbf{a}_{i\alpha}, \mathbf{c}_{\beta j}\} \;=\; & \mathbf{a}_{i\alpha}Z_{ij} - \delta_{\alpha\beta}Z_{ij} - \frac{1}{2}\delta_{i\neq j}\frac{\mathcal{Q}_i + \mathcal{Q}_j}{\mathcal{Q}_i - \mathcal{Q}_j}(\mathbf{a}_{i\alpha} - \mathbf{a}_{j\alpha})\mathbf{c}_{\beta j} + \mathbf{a}_{i\alpha}\sum_{\gamma=1}^{\beta-1}\mathbf{a}_{i\gamma}\mathbf{c}_{\gamma j} - \delta_{\alpha\beta}\sum_{\gamma=1}^{\beta-1}\mathbf{a}_{i\gamma}\mathbf{c}_{\gamma j} \\
& - \frac{1}{2}\mathbf{a}_{j\alpha}\mathbf{c}_{\beta j}\sum_{\gamma=1}^{\ell}\epsilon(\alpha,\gamma)\mathbf{a}_{i\gamma} - \frac{1}{2}\mathbf{a}_{i\alpha}\mathbf{c}_{\beta j}\sum_{\gamma,\delta=1}^{\ell}\epsilon(\gamma,\delta)\mathbf{a}_{i\gamma}\mathbf{a}_{j\delta} + \frac{1}{2}\mathbf{a}_{i\alpha}\mathbf{a}_{i\beta}\mathbf{c}_{\beta j} - \frac{1}{2}\delta_{\alpha\beta}\mathbf{a}_{i\alpha}\mathbf{c}_{\beta j}\,, \\
\{\mathbf{c}_{\alpha i}, \mathbf{c}_{\beta j}\} \;=\; & \frac{1}{2}\delta_{i\neq j}\frac{\mathcal{Q}_i + \mathcal{Q}_j}{\mathcal{Q}_i - \mathcal{Q}_j}(\mathbf{c}_{\alpha i}\mathbf{c}_{\beta j} + \mathbf{c}_{\alpha j}\mathbf{c}_{\beta i}) - \mathbf{c}_{\alpha i}Z_{ij} + \mathbf{c}_{\beta j}Z_{ji} - \frac{1}{2}\epsilon(\beta,\alpha)\mathbf{c}_{\alpha j}\mathbf{c}_{\beta i} \\
& - \mathbf{c}_{\alpha i}\sum_{\gamma=1}^{\beta-1}\mathbf{a}_{i\gamma}\mathbf{c}_{\gamma j} + \mathbf{c}_{\beta j}\sum_{\gamma=1}^{\alpha-1}\mathbf{a}_{j\gamma}\mathbf{c}_{\gamma i} + \frac{1}{2}\mathbf{c}_{\alpha i}\mathbf{c}_{\beta j}\sum_{\gamma,\delta=1}^{\ell}\epsilon(\gamma,\delta)\mathbf{a}_{i\gamma}\mathbf{a}_{j\delta} + \frac{1}{2}(\mathbf{a}_{j\alpha} - \mathbf{a}_{i\beta})\mathbf{c}_{\alpha i}\mathbf{c}_{\beta j}\,.
\end{aligned} \tag{A.3.3}$$

We draw the attention of the reader on the fact that the brackets (A.3.3) include terms of order four in the invariant spins, while (A.3.2) contain terms up to order three.

Appendix B
Details on Basso-Dixon integrals

B.1 Diagram technique

The functions and kernels of integral operators considered in the main body of the paper are represented in the form of two-dimensional Feynman diagrams. The propagator which is shown by the arrow directed from w to z and index α attached to it is given by the following expression

$$\frac{1}{[z-w]^{\alpha}} \equiv \frac{1}{(z-w)^{\alpha}(z^*-w^*)^{\bar{\alpha}}} = \frac{(z^*-w^*)^{\alpha-\bar{\alpha}}}{|z-w|^{2\alpha}}\,, \tag{B.1.1}$$

where the difference $\alpha-\bar{\alpha}$ is integer: $\alpha-\bar{\alpha}\in\mathbb{Z}$.[1] The flip of the arrow in propagator gives an additional sign factor $(-1)^{\alpha-\bar{\alpha}}$ for which we shall use the shorthand notation

$$(-1)^{[\alpha]} = (-1)^{\alpha-\bar{\alpha}} \tag{B.1.2}$$

so that

$$\frac{1}{[z-w]^{\alpha}} = \frac{(-1)^{\alpha-\bar{\alpha}}}{[w-z]^{\alpha}} = \frac{(-1)^{[\alpha]}}{[w-z]^{\alpha}}\,. \tag{B.1.3}$$

The evaluation of Feynman diagrams is based on their transformation with the help of the certain rules, namely:

- Chain relation:

$$\int d^2w \frac{1}{[z_1-w]^{\alpha}[w-z_2]^{\beta}} = (-1)^{[\gamma]} a(\alpha,\beta,\gamma)\frac{1}{[z_1-z_2]^{\alpha+\beta-1}}\,, \tag{B.1.4}$$

  where $\gamma = 2-\alpha-\beta,\ \bar{\gamma} = 2-\bar{\alpha}-\bar{\beta}$.

- Special case of the chain relation

$$\int d^2w \frac{1}{[z_1-w]^{1-\alpha}[w-z_2]^{1+\alpha}} = -\pi^2\,\frac{(-1)^{[\alpha]}}{\alpha\bar{\alpha}}\,\delta^2(z_1-z_2)\,, \tag{B.1.5}$$

[1] Note that the star * is used for the usual complex conjugation whether as the meaning of the bar is explained in eq.(3.2.10),(3.2.11).

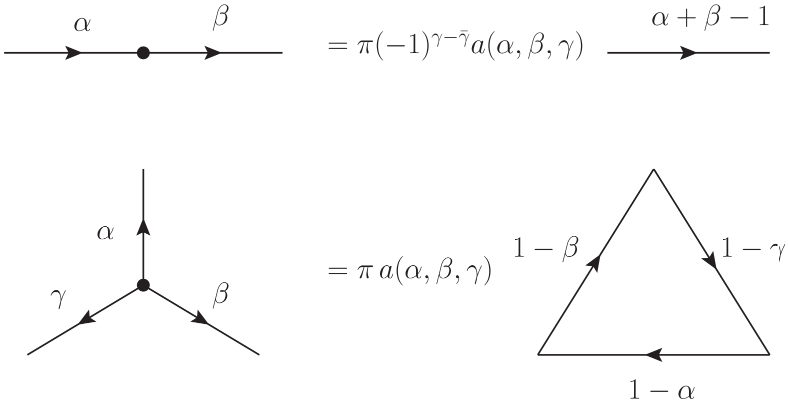

Figure B.1: The chain and star–triangle relations, $\alpha+\beta+\gamma=2$.

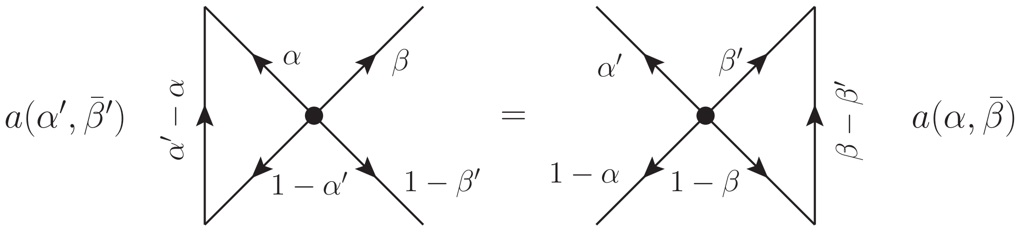

Figure B.2: The cross relation, $\alpha+\beta=\alpha'+\beta'$.

- Star–triangle relation:

$$\int d^2w \frac{1}{[z_1-w]^{\alpha}[z_2-w]^{\beta}[z_3-w]^{\gamma}} = \frac{\pi a(\alpha,\beta,\gamma)}{[z_2-z_1]^{1-\gamma}[z_1-z_3]^{1-\beta}[z_3-z_2]^{1-\alpha}}\,, \tag{B.1.6}$$

  where $\alpha+\beta+\gamma=2$ and $\bar{\alpha}+\bar{\beta}+\bar{\gamma}=2$.

- Cross relation:

$$\frac{1}{[z_1-z_2]^{\alpha'-\alpha}} \int d^2w \frac{a(\alpha',\bar{\beta}')}{[w-z_1]^{\alpha}[w-z_2]^{1-\alpha'}[w-z_3]^{\beta}[w-z_4]^{1-\beta'}} =$$
$$= \frac{1}{[z_3-z_4]^{\beta'-\beta}} \int d^2\zeta \frac{a(\alpha,\bar{\beta})}{[w-z_1]^{\alpha'}[w-z_2]^{1-\alpha}[w-z_3]^{\beta'}[w-z_4]^{1-\beta}}\,, \tag{B.1.7}$$

  where $\alpha+\beta=\alpha'+\beta'$.

These relations are shown in diagrammatic form in Figs. B.1, B.2. Here the notation $a(\alpha,\beta,\gamma,\ldots)=a(\alpha)a(\beta)a(\gamma)\ldots$ is introduced for the product of special function $a(\alpha)$ for different values of arguments. The definition of the function $a(\alpha)$ is the following

$$a(\alpha) = \frac{\Gamma(1-\bar{\alpha})}{\Gamma(\alpha)}. \tag{B.1.8}$$

Note that this function depends on two parameters α and $\bar{\alpha}$, where the difference $\alpha-\bar{\alpha}$ should be integer, but for the sake of simplicity we shall use the shorthand notation $a(\alpha)$. There are some useful relations for this function

$$a(1+\alpha) = -\frac{a(\alpha)}{\alpha\bar{\alpha}}, \quad a(\alpha)a(1-\alpha) = (-1)^{[\alpha]}, \quad a(1+\alpha)a(1-\alpha) = -\frac{(-1)^{[\alpha]}}{\alpha\bar{\alpha}} \tag{B.1.9}$$

B.2 Reduction and duality

We start from the simplest example $N = 1\,, L = 1$, make the reduction by sending $w_0 \to \infty$ and drop the corresponding propagator. We want to reduce the original quantity

$$I^{BD}_{1,1}(z_0, z_1, w_0, w_1) = \int d^2w \frac{1}{[w-z_1]^{1-\gamma}[w_1-w]^{1-\gamma}[w-w_0]^{\gamma}[z_0-w]^{\gamma}} \to$$
$$\to G_{1,1}(z_1, w_1|z_0) = \int d^2w \frac{1}{[w-z_1]^{1-\gamma}[w_1-w]^{1-\gamma}[z_0-w]^{\gamma}}$$

We can always restore the original quantity $I^{BD}_{1,1}(z_0, z_1, w_0, w_1)$ from $G_{1,1}(z_1, w_1|z_0)$ using its conformal symmetry, i.e. by applying the shift+inversion transformation:

$$G_{1,1}\left(\frac{1}{z_1}, \frac{1}{w_1}\middle|\, \frac{1}{z_0}\right) = \int \frac{d^2w}{[w]^2} \frac{1}{[1/w-1/z_1]^{1-\gamma}[1/w_1-1/w]^{1-\gamma}[1/z_0-1/w]^{\gamma}} =$$
$$= [z_1]^{1-\gamma}[w_1]^{1-\gamma}[z_0]^{\gamma} \int \frac{d^2w}{[w]^{\gamma}[z_1-w]^{1-\gamma}[w-w_1]^{1-\gamma}[w-z_0]^{\gamma}}$$
$$= [z_1]^{1-\gamma}[w_1]^{1-\gamma}[z_0]^{\gamma}\, I^{BD}_{1,1}(z_0, z_1, 0, w_1)$$
$$= [z_1]^{1-\gamma}[w_1]^{1-\gamma}[z_0]^{\gamma}\, I^{BD}_{1,1}(z_0+w_0, z_1+w_0, w_0, w_1+w_0)$$

or

$$I^{BD}_{1,1}(z_0, z_1, w_0, w_1) = [z_1-w_0]^{\gamma-1}[w_1-w_0]^{\gamma-1}[z_0-w_0]^{-\gamma} G_{1,1}\left(\frac{1}{z_1-w_0}, \frac{1}{w_1-w_0}\middle|\, \frac{1}{z_0-w_0}\right).$$

Analogously, the formula for the general N, L looks as follows:

$$I^{BD}_{L,N}(z_0, z_1, w_0, w_1) = [z_1-w_0]^{N(\gamma-1)}[w_1-w_0]^{N(\gamma-1)}[z_0-w_0]^{-L\gamma} \times \tag{B.2.1}$$
$$\times\; G_{L,N}\left(\frac{1}{z_1-w_0}, \frac{1}{w_1-w_0}\middle|\, \frac{1}{z_0-w_0}\right), \tag{B.2.2}$$

where

$$I^{\mathrm{BD}}_{L,N}(z_0, z_1, w_0, w_1) = \int \prod_{l=1}^{L}\prod_{n=1}^{N} d^2z_{ln} \left(\prod_{(l,n)\in\mathcal{L}_{L,N}} \frac{1}{|z_{l,n}-z_{l,n+1}|^{1+2\omega}\,|z_{l,n}-z_{l+1,n}|^{1-2\omega}}\right). \tag{B.2.3}$$

Taking into account (3.2.46) and (3.2.52) and setting:

$$z_1' = (z_1-w_0)^{-1}, \quad z_0' = (z_0-w_0)^{-1}, \quad w_1' = (w_1-w_0)^{-1}, \;\text{ and }\; \eta' = \frac{w_1'-z_0'}{z_1'-z_0'},$$

we can give an explicit expression for the last factor in (B.2.2) in terms of function $B_{L,N}(\eta)$:

$$G_{L,N}(z_1', w_1'|z_0') = ([z_0'-z_1'][z_0'-w_1'])^{N\frac{\gamma-1}{2}} B_{L,N}(\eta')$$

$$= \left(\frac{[z_0 - z_1]}{[z_0 - w_0][z_1 - w_0]} \right)^{(\gamma-1)N} \quad [\eta]^{\frac{\gamma-1}{2}N} B_{L,N}(\eta) \ ,$$

where η is the anharmonic ratio of the graph $I^{BD}_{L,N}$:

$$\eta = \frac{(w_1 - z_0)(z_1 - w_0)}{(z_1 - z_0)(w_1 - w_0)} \,. \tag{B.2.4}$$

By definition (3.2.2) our graphs should have a duality symmetry, namely:

$$I^{BD}_{L,N}(z_0, z_1, w_0, w_1) \ = \ I^{BD}_{N,L}(z_1, w_0, w_1, z_0) \,. \tag{B.2.5}$$

Namely we can rotate the whole diagram anti-clockwise by an angle $\frac{\pi}{2}$ and repeat our computation by eigenfunction expansion step by step with some changes:

- $L \rightleftarrows N$
- $\gamma \rightleftarrows 1 - \gamma$, so that now horizontal lines have index γ and vertical $1 - \gamma$

and we derive a different representation for the same quantity

$$I^{BD}_{N,L}(z_0, z_1, w_0, w_1) = \frac{[w_0 - z_1]^{-\gamma L}[z_0 - w_1]^{-\gamma L}}{[z_1 - w_1]^{-\gamma L + (1-\gamma)N}} \ [\eta]^{\frac{\gamma}{2}L} \ B^{(1-\gamma)}_{N,L} \left(\frac{1}{\eta} \right) \tag{B.2.6}$$

B.3 Details of the derivation of the formula (3.2.58)

The derivation of the formula (3.2.58) contains three steps:

- calculate integrand at $\nu = \frac{in}{2} + ik - i\varepsilon$

$$(-1)^{Mn} \frac{\Gamma^M(2 - 2\bar{s} + k - \varepsilon)\Gamma^M(-k + \varepsilon)}{\Gamma^M(2s - n - k + \varepsilon)\Gamma^M(n + k - \varepsilon)} \, \eta^{n+k-\varepsilon} \bar{\eta}^{k-\varepsilon} \tag{B.3.1}$$

- use twice the Euler reflection formula

$$\Gamma(-k + \varepsilon) = \frac{1}{\varepsilon} \frac{(-1)^k \, \Gamma(1 + \varepsilon)\Gamma(1 - \varepsilon)}{\Gamma(1 + k - \varepsilon)} \,,$$

$$\frac{1}{\Gamma(2s - n - k + \varepsilon)} = \frac{(-1)^{n+k}\Gamma(2s + \varepsilon)\Gamma(1 - 2s - \varepsilon)}{\Gamma(1 - 2s + n + k - \varepsilon)} \,,$$

  to transform (B.3.1) to the form

$$\frac{1}{\varepsilon^M} \frac{\Gamma^M(1 + \varepsilon)\Gamma^M(1 - \varepsilon)}{\Gamma^M(2s + \varepsilon)\Gamma^M(1 - 2s - \varepsilon)} \frac{\Gamma^M(1 - 2s + n + k - \varepsilon)}{\Gamma^M(n + k - \varepsilon)} \frac{\Gamma^M(2 - 2\bar{s} + k - \varepsilon)}{\Gamma^M(1 + k - \varepsilon)} \, \eta^{n+k-\varepsilon} \bar{\eta}^{k-\varepsilon}$$

- extract the coefficient in front of $\frac{1}{\varepsilon}$ and multiply it by $(-i)$.

Appendix C
Details on chiral CFT_4

C.1 Notation and conventions

As a convention, the metric tensor of the four dimensional Euclidean space is taken to be

$$g_{\mu\nu} = \delta_{\mu\nu} = \text{diag}(\ 1, 1, 1, 1\ )\,, \tag{C.1.1}$$

where $\mu, \nu = 0, 1, 2, 3$ are spacetime vector indices. The massless scalar propagators are defined in configuration and momentum space as follows

$$\frac{1}{(x_{12}^2)^{\alpha}} = \frac{1}{4^{\alpha}\pi^{D/2}}\frac{\Gamma(2-\alpha)}{\Gamma(\alpha)}\int d^D k \frac{e^{ik\cdot x_{12}}}{(k^2)^{D/2-\alpha}}\,, \tag{C.1.2}$$

and the same for the fermionic propagators

$$\frac{\not{x}_{12}}{(x_{12}^2)^{\alpha+1/2}} = \frac{-i}{4^{\alpha}\pi^{D/2}}\frac{\Gamma\left(\frac{5}{2}-\alpha\right)}{\Gamma\left(\frac{1}{2}+\alpha\right)}\int d^D k \frac{e^{ik\cdot x_{12}}\not{k}}{(k^2)^{D/2-\alpha+1/2}}\,, \tag{C.1.3}$$

where $\not{x}$ stands for the position x contracted with the spin structure matrix, and the same for $\not{k}$. The positions satisfies the following identity

$$x_{ij}\cdot x_{kl} = \frac{1}{2}(x_{il}^2 + x_{jk}^2 - x_{ik}^2 - x_{jl}^2)\,. \tag{C.1.4}$$

We can represent the four-dimensional gamma-matrices to have the off-block diagonal form

$$\gamma^{\mu} = \begin{pmatrix} 0 & (\sigma^{\mu})_{\alpha\dot{\beta}} \\ (\bar{\sigma}^{\mu})^{\dot{\alpha}\beta} & 0 \end{pmatrix}\,, \tag{C.1.5}$$

by introducing the 2×2 Euclidean σ matrices

$$\sigma^{\mu} = (-i\vec{\boldsymbol{\sigma}}, \mathbb{I}_{2\times 2}) \qquad \text{and} \qquad \bar{\sigma}^{\mu} = (i\vec{\boldsymbol{\sigma}}, \mathbb{I}_{2\times 2})\,, \tag{C.1.6}$$

where $\vec{\boldsymbol{\sigma}}$ are the *Pauli matrices.* We use the standard convention for raising/lowering of two-component spinor indices α, $\dot{\alpha}$

$$\psi_{\alpha} = \epsilon_{\alpha\beta}\psi^{\beta}, \quad \psi^{\alpha} = \epsilon^{\alpha\beta}\psi_{\beta}, \quad \bar{\psi}_{\dot{\alpha}} = \epsilon_{\dot{\alpha}\dot{\beta}}\bar{\psi}^{\dot{\beta}}, \quad \bar{\psi}^{\dot{\alpha}} = \epsilon^{\dot{\alpha}\dot{\beta}}\bar{\psi}_{\dot{\beta}}\,, \tag{C.1.7}$$

where we introduced the tensors ϵ as

$$\epsilon_{\alpha\beta} = \epsilon_{\dot{\alpha}\dot{\beta}} = i\sigma^2 \,, \qquad \epsilon^{\alpha\beta} = \epsilon^{\dot{\alpha}\dot{\beta}} = -i\sigma^2 \,, \tag{C.1.8}$$

and the following relations hold

$$(\bar{\sigma}^{\mu})^{\dot{\alpha}\alpha} = \epsilon^{\dot{\alpha}\dot{\beta}}\epsilon^{\alpha\beta}\sigma^{\mu}_{\dot{\beta}\beta}, \qquad \epsilon^{\dot{\alpha}\dot{\beta}}\epsilon_{\dot{\beta}\dot{\gamma}} = \delta^{\dot{\alpha}}_{\dot{\gamma}} \qquad \epsilon^{\alpha\beta}\epsilon_{\beta\gamma} = \delta^{\alpha}_{\gamma} \,. \tag{C.1.9}$$

The σ matrices satisfy

$$\bar{\sigma}_{\mu}\sigma_{\nu} + \bar{\sigma}_{\nu}\sigma_{\mu} = 2\delta_{\mu\nu}\mathbb{I}_{2\times 2} \qquad \text{and} \qquad \sigma_{\mu}\bar{\sigma}_{\nu} + \sigma_{\nu}\bar{\sigma}_{\mu} = 2\delta_{\mu\nu}\mathbb{I}_{2\times 2} \,, \tag{C.1.10}$$

and the trace identities are

$$\begin{aligned}
&\mathrm{tr}(\textit{odd number of } \sigma\textit{'s}) = 0, \\
&\mathrm{tr}(\sigma^{\mu}\bar{\sigma}^{\nu}) = \mathrm{tr}(\bar{\sigma}^{\mu}\sigma^{\nu}) = 2\delta^{\mu\nu}, \\
&\mathrm{tr}\left(\sigma_{\mu}\overline{\sigma}_{\rho}\sigma_{\eta}\overline{\sigma}_{\nu}\right) = 2\left(\delta_{\mu\rho}\delta_{\eta\nu} - \delta_{\mu\eta}\delta_{\rho\nu} + \delta_{\mu\nu}\delta_{\rho\eta} - \epsilon_{\mu\rho\eta\eta}\right), \\
&\mathrm{tr}\left(\overline{\sigma}_{\mu}\sigma_{\rho}\overline{\sigma}_{\eta}\sigma_{\nu}\right) = 2\left(\delta_{\mu\rho}\delta_{\eta\nu} - \delta_{\mu\eta}\delta_{\rho\nu} + \delta_{\mu\nu}\delta_{\rho\eta} + \epsilon_{\mu\rho\eta\eta}\right) .
\end{aligned} \tag{C.1.11}$$

C.2 Cancellation of the spurious poles

In order to confirm the validity of equation (4.2.27) we should show that the *physical poles* given by the zeroes of the spectral equation (4.2.25) are the only contributions to the four-point correlators under study. This fact, well known for the bi-scalar reduction of our theory (see Appendix B in [37]), needs a proof for the full χCFT. It appears that additional possible contributions could come from the extra poles in $g_{\Delta,S}(u,v)$ and the measure factor $1/c_2(\Delta,S)$. In this appendix we will show that these contributions cancel each other thanks to a symmetry relation fulfilled by the eigenvalues $h_{i\,\Delta,S}$ of the Bethe-Salpeter kernels.

The conformal block $g_{\Delta,S}(u,v)$ has simple poles at $\Delta_{S-n} = S+3-n$ (with $n = 1,2,\ldots,S$), namely $2i\nu_n = S+1-n$. Its residue at the pole $\nu = \nu_n$ is given by $r_n\, g_{S+3,S-n}(u,v)$ where (see for example Appendix B in [193]):

$$r_n = (-1)^n \frac{in\Gamma^2\left(\frac{1}{2}\left(n-\Delta_1+\Delta_2+1\right)\right)}{2\Gamma(n+1)^2\Gamma^2\left(\frac{1}{2}\left(-n-\Delta_1+\Delta_2+1\right)\right)} \,. \tag{C.2.1}$$

This results in the following extra contribution to (4.2.27):

$$R^{g}_{S,m} = \left(\frac{r_m}{c_2(\Delta_{S-m},S)}\frac{h_{B\,\Delta_{S-m},S}}{1-\chi_B h_{B\,\Delta_{S-m},S} - \chi_F h_{F\,\Delta_{S-m},S}}\right) g_{S+3,S-m}(u,v) \;\;,\;\; 1 \le n \le S < \infty \,. \tag{C.2.2}$$

In addition to that, the measure factor $1/c_2(\Delta,S)$ develops poles at $\Delta = S+3+k,\ k = 0,1,2,\ldots$. The corresponding contribution can be expressed as

$$R^{c_2}_{S,k} = -\left(\frac{r_k}{c_2(\Delta_S,S+k)}\frac{h_{B\,\Delta_{S+k},S}}{1-\chi_B h_{B\,\Delta_{S+k},S} - \chi_F h_{F\,\Delta_{S+k},S}}\right) g_{S+3+k,S}(u,v) \;\;,\;\; 0 \le S,k < \infty \,. \tag{C.2.3}$$

The overall contribution of these terms is the sum over all non-negative integers S, k of the generic term

$$R^{c_2}_{S,k} + R^{g}_{S+k,k} = -\left(\frac{r_k}{c_2(\Delta_S, S+k)}\, g_{S+3+k,S}(u,v)\right) \times \qquad \text{(C.2.4)}$$
$$\times \left[\frac{h_{B\,\Delta_{S+k},S}}{1-\chi_B h_{B\,\Delta_{S+k},S} - \chi_F h_{F\,\Delta_{S+k},S}} - \frac{h_{B\,\Delta_S,S+k}}{1-\chi_B h_{B\,\Delta_S,S+k} - \chi_F h_{F\,\Delta_S,S+k}}\right].$$

A possible vanishing condition for the full contribution is then

$$r_k[h_{b\,\Delta_{S+k},S}(1-\chi_b h_{B\,\Delta_{S+k},S} - \chi_F h_{F\,\Delta_{S+k},S}) - h_{B\,\Delta_{S+k},S}(1-\chi_B h_{B\,\Delta_{S+k},S} - \chi_F h_{F\,\Delta_{S+k},S})] = 0\,, \qquad \text{(C.2.5)}$$

for any $k \in \mathbb{N}$. We can actually verify in both sectors under study that the following set of stronger conditions is fulfilled

$$r_k(h_{B\,3+S+k,S} - h_{B\,3+S,S+k}) = 0 \quad , \quad k = 0,1,2,\ldots \qquad \text{(C.2.6)}$$
$$r_k(h_{F\,3+S+k,S} - h_{F\,3+S,S+k}) = 0 \quad , \quad k = 0,1,2,\ldots\,. \qquad \text{(C.2.7)}$$

It is easy to check that plugging (C.2.6) into (C.2.5), one is left with the condition (C.2.7), which means that (C.2.6) together with (C.2.7) are a sufficient condition for (C.2.5). To prove these equations hold, we notice first of all that at $\Delta_1 = \Delta_2 = 1$ (C.2.1) vanishes at odd n, so it would be sufficient to prove (C.2.6), (C.2.7) at even $k \in 2\mathbb{N}$. Moreover, equation (C.2.6) has been checked in [37], where it was enough to state the cancelation of spurious poles in Tr $[\phi_1^2]$ sector. Let us verify the second condition (C.2.7) at even integer k. Starting from the sector Tr $[\phi_1^2]$ it is equivalent to

$$\tilde{h}_{F\,3+S+k,S} - \tilde{h}_{F\,3+S,S+k} = 0\,, \qquad \text{(C.2.8)}$$

where we recalled the definition of $\tilde{h}_{F\,\Delta,S}$ (4.3.25). Equation (C.2.8) actually coincides with the vanishing condition for spurious contribution in the "one-magnon" Tr $[\phi_1^2\phi_2]$ sector of bi-scalar theory, and is verified in [37].

C.3 Operator mixing and logarithmic multiplet

The sector Tr $[\phi_1^2]$ of our theory the exchanged physical operators in the OPE s-channel of the 4-point correlators under analysis present mixing. Namely, due to the wide matter content of the theory, the renormalized operators are not just rescaled and normal-ordered monomials of elementary fields and derivatives, but linear coupling-dependant combination of several such terms which share the same symmetries. Concretely, in our theory we deal with single trace primary operators as

$$\mathcal{O}_1(x) = \mathrm{tr}[\chi_{i_1}\chi_{i_2}\cdots\chi_{i_L}](x)\,, \qquad \text{(C.3.1)}$$

made up of elementary fields of the theory $\chi_{i_k}(x)$ eventually dressed by tensor structures and derivatives. Given the quantum numbers of such a term $\mathcal{O}_1$, that is Cartan's $U(1)^{\otimes 3}$ charge, twist and tensor rank S, it is usually possible to write a few other conformal primaries with the same numbers, say $\{\mathcal{O}_2,\, \mathcal{O}_3\, \dots\}$. This allows in general some of the two-point functions $\langle \mathcal{O}_i(x)\mathcal{O}_j(0)^\dagger\rangle$ to not vanish at $i \neq j$, that is to have transitions $\mathcal{O}_i \to \mathcal{O}_j$. We define the anomalous dimension matrix γ_{ij} as

$$-\mu\frac{d}{d\mu}\, Z_{O_i} \;=\; \gamma_{ij}\, Z_{\mathcal{O}_j}\,, \tag{C.3.2}$$

being Z_{O_i} the renormalization of operator $\mathcal{O}_i$ and μ the scale. In absence of transitions, namely $\gamma_{ij} = \delta_{ij}\gamma_i$, mixing does not happen and each operator $\mathcal{O}_i$ has anomalous dimension γ_i. Otherwise, one has to bring the *mixing matrix* γ_{ij} into diagonal form via a rotation over the basis of local primaries $\{\mathcal{O}_1,\, \mathcal{O}_2\, \dots\}$. The operators of the new basis are linear combinations of the kind

$$\mathcal{O}'_i(x) \;=\; c_{1,i}(\xi)\,\mathcal{O}_1 + c_{2,i}(\xi)\,\mathcal{O}_2 + \dots \tag{C.3.3}$$

and they do not mix among each other. The anomalous dimension of $\mathcal{O}'_i(x)$ is the corresponding eigenvalue of the matrix, namely γ'_i. The existence of a basis of eigenvectors for γ_{ij}-matrix is ensured by its hermiticity in unitary theories. The absence of invariance under hermitian conjugation of (1.2.2) prevent to come to similar conclusions for χCFT theory. In particular, performing the planar limit can lead to "one-way" transitions

$$\langle \mathcal{O}_i(x)\mathcal{O}_j(0)^\dagger\rangle \neq 0 \qquad \langle \mathcal{O}_i(x)\mathcal{O}_j(0)^\dagger\rangle = 0\,, \tag{C.3.4}$$

and the correspondent mixing matrix can be only brought into Jordan canonical form, e.g. for the mixing of four primaries:

$$\gamma_{ij} \;\longrightarrow\; (S\gamma S^{-1})_{ij} \;=\; \begin{bmatrix} 0 & 1 & 0 & 0\\ 0 & 0 & 0 & 0\\ 0 & 0 & \gamma'_3 & 0\\ 0 & 0 & 0 & \gamma'_4 \end{bmatrix}. \tag{C.3.5}$$

The matrix (C.3.5) contains a 2×2 Jordan block, together with two diagonal terms γ'_3 and γ'_4, corresponding to two renormalized operators with such anomalous dimensions. The physical interpretation of Jordan blocks leads to the formulation of logarithmic CFT (see [105],[110]). In the example (C.3.5) the block corresponds to a rank-2 logarithmic multiplet. This means that the corresponding operators of the new basis, $\mathcal{O}'_1, \mathcal{O}'_2$ show 2-point functions of the kind

$$\langle \mathcal{O}'_1(x)\mathcal{O}'^\dagger_1(0)\rangle = \frac{k\,\ln(\mu^2x^2)}{(x)^{2\Delta_0}} \qquad\qquad \langle \mathcal{O}'_1(x)\mathcal{O}_2'^\dagger(0)\rangle = \frac{k}{(x)^{2\Delta_0}} \tag{C.3.6}$$

$$\langle \mathcal{O}'_2(x)\mathcal{O}'^\dagger_1(0)\rangle = \frac{k}{(x)^{2\Delta_0}} \qquad\qquad \langle \mathcal{O}'_2(x)\mathcal{O}'^\dagger_2(0)\rangle = 0\,, \tag{C.3.7}$$

where Δ_0 is the bare dimension of $\mathcal{O}_i$ operators, and μ the energy scale. This phenomenon, the presence of log-multiplets in χCFT has first be noticed by J.Caetano

[38] for its bi-scalar reduction (2.1.3) and some examples of its occurance in the context of fishnet CFT have been presented in [39]. Despite such logarithmic operators appear in our theory, we are mostly interested in selecting the non-logarithmic ones: indeed these are the only exchanged in the OPE of the correlators under study, as the solutions of spectral equations (4.3.26) correspond to non-protected operators $\Delta(\xi) \neq \Delta_0$.

tr$[\phi_1^2]$ sector This first sector is characterized by the Cartan R-charge of two ϕ_1 fields $(2, 0, 0)$. The equation (4.3.26) shows physical solutions for every even twist. In particular there is only one solution at twist-2 (4.3.29), and two at twist-4 (4.3.30) and higher (4.3.31) both for spin $S = 0$ and $S > 0$. The twist-2 solution is easily interpreted as the scaling dimension of

$$\mathrm{tr}[\phi_1 (n \cdot \partial)^S \phi_1] + \text{permutations} \qquad S = 0, 2, \dots\,, \tag{C.3.8}$$

indeed for any S there is no other twist-2 conformal primary with charge $(2, 0, 0)$. On the other hand for $\Delta_0 - S = t \geq 4$ we can list several primaries with the right set of Cartan's charges. Let us concentrate on the scalar case $S = 0$ of twist four; we find 9 scalar conformal primaries which have the right set of charges

$$\begin{aligned} &\mathcal{O}_1 = \mathrm{tr}[\phi_1^3 \phi_1^\dagger] \qquad \mathcal{O}_j = \mathrm{tr}[\phi_1^2 \phi_j \phi_j^\dagger] \qquad \mathcal{O}_{2+j} = \mathrm{tr}[\phi_1^2 \phi_j^\dagger \phi_j] \qquad \mathcal{O}_{4+j} = \mathrm{tr}[\phi_1 \phi_j \phi_1 \phi_j^\dagger] \\ &\mathcal{O}_8 = \mathrm{tr}[\bar\psi_2 \bar\psi_3 \phi_1] \qquad \mathcal{O}_9 = \mathrm{tr}[\bar\psi_3 \bar\psi_2 \phi_1], \quad j = 2, 3. \end{aligned}$$

As also the structure of (4.3.1) shows, this sector is fully described in terms of the χ_0CFT, thus the mixing transitions are realized by the vertices of (1.2.4). At any coupling $\mathcal{O}_1$ shows no planar transitions, and we deal with a set of 8 conformal primaries which at non-zero couplings ξ_2, ξ_3 mix among themselves. This fact is apparently in contrast with the presence of only two twist-4 exchanged operators in the OPE expansion of Sec.(4.3.5), and can be explained with the arising of logarithmic multiplets of operators with $\Delta = \Delta_0 = 4$, not being solutions of (4.3.26). Indeed, for instance, the following planar transitions

$$\mathcal{O}_{4+j} \longrightarrow \mathcal{O}_2, \mathcal{O}_5 \qquad \mathcal{O}_8 \longrightarrow \mathcal{O}_4, \mathcal{O}_3, \tag{C.3.9}$$

can happen respectively starting from order ξ^2 and ξ^3, while they lack the hermitian conjugate due to chirality of (1.2.4). One can actually check that there is no conjugate transition to (C.3.9) at any order. This suggest that matrix γ_{ij} won't be diagonalizable and presents Jordan blocks in its canonical form, i.e. logarithmic operators.

Bibliography

[1] J. Liouville, *"Note sur l'intégration des équations différentielles de la Dynamique, présentée au Bureau des Longitudes le 29 juin 1853."*, Journal de Mathématiques Pures et Appliquées , 137 (1855).

[2] V. I. Arnold, *"Mathematical Methods of Classical Mechanics"*.

[3] G. Arutyunov, *"Elements of Classical and Quantum Integrable Systems"*.

[4] R. Esposito, *"Appunti dalle lezioni di meccanica razionale"*, Aracne (1999).

[5] H. Bethe, *"Zur theorie der metalle"*, Zeitschrift für Ph 71, 205 (1931).

[6] L. D. Faddeev, *"How algebraic Bethe ansatz works for integrable model"*, arXiv:9605187, in: *"Relativistic gravitation and gravitational radiation. Proceedings, School of Physics, Les Houches, France, September 26-October 6, 1995"*, pp. 149-219p.

[7] E. K. Sklyanin, *"Separation of variables in the Gaudin model"*, J. Sov. Math. 47, 2473 (1989).

[8] E. K. Sklyanin, *"Functional Bethe Ansatz"*, in: *"Integrable and Superintegrable Systems"*, WORLD SCIENTIFIC (1990), 8-33p.

[9] R. J. Baxter, *"Exactly solved models in statistical mechanics"*, Elsevier (1982).

[10] V. E. Korepin, N. M. Bogoliubov and A. G. Izergin, *"Quantum Inverse Scattering Method and Correlation Functions"*.

[11] F. Calogero, *"Solution of a Three-Body Problem in One Dimension"*, Journal of Mathematical Physics 10, 2191 (1969).

[12] F. Calogero, *"Exactly solvable one-dimensional many-body problems"*, Lettere al Nuovo Cimento 13, 411 (1975).

[13] N. Beisert et al., *"Review of AdS/CFT Integrability: An Overview"*, Lett. Math. Phys. 99, 3 (2012), arXiv:1012.3982.

[14] G. Arutyunov and S. Frolov, *"Foundations of the $AdS_5 \times S^5$ superstring: I"*, Journal of Physics A: Mathematical and Theoretical 42, 254003 (2009).

[15] O. Babelon and C.-M. Viallet, *"Hamiltonian structures and Lax equations"*, Physics Letters B 237, 411 (1990).

[16] E. K. Sklyanin, *"Quantum inverse scattering method. Selected topics"*, hep-th/9211111.

[17] P. Di Francesco, P. Mathieu and D. Senechal, *"Conformal Field Theory"*, Springer-Verlag (1997), New York.

[18] S. N. M. Ruijsenaars and H. Schneider, *"A new class of integrable systems and its relation to solitons"*, Annals of Physics 170, 370 (1986).

[19] E. D'Hoker and D. H. Phong, *"Seiberg-Witten Theory and Calogero-Moser Systems"*, Progress of Theoretical Physics Supplement 135, 75 (1999), hep-th/9906027v1.

[20] M. Isachenkov and V. Schomerus, *"Integrability of conformal blocks. Part I. Calogero-Sutherland scattering theory"*, Journal of High Energy Physics 2018, V. Schomerus (2018).

[21] S. N. M. Ruijsenaars, *"Complete integrability of relativistic Calogero-Moser systems and elliptic function identities"*, Communications in Mathematical Physics 110, 191 (1987).

[22] V. G. Drinfel'd, *"Hamiltonian structures on Lie groups, Lie bialgebras and the geometric meaning of the classical Yang-Baxter equations"*, in: *"Yang-Baxter Equation in Integrable Systems"*, WORLD SCIENTIFIC (1990), 222-225p.

[23] J. Avan and A. Doikou, *"Commuting quantum traces: the case of reflection algebras"*, math/0305424v2.

[24] I. Krichever and A. Zabrodin, *"Spin generalization of the Ruijsenaars-Schneider model, the non-Abelian 2D Toda chain, and representations of the Sklyanin algebra"*, Russian Mathematical Surveys 50, 1101 (1995).

[25] N. Reshetikhin, *"Degenerately Integrable Systems"*, Journal of Mathematical Sciences 213, 769 (2016).

[26] J. M. Maldacena, *"The Large N limit of superconformal field theories and supergravity"*, Adv.Theor.Math.Phys. 2, 231 (1998), hep-th/9711200.

[27] G. Arutyunov and S. Frolov, *"Foundations of the $AdS\_5 \times S^5$ Superstring. Part I"*, J. Phys. A 42, 254003 (2009), arXiv:0901.4937.

[28] V. Kazakov and E. Olivucci, *"Biscalar Integrable Conformal Field Theories in Any Dimension"*, Phys. Rev. Lett. 121, 131601 (2018), arXiv:1801.09844.

[29] S. Derkachov, V. Kazakov and E. Olivucci, *"Basso-Dixon Correlators in Two-Dimensional Fishnet CFT"*, JHEP 1904, 032 (2019), arXiv:1811.10623.

[30] S. Derkachov and E. Olivucci, *"Exactly solvable magnet of conformal spins in four dimensions"*, arXiv:1912.07588v3.

[31] V. Kazakov, E. Olivucci and M. Preti, *"Generalized fishnets and exact four-point correlators in chiral CFT_4"*, JHEP 1906, 078 (2019), arXiv:1901.00011.

[32] O. Gurdogan and V. Kazakov, *"New integrable non-gauge 4D QFTs from strongly deformed planar N=4 SYM"*, arXiv:1512.06704.

[33] L. N. Lipatov, *"High Energy Asymptotics of Multi–Colour QCD and Exactly Solvable Lattice Models"*, hep-th/9311037v1.

[34] N. I. Usyukina and A. I. Davydychev, *"Exact results for three and four point ladder diagrams with an arbitrary number of rungs"*, Phys. Lett. B305, 136 (1993).

[35] B. Basso and L. J. Dixon, *"Gluing Ladder Feynman Diagrams into Fishnets"*, Phys. Rev. Lett. 119, 071601 (2017), arXiv:1705.03545.

[36] D. Grabner, N. Gromov, V. Kazakov and G. Korchemsky, *"Strongly gamma-deformed N=4 SYM as an integrable CFT"*, arXiv:1711.04786.

[37] N. Gromov, V. Kazakov and G. Korchemsky, *"Exact Correlation Functions in Conformal Fishnet Theory"*, arXiv:1808.02688.

[38] J. Caetano, *"To be published"*, To be published.

[39] N. Gromov, V. Kazakov, G. Korchemsky, S. Negro and G. Sizov, *"Integrability of Conformal Fishnet Theory"*, arXiv:1706.04167.

[40] M. A. Semenov-Tian-Shansky, *"Dressing transformations and Poisson group actions"*, Publications of the Research Institute for Mathematical Sciences 21, 1237 (1985).

[41] J.-H. Lu, *"Momentum Mappings And Reduction of Poisson Actions"*, edited by P. Dazord and A. Weinstein, in: *"Symplectic Geometry, Groupoids, and Integrable Systems"*, edited by P. Dazord and A. Weinstein, Springer US (1991), New York, NY, 209–226p.

[42] F. Delduc, S. Lacroix, M. Magro and B. Vicedo, *"On q-deformed symmetries as Poisson–Lie symmetries and application to Yang–Baxter type models"*, J. Phys. A 49, 415402 (2016), arXiv:1606.01712.

[43] P. A. M. Dirac, *"Generalized Hamiltonian Dynamics"*, Canadian Journal of Mathematics 2, 129–148 (1950).

[44] J. Marsden and A. Weinstein, *"Reduction of symplectic manifolds with symmetry"*, Rept. Math. Phys. 5, 121 (1974).

[45] D. Kazhdan, B. Kostant and S. Sternberg, *"Hamiltonian group actions and dynamical systems of calogero type"*, Communications on Pure and Applied Mathematics 31, 481 (1978).

[46] L. Feher and T. F. Gorbe, *"The full phase space of a model in the Calogero-Ruijsenaars family"*, Journal of Geometry and Physics 115, 139 (2017), arXiv:1603.02877v1.

[47] L. Fehér, *"Poisson-Lie analogues of spin Sutherland models"*, Nuclear Physics B 949, 114807 (2019).

[48] O. Chalykh and M. Fairon, *"On the Hamiltonian formulation of the trigonometric spin Ruijsenaars-Schneider system"*, arXiv:1811.08727v2.

[49] A. Zabrodin, *"Quantum Spin Chains and Integrable Many-Body Systems of Classical Mechanics"*, in: *"Springer Proceedings in Physics"*, Springer International Publishing (2015), 29-48p.

[50] A. Grekov, I. Sechin and A. Zotov, *"Generalized model of interacting integrable tops"*, Journal of High Energy Physics 2019, A. Zotov (2019).

[51] I. G. Macdonald, *"Symmetric functions and Hall polynomials"*.

[52] K. Hasegawa, *"Ruijsenaars' Commuting Difference Operators as Commuting Transfer Matrices"*, Communications in Mathematical Physics 187, 289 (1997).

[53] A. Antonov, K. Hasegawa and A. Zabrodin, *"On trigonometric intertwining vectors and non-dynamical R-matrix for the Ruijsenaars model"*, Nuclear Physics B 503, 747 (1997).

[54] G. E. Arutyunov, L. O. Chekhov and S. A. Frolov, *"Quantum dynamical R-matrices"*.

[55] L. Fehér and C. Klimčík, *"Poisson–Lie Generalization of the Kazhdan–Kostant–Sternberg Reduction"*, Letters in Mathematical Physics 87, 125 (2009).

[56] L. Feher and C. Klimcik, *"Poisson-Lie interpretation of trigonometric Ruijsenaars duality"*, arXiv:0906.4198v3.

[57] G. E. Arutyunov and S. A. Frolov, *"Quantum Dynamical R-Matrices and Quantum Frobenius Group"*.

[58] G. E. Arutyunov, S. A. Frolov and P. B. Medvedev, *"Elliptic Ruijsenaars - Schneider model via the Poisson reduction of the affine Heisenberg double"*, Journal of Physics A: Mathematical and General 30, 5051 (1997).

[59] V. V. Fock and A. A. Rosly, *"Moduli Space of Flat Connections as a Poisson Manifold"*, International Journal of Modern Physics B 11, 3195 (1997).

[60] Y. B. Suris, *"A new integrable system related to the Toda lattice"*, solv-int/9605010v1.

[61] J. Avan and G. Rollet, *"The Classical r-Matrix for the Relativistic Ruijsenaars-Schneider System"*, hep-th/9510166v1.

[62] O. Babelon and D. Bernard, *"The sine-Gordon solitons as an N-body problem"*, Physics Letters B 317, 363 (1993).

[63] F. W. Nijhoff, V. B. Kuznetsov, E. K. Sklyanin and O. Ragnisco, *"Dynamicalr-matrix for the elliptic Ruijsenaars - Schneider system"*, Journal of Physics A: Mathematical and General 29, L333 (1996).

[64] E. K. Sklyanin, *"Dynamical r-matrices for the Elliptic Calogero-Moser Model"*, hep-th/9308060v1.

[65] J.-L. Gervais and A. Neveu, *"Novel triangle relation and absence of tachyons in Liouville string field theory"*, Nuclear Physics B 238, 125 (1984).

[66] G. Felder, *"Conformal field theory and integrable systems associated with elliptic curves"*, hep-th/9407154v1.

[67] M. A. Semenov-Tian-Shansky, *"Poisson Lie groups, quantum duality principle, and the quantum double"*.

[68] Z. Nagy, J. Avan, A. Doikou and G. Rollet, *"Commuting quantum traces for quadratic algebras"*.

[69] G. E. Arutyunov and S. A. Frolov, *"On Hamiltonian structure of the spin Ruijsenaars-Schneider model"*, Journal of Physics A: Mathematical and General 31, 4203 (1998), hep-th/9703119v2.

[70] A. Gorsky and N. Nekrasov, *"Relativistic Calogero-Moser model as gauged WZW theory"*, Nuclear Physics B 436, 582 (1995).

[71] M. Fairon, *"Spin versions of the complex trigonometric Ruijsenaars-Schneider model from cyclic quivers"*, arXiv:1811.08717v2.

[72] O. Chalykh and M. Fairon, *"Multiplicative quiver varieties and generalised Ruijsenaars-Schneider models"*, arXiv:1704.05814v1.

[73] G. Arutyunov, R. Klabbers and E. Olivucci, *"Quantum Trace Formulae for the Integrals of the Hyperbolic Ruijsenaars-Schneider model"*, arXiv:1902.06755v2.

[74] H. Flaschka and T. Ratiu, *"A convexity theorem for Poisson actions of compact Lie groups"*.

[75] R. Rattazzi, V. S. Rychkov, E. Tonni and A. Vichi, *"Bounding scalar operator dimensions in 4D CFT"*, JHEP 0812, 031 (2008), arXiv:0807.0004.

[76] S. El-Showk, M. F. Paulos, D. Poland, S. Rychkov, D. Simmons-Duffin and A. Vichi, *"Solving the 3D Ising Model with the Conformal Bootstrap"*, Phys. Rev. D86, 025022 (2012), arXiv:1203.6064.

[77] N. Gromov, V. Kazakov, S. Leurent and D. Volin, *"Quantum Spectral Curve for Planar $\mathcal{N} = 4$ Super-Yang-Mills Theory"*, Phys. Rev. Lett. 112, 011602 (2014), arXiv:1305.1939.

[78] N. Gromov, V. Kazakov, S. Leurent and D. Volin, *"Quantum spectral curve for arbitrary state/operator in AdS_5/CFT_4"*, JHEP 1509, 187 (2015), arXiv:1405.4857.

[79] N. Gromov, *"Introduction to the Spectrum of $N = 4$ SYM and the Quantum Spectral Curve"*, arXiv:1708.03648.

[80] V. Kazakov, *"Quantum Spectral Curve of γ-twisted $\mathcal{N} = 4$ SYM theory and fishnet CFT"*, arXiv:1802.02160, [Rev. Math. Phys.30,no.07,1840010(2018)].

[81] N. Beisert and R. Roiban, *"Beauty and the twist: The Bethe ansatz for twisted N=4 SYM"*, JHEP 0508, 039 (2005), hep-th/0505187.

[82] S. Frolov, *"Lax pair for strings in Lunin-Maldacena background"*, JHEP 0505, 069 (2005), hep-th/0503201.

[83] V. Kazakov, S. Leurent and D. Volin, *"T-system on T-hook: Grassmannian Solution and Twisted Quantum Spectral Curve"*, arXiv:1510.02100.

[84] C. Sieg and M. Wilhelm, *"On a CFT limit of planar γ_i-deformed $\mathcal{N} = 4$ SYM theory"*, Phys. Lett. B756, 118 (2016), arXiv:1602.05817.

[85] J. Fokken, C. Sieg and M. Wilhelm, *"Non-conformality of γ_i-deformed $N = 4$ SYM theory"*, J. Phys. A47, 455401 (2014), arXiv:1308.4420.

[86] B. Basso, S. Komatsu and P. Vieira, *"Structure Constants and Integrable Bootstrap in Planar N=4 SYM Theory"*, arXiv:1505.06745.

[87] T. Fleury and S. Komatsu, *"Hexagonalization of Correlation Functions"*, JHEP 1701, 130 (2017), arXiv:1611.05577.

[88] B. Eden and A. Sfondrini, *"Tessellating cushions: four-point functions in $\mathcal{N} = 4$ SYM"*, JHEP 1710, 098 (2017), arXiv:1611.05436.

[89] F. Coronado, *"Bootstrapping the simplest correlator in planar $\mathcal{N} = 4$ SYM at all loops"*, arXiv:1811.03282.

[90] T. Bargheer, J. Caetano, T. Fleury, S. Komatsu and P. Vieira, *"Handling Handles I: Nonplanar Integrability"*, arXiv:1711.05326.

[91] J. Caetano, O. Gurdogan and V. Kazakov, *"Chiral limit of $N = 4$ SYM and ABJM and integrable Feynman graphs"*, Journal of High Energy Physics 117, V. Kazakov (2016), arXiv:1612.05895.

[92] A. B. Zamolodchikov, *""Fishnet" diagrams as a completely integrable system"*, Phys. Lett. 97B, 63 (1980).

[93] C. Ahn, Z. Bajnok, D. Bombardelli and R. I. Nepomechie, *"TBA, NLO Luscher correction, and double wrapping in twisted AdS/CFT"*, JHEP 1112, 059 (2011), arXiv:1108.4914.

[94] D. Chicherin, V. Kazakov, F. Loebbert, D. Mueller and D.-l. Zhong, *"Yangian Symmetry for Bi-Scalar Loop Amplitudes"*, arXiv:1704.01967.

[95] D. Chicherin, V. Kazakov, F. Loebbert, D. Mueller and D.-l. Zhong, *"Yangian Symmetry for Fishnet Feynman Graphs"*, Phys. Rev. D96, 121901 (2017), arXiv:1708.00007.

[96] G. P. Korchemsky, *"Exact scattering amplitudes in conformal fishnet theory"*, arXiv:1812.06997.

[97] R. Ben-Israel, A. G. Tumanov and A. Sever, *"Scattering Amplitudes – Wilson Loops Duality for the First Non-planar Correction"*, arXiv:1802.09395.

[98] O. Mamroud and G. Torrents, *"RG stability of integrable fishnet models"*, JHEP 1706, 012 (2017), arXiv:1703.04152.

[99] R. G. Leigh and M. J. Strassler, *"Exactly marginal operators and duality in four-dimensional N=1 supersymmetric gauge theory"*, Nucl. Phys. B447, 95 (1995).

[100] O. Lunin and J. M. Maldacena, *"Deforming field theories with U(1) x U(1) global symmetry and their gravity duals"*, JHEP 0505, 033 (2005), hep-th/0502086.

[101] A. A. Tseytlin and K. Zarembo, *"Effective potential in nonsupersymmetric SU(N) x SU(N) gauge theory and interactions of type 0 D3-branes"*, Phys. Lett. B457, 77 (1999), arXiv:9902095.

[102] A. Dymarsky, I. R. Klebanov and R. Roiban, *"Perturbative search for fixed lines in large N gauge theories"*, JHEP 0508, 011 (2005), arXiv:0505099.

[103] J. Fokken, C. Sieg and M. Wilhelm, *"A piece of cake: the ground-state energies in γ_i -deformed $\mathcal{N} = 4$ SYM theory at leading wrapping order"*, JHEP 1409, 78 (2014), arXiv:1405.6712.

[104] E. Pomoni and L. Rastelli, *"Large N Field Theory and AdS Tachyons"*, JHEP 0904, 020 (2009), arXiv:0805.2261.

[105] V. Gurarie, *"Logarithmic operators in conformal field theory"*, Nuclear Physics B 410, 535 (1993), arXiv:9303160[hep-th].

[106] T. Banks and A. Zaks, *"On the Phase Structure of Vector-Like Gauge Theories with Massless Fermions"*, Nucl. Phys. B196, 189 (1982).

[107] N. Gromov, V. Kazakov, S. Leurent and D. Volin, *"Quantum Spectral Curve for Planar $\mathcal{N} =$ Super-Yang-Mills Theory"*, Phys. Rev. Lett. 112, 011602 (2014).

[108] N. Gromov, V. Kazakov and P. Vieira, *"Exact Spectrum of Anomalous Dimensions of Planar N=4 Supersymmetric Yang-Mills Theory"*, Phys. Rev. Lett. 103, 131601 (2009), arXiv:0901.3753.

[109] A. G. Grozin, *"Massless two-loop self-energy diagram: Historical review"*, Int. J. Mod. Phys. A27, 1230018 (2012), arXiv:1206.2572.

[110] M. Hogervorst, M. Paulos and A. Vichi, *"The ABC (in any D) of Logarithmic CFT"*, JHEP 1710, 201 (2017), arXiv:1605.03959.

[111] D. Chicherin, S. Derkachov and A. P. Isaev, *"Conformal group: R-matrix and star-triangle relation"*, JHEP 1304, 020 (2013), arXiv:1206.4150.

[112] F. A. Dolan and H. Osborn, *"Conformal Partial Waves: Further Mathematical Results"*, Phys. Lett 718, 169 (2011), arXiv:1108.6194.

[113] V. K. Dobrev et al., *"Harmonic Analysis on the n-Dimensional Lorentz Group and Its Application to Conformal Quantum Field Theory"*, Lect.Notes Phys. 63 12, 059 (1977).

[114] E. S. Fradkin and M. Ya. Palchik, *"Recent Developments in Conformal Invariant Quantum Field Theory"*, Phys. Rept. 44, 249 (1978).

[115] L. N. Lipatov, *" High energy asymptotics of multi-color QCD and exactly sol vable lattice models"*, JETP Lett. 59 (1994) 596-599; 12, L. N. Lipatov (1994), arXiv:9311037v1.

[116] G. P. Korchemsky, *"Conformal bootstrap for the BFKL pomeron"*, Nucl. Phys. B550, 397 (1999), arXiv:9711277.

[117] S. E. Derkachov, G. P. Korchemsky and A. N. Manashov, *"Noncompact Heisenberg spin magnets from high-energy QCD: 1. Baxter Q operator and separation of variables"*, Nucl. Phys. B617, 375 (2001), arXiv:0107193.

[118] H. J. De Vega and L. N. Lipatov, *"Interaction of reggeized gluons in the Baxter-Sklyanin representation"*, Phys. Rev. D64, 114019 (2001), arXiv:0107225.

[119] I. Balitsky, V. Kazakov and E. Sobko, *"Two-point correlator of twist-2 light-ray operators in N=4 SYM in BFKL approximation"*, arXiv:1310.3752.

[120] I. Balitsky, V. Kazakov and E. Sobko, *"Three-point correlator of twist-2 light-ray operators in N=4 SYM in BFKL approximation"*, arXiv:1511.03625.

[121] I. Balitsky, V. Kazakov and E. Sobko, *"Structure constant of twist-2 light-ray operators in the Regge limit"*, Phys. Rev. D93, 061701 (2016), arXiv:1506.02038.

[122] D. J. Gross and V. Rosenhaus, *"All point correlation functions in SYK"*, JHEP 1712, 148 (2017), arXiv:1710.08113.

[123] B. Eden, Y. Jiang, D. le Plat and A. Sfondrini, *"Colour-dressed hexagon tessellations for correlation functions and non-planar corrections"*, JHEP 1802, 170 (2018), arXiv:1710.10212.

[124] T. Bargheer, J. Caetano, T. Fleury, S. Komatsu and P. Vieira, *"Handling Handles I: Nonplanar Integrability"*, arXiv:1711.05326.

[125] B. Basso and L. J. Dixon, *"Gluing Ladder Feynman Diagrams into Fishnets"*, Phys. Rev. Lett. 119, 071601 (2017), arXiv:1705.03545.

[126] G. 't Hooft, *"A Planar Diagram Theory for Strong Interactions"*, Nucl. Phys. B72, 461 (1974).

[127] A. P. Isaev, *"Operator approach to analytical evaluation of Feynman diagrams"*, Phys. Atom. Nucl. 71, 914 (2008), arXiv:0709.0419, in: *"Proceedings, XII International Conference on Symmetry Methods in Physics: Yerevan, Armenia, July 3-8, 2006"*, 914-924p.

[128] D. Chicherin, S. Derkachov and A. P. Isaev, *"Conformal group: R-matrix and star-triangle relation"*, JHEP 1304, 020 (2013), arXiv:1206.4150.

[129] A. V. Belitsky, S. E. Derkachov and A. N. Manashov, *"Quantum mechanics of null polygonal Wilson loops"*, Nucl. Phys. B882, 303 (2014), arXiv:1401.7307.

[130] S. E. Derkachov and A. N. Manashov, *"Iterative construction of eigenfunctions of the monodromy matrix for $SL(2,\mathbb{C})$ magnet"*, J. Phys. A47, 305204 (2014), arXiv:1401.7477.

[131] E. K. Sklyanin, *"The Quantum Toda Chain"*, Lect. Notes Phys. 226, 196 (1985), in: *"Non-Linear Equations in Classical and Quantum Field Theory"*, Springer Berlin Heidelberg (1985), 196-233p.

[132] E. K. Sklyanin, *"Separation of variables - new trends"*, Prog. Theor. Phys. Suppl. 118, 35 (1995).

[133] E. K. Sklyanin, *"Quantum inverse scattering method. Selected topics"*, hep-th/9211111.

[134] M. Preti, *"STR: a Mathematica package for the method of uniqueness"*, arXiv:1811.04935.

[135] K. K. Kozlowski, *"Unitarity of the SoV Transform for the Toda Chain"*, Commun. Math. Phys. 334, 223 (2015), arXiv:1306.4967.

[136] S. E. Derkachov, K. K. Kozlowski and A. N. Manashov, *"On the separation of variables for the modular XXZ magnet and the lattice Sinh-Gordon models"*, arXiv:1806.04487.

[137] G. Schrader and A. Shapiro, *"On b-Whittaker functions"*, ArXiv e-prints 334, A. Shapiro (2018), arXiv:1806.00747.

[138] E. Brezin, C. Itzykson, G. Parisi and J. B. Zuber, *"Planar Diagrams"*, Commun. Math. Phys. 59, 35 (1978).

[139] C. Itzykson and J. B. Zuber, *"The Planar Approximation. 2."*, J. Math. Phys. 21, 411 (1980), in: *"4th Workshop on Current Problems in High-Energy Particle Theory Bad Honnef, Germany, June 2-4, 1980"*, 411p.

[140] V. S. Dotsenko and V. A. Fateev, *"Conformal Algebra and Multipoint Correlation Functions in Two-Dimensional Statistical Models"*, Nucl. Phys. B240, 312 (1984), [,653(1984)].

[141] G. P. Korchemsky, *"Conformal bootstrap for the BFKL Pomeron"*, hep-ph/9711277v2.

[142] A. Levin and G. Racinet, *"Towards multiple elliptic polylogarithms"*, ArXiv Mathematics e-prints B240, G. Racinet (2007), math/0703237.

[143] G. Passarino, *"Elliptic Polylogarithms and Basic Hypergeometric Functions"*, Eur. Phys. J. C77, 77 (2017), arXiv:1610.06207.

[144] J. Bartels, L. N. Lipatov and A. Prygarin, *"Integrable spin chains and scattering amplitudes"*, J. Phys. A44, 454013 (2011), arXiv:1104.0816.

[145] L. N. Lipatov, *"Integrability of scattering amplitudes in N=4 SUSY"*, J. Phys. A42, 304020 (2009), arXiv:0902.1444.

[146] L. D. Faddeev and G. P. Korchemsky, *"High-energy QCD as a completely integrable model"*, Phys. Lett. B342, 311 (1995), arXiv:9404173.

[147] D. Grabner, N. Gromov, V. Kazakov and G. Korchemsky, *"to appear"*.

[148] V. Kazakov, *"Quantum Spectral Curve of γ-twisted $\mathcal{N}=4$ SYM theory and fishnet CFT"*, arXiv:1802.02160.

[149] B. Basso and D.-l. Zhong, *"Continuum limit of fishnet graphs and AdS sigma model"*, arXiv:1806.04105.

[150] V. E. Korepin, N. M. Bogoliubov and A. G. Izergin, *"Quantum inverse scattering method and correlation functions"*, Cambridge university press (1997).

[151] L. D. Faddeev, *"Symmetries quantiques"*, North Holland (1998).

[152] V. S. Fadin, E. Kuraev and L. Lipatov, *"On the Pomeranchuk singularity in asymptotically free theories"*, Physics Letters B 60, 50 (1975).

[153] Y. Y. Balitskii and L. Lipatov, *"Pomeranchuk singularity in quantum chromodynamics"*, Sov. J. Nucl. Phys. 28, L. Lipatov (1978).

[154] V. K. Dobrev, G. Mack, V. B. Petkova, S. G. Petrova and I. T. Todorov, *"Harmonic Analysis on the n-Dimensional Lorentz Group and Its Application to Conformal Quantum Field Theory"*, Lect. Notes Phys. 63, 1 (1977).

[155] L. N. Lipatov, *"Integrability properties of high energy dynamics in the multi-color QCD"*, Physics-Uspekhi 47, 325 (2004).

[156] E. K. Sklyanin, *"Separation of variables in the quantum integrable models related to the Yangian Y[sl(3)]"*, J. Math. Sci. 80, 1861 (1996).

[157] B. Basso, S. Komatsu and P. Vieira, *"Structure Constants and Integrable Bootstrap in Planar N=4 SYM Theory"*, arXiv:1505.06745.

[158] T. Fleury and S. Komatsu, *"Hexagonalization of Correlation Functions"*, JHEP 1701, 130 (2017), arXiv:1611.05577.

[159] B. Eden and A. Sfondrini, *"Tessellating cushions: four-point functions in $\mathcal{N} = 4$ SYM"*, JHEP 1710, 098 (2017), arXiv:1611.05436.

[160] S. E. Derkachov and A. N. Manashov, *"Iterative construction of eigenfunctions of the monodromy matrix for SL(2,C) magnet"*, J.Phys. A47 (2014) 305204 47, 305204 (2014).

[161] M. D'Eramo, G. Parisi and L. Peliti, *"THEORETICAL PREDICTIONS FOR CRITICAL EXPONENTS AT THE lambda POINT OF BOSE LIQUIDS"*, Lett. Nuovo Cim. 2, 878 (1971).

[162] A. P. Isaev, *"Multiloop Feynman integrals and conformal quantum mechanics"*, Nucl. Phys. B662, 461 (2003), arXiv:0303056.

[163] A. N. Vasilev, *"The field theoretic renormalization group in critical behavior theory and stochastic dynamics"*, Chapman and Hall/CRC (2004).

[164] P. P. Kulish, N. Y. Reshetikhin and E. K. Sklyanin, *"Yang-Baxter equation and representation theory: I"*, Letters in Mathematical Physics 5, 393 (1981).

[165] B. Basso, J. Caetano and T. Fleury, *"Hexagons and Correlators in the Fishnet Theory"*, .

[166] T. Fleury and S. Komatsu, *"Hexagonalization of Correlation Functions II: Two-Particle Contributions"*, JHEP 1802, 177 (2018), arXiv:1711.05327.

[167] D. J. Broadhurst, *"Evaluation of a Class of Feynman Diagrams for All Numbers of Loops and Dimensions"*, Phys. Lett. B164, 356 (1985).

[168] E. Panzer, *"Feynman integrals and hyperlogarithms"*, arXiv:1506.07243, https://inspirehep.net/record/1377774/files/arXiv:1506.07243.pdf.

[169] N. Gromov and A. Sever, *"Derivation of the Holographic Dual of a Planar Conformal Field Theory in 4D"*, Phys. Rev. Lett. 123, 081602 (2019), arXiv:1903.10508.

[170] N. Gromov and A. Sever, *"Quantum fishchain in AdS_5"*, JHEP 1910, 085 (2019), arXiv:1907.01001.

[171] N. Gromov and A. Sever, *"The Holographic Dual of Strongly γ-deformed N=4 SYM Theory: Derivation, Generalization, Integrability and Discrete Reparametrization Symmetry"*, arXiv:1908.10379.

[172] J. M. Maillet and G. Niccoli, *"On quantum separation of variables"*, J. Math. Phys. 59, 091417 (2018), arXiv:1807.11572.

[173] J. M. Maillet and G. Niccoli, *"On quantum separation of variables beyond fundamental representations"*, arXiv:1903.06618.

[174] N. Gromov, F. Levkovich-Maslyuk and G. Sizov, *"New Construction of Eigenstates and Separation of Variables for SU(N) Quantum Spin Chains"*, JHEP 1709, 111 (2017), arXiv:1610.08032.

[175] A. Cavaglià, N. Gromov and F. Levkovich-Maslyuk, *"Separation of variables and scalar products at any rank"*, JHEP 1909, 052 (2019), arXiv:1907.03788.

[176] P. Ryan and D. Volin, *"Separated variables and wave functions for rational $gl(N)$ spin chains in the companion twist frame"*, arXiv:1810.10996.

[177] N. Gromov, F. Levkovich-Maslyuk, P. Ryan and D. Volin, *"Dual Separated Variables and Scalar Products"*, arXiv:1910.13442.

[178] I. Kostov, V. B. Petkova and D. Serban, *"Determinant Formula for the Octagon Form Factor in N=4 Supersymmetric Yang-Mills Theory"*, Phys. Rev. Lett. 122, 231601 (2019), arXiv:1903.05038.

[179] Y. Jiang, S. Komatsu and E. Vescovi, *"Structure Constants in $\mathcal{N} = 4$ SYM at Finite Coupling as Worldsheet g-Function"*, arXiv:1906.07733.

[180] A. Pittelli and M. Preti, *"Integrable fishnet from γ-deformed $\mathcal{N} = 2$ quivers"*, Phys. Lett. B798, 134971 (2019), arXiv:1906.03680.

[181] B. Basso, G. Ferrando, V. Kazakov and D.-l. Zhong, *"Thermodynamic Bethe Ansatz for Fishnet CFT"*, arXiv:1911.10213.

[182] S. E. Derkachov and A. N. Manashov, *"General solution of the Yang-Baxter equation with symmetry group SL(n,C)"*, St. Petersburg Math. J. 21, 513 (2010), [Alg. Anal.21N4,1(2009)].

[183] V. K. Dobrev, G. Mack, V. B. Petkova, S. G. Petrova and I. T. Todorov, *"Harmonic Analysis on the n-Dimensional Lorentz Group and Its Application to Conformal Quantum Field Theory"*, Lect. Notes Phys. 63, 1 (1977).

[184] E. S. Fradkin and M. Ya. Palchik, *"Recent Developments in Conformal Invariant Quantum Field Theory"*, Phys. Rept. 44, 249 (1978).

[185] F. A. Dolan and H. Osborn, *"Conformal four point functions and the operator product expansion"*, Nucl. Phys. B599, 459 (2001), arXiv:0011040.

[186] F. A. Dolan and H. Osborn, *"Conformal Partial Waves: Further Mathematical Results"*, arXiv:1108.6194.

[187] M. Preti, *"The Game of Triangles"*, arXiv:1905.07380, in: *"19th International Workshop on Advanced Computing and Analysis Techniques in Physics Research: Empowering the revolution: Bringing Machine Learning to High Performance Computing (ACAT 2019) Saas-Fee, Switzerland, March 11-15, 2019"*.

[188] A. G. Grozin, *"Massless two-loop self-energy diagram: Historical review"*, Int. J. Mod. Phys. A27, 1230018 (2012), arXiv:1206.2572.

[189] N. I. Usyukina and A. I. Davydychev, *"An Approach to the evaluation of three and four point ladder diagrams"*, Phys. Lett. B298, 363 (1993).

[190] A. C. Ipsen, M. Staudacher and L. Zippelius, *"The One-Loop Spectral Problem of Strongly Twisted $\mathcal{N}$=4 Super Yang-Mills Theory"*, arXiv:1812.08794.

[191] B. Basso, J. Caetano and T. Fleury, *"Hexagons and Correlators in the Fishnet Theory"*, arXiv:1812.09794.

[192] G. Arutyunov and E. Olivucci, *"Hyperbolic spin Ruijsenaars-Schneider model from Poisson reduction"*, arXiv:1906.02619v2.

[193] D. Simmons-Duffin, D. Stanford and E. Witten, *"A spacetime derivation of the Lorentzian OPE inversion formula"*, arXiv:1711.03816.

Eidesstattliche Erklärung

Hiermit erkläre ich an Eides statt, dass ich die vorliegende Dissertationsschrift selbst verfasst und keine anderen als die angegebenen Quellen und Hilfsmittel benutzt habe.

Hamburg, den 29 April 2020 Unterschrift